PDZD11: a novel PLEKHA7 interactor at adherens junctions

Guerrera, Diego

UNIVERSITE DE GENÈVE
Section de Biologie
Département de Biologie Cellulaire

FACULTE DES SCIENCES
Prof. Sandra Citi

PDZD11: a novel PLEKHA7 interactor at adherens junctions

THÈSE
Présentée à la Faculté des sciences de l'Université de Genève
Pour obtenir le grade de Doctor ès science, mention Biologie

par
DIEGO GUERRERA
de
Benevento (Italie)

Thèse N° 4962

GENÈVE
Atelier d'impression Repromail
2016

UNIVERSITÉ
DE GENÈVE

FACULTÉ DES SCIENCES

Doctorat ès sciences
Mention biologie

Thèse de *Monsieur Diego GUERRERA*

intitulée :

"PDZD11: a Novel PLEKHA7 Interactor at Adherens Junctions"

La Faculté des sciences, sur le préavis de Madame S. CITI, professeure et directrice de thèse (Département de biologie cellulaire), Monsieur E. FERAILLE, professeur (Département de physiologie cellulaire et métabolisme) et Monsieur A. LE BIVIC, professeur (Institut de la biologie du développement, Université d'Aix-Marseille, Marseille, France), autorise l'impression de la présente thèse, sans exprimer d'opinion sur les propositions qui y sont énoncées.

Genève, le 22 juillet 2016

Thèse - 4962 -

p.o.

Le Doyen

N.B. - La thèse doit porter la déclaration précédente et remplir les conditions énumérées dans les "Informations relatives aux thèses de doctorat à l'Université de Genève"

Table of contents

Résumé

Les cellules épithéliales fournissent une barrière entre les environnements externe et interne du corps et définissent une compartimentation tissulaire dans les organes, en recouvrant toutes les surfaces et les cavités internes du corps. Les cellules épithéliales polarisées des vertébrés sont caractérisées par un complexe jonctionnel comprenant les jonctions serrées, les jonctions adhérentes et les desmosomes. Le complexe jonctionnel est responsable de l'adhésion épithéliale par l'établissement de contacts cellules-cellules spécifiques entre les cellules épithéliales voisines, et joue un rôle dans les fonctions fondamentales de la polarité épithéliale, la barrière paracellulaire et la morphogenèse cellulaire.

PLEKHA7 est une protéine récemment identifié appartenant aux jonctions adhérentes, où elle est présente dans les deux complexes majeures d'adhésions, basé sur les cadherines et les nectines, à travers l'interaction d'avec les composants cytoplasmiques p120ctn et afadine [5-7]. PLEKHA7 fait partie d'un complexe connectant l'E-cadherine aux microtubules du cytosquelette, et stabilise la *zonula adhaerens* (ZA) [5]. Des études génétiques et génomiques ont montré que PLEKHA7 est impliquée dans la régulation de la signalisation des micro ARNs, dans l'hypertension, dans la régulation de la contractilité cardiaque et dans le glaucome [8-11]. Toutefois, les mécanismes moléculaires à travers lesquels PLEKHA7 participe dans la physiologie et la pathologie des différents tissues restent inconnus. Dans ma thèse, je rapporte de nouveaux résultats qui ont aidé à découvrir les fonctions de PLEKHA7 dans les cellules épithéliales et endothéliales, à travers

l'identification d'une nouvelle molécule qui interagit avec PLEKHA7, PDZD11, par le criblage à deux hybrides de levures, des analyses de spectrométrie de masse, de co-immunoprécipiation et de pull-down. J'ai analysé les bases structurelles de leur interaction, montrant que le domaine WW de PLEKHA7 se lie à la région N-terminale de PDZD11; cette interaction est fonctionnellement essentielle, car PLEKHA7 est responsable du recrutement de PDZD11 aux jonctions cellule-cellule. Ainsi, j'ai identifié PDZD11 comme une nouvelle protéine des jonctions adhérentes. Par ailleurs, j'ai fourni des preuves que PDZD11 forme un complexe avec les nectines dans les jonctions adhérentes, et que son domaine PDZ se lie au motif des nectines liant PDZ. PDZD11 stabilise les nectines et régule le début des premières étapes de l'assemblage jonctionnel. En résumé, mon travail a permis de découvrir une nouvelle fonction de PLEKHA7 dans le recrutement de PDZD11 dans les jonctions adhérentes, et a montré que le complexe PLEKHA7-PDZD11 stabilise le complexe des nectines dans les jonctions adhérentes, promouvant l'efficacité des premières étapes dans l'assemblage des jonctions. Ces résultats suggèrent un rôle de PLEKHA7 dans le recrutement et la stabilisation des protéines liant PDZ aux jonctions adhérentes, ouvrant de nouvelles perspectives dans la compréhension des mécanismes moléculaires sous-jacents le rôle de PLEKHA7 dans la physiologie et pathologie cellulaire.

ABSTRACT

Epithelial cells provide a barrier between the external and internal body environments and define tissue compartmentalization within organs, by covering all body surfaces and lining all internal body cavities. Vertebrate polarized epithelial cells are characterized by a junctional complex, comprising tight junctions (TJ), adherens junctions (AJ) and desmosomes (D). The junctional complex is responsible for epithelial adhesion through the establishment of specific cell-cell contacts between neighboring epithelial cells, and mediates fundamental functions in epithelial polarity, paracellular barrier, and cell morphogenesis.

PLEKHA7 is a recently identified protein of the AJ, where it is present at both major adhesive protein complexes, based on cadherin and nectin, respectively, through its interaction with the cytoplasmic components p120ctn and afadin [5-7]. PLEKHA7 is part of a complex which connects E-cadherin to the microtubule cytoskeleton, and stabilizes the *zonula adhaerens* (ZA) [5]. PLEKHA7 has been involved by genetic and genomic studies in the regulation of micro-RNA signaling, hypertension, regulation of cardiac contractility, and glaucoma [8-11]. However, the molecular mechanisms through which PLEKHA7 participates in tissue physiology and pathology remain unknown. In my thesis I report novel results which help to uncover PLEKHA7 functions in epithelial and endothelial cells, through the identification of a novel molecular interactor of PLEKHA7, PDZD11, by yeast two-hybrid screening, mass spectrometry analysis, co-immunoprecipitation and pulldown assays. I dissected the structural basis of their interaction, showing that the WW

domain of PLEKHA7 binds to the N-terminal region of PDZD11; this interaction is functionally relevant, since it mediates the junctional recruitment of PDZD11 in vivo. Thus, I identified PDZD11 as a novel AJ protein. Furthermore, I provided evidence that PDZD11 forms a complex with nectins at AJ, and its PDZ domain binds to the PDZ-binding motif of nectins. PDZD11 stabilizes nectin adhesion molecules and thus promotes the early steps of junction assembly. In summary, my work uncovered a new function for PLEKHA7 in recruiting PDZD11 to AJ, and showed that the PLEKHA7-PDZD11 complex stabilizes the nectin complex at AJ, promoting efficient early steps in junctional assembly. These results suggest a role for PLEKHA7 in the recruitment and stabilization of PDZ-binding proteins at AJ, opening new perspectives in the dissection of the molecular mechanisms underlying PLEKHA7 role in tissue physiology and pathology.

INTRODUCTION

The complexity of multicellular organisms is achieved through the interplay and interactions of different cell types, which are organized into tissues and organs. This is made possible by the presence of specific adhesion molecules on the cell surface, which allow the interaction between neighboring cells and with the extracellular matrix.

Epithelial cells constitute 60% of the cells in human body; they cover body surfaces, line internal organs and cavities, thus forming a protective barrier to the outside, separating and defining functionally different body compartments, and regulating the exchange of solutes between them. In addition, epithelial cells constitute glandular tissues.

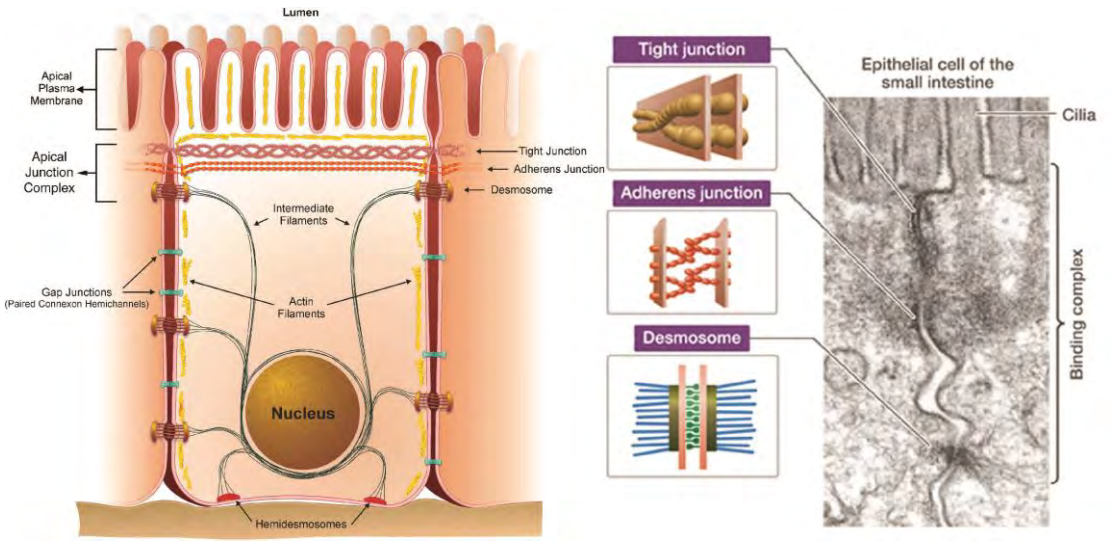

Figure 1. The junctional complex of vertebrate epithelial cells.
Schematic representation of an epithelial cell with highlighted the junctional complex components: tight junction, adherens junction and desmosome. These components are also shown in an electron microscopy image of an epithelial intestinal cell (adapted from [3] and CSLS/The University of Tokyo).

Along with the increasing complexity of organisms throughout evolution from Invertebrate to Vertebrate species, there has been a corresponding

increase in the complexity, protein redundance and functional specializations of cell-cell junctions. In fact, invertebrate organisms have epithelial cells with two basic types of junctions: septate junctions (SJ) and adherens junction (AJ) [12]. In contrast, epithelial cells of vertebrates are characterized by a junctional complex which comprises, from apical to basal: tight junctions (TJ), which are the functional counterpart of the SJ of invertebrates, adherens junctions (AJ) and desmosomes (D) [13] (Fig. 1).

The junctional complex is responsible for epithelial adhesion through the establishment of specialized points of contact between neighboring epithelial cells. Moreover, it plays crucial functions in epithelial polarity, barrier, and cell morphology. AJ represent the first contact that is established between cells, and they are linked to the actin cytoskeleton and to microtubules, conferring mechanical resistance to junctions, together with desmosomes, which are linked to intermediate filaments [14]. The junctional complex is responsible for the establishment and maintenance of apico-basal polarity through different polarity complexes present either at TJ or along basolateral membrane, structurally separating functionally distinct proteins and lipids of the apical and basolateral membranes [15]. Besides their potential or established roles in cell-cell adhesion, transmembrane proteins of the TJ, establish a paracellular barrier, which controls the passage of ions and solutes in the space between neighboring cells [16]. Furthermore, the junctional complex is also involved in the regulation of cell morphology and migration, through its association with and organization of the actin cytoskeleton. Finally, numerous recent studies implicate the junctional complex in the regulation of signaling pathways, which control the activity of

Rho GTPases, cell proliferation, differentiation and gene expression [4, 17, 18]. Despite the great advances in this field in the last thirty years, further studies are still needed to clarify the molecular mechanisms at the basis of the regulation of junction assembly, and their involvement in the physiology and pathology of epithelial cells and tissues.

TIGHT JUNCTIONS (TJ)

In vertebrate polarized epithelial cells TJ are the most apical element of the junctional complex. The ultrastructure of TJ was first described by Farquhar and Palade in 1963, in intestinal epithelial cells. On thin section electron micrographs TJ appear as points of contact between the outer leaflets of the plasma membrane of neighboring cells, where membranes appear to "fuse" together, merging into a single leaflet of the same thickness of each of the original layer [13] (Fig. 1). TJ have different functions, among which the best known is to control the flux of solutes and ions across paracellular pathway (barrier function). The barrier function is accomplished by transmembrane proteins that seal the space between neighboring cells and form selective paracellular channels/pores for the passage of solutes and ions. Different tissues display different paracellular permeability properties, depending on which of the isoforms of the claudin family of proteins is expressed. This property can be studied for example by measuring the transepithelial electrical resistance (TER) of a cell monolayer; a high value of TER corresponds to low ionic permeability [19-21]. TJ also provide a barrier against large molecules and pathogens [22]. A second major "canonical"

function of TJ is the "fence" function, which refers to the maintenance of the apico-basal polarized distribution of proteins and lipids in the plasma membrane [16].

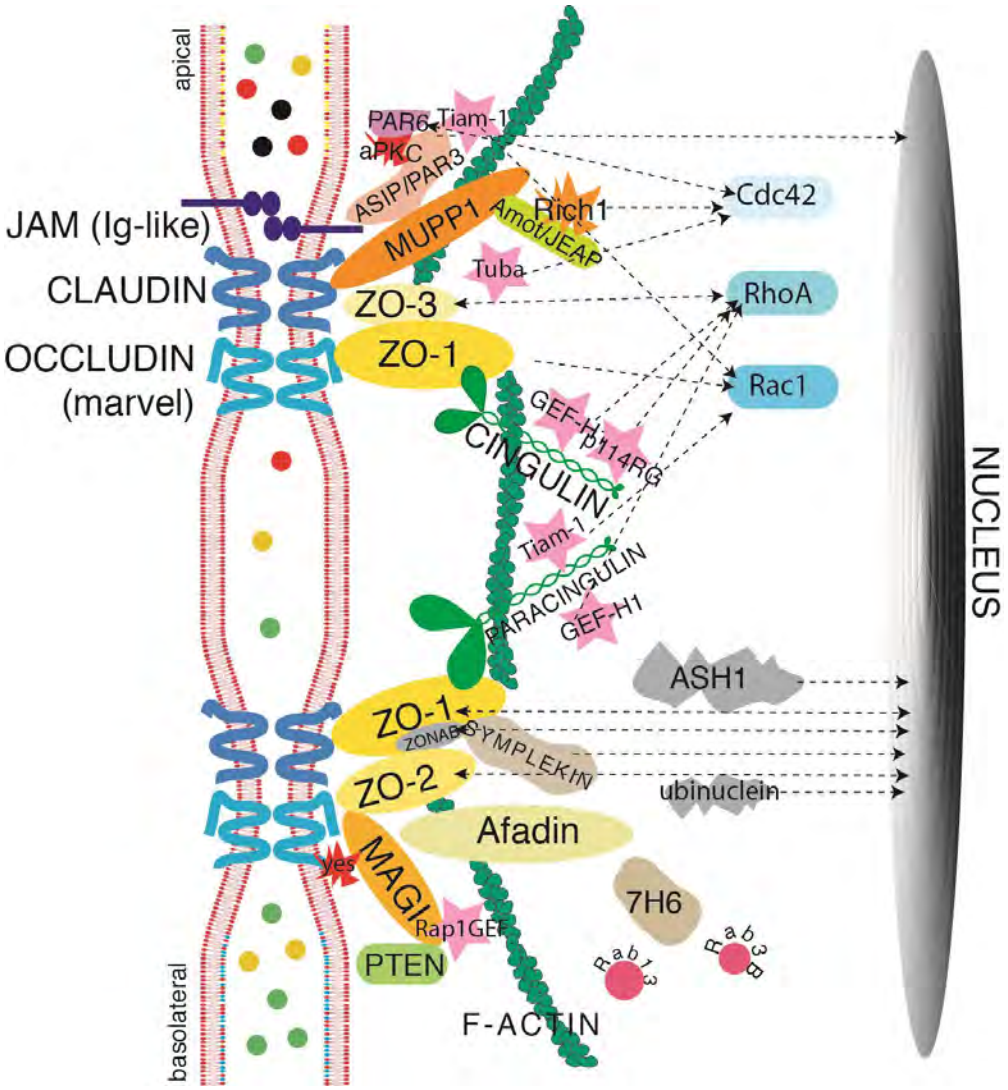

Figure 2. Schematic organization of TJ proteins.
Integral membrane proteins of TJ (occludin, claudins, and Ig-lile adhesion molecules such as JAMs) are shown connected with the counterpart on neighboring cell. The cytoplasmic plaque is also shown, with the protein interaction networks mediating connection to the actin cytoskeleton, regulation of Rho family GTPases and signaling. PDZ-containing proteins are represented: ZO proteins, AF-6/afadin, PAR3, PAR6, MAGI and MUPP1. The scaffolding proteins cingulin and paracingulin, GEFs (GEF-H1, p114RhoGEF, Tiam1, Tuba, Rap1GEF), GTPases (RhoA, Rac1, Cdc42) and trascription factors are also represented (adapted from [4])

In addition to these canonical functions, increasing lines of evidence suggest a role of TJ in the regulation of gene expression and proliferation, through

different junctional proteins that can either directly shuttle to the nucleus (for example ZO-2 and symplekin), or sequester transcription factors at junctions (ZO proteins and AMOT) [4, 23-25]. Additional proteins, like cingulin and paracingulin, can regulate gene expression and proliferation by controlling the subcellular localization of GEFs and GAPs for Rho GTPases [26, 27].

In addition to transmembrane proteins, TJ comprise several cytoplasmic proteins, including scaffolding proteins, which link transmembrane proteins to the cytoskeleton, adaptor and signaling proteins [4, 28] (Fig. 2).

Transmembrane proteins

TJ comprise two types of transmembrane proteins: 1) tetraspan proteins, such as occludin, claudins and tricellulin, which cross the membrane four times, and display cytoplasmic amino and carboxyl terminal regions, and two extracellular loops; 2) single-pass immunoglobulin-like adhesion proteins, such as junctional adhesion molecule (JAM) and coxsackievirus and adenovirus receptor (CAR) [28].

The first transmembrane protein of TJ (occludin) was identified in the Tsukita laboratory in 1993, by generating monoclonal antibodies against a liver junctional fraction; the name occludin derives from latin “occludere”, which means to occlude/seal [29]. **Occludin** is a 65 KDa protein characterized by four transmembrane domains and two extracellular loops; its cytoplasmic region is rich of serine, threonine and tyrosine residues, whose phosphorylation state determines occludin accumulation at TJ [30, 31]. The

carboxyl terminal region of occludin directly binds to actin and to ZO proteins [28, 32, 33]. Early evidence about the importance of occludin in TJ structure and function came from experiments showing that exogenous expression of occludin in fibroblasts (lacking TJ) leads to the formation of TJ-like structures; and that exposure of epithelial cells to a peptide corresponding to the extracellular loops of occludin perturbs TJ formation and permeability barrier [34, 35]. However, either depletion or knockout (KO) of occludin in cell lines and mice does not lead to abnormalities in the morphology and physiology of TJ [36, 37], possibly due to the redundant expression of tricellulin. Tricellulin shows sequence similarities to occludin, it is normally present at tricellular TJ, but localizes along all TJ when occludin is depleted [28].

The lack of strong phenotypes in occludin KO mice led the Tsukita group to search for additional transmembrane components of TJ; thus, they identified two new transmembrane proteins, claudin-1 and claudin-2, whose name derives from latin “claudere” (to close) [38]. Freeze fracture electron microscopy revealed the presence of claudins as main components of TJ membrane strands [38].The claudin family of proteins contains over 25 members, which have a size of 20-27 kDa and display four transmembrane domains and two extracellular loops, without significant sequence similarity to occludin [39]. The last amino acids of the C-terminal tail of claudins are highly conserved and contain a PDZ (PsD-95/Disc-large/ZO-1)-binding consensus sequence, through which claudins can bind the PDZ domain of ZO proteins, PATJ and MUPP1 [40-42]. Claudins can form homo or hetero-dimers, by interacting in cis or in trans with other members of the claudin family. Different combinations of interacting claudins give rise to different patterns in the TJ

strands [43]. The main function of claudins is to control the paracellular permeability of epithelial sheets; the expression of different claudins and their combination provide tissues with their specific permeability properties, which are adapted to the physiological requirements of each tissue. The crucial role played by claudins in the barrier function of epithelia is highlighted by the observation that in claudin-1 KO mice a defective epidermal barrier leads to the death of newborn mice, by dehydration [44]. Mutation or altered expression of claudin genes are associated with several different human pathologies [45].

JAM and CAR are single transmembrane domain proteins of TJ, which display an extracellular region with two Ig-like domains, and an intracellular tail bearing a PDZ-binding consensus motif, which allows JAM to interact with afadin, Par3 and ZO-1 [46-48]. In addition, CAR (Coksackie-adenovirus receptor) can bind ZO-1 [49]. Knockdown studies in epithelial cells demonstrated that JAM and CAR are involved in the regulation of the barrier function [49, 50].

Cytoplasmic proteins

The cytoplasmic region of TJ contains a variety of protein components that can be subdivided in two large groups: PDZ proteins, which form scaffolds to anchor membrane proteins of TJ to the cytoskeleton, and non-PDZ proteins, which include signaling proteins, kinases, transcription factors and adaptor proteins.

The PDZ proteins of TJ include the ZO proteins; the membrane-associated guanylate kinase inverted proteins (MAGIs); the multi-PDZ protein MUPP1; afadin; the members of the polarity complex involved in the establishment of apico-basal polarity, PAR-3, PAR6, PALS-1, and PATJ. The PDZ domain is responsible for the interaction with membrane proteins, binding the consensus motif at their C-terminal tail, and mediates also the interaction with the PDZ domain of other proteins, creating scaffolding networks [4].

ZO proteins (ZO-1, ZO-2 and ZO-3) are scaffolding proteins belonging to the membrane-associated guanylate kinase (MAGUK) family. They contain three PDZ domains, followed by a Src-homology (SH3) domain and a guanylate kinase (GUK) domain. The SH3 domain binds proline-rich regions, mediating the association with signaling proteins. Moreover, the GUK domain of ZO proteins lacks crucial residues that are necessary for kinase activity, and is likely only involved in protein interactions [51]. ZO-1 is a M_r 220 kDa protein, and it was the first identified protein of TJ [52]. Subsequently ZO-2 (160 kDa) and ZO-3 (130 kDa) were identified as proteins, through their co-immunoprecipitation with ZO-1 [53, 54]. The first PDZ domain of ZO-1 mediates its homodimerization, whereas the second PDZ domain is responsible for heterodimerization with ZO-2 and ZO-3 [55]. The first PDZ domain of ZO proteins is responsible for the interaction with the cytoplasmic tail of claudins. This interaction is crucial for the assembly of claudin fibrils/strands. ZO-1 and ZO-2 show redundant function and only when both are depleted do claudins fail to assemble into TJ fibrils, with consequent impairment of the barrier function [56]. In contrast, ZO-3 does not appear to

be required for TJ formation in epithelia [57]. ZO-1 interacts also with occludin and α-catenin through the SH3-GUK domain, and through its C-terminal region with afadin and cingulin (CGN), and is crucial for the junctional recruitment of the latter [58-60]. The C-terminal region of ZO-1 and ZO-2 contains also an actin-binding domain, allowing them to connect transmembrane TJ proteins to the actin cytoskeleton [61]. Finally, ZO-1 can associate through its PDZ3-SH3-GUK domain to the transcription factor Dbpa/ZONAB, and all three ZO proteins redundantly regulate its sequestration at TJ [24]. In vivo the KO of either ZO-1 or ZO-2 is not compatible with life, with mice dying at early embryonic stage, due to failure in development of the yolk sac and annexed tissues [62, 63]; whereas, mice KO for ZO-3 are viable and don't show any defect in TJ morphology and function, except for defective blood-sperm barrier [57].

Other PDZ protein of the TJ include the **polarity complex proteins**. Three polarity complexes mediate the establishment of the apico-basal polarity in epithelial cells: two localized apically at TJ, the PAR and Crumb complexes; one localized at lateral membrane, the Scribble complex. The PAR complex, originally described in *C. elegans*, in mammals comprises the scaffolding PDZ containing proteins PAR3 and PAR6 and the catalytic protein atypical protein kinase C (aPKC) [64]. PAR3 localizes at TJ by interacting through its second PDZ domain with JAM, and subsequently recruits the other two members of the complex (PAR6 and aPKC) [48, 65, 66]. It also interacts with Tiam1, thus regulating the spatial activation of Rac1 and the junction assembly [67]. PAR6 mediates the interaction of PAR3 with aPKC, once activated by either Cdc42 or Rac1, thus driving junction formation and polarity

establishment [64, 66]. The second apical polarity complex, Crumb, comprises the transmembrane protein CRB, which binds to the cytoplasmic PDZ containing protein PALS1; PALS1 in turn is connected to the other cytoplasmic members PATJ and MUPP1. PATJ interacts through its PDZ domain to ZO-3 and claudin-1 [42], and its depletion affects the stability of TJ and of the Crumb polarity complex [68]. MUPP1 instead interacts with JAM, CAR and claudins and may serve as linker between these transmembrane TJ proteins [64].

In addition to the above mentioned PDZ proteins, the cytoplasmic side of TJ comprises several non-PDZ proteins, including signaling and scaffolding proteins; among them we will examine in further detail cingulin and paracingulin.

Cingulin

Cingulin is a 140 kDa cytoplasmic protein exclusively found at TJ of epithelial and endothelial cells of vertebrates. It was discovered in 1988 as a protein, which copurified with non-muscle myosin II from chicken intestinal epithelial cells, and it has a similar domain organization to myosin. Its name derives from latin "*cingere*" (to form a belt around), since it localizes in an apical circumferential belt in epithelial cells [69]. At the structural level, cingulin is characterized at the N-terminal region by a globular head, followed by a coiled-coil rod domain and a small globular tail at the C-terminal region [58] (Fig. 3). Cingulin exists as a parallel homodimer, thanks to the interaction of the alpha-helices of each monomer, to form a coiled-coil rod domain. In

vitro cingulin can bind to and bundle actin filaments, but it does not appear to be involved in the regulation of actin filaments architecture in vivo [70]. The N-terminal region of cingulin is a site of interaction for many different molecular partners, like ZO proteins, afadin and JAM [46, 58]. The AMPK-mediated phosphorylation on specific serines in this region mediates the association of cingulin with a planar apical network of microtubules, thus mediating the association of microtubules with TJ [71]. This association is important for TJ-related regulation of epithelial morphogenesis [71]. The globular head of cingulin is responsible for the interaction with the ZO proteins, afadin and JAM [46, 58]. The interaction with ZO-1 is fundamental for cingulin localization at TJ; this interaction is mediated by a small region called ZO-1 interaction motif (ZIM) [72] (Fig. 3). Cingulin accumulation at TJ is lost in epithelial cell lines lacking ZO-1, but not ZO-2, suggesting no redundancy of ZO-1 and ZO-2 concerning cingulin junctional recruitment [73]. The KO of cingulin in embryoid bodies does not affect TJ organization and function, but leads to altered expression of over 800 genes, including, occludin, several claudins, and the transcription factors GATA-4, GATA-6 and HFN-4α, which are implicated in endodermal differentiation [74]. The role of cingulin in regulating gene expression was partially confirmed by experiments using cingulin knockdown (KD) epithelial (MDCK) cell lines, which show altered expression of claudin-2 and ZO-3, and increased cell proliferation. The ability of cingulin to regulate gene expression and cell proliferation depends on its ability to control cellular RhoA activation; in fact, cingulin binds and sequesters at junction the guanine nucleotide exchange factor (GEF) GEF-H1, preventing its activation of RhoA [26, 75]. Cingulin KO mice display normal TJ morphology and function, but

have altered expression of claudin-2 and an exacerbated response upon pharmacologically induced duodenal injury [76]. Furthermore, cingulin is implicated in the junctional recruitment of an additional GEF, p114RhoGEF, important for junction assembly in epithelial corneal cells [77]. However, experiments on KD MDCK cells indicate that cingulin does not affect TJ assembly and barrier function, suggesting that the role of cingulin in barrier function is cell-context dependent. This idea is confirmed by the observation that endothelial cells overexpressing cingulin show increased barrier function, and mice KO for cingulin display impaired blood brain barrier function [78].

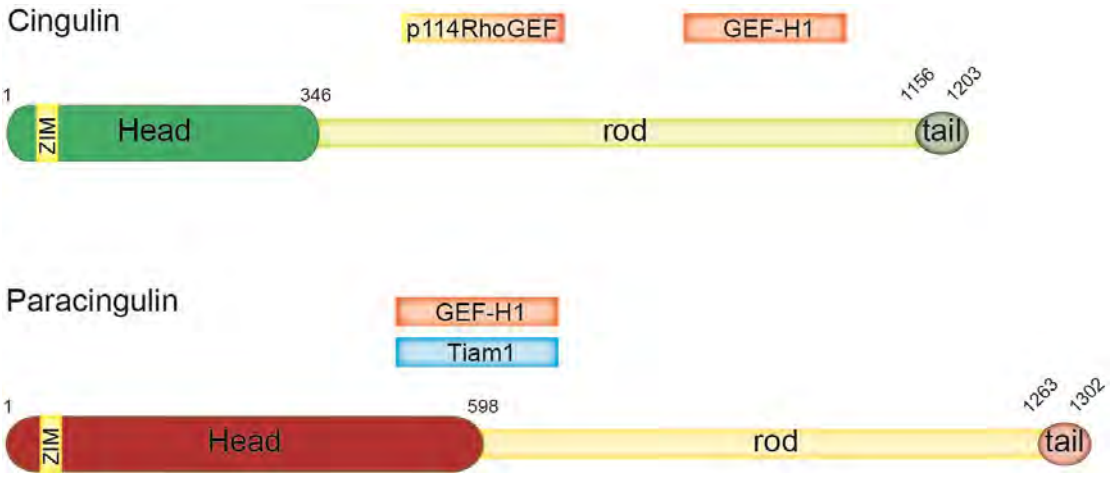

Figure 3. Schematic representation of the domain organization of cingulin and paracingulin.
Human cingulin and paracingulin protein domains are indicated with the correspondent amino acidic residues. ZIM (ZO-1 interacting motif) sequence is indicated, along with the correspondent GEFs molecular partners of each protein.

Paracingulin

Paracingulin (also known as JACOP, or cingulin-like1-CGNL1) is a 160 kDa junctional protein which shows sequence and domain organization similarities with cingulin [79]. It has a globular head bigger than cingulin, a shorter coiled-coil rod domain, and a globular tail (Fig. 3).

Due to the structural similarity with cingulin, it is likely that paracingulin also forms homodimers. Although the two proteins form a complex detectable by co-immunoprecipitation, they are not likely to function as a unit, since their junctional recruitment and dynamics are independent [80]. Unlike cingulin, paracingulin has been immunolocalized both at TJ and AJ [79]. Similarly to cingulin, it presents a ZIM sequence in its globular head that mediates its interaction with ZO-1, responsible for paracingulin accumulation at TJ [81]. In contrast, paracingulin is recruited to AJ through the interaction of its globular head domain with PLEKHA7[81]. Possibly due to the association with PLEKHA7, which mediates the conneciton between E-cadherin and the microtubule cytoskeleton, perturbing microtubule organization results in the loss of junctional paracingulin [80]. Paracingulin is involved in the regulation of the Rho family GTPases RhoA and Rac1 through the GEFs GEF-H1 and Tiam1, respectively [27] (Fig. 3). Similarly to cingulin, paracingulin interacts with GEF-H1, sequestering it at junctions and preventing RhoA activation. Paracingulin-depleted cells also show altered expression of claudin-2 and ZO-3, and increased proliferation [27]. Furthermore, paracingulin is involved in the regulation of junction assembly by interacting, through its head domain, with the Rac1 GEF Tiam1, which locally activates Rac1 driving junction formation. Epithelial cells depleted of paracingulin lose junctional recruitment of Tiam1, showing decreased Rac1 activation and delayed junction formation [27].

ADHERENS JUNCTIONS (AJ)

AJ comprise cell-cell adhesion structures found in a variety of cell types, e.g., AJ are not restricted to epithelial cells, like TJ. In polarized epithelial cells, AJ are localized immediately basal to TJ. By electron microscopy, AJ appear as sites where the opposing plasma membranes of neighboring cells are separated by an extracellular space of ~200 Å [13]. Actin filaments are densely associated with the cytoplasmic face of the AJ plasma membrane [82]. Within vertebrate polarized epithelial cells AJ can be distinguished into two subdomains: 1) a circumferential apical ring called "*zonula adhaerens*" (ZA) or adhesion belt, just below TJ, which contains a circumferential actin belt in the cytoplasm, which runs parallel to the membrane; 2) along the lateral membrane in a punctate pattern, called *puncta adhaerentia*, or lateral contacts, where actin filaments terminate more perpendicularly [83]. In non-epithelial cell types AJ have different morphologies, but are typically discontinuous, in the form of spot-like adhesion contacts, where actin filaments terminate in a perpendicular fashion, similar to *puncta adhaerentia* [18, 84]. AJ are responsible for the initiation and maintenance of cell-cell adhesion, for coordinating tissue organization and integrity, and for regulating cell shape and motility through rearrangements of the cytoskeleton. For example, the disruption of AJ leads to the loosening of cell contacts and disorganization of tissue architecture [18]. AJ are connected both to actin and microtubule cytoskeletons. The interaction with the actin cytoskeleton is mediated by several cytoplasmic proteins, comprising α-catenin, afadin, eplin, vinculin and α-actinin [85-89]. AJ can drive epithelial

shape changes through the contraction of the AJ-associated actomyosin belt, and this is a fundamental role of AJ in tissue remodeling during development [18, 90]. AJ can also interact with microtubules, although this interaction is less well characterized, compared to interaction with actin. β-catenin interacts with the motor protein dynein [91], and a complex comprising p120ctn, PLEKHA7 and nezha links E-cadherin to the microtubules minus end [5] (Fig. 4).

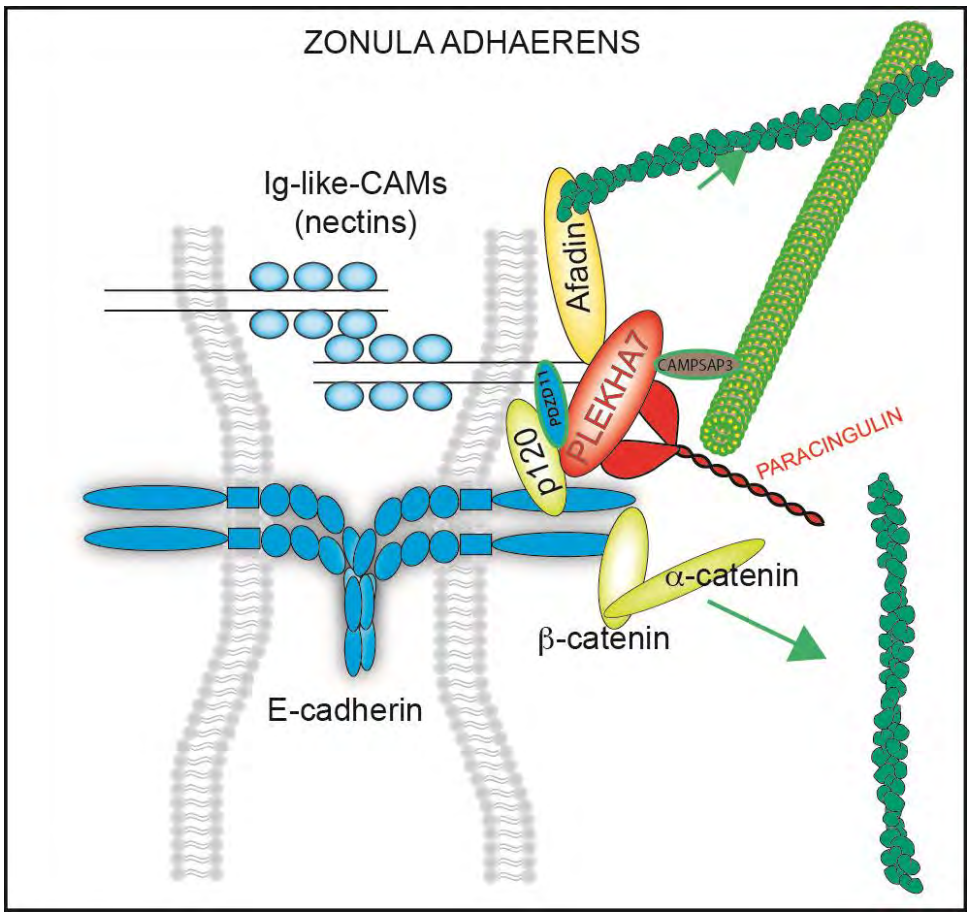

Figure 4. Schematic representation of AJ.
Semplified representation of AJ organization, with the two major adhesion molecules, nectin and cadherin, connected together or either with the actin or microtubule cytoskeleton through their cytoplasmic partners.

Besides their role in adhesion and linkage to cytoskeleton, AJ are also involved in signaling and regulation of gene expression. Cytoplasmic proteins,

such as β-catenin and p120ctn, can directly translocate to the nucleus, where they interact with transcription factors, whereas PLEKHA7 regulates the processing of miRNAs [8]. Furthermore, both p120ctn and afadin can modulate gene expression through the regulation of RhoA and Rac1 activity [92, 93]. Finally, α-catenin is involved in the junctional retention of the transcription factor YAP [94, 95].

Cadherins and nectins are two major types of transmembrane adhesion proteins of AJ and they are connected through their cytoplasmic partners to the cytoskeleton (Fig. 4). They are discussed in further detail below.

Cadherins

Cadherins are a superfamily of adhesion molecules comprising more than 40 different members, and they mediate various types of cell-cell interactions. In mammalian species, a subset of the family of cadherins are the "classical" cadherin family and they comprise 20 members, that share a similar domain organization. They are single-span transmembrane proteins with an extracellular domain constituted of five cadherin repeats (EC domain), and a short cytoplasmic domain. The family members are named after the tissue of their predominant expression, such as epithelial cadherin (E-cadherin), neural (N-cadherin), vascular endothelial (VE-cadherin) and placental (P-cadherin) [96, 97]. The EC domain contains calcium binding sequences, and calcium binding to the extracellular region is required for the trans-interaction between cadherins of neighboring cells to occur [98].

Furthermore, cadherins can homodimerize in cis, and their clustering strengthens cell-cell contacts [99, 100]. Besides the well-conserved EC domains there are some sequences in the extracellular region that vary between the family members and confer adhesive specificity [96]. Homotypic interactions have higher affinity than heterotypic ones, allowing segregation and sorting of different cell types [96]. Non-classical cadherins have a similar extracellular domain organization, but differences in the cytoplasmic domain sequence and molecular interactions. Among them are the desmosomal cadherins (desmocollins and desmogleins), protocadherins and Fat cadherins [18, 101, 102].

E-cadherin

E-cadherin is the major calcium-dependent transmembrane protein of epithelial AJ. The cytoplasmic region of E-cadherin is divided in two parts: the juxtamembrane domain (JMD), responsible for the interaction with p120ctn, and the C-terminal, catenin-binding domain (CBD), which mediates the interactions with β-catenin and plakoglobin [103-105]. The interaction with p120ctn stabilizes E-cadherin at AJ, since p120ctn binding masks the residues implicated in clathrin-mediated endocytosis and Hakai-dependent ubiquitination [106, 107]. Thus, p120 binding to E-cadherin prevents its endocytosis, which can drive junction disassembly [108]. The association of E-cadherin with microtubules, which is mediated by the p120ctn-PLEKHA7-nezha complex, also stabilizes E-cadherin at AJ. The kinesin motor KIFC3, which is bound to microtubules, recruits the USP47 deubiquitinase to AJ

[109], thus counteracting Hakai-dependent ubiquitination, which promotes endocytosis. E-cadherin association with β-catenin is promoted by the phosphorylation of E-cadherin on three specific serine residues [110]. The binding to β-catenin also stabilizes E-cadherin at AJ, since it allows the interaction with α-catenin and in turns with the actin cytoskeleton, and strengthens cell-cell contacts [111]. The interaction between E-cadherin and β-catenin may also be involved in Wnt/β-catenin signaling, since E-cadherin sequesters β-catenin at AJ, thus reducing the cytoplasmic pool, which can translocate to the nucleus to regulate gene expression [112]. Despite the central role of E-cadherin in cell-cell adhesion, epithelial cells depleted of E-cadherin display normal AJ, TJ and apico-basal polarization. However, depletion of E-cadherin affects the establishment of cell-cell junctions, pointing to a central role of E-cadherin in driving junction assembly, rather than a role in their maintenance [113].

Genetic approaches targeting E-cadherin in mice have revealed the central role of E-cadherin in epithelial development and morphogenesis. E-cadherin KO mice die at early embryonic stage due to failure in the formation of trophectoderm [114]. Conditional KO of E-cadherin in postnatal epidermis results in loss of AJ, loss of hair follicles, and altered epidermal differentiation [115]. The conditional targeting of E-cadherin in embryonic skin epithelium impairs TJ formation and barrier function, causing postnatal death due to dehydration [116]. E-cadherin regulation and turnover is necessary to drive physiological morphogenetic events such as epithelial to mesenchymal transition (EMT). Furthermore, downregulation or loss of E-cadherin is

associated with epithelial tumors and correlates with malignancy and the metastatic process in mouse models and human patients [117].

Nectins

Nectins are calcium-independent type-I single pass Ig-like transmembrane adhesion proteins of AJ. The nectin family of proteins comprises four members (nectin-1 to 4) and shares similarities with the members of a related family of non-canonical components of AJ, the nectin-like molecules (Necls) [118]. Nectins consist of an extracellular domain, comprising three Ig-like domains with a distal IgV followed by two IgC domains, followed by a transmembrane region and a cytoplasmic tail with a terminal four conserved residues that constitutes a PDZ-binding motif (Fig. 5). Nectins were first identified as viral receptor proteins, they are also known as poliovirus receptor-like proteins (PVRL1-4) [119, 120].

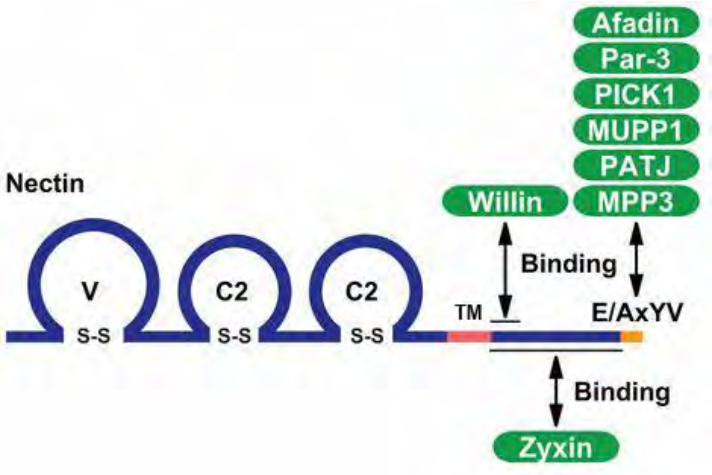

Figure 5. Schematic representation of nectins domain organization.
Nectins domain organization with the three extracellular loop, the transmembrane domain in pink and the PDZ consensus sequence in yellow. Nectins interactors and the region of binding are also represented (adapted from [1]).

The first extracellular loop of nectins mediates the homophylic and heterophylic trans-interaction with nectins on neighboring cells, whereas the second and third extracellular loops mediate cis-interaction. Nectins form trans-hetero-dimers in different combinations, and heterophylic interactions are stronger than homophylic ones, with the nectin-1/nectin-3 hetero-dimer being the strongest affinity interaction [121, 122]. Within the cytoplasmic region the last four residues of nectins bind to the PDZ domain of different proteins, among which the best characterized is afadin [123]. Depending on nectin isoform, nectins have been reported to interact with additional PDZ proteins, such as the polarity complex protein Par3, and the PDZ proteins PICK-1, MUPP1 and PATJ [124-126] (Fig. 5). These interactions are required for the regulation of TJ and AJ in epithelial cells. Nectin-1 and -3 also bind willin, whereas nectin-2 and -4 bind zyxin, mediating the recruitment of these proteins to cell-cell adhesion sites [127, 128] (Fig. 5). The interaction of nectins with afadin is important for their association with the actin cytoskeleton, and for the link with E-cadherin based complexes, through afadin interaction with α-catenin [129, 130] (Fig. 4). Nectins first cis-interact and then trans-interact at joining protrusion sites of neighboring cells, thus independently initiating and driving the formation of cell-cell junctions, followed by E-cadherin interactions. This first interactions give rise to spot-like junctions, which subsequently mature into belt-like AJ. Nectins and E-cadherin cooperatively organize AJ, during junction formation [131]. Nectins organize E-cadherin-based nascent complexes by connecting through them via their cytoplasmic partners afadin-ponsin and vinculin-α-catenin, respectively [131, 132] (Fig. 4). However, nectins alone can efficiently drive

the formation of AJ and TJ even without the cooperation of E-cadherin [133, 134]. Studies on nectin function in epithelial cells show their importance in junction formation [135]. Nectin mutations in the extracellular domain, which prevent the trans-interactions, affect junction assembly, delaying AJ formation [135].

Despite their importance in cell-cell adhesion in different tissues, the individual KO of nectins in mice do not lead to either embryonic lethality or strong phenotypes, probably due to the functional redundancy among nectin family members. However, nectin KO mice display developmental and functional abnormalities, for example either nectin-2 or nectin-3 KO leads to male infertility, due to defective formation and maintenance of sertoli-spermatid junctions [136]. Moreover, nectin-1 and nectin-3 are required for correct eye development, since they mediate the apex-apex adhesion between the ciliary epithelial cell layers [137]. Mice lacking these nectins display microphthalmia and separation of the pigment and non-pigment epithelia of the ciliary body [137]. These two nectins are also responsible for the adhesion of auditory sensory epithelial cells, being important for the development of the mammalian inner ear [138]. Finally, nectins may contribute to tumorigenesis, since several nectins are overexpressed in breast and ovarian cancer tissues, and in non-small-cell lung cancers [121].

Catenins

Catenins mediates the linkage of E-cadherin to the cytoskeleton and are divided in two subfamilies: 1) catenins which contain armadillo repeats, for

example β-catenin, p120ctn and plakophilins; 2) non-armadillo catenins, such as α-catenin, which does not share sequence similarities with other catenins, but is more similar to vinculin.

α-catenin

Similarly to cadherins, α-catenin is found in different isoforms named after the tissues in which they are predominantly expressed. Three isoforms of α-catenin have been characterized: αE-catenin in epithelial tissue, αN-catenin in neural tissue and αT-catenin in heart. α–catenin is responsible for the stabilization of AJ, since it mediates the connection of E-cadherin complex to the actin cytoskeleton and to the nectin complex. Unlike other catenins, α–catenin does not bind directly to E-cadherin, but indirectly through the interaction with β–catenin [139]. One prominent feature of α–catenin is that it can directly bind and bundle actin filaments, and interact with additional actin binding proteins, which regulate actin filament turnover, providing the connection of AJ with the circumferential F-actin belt [85, 140]. The importance of α–catenin in cell-cell adhesion is shown by the observation that cells depleted of this protein fail to adhere. Furthermore, α–catenin KO is lethal at the embryonic stage in mice [141]. The conditional KO of α-catenin in the skin results in a more severe phenotype compared to that of E-cadherin, with hyperproliferation and defects in cell adhesion in epidermis [142]. Finally, α–catenin is also involved in contact-dependent inhibition of cell proliferation,

by binding and sequestering the transcriptional coactivator YAP at cell junctions, when cells grow at high density [94].

β-catenin

β–catenin belongs to the armadillo repeat subfamily of catenins, since it contains 12 armadillo repeats (a conserved 40 residue motif). β–catenin is found in different pools: 1) associated with AJ, 2) in the cytoplasm and 3) in the nucleus, reflecting the different functions of the protein. In fact, β–catenin regulates cell-cell adhesion but is also involved in transcriptional regulation by the Wnt signaling pathway [143]. Its different roles are mediated by differential interaction with molecular partners. β–catenin interacts with E-cadherin, in a phosphorylation-dependent way, through a central armadillo repeat, the N-terminal domain of β–catenin mediates its interaction with α–catenin, whereas the C-terminal region mediates the transcriptional activation function [103, 143]. Under normal conditions the majority of β–catenin is associated with E-cadherin at AJ, with low levels of the cytoplasmic pool, since excess cytoplasmic β–catenin is phosphoryated, recruited to the APC complex, ubiquitinated, and degraded by the proteasome. Upon activatio then of Wnt pathway, the APC-mediated degradation of the cytoplasmic β–catenin is inhibited, and β–catenin can translocate to the nucleus, where it binds the Tcf/Lef transcription factor, activating the transcription of Wnt target genes [143-145]. β–catenin promotes E-cadherin based adhesion through two mechanisms: 1) by regulating cadherin trafficking from the endoplasmic

reticulum (ER) to the plasma membrane and 2) by stabilizing E-cadherin at AJ through the association with α–catenin [146, 147]. The KO of β–catenin in mice leads to early embryonic lethality, due to failure in mesoderm development. In addiiton, conditional KO of β–catenin in different tissues leads to defective cell differentiation and altered tissue integrity [148].

p120-catenin

p120-catenin (p120ctn) is a protein of the armadillo family, which is fundamental for the stability and dynamics of cadherins. It contains 9 armadillo repeats, through which it binds to the JMD domain of E-cadherin, and an N-terminal region, which contains regulatory phosphorylation domains [149], [150]. By binding to E-cadherin, p120ctn prevents E-cadherin ubiquitination and endocytosis, since it competes for the binding with Hakai, an E3 ubiquitin ligase which ubiquitinates E-cadherin and promotes its internalization [151, 152]. By binding to PLEKHA7 through its N-terminal region, p120ctn promotes the association of E-cadherin with microtubules and its stabilization, since this linkage allow the ZA localization of USP47, the deubiquitinase that counteracts the action of Hakai [5, 109].

p120ctn is involved in cell motility and cancer cell invasiveness through its ability to influence the assembly and contractility of the actin cytoskeleton, by regulating the activities of Rho GTPases. Specifically, p120ctn can inhibit RhoA activation, either by acting as a GDP dissociation inhibitor (GDI) and directly binding to RhoA, or by interacting with p190RhoGAP, to decrease RhoA activity at site of cell-cell contact [153, 154]. By regulating RhoA activity

p120ctn controls epithelial cell shape maturation and lumenogenesis [155]. Epithelial cells depleted of p120ctn show altered morphogenesis, with disrupted apical surface and altered lumen formation [155]. Similarly to β-catenin, p120ctn can also localize in the nucleus [156]. Either p120ctn phosphorylation or E-cadherin depletion can trigger the translocation of p120ctn from AJ to the nucleus, where it binds to the transcriptional repressor Kaiso. p120ctn binding to the transcriptional repressor Kaiso promotes the dissociation of Kaiso from DNA, activating the transcription of genes such as cyclin D1 and matrilysin, which are also activated by the β-catenin/Tcf pathway [156]. p120ctn seems to have a dual role in human cancers, on one side it acts as tumor suppressor by stabilizing E-cadherin, on the other side recent findings highlight the presence of a p120ctn tumor promoting basolateral complex, where Src-phosphorylated p120ctn is associated with proteins involved in cell cycle, signaling and tumor progression like cyclin D1, MYC and SNAIL [8]. This tumor promoting basolateral complex was proposed to act in antagonsim to the apical complex, where p120ctn is associated with PLEKHA7. The apical complex recruits components of the micro-RNA processing complex to the ZA, and promotes the maturation of miRNAs targeting the basolateral tumor promoting proteins [8, 157].

The fundamental importance of p120ctn in vertebrates is confirmed by the strong phenotypes of p120ctn KO mice. The global KO of p120ctn is embryonic lethal, and the conditional KO of p120ctn in various tissues cause defects in morphology, function and differentiation of epithelial tissues, due to defects in adhesion, increased inflammation and proliferation [158-160].

Afadin

Afadin is a Mr 205 kDa protein that has been immunolocalized at both AJ and TJ [59, 86]. At the structural level its N-terminal region contains two Ras-associated domains (RA), a fork head-associated domain (FHA), a dilute domain (DIL) followed by a PDZ and two proline-rich domains. The C-terminal tail of the long isoform of afadin (l-afadin) contains a F-actin binding region, which is missing in the shorter splicing variant of afadin (s-afadin) [86]. L-afadin is ubiquitously expressed, whereas s-afadin is specifically expressed in neurons [86]. Afadin is a target of Ras, and through its RA domain it binds the small G protein Rap1 [118]. Through the same domain afadin interacts with ZO-1 at TJ, and this association is inhibited by activated Ras, whose activity perturb cell-cell contacts [59]. Afadin also forms a complex with cingulin [58, 59], and has multiple additional partners, that associate to its PDZ domain. For example afadin forms complexes with nectins, c-Src and JAM at AJ [47, 123, 161] (Fig. 6). The F-actin binding region of afadin allows to connect nectins to the actin cytoskeleton, and afadin interaction with profilin might modulate actin modeling at the AJ [162]. In addition, afadin connects the nectin complex to the E-cadherin complex through multiple interactions. For example, afadin can bind α-catenin either directly, or indirectly through ponsin (which interacts with vinculin), or through ADIP and LMO7 (which interact with the α-catenin partner α-actinin) [98, 118, 130, 132, 163] (Fig. 6). Finally, afadin interacts with PLEKHA7 through two regions, one comprising the RA domains, and one comprising the PDZ domain, thus recruiting PLEKHA7 to nectin-based AJ [7]. Afadin plays key roles in the junctional organization and

establishment of apico-basal polarity. Depletion of afadin in cultured cells inhibits cadherin-based AJ formation and also TJ formation [133, 134, 164]. Afadin KO in mice leads to embryonic lethality due to failure in gastrulation, with disorganized mesoderm and impaired migration of mesoderm. TJ and AJ are improperly organized with loss of polarization in the ectoderm of afadin-KO mice and embryoid bodies, reflecting afadin importance in the formation of cell-cell junctions, development of cell polarity and differentiation [165, 166].

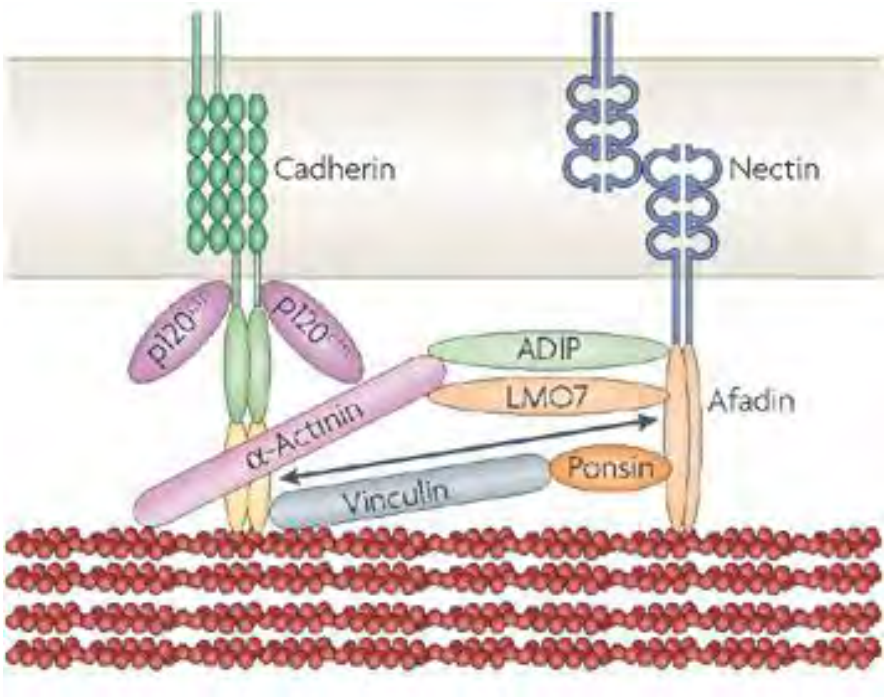

Figure 6. Scematic representation of afadin interactors at AJ.
The organization of AJ and afadin direct and indirect interactors at nectin and E-cadherin complexes are represented. Arrow indicates direct interaction between afadin and α-catenin (in yellow) (adapted from [2]).

PLEKHA7

Pleckstrin Homology domain-containing family A member 7 (PLEKHA7) is a recently identified protein of the *zonula adhaerens*, which

interacts with the AJ cytoplasmic proteins p120ctn, nezha, paracingulin and afadin. PLEKHA7 was independently identified by mass spectrometry as an interactor of the N-terminal domain of p120ctn [5], and by yeast two-hybrid screening as an interactor of paracingulin [6, 81]. Unlike other AJ proteins and similarly to afadin, PLEKHA7 localizes exclusively to the apical zonular region, being excluded from lateral punctate AJ. PLEKHA7 exists in two isoforms and migrates as Mr 135-145 KDa polypeptides; its mRNA is detected in several tissues, including brain, colon, liver, kidney, placenta, skeletal muscle, spleen, small intestine, lung and heart [6]. However, the functional differences between the two isoforms have not been characterized yet.

The N-terminal region of PLEKHA7 comprises two tryptophan domains (WW), each comprising 33 residues spaced by a region of 11 residues, a pleckstrin homology (PH) domain consisting of 120 residues (Fig. 7), which allows it to bind phospholipids [10], thus providing a possible anchorage to plasma membrane. The C-terminal region of PLEKHA7 comprises two coiled-coil (CC) and two proline-rich (Pro) domains. By binding p120ctn and nezha, PLEKHA7 is part of a protein complex, which links E-cadherin to microtubules minus end, thus stabilizing E-cadherin complex at the *zonula adhaerens*. PLEKHA7 as part of this complex is responsible for the accumulation of the kinesin motor KIFC3 to AJ, which brings at junction the deubiquitinase USP47, counteracting the effects of the E3-ubiquitin ligase Hakai that promotes E-cadherin internalization. In fact, epithelial cells depleted of PLEKHA7 show loss of junctional KIFC3 and reduced E-cadherin levels [5, 109]. A region in the N-terminal of PLEKHA7 (aa 120–374), comprising the PH domain, is responsible for the binding to afadin [7] (Fig. 7). PLEKHA7 is

independently recruited at AJ by p120ctn at E-cadherin based AJ, whereas through the interaction with afadin is recruited at nectin based AJ, both interactions are important for the stabilization of the *zonula adhaerens* [5, 7]. A region comprising the first proline-rich domain (aa 538-696) is responsible for binding to p120ctn, whereas nezha and paracingulin interact with overlapping regions of PLEKHA7, comprising the first coiled-coil domain (aa 680-821 and aa 620-769 respectively) [5, 81] (Fig. 7). Through this interaction PLEKHA7 is responsible for the recruitment of paracingulin at AJ.

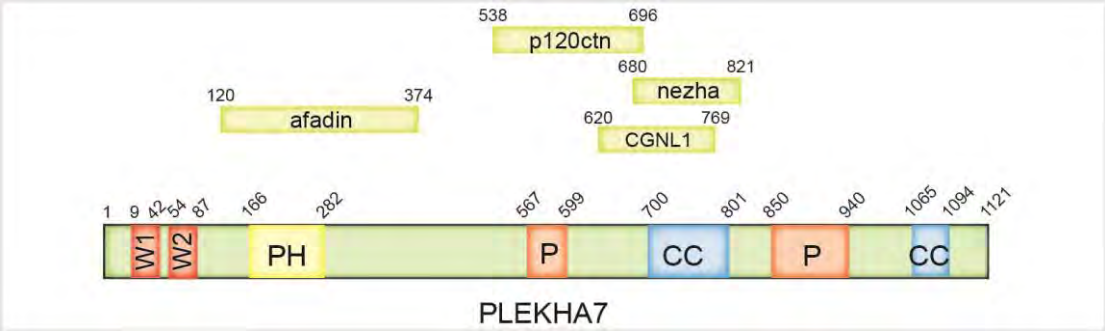

Figure 7. Schematic representation of PLEKHA7 protein organization.
Highlighted PLEKHA7 conserved domains and residues: two WW Trp-Trp domain; PH plekstrin homology domain; two P prolin-rich domains; two CC coiled-coil domains. PLEKHA7 residues of interaction with its molecular partners are also shown.

Recent studies show a role for PLEKHA7 in the maturation of specific miRNAs through the recruitment of components of the miRNA processing machinery, DROSHA and DGCR8, at the ZA [8]. Thus, PLEKHA7 is responsible for the local maturation of specific miRNA, which suppress the expression of growth promoting proteins, such as SNAIL, MYC and cyclin D1 [8]. In this model, PLEKHA7 defines an apical, tumor-suppressing p120ctn complex, which antagonizes the effects of the basolateral tumor-promoting p120ctn complex, characterized by src-phosphorylated p120ctn associated with proteins involved in cell cycle progression and cancer. Accordingly,

epithelial colon cancer (Caco2) cells depleted of PLEKHA7 show increased anchorage independent growth and the expression of mesenchymal and transformation markers [8]. Indeed, several human tumors, including breast and renal carcinoma, display a mislocalized, reduced or lost expression of PLEKHA7 [157, 167].

Genome-wide analyses have identified SNPs in PLEKHA7 associated with either high systolic blood pressure or primary angle closure glaucoma [9, 11]. Genetic studies in vivo showed the implication of Hadp1, the PLEKHA7 homolog in zebrafish, in cardiac development and contractility, pointing to a role in the regulation of intracellular calcium response in cardiomyocytes [10]. Furthermore, genome-wide data were confirmed in vivo by analysis of a PLEKHA7-KO rat model, where the absence of PLEKHA7 reduced the blood pressure and attenuated the salt induced hypertension. Aortic endothelial cells from PLEKHA7-KO rats showed increased intracellular calcium levels and synthesis of nitric oxide [168].

REGULATION OF JUNCTION FORMATION AND STABILITY

The organization, assembly and stabilization of the junctional complex is a spatially and temporally fine-tuned process which requires the actomyosin and microtubule cytoskeletons, and regulated by Rho family GTPases. The actomyosin cytoskeleton regulates the distribution, clustering and stability of junctional proteins. The contractility of the apical actomyosin ring is fundamental in the regulation of junction integrity, barrier function, and changes in morphogenesis during development. Both AJ and TJ are

physically and functionally associated with the actin cytoskeleton through different molecular partners. Studies with constitutively active and dominant negative Rho GTPases show inhibited or altered junction assembly in both cases, revealing the importance in the cycling from active to inactive state for their proper regulation of junction assembly [169-171]. Correct junction assembly is achieved through a finely tuned balance of the activities of RhoA, Rac1 and Cdc42, resulting from the coordinated interplay between these Rho GTPases, their regulators GEFs and GAPs and the junctional proteins. Rac1 and Cdc42 play a fundamental role in the initial steps of junction assembly. Following initial cell-cell adhesion, the accumulation of nectin and cadherin adhesion molecules, is promoted by and stimulates Rac1 activity, to drive actin polymerization and further accumulation of adhesion and other junctional proteins. Rac1 promote the activation of the Arp2/3 complex, driving the polymerization of actin filaments [172, 173]. Furthermore, Cdc42 is required for the formation of the Par3-Par6-aPKC polarity complex, and it phosphorylates and activates , which initiates the establishment of apico-basal polarity, driving the segregation of junctional proteins and the formation of mature AJ and TJ [64]. During the initial steps, the junctional surface is expanded and nascent junctions are stabilized. This requires inactivation of RhoA at sites of cell-substrate interaction, and activation at junctions. RhoA is important in the establishment and maintenance of junctions, through the activation of its effectors ROCK and Dia, which promote actin filaments polymerization, bundling and contractility, keeping the tension necessary to strengthen apical junctions, and promoting TJ barrier formation [174]. A balance in the activity of RhoA versus Rac1 is needed, since excessive RhoA

activation can lead to junction disruption and disassembly [175]. These dynamic processes must therefore be spatially and temporally regulated by the Rho GTPases regulators guanine nucleotide exchange factors (GEFs) and GTPase activating proteins (GAPs), which, by promoting either the exchange from GDP to GTP, or the hydrolysis of GTP, respectively, can activate or inhibit Rho GTPases. GEFs and GAPs are recruited to junctions by junctional adaptor proteins, which can regulate their spatial and temporal activity. One mechanism of regulation of RhoA activity is through the TJ proteins cingulin and paracingulin [27, 75]. Both of them can bind and inactivate GEF-H1 at junctions, thus preventing activation of RhoA and stress fiber formation in the cytoplasm, and its downstream induction of gene expression and proliferation [27, 75]. In a similar manner, in some types of epithelial cells, cingulin can bind and recruit p114RhoGEF to junctions, in this case locally promoting its action towards RhoA, activating it and promoting junctional tension [77]. It has been shown that also the polarity protein PatJ can bind p114RhoGEF promoting its action at junctional sites [176]. Another TJ protein, ZO-1, can interact with the Rho GEF ARHGEF11, constituting an important interaction for the local activation of RhoA and the efficient apical junction assembly [177]. Furthermore, the E-cadherin-α-catenin complex recruits the Rho GEF ECT2 to AJ, resulting in the local activation of RhoA, and maintenance of junction integrity [178]. But to fine-tune RhoA activity and prevent its excessive activation junctional proteins can recruit also Rho GAPs. For example, p190RhoGAP is recruited to AJ by p120ctn, and can temporally restrict and modulate RhoA activation [154]. Another member of the Rho family GTPases, Rac1, is essential in the early phases of junction assembly

and its activation is mediated by the GEF Tiam1, which is fundamental to drive junction assembly and efficient TJ formation. Tiam1 interacts and is recruited at junctions by paracingulin, since epithelial cells depleted of paracingulin show impaired junctional recruitment of Tiam1 and a delay in junction assembly [27]. The positive action of Tiam1 towards Rac1 is inhibited in confluent cells by the interaction with Par3. The inhibitory effect of Par3 is counteracted, during junction assembly, by β2-syntrophin, which prevents their interaction and establishes a gradient of apico-basal Rac1 activity [179]. The inhibition of Rac1 activity at TJ in confluent cells is also mediated by the GAP Rich-1, which is recruited at that site by its interacting partner AMOT [180]. Moreover, the regulation of Rac1 activity is carried out through the same E-cadherin-α-catenin complex that recruits ECT2, but can also recruit another component of the centralspindlin complex (MgcRacGAP), which can inhibit Rac1 activation [178]. Finally, together with Rac1, Cdc42 is also fundamental in junction assembly and stability. The GEF Tuba interacts at junctions with ZO-1, and its Cdc42-mediated activation is important for junctional stability and maintenance [181]. Furthermore, the confinement of Cdc42 activity is mediated by the GAP SH3BP1, which interacts with paracingulin, and is important for junction formation and actin remodeling in mature junctions [182]. However, since over 100 among GEFs and GAPs have been identified so far, the precise mechanisms of regulation of Rho family GTPases at junctions of different types of epithelia are far from being understood in detail [17, 183].

ZONULAR PROTEINS: THE MOLECULAR LINKAGE BETWEEN AJ AND TJ

AJ and TJ are closely neighbouring structures, and both of them are connected to an apical circumferential (zonular) ring of actin filaments. Several proteins of TJ and AJ have been detected at both types of junction and have been shown to associate with molecular partners present in both types of junctions, suggesting a possible molecular linkage between AJ and TJ. For example, ZO-1 has been detected in the AJ fraction of cardiac muscle and fibroblastic cells, revealing a new localization in addition to the classical TJ localization found in epithelial and endothelial cells. ZO-1 accumulation at AJ is mediated by its direct interaction with α-catenin and actin filaments, showing its involvement also in cadherin-based cell adhesions [184-186].

Paracingulin is another protein, which has been localized either at TJ or AJ, depending on the tissue [79]. The localization of paracingulin at TJ appears to require ZO-1 [81], and paracingulin forma a complex with the related protein cingulin. In specific cell types, the absence of ZO-1 only delays paracingulin accumulation at junctions, and this may be due to the fact that paracingulin can be independently recruited to zonular junctions by PLEKHA7 [81].

Afadin is another junctional protein showing a double localization at AJ and TJ. Similarly to paracingulin, the molecular partners of afadin at TJ are ZO-1 and cingulin [58, 59]. At AJ afadin is part of the nectin complex, and is a fundamental mediator of the interaction between the nectin and the E-cadherin complexes, and the actin cytoskeleton [123, 130].

Unlike other junctional proteins and similarly to afadin, PLEKHA7 is present only at the apical zonular belt, being absent from lateral punctate AJ. It is present in both nectin and E-cadherin complexes, being independently recruited by afadin and p120ctn, respectively [5, 7]. Furthermore, PLEKHA7 interacts with paracingulin, being responsible for its recruitment to AJ [81]. All the mentioned proteins are connected with the circumferential (zonular) actin belt underlying TJ and AJ; with their dual localization and their cross-interactions it is likely that they provide a molecular framework which connects TJ to AJ.

RESEARCH PROJECT

Despite the great advances in the field of the cell biology of intercellular junctions in the last thirty years, with the identification and characterization of most of the molecular components of the junctional complex, understanding the functional organization of the junctional complex is still in progress. New molecular components are still being identified, and further studies are needed to clarify the molecular mechanisms behind the regulation of junction assembly and their involvement in signaling and physiology of epithelial cells.

PLEKHA7 is a recently identified component of the ZA. Its molecular interactors and function at E-cadherin based AJ are well characterized. In contrast,, less is known about its role at nectin based AJ [5-7, 81, 109]. Furthermore, despite an increasing number of studies which implicate PLEKHA7 in tumor growth regulation, hypertension, regulation of cardiac development and contractility, and glaucoma [8-11, 168], the molecular

mechanisms through which PLEKHA7 participates in tissue physiology and pathology remain mainly unknown.

The scope of my thesis project was to identify and characterize novel molecular interactors of PLEKHA7 and elucidate the functional basis of their interaction, to gain new insight in the role of PLEKHA7 in junction biology and in the pathogenesis of human disease.

PAPERS

ORIGINAL ARTICLES:

1. Paschoud et al. PLEKHA7 modulates epithelial tight junction barrier function. Tissue Barriers. 2014 Jan 1;2(1):e28755.
2. Guillemot et al. MgcRacGAP interacts with cingulin and paracingulin to regulate Rac1 activation and development of the tight junction barrier during epithelial junction assembly. Mol Biol Cell. 2014 Jul 1;25(13):1995-2005.
3. Popov et al. The adherens junctions control susceptibility to Staphylococcus aureus α-toxin. Proc Natl Acad Sci U S A. 2015 Nov 17;112(46):14337-42.
4. Guerrera et al. PLEKHA7 recruits PDZD11 to adherens junctions to stabilize nectins. J Biol Chem. 2016 May 20;291(21):11016-29.

REVIEWS:

1. Citi et al. Epithelial junctions and Rho family GTPases: the zonular signalosome. Small GTPases. 2014;5(4):1-15.
2. Shah et al. PLEKHA7: cytoskeletal adaptor protein at center stage in junctional organization and signaling. Int J Biochem Cell Biol. 2016 Jun;75:112-6.

PLEKHA7 modulates epithelial tight junction barrier function

In epithelial and endothelial cells TJ are fundamental for the establishment of the barrier. TJ are part of the apical junctional complex with AJ, with both structures associated with the circumferential actin belt underlying ZA. The establishment of AJ precedes and drives the formation of TJ. It was previously shown that E-cadherin is required for the proper regulation of TJ barrier function. Moreover, studies in which the microtubule cytoskeleton was perturbed revealed a role for microtubules in the regulation of TJ barrier function [187, 188]. PLEKHA7 is a recently identified protein of ZA, part of a complex linking E-cadherin to microtubules, and it is required for stabilization of ZA. In this paper we addressed the role of PLEKHA7 in the regulation of the TJ barrier in epithelial cells, through its stabilizing activity on E-cadherin-microtubules complex. By overexpression experiment of full length and different fragments of PLEKHA7 in MDCK epithelial cell line we show that all the fragments are targeted at junctions and, surprisingly, unlike the endogenous PLEKHA7, they are present also at lateral contact of AJ, suggesting differential affinities for the apical and the lateral complexes. PLEKHA7 fragments, except the central one, increased the accumulation of E-cadherin and of the other components of E-cadherin complex at ZA and lateral AJ. Moreover, the same increase was observed in the apical accumulation of paracingulin but not of other proteins of TJ. The exogenous expression of PLEKHA7 did not affect the development and the steady-state value of transepithelial resistance (TER), but protected from disruption of TJ barrier, attenuating the fall in TER after calcium removal. Treatment with

microtubules destabilizing drugs revealed that these effects are dependent on microtubule cytoskeleton. Finally, we showed that PLEKHA7 can form a complex with the TJ proteins cingulin and ZO-1, providing a link between ZA and TJ, independently of the microtubule cytoskeleton.

I contributed to this publication with the co-immunoprecipitation analysis of PLEKHA7 with junctional proteins (Figure 7).

RESEARCH PAPER

Tissue Barriers 2, e28755; April 2014; © 2014 Landes Bioscience

PLEKHA7 modulates epithelial tight junction barrier function

Serge Paschoud[1,2], Lionel Jond[1,2], Diego Guerrera[1,2], and Sandra Citi[1,2]

[1]Departments of Cell Biology and Molecular Biology; University of Geneva; Geneva; [2]Institute of Genetics and Genomics in Geneva; University of Geneva; Geneva, Switzerland

Keywords: PLEKHA7, microtubules, paracingulin, cingulin, barrier, epithelium

PLEKHA7 is a recently identified protein of the epithelial *zonula adhaerens* (ZA), and is part of a protein complex that stabilizes the ZA, by linking it to microtubules. Since the ZA is important in the assembly and disassembly of tight junctions (TJ), we asked whether PLEKHA7 is involved in modulating epithelial TJ barrier function. We generated clonal MDCK cell lines in which one of four different constructs of PLEKHA7 was inducibly expressed. All constructs were localized at junctions, but constructs lacking the C-terminal region were also distributed diffusely in the cytoplasm. Inducible expression of PLEKHA7 constructs did not affect the expression and localization of TJ proteins, the steady-state value of transepithelial resistance (TER), the development of TER during the calcium switch, and the flux of large molecules across confluent monolayers. In contrast, expression of three out of four constructs resulted both in enhanced recruitment of E-cadherin and associated proteins at the apical ZA and at lateral *puncta adherentia* (PA), a decreased TER at 18 h after assembly at normal calcium, and an attenuation in the fall in TER after extracellular calcium removal. This latter effect was inhibited when cells were treated with nocodazole. Immunoprecipitation analysis showed that PLEKHA7 forms a complex with the cytoplasmic TJ proteins ZO-1 and cingulin, and this association does not depend on the integrity of microtubules. These results suggest that PLEKHA7 modulates the dynamics of assembly and disassembly of the TJ barrier, through E-cadherin protein complex- and microtubule-dependent mechanisms.

Introduction

Zonulae occludentes (also called Tight Junctions: TJ) of vertebrate polarized epithelial and endothelial cells are crucial for the establishment and maintenance of barriers between body compartments.[1] TJ are topologically associated with *zonulae adhaerentes* (ZA) in the "apical junctional complex" (AJC) at the apicolateral border of polarized cells.[2] TJ and ZA are formed by specific transmembrane proteins (claudins, occludin/tricellulin, JAM-A for TJ, E-cadherin and nectins for ZA) that are linked intracellularly to cytoplasmic adaptor proteins, for example ZO-1, ZO-2, cingulin and polarity complex proteins at TJ, and β-catenin, p120-catenin, α-catenin, and afadin at ZA.[3-5] In addition, specific cytoplasmic adaptor proteins of TJ and ZA are directly or indirectly linked to the actomyosin cytoskeleton, which forms a circumferential contractile belt underlying the ZA.[6-8]

Several lines of evidence show that the assembly and integrity of the ZA is essential for the establishment and maintenance of TJ. Antibodies against the extracellular domain of E-cadherin inhibit the assembly of TJ,[9] and studies both on cultured cells and in vivo confirm the crucial role of E-cadherin in the regulation of TJ barrier function.[10,11] Modulation of the concentration of extracellular calcium, which controls cadherin-dependent adhesion, results in the modulation of the TJ barrier function, as determined by the measurement of the transepithelial electrical resistance (TER) of cultured cell monolayers in either "calcium switch" or calcium depletion assays.[12-14] The circumferential actomyosin belt associated with the ZA is critically important in the physiological and pathological regulation of TJ barrier function,[15-19] and disruption of E-cadherin-dependent adhesion affects the integrity of the TJ barrier through phosphorylation signals that control the contractility of the actomyosin cytoskeleton.[20]

Recent studies have demonstrated that the E-cadherin complex is linked to the microtubule cytoskeleton, through a protein complex containing p120ctn, PLEKHA7, paracingulin (CGNL1) and nezha (CAMSAP3).[21-23] Moreover, studies with drugs that inhibit microtubule polymerization show that the integrity of microtubules is required to maintain TJ barrier function in different types of epithelial and endothelial cells.[24-26] Microtubules have also been implicated in the perturbation of the TJ barrier by enteric pathogens.[27] These observations raise a key question: does the protein complex that connects E-cadherin to microtubules regulate the TJ barrier?

PLEKHA7 links the microtubule cytoskeleton to the ZA, by binding to p120ctn and nezha.[21-23] Unlike most other ZA proteins, including E-cadherin, p120ctn, α-catenin, and β-catenin, PLEKHA7 is not localized along the lateral

Correspondence to: Sandra Citi, E-mail: sandra.citi@unige.ch
Submitted: 03/17/14; Accepted: 03/21/14; Published Online: 04/02/14
Citation: Paschoud S, Jond L, Guerrera D, Citi S. PLEKHA7 modulates epithelial tight junction barrier function. Tissue Barriers 2014; 2:e28755; http://dx.doi.org/10.4161/tisb.28755

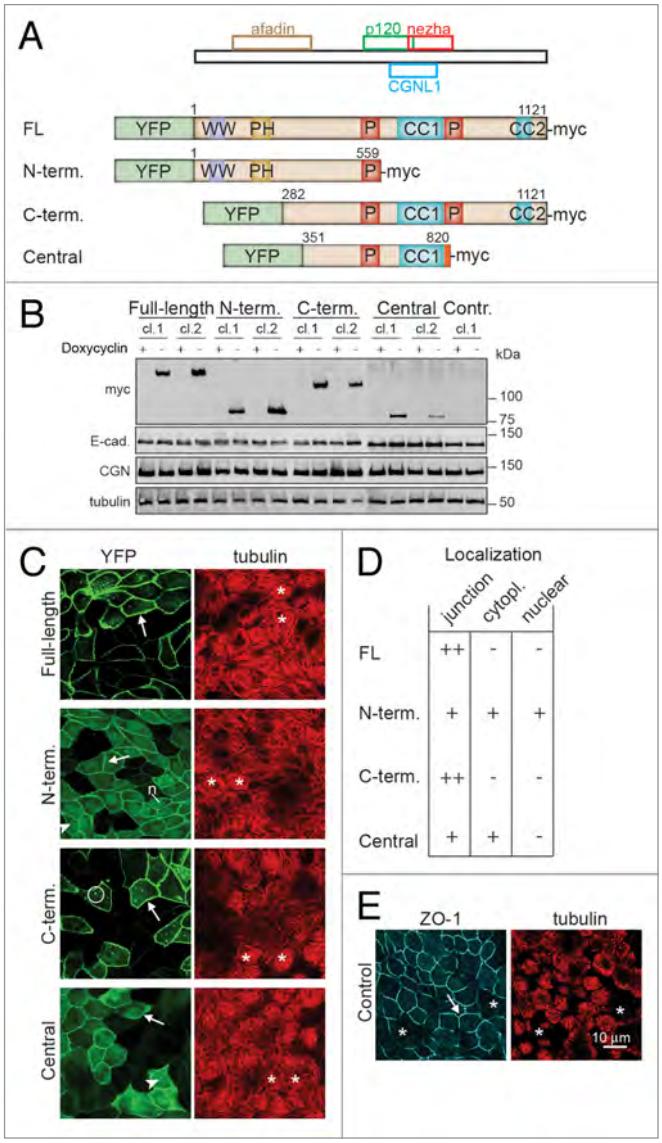

Figure 1. Generation of stable MDCK tet-off cell clones with inducible expression of PLEKHA7 constructs. (**A**) Schematic diagrams showing the putative minimal regions of PLEKHA7 which can interact with afadin (residues 120–374 in human PLEKHA7), p120ctn (538–696), CGNL1 (620–769), or nezha (680–821),[21,23,29] and schematic structure of the PLEKHA7 constructs (Full-length FL, N-terminal = N-term., C-terminal = C-term., Central) used to generate stable clones of MDCK tet-off cells. Constructs were tagged N-terminally with YFP, and C-terminally with myc. Putative structural domains are indicated: WW (purple), PH (brown), Pro-rich (P, red), and coiled-coil (CC, blue, CC1 = residues 686–835, and CC2 = residues 1055–1095, based on Phyre2 analysis). Numbers indicate position of PLEKHA7 amino acid residues within constructs. (**B**) Immunoblotting analysis of lysates of MDCK cell lines (two clones for each construct shown) cultured either in the presence (+) or in the absence (-) of doxycycline, using antibodies against the myc tag (to detect exogenous PLEKHA7), E-cadherin (E-cad.), cingulin (CGN) and tubulin (loading control). Numbers on the right indicate the migration of pre-stained markers (kDa). (**C**) Confocal immunofluorescent analysis of induced cultures of stable clones showing the localization of exogenous PLEKHA7 constructs (green, YFP) and α-tubulin (red), on the apical plane of focus (ZO-1 labeling is shown for control cells, panel E). Arrows = junctional labeling; arrowheads = cytoplasmic labeling; circle = cytoplasmic dots; n = nuclear labeling. (**D**) Table summarizing the subcellular localization of each YFP-tagged construct, based on immunofluorescence on paraformaldehyde-fixed cells. (**E**) Immunofluorescent labeling of control Tet-off cells showing tubulin and ZO-1 in the apical plane of focus. Bar = 10 µm.

membranes of polarized epithelial cells, but only at the apical circumferential ZA.[22] Depletion of the PLEKHA7 complex in Caco2 cells perturbs the organization of the ZA,[21] suggesting that it may indirectly affect the stability of the neighboring TJ. However, the role of PLEKHA7 in regulating TJ barrier function has not yet been investigated. PLEKHA7 is expressed in organs, such as kidney and intestine, where modulation of epithelial barrier function is critical for physiology.[22] Moreover, its involvement in the pathogenesis of glaucoma may depend on a hypothetical role in controlling the TJ barrier.[28] For these reasons, it is important to examine whether PLEKHA7 is implicated in the modulation of the TJ barrier. In the present paper we address this question, by studying the effects of exogenous expression of different PLEKHA7 constructs on the molecular organization and paracellular permeability of TJ of MDCK cells. Our results provide evidence that PLEKHA7 contributes to modulating the dynamic assembly and disassembly of the TJ barrier in a microtubule-dependent manner, through the junctional enrichment of E-cadherin complex proteins.

Results

PLEKHA7 constructs containing either N-terminal or central domains are targeted to junctions

We reasoned that if PLEKHA7 contributes to ZA stability, and ZA integrity affects TJ barrier function, exogenous expression of PLEKHA7 in cultured epithelial cells might influence the paracellular permeability barrier, in experimental models of junction assembly/disassembly induced either by calcium switch or calcium depletion, respectively. To test this hypothesis, we generated stable clones of MDCK-tet-off cells, where expression of exogenous human PLEKHA7 constructs was induced by removal of doxycycline (Dox) from the culture medium (**Fig. 1**).

To design the constructs, we took into account the putative regions of PLEKHA7 which have been implicated in the interaction with different protein partners, namely afadin, p120ctn, CGNL1 and nezha (CAMSAP3) (**Fig. 1A**).[21,23,29] The Full-length (FL) construct contained all the putative interactor binding sites, the « N-terminal » (N-term.) construct contained the afadin-binding, and part of the p120ctn-interacting sequences. The C-terminal (C-term.) construct contained part of the afadin-binding sequence, and the sequences involved in the interaction with p120ctn, CGNL1 and nezha. The « Central » construct lacked both the afadin-binding region, and additional sequences downstream of the first coiled-coil region, but it comprised the p120ctn, CGNL1, and part of the nezha-binding domains. (**Fig. 1A**). Constructs were tagged N-terminally with

YFP, to directly visualize their expression in induced cells (**Fig. 1A**).

Immunoblotting analysis showed that the exogenous proteins were expressed at very low or undetectable levels in the presence of Dox, and were strongly upregulated following Dox removal (**Fig. 1B**). Expression of exogenous PLEKHA7 constructs did not result in detectable changes in the levels of expression of ZA and TJ proteins, including E-cadherin, cingulin (**Fig. 1B**), α-catenin, β-catenin, p120ctn, paracingulin, and ZO-1 (data not shown). Immunofluorescence analysis confirmed that fluorescent exogenous protein was very low or undetectable in cells grown in the presence of Dox (**Fig. 2**, and data not shown).

Next, we examined the localization of the exogenous constructs by immunofluorescence. All constructs were targeted to cell-cell junctions (arrows in **Fig. 1C**, and **Fig. 1D**), indicating that they all contained sequences that are sufficient for the junctional recruitment of PLEKHA7. The Full-length and C-terminal constructs showed a selective accumulation at junctions, and little or no cytoplasmic labeling (**Fig. 1 C-D**). In contrast, the N-terminal and Central constructs showed not only an accumulation at junctions, but also a finely diffuse cytoplasmic labeling (arrowheads in **Fig. 1C** and **Fig. 1D**, see also **Figs. S1–S3**). In the case of the N-terminal construct, labeling was also detected in the nuclei (« n » in **Fig. 1C**, **Fig. 1D**, see also **Figs. S1–S3**). Cytoplasmic dots were often detected in cells expressing low/medium amounts of exogenous proteins, and additional granular cytoplasmic labeling was detected in cells expressing high levels of exogenous proteins (circles in **Fig. S1**, see also **Fig. S2, S3**), suggesting that exogenous PLEKHA7 proteins may ectopically associate with centrosomes, primary cilia, and the minus ends of cytoplasmic microtubules.

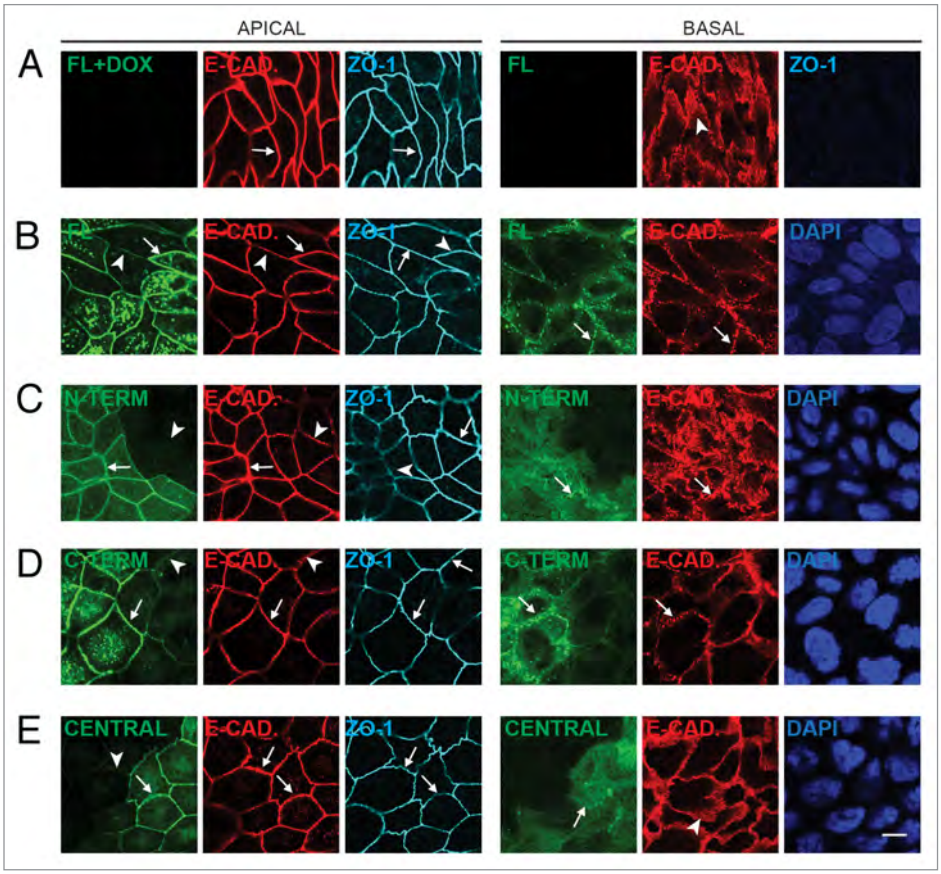

Figure 2. Exogenous expression of full-length, N-terminal, C-terminal, but not Central PLEKHA7 constructs enhances ZA recruitment and PA clustering of E-cadherin. Confocal immunofluorescence analysis of clonal lines of MDCK cells showing labeling for exogenous constructs (green) and E-cadherin, either in the apical plane of focus (ZO-1, gray, left panels), which contains ZA (*zonula adhaerens*), or in the basal plane (nuclei, blue DAPI, right panels), which contains PA (*puncta adhaerentia*). (**A**) Full-length, uninduced (FL+DOX); (**B**) Full-length, induced (FL); (**C**) N-terminal, induced (N-TERM); (**D**) C-terminal, induced (C-TERM; (**E**) Central, induced. Matched arrows indicate matched normal junctional labeling (using ZO-1 as a reference fore the apical plane), and matched arrowheads indicate matched decreased junctional labeling (B, C, D, apical plane) or diffuse lateral labeling (A and E, basal). Within each panel, arrows indicate stronger labeling than arrowheads. The basal plane was typically 10–15 μm below the apical plane. Bar = 10 μm.

Since PLEKHA7 is part of a complex that is associated with microtubules, we asked whether the organization of microtubules is affected by exogenous expression of PLEKHA7 constructs. Tubulin staining in confluent MDCK monolayers was concentrated in the apical plane of focus, containing the TJ marker ZO-1 (arrow in **Fig. 1E**), whereas it was much weaker in the sub-apical and basal planes, below ZO-1 (asterisks in **Fig. 1E**, see also **Fig. S3**). In cells expressing exogenous PLEKHA7 constructs, we selected regions of the monolayer where neighboring cells expressed different levels of exogenous protein, to directly compare tubulin staining. No difference was observed in the distribution of microtubule labeling between cells expressing either low or high amounts of exogenous PLEKHA7 constructs, either under normal conditions (matched asterisks in **Fig. 1C**) or after treatment with nocodazole (**Fig. S3**). This indicated that PLEKHA7 exogenous proteins did not induce a detectable reorganization of the microtubule cytoskeleton, nor did they induce an accumulation of ectopic microtubules along cell-cell junctions.

Exogenous expression of full-length, N-terminal and C-terminal, but not central PLEKHA7 constructs enhances the zonular accumulation and lateral clustering of E-cadherin complex proteins

We next examined whether expression of exogenous constructs of PLEKHA7 modified the distribution of proteins

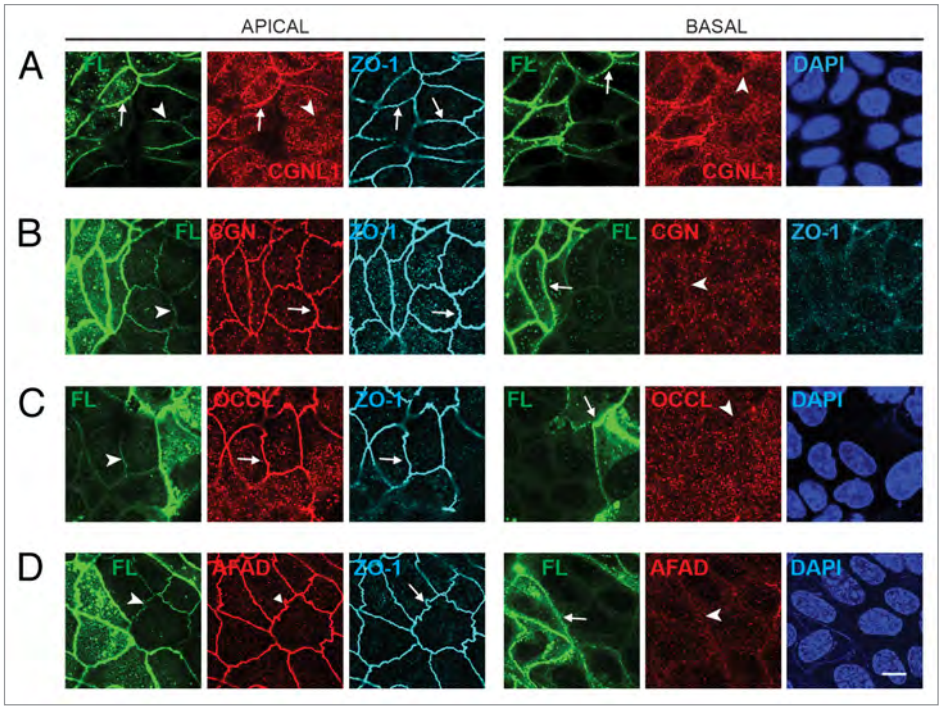

Figure 3. Exogenous expression of full-length PLEKHA7 enhances the ZA recruitment of paracingulin, but not cingulin, ZO-1, occludin and afadin. Confocal immunofluorescence analysis of MDCK cells expressing the Full-length construct cells with labeling for exogenous protein (green) and either paracingulin (CGNL1, (**A**)), cingulin (CGN, (**B**)) occludin (OCCL, (**D**)), or afadin (AFAD), (**E**)) in red. ZO-1 labeling in triple-stained cells is shown in gray in apical, left panels, and in basal plane (**B**). See legend to **Figure 1** for arrow/arrowheads description. Bar = 10 μm.

of the cadherin complex, which includes E-cadherin, p120-ctn, and β-catenin. All of these proteins are localized in polarized epithelial cells at two distinct localizations: at the apical circumferential belt (*zonula adhaerens*, ZA), where endogenous PLEKHA7 is also detected, and at the lateral *puncta adhaerentia* (PA), where PLEKHA7 is not detected.[22] We examined regions of the monolayer where neighboring cells expressed different levels of exogenous protein, to ask whether increased exogenous (PLEKHA7) protein correlated with increased labeling for either E-cadherin, p120ctn, and β-catenin. Images were taken both at the apical, zonular ZA plane, using ZO-1 as a marker (**Fig. 2**, apical), and at a more basal plane which did not contain ZO-1, but contained prominent nuclear labeling (**Fig. 2**, basal). In confluent cultures grown in the presence of Dox, which inhibits transgene expression, no labeling either for the full-length construct (**Fig. 2A**), or for any of other exogenous constructs (data not shown) was detectable in either plane of focus. E-cadherin labeling in the apical plane was distributed along along circumferential ZA, similar to ZO-1 (arrows in **Fig. 2A**). In a more basal plane of focus, E-cadherin was distributed diffusely and along discontinuous spots throughout the lateral membrane, corresponding to PA (arrowhead in **Fig. 2A**, basal). Upon induction of expression, labeling for the exogenous proteins was detected not only at cell-cell junctions in the ZA plane of focus, but also at cell-cell contact areas in the basal planes of focus, throughout the lateral membrane (**Fig. 2, Fig. 3**, basal). This indicated that although PLEKHA7 is localized in normal tissues in situ exclusively at the ZA,[22] when exogenously expressed it can also be recruited to lateral PA. Close examination of E-cadherin labeling in the apical plane of focus, using ZO-1 as a marker, clearly showed increased zonular E-cadherin labeling in cells expressing higher levels of exogenous Full-length, N-terminal, and C-terminal constructs (compare arrows/stronger labeling with arrowheads/weaker labeling in **Fig. 2B-D**, apical). In contrast, no increase of E-cadherin labeling at the ZA was observed in cells expressing the Central construct (**Fig. 2E**, apical). Furthermore, in the basal plane of focus of expressing cells, E-cadherin was no longer distributed diffusely in PA along the lateral membrane, but was accumulated in fewer, more brighly labeled spots, which precisely co-localized with exogenous PLEKHA7 (matching arrows in **Fig. 2B-D**, basal, see **Fig. S1E** for a scheme). Again, this lateral clustering effect was observed with the Full-length, N-terminal, and C-terminal constructs (**Fig. 2B-D**), but not with the Central construct, where cells showed diffuse lateral E-cadherin labeling, similarly to cells grown in the presence of Dox (arrowhead in **Fig. 2E**, basal). Essentially identical observations were made when examining the localization of additional protein components of the E-cadherin complex, namely p120-ctn, α-catenin, and β-catenin: in cells expressing Full-length, N-terminal, and C-terminal, but not Central PLEKHA7 constructs, zonular labeling of the ZA protein was increased, and the more basal, lateral PA labeling was clustered, and co-localized with clustered exogenous PLEKHA7 (**Fig. S1A-D** and data not shown).

In summary, these observations showed that exogenous expression of all PLEKHA7 constructs, except for the Central construct, results in enhanced ZA recruitment of E-cadherin-complex proteins, and their clustering along the lateral cell-cell contact regions (**Fig. S1E**).

Exogenous expression of PLEKHA7 constructs does not affect the localization of zonular membrane and cytoplasmic components of the apical junctional complex, with the exception of paracingulin

The ZA, together with the TJ, forms the « apical junctional complex » (AJC), which is characterized by proteins whose distribution is exclusively «zonular », e.g., in a continuous circumferential belt. These include 1) specific TJ and membrane proteins, such as cingulin, occludin and ZO-1; 2) paracingulin, which is localized both at TJ and ZA, and 3) afadin and

PLEKHA7, which, unlike most proteins of the E-cadherin complex, are localized at the ZA, but not at lateral PA.[22,23] So, we asked whether expression of exogenous PLEKHA7 constructs influenced the junctional recruitment and subcellular localization of zonular AJC proteins.

We found that paracingulin labeling in the apical plane of focus was increased in cells expressing higher levels of exogenous Full-length, N-terminal, and C-terminal, but not Central constructs (**Fig. 3A**, apical, and **Fig. S2**). Unlike E-cadherin complex proteins, we did not observe a significant increase of lateral paracingulin labeling in cells expressing the Full-length, N-terminal, and C-terminal constructs, indicating that PLEKHA7 does not induce the ectopic lateral recruitment of CGNL1 (**Fig. 3A**, basal, and **Fig. S2**). In contrast to CGNL1, the zonular labeling for cingulin, ZO-1, occludin, and afadin was not affected by exogenous expression of PLEKHA7 constructs, and no labeling was detected at junctions in more basal planes of focus, where exogenous PLEKHA7 constructs were still detected (**Fig. 3B-D**, and **Fig. S2**).

Exogenous expression of PLEKHA7 does not affect either the establishment of the TJ paracellular permeability barrier to ions during the calcium switch, or the barrier to large solutes

The observation that exogenous expression of specific PLEKHA7 constructs promotes the accumulation of E-cadherin complex proteins at the ZA raises the possibility that E-cadherin-dependent modulation of TJ barrier function may be affected in these cells. To test this hypothesis, we first measured the development of the transepithelial electrical resistance (TER) of the different clonal lines in the « calcium switch » assay, where junction re-assembly is rapidly induced by adding calcium to cultures incubated for 16–18 h in the absence of extracellular calcium. In this assay, the TER profile of MDCK cells shows a characteristic peak between 4 and 8 h after the switch.[30,31] Clonal lines were assayed either in the presence (uninduced) or absence (induced) of Dox. All clonal lines showed a peak of TER between 4 and 8 h, with a resistance value between 200–400 ohm.cm^2. We observed no significant difference when comparing the profiles of each pair of cultures, either in the presence or the absence of Dox (**Fig. 4**). Immunofluorescent analysis of the localization of ZA and TJ proteins at different times during the calcium switch confirmed that there was no detectable difference in the dynamics of junction assembly, whether the exogenous PLEKHA proteins were expressed or not (data not shown).

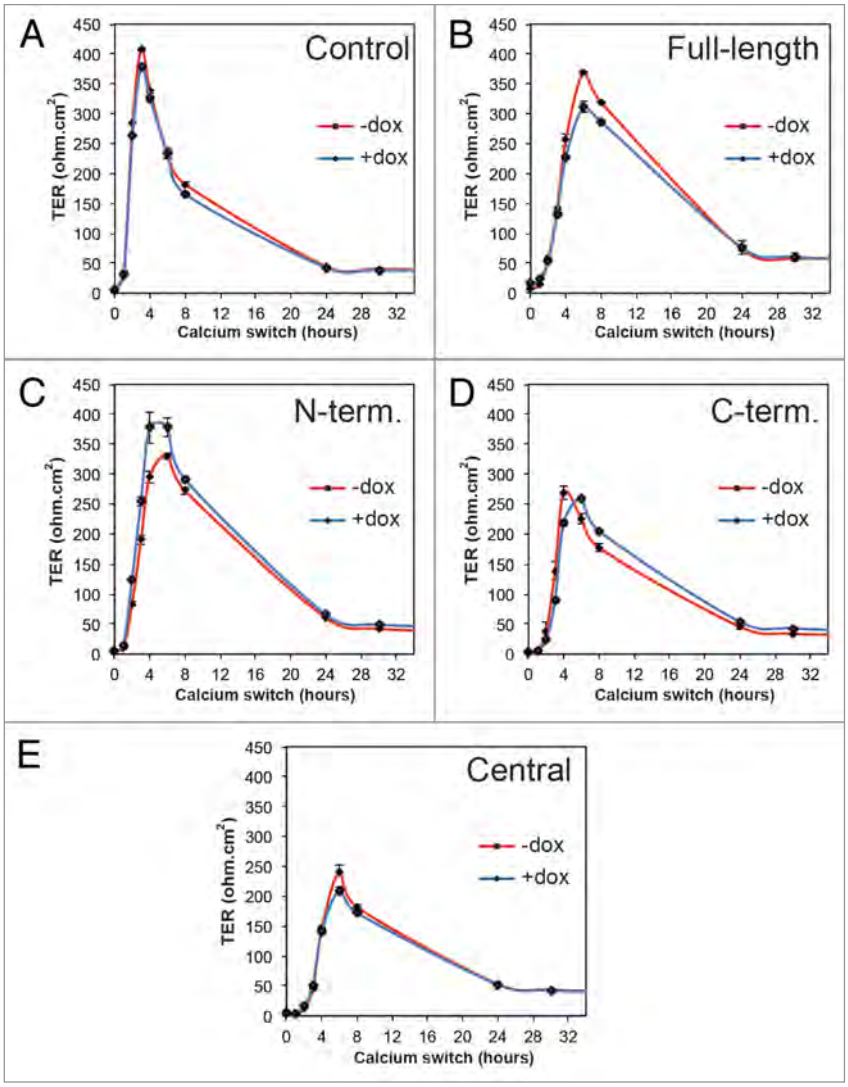

Figure 4. Expression of exogenous PLEKHA7 constructs does not affect TER development during the calcium switch in MDCK cells. Transepithelial electrical resistance (TER, ohm.cm^2) profiles of representative clonal lines of MDCK cells expressing YFP (Control) or YFP-tagged constructs of PLEKHA7 (see legends), either in the absence (red) or presence (blue) of doxycycline, during the calcium switch.

Next, we asked whether the barrier to large solutes is affected in cells expressing exogenous PLEKHA7 constructs, by measuring the flux of fluorescently labeled dextran. In normal calcium medium all clones showed a very low permeability to dextran, which was similar to that of control cells, and was not dependent, for each clone, on whether the exogenous protein was repressed or induced (plus or minus Dox) (**Fig. 5**). One hour after calcium removal, the flux was increased 10-fold to 30-fold, depending on the clone, and independently of the presence of Dox (**Fig. 5**).

Taken together, these observations show that inducible expression of exogenous constructs of PLEKHA7 does not significantly affect either the establishment of the TJ barrier to ions in the calcium switch, or the flux to large molecules in confluent monolayers at steady-state.

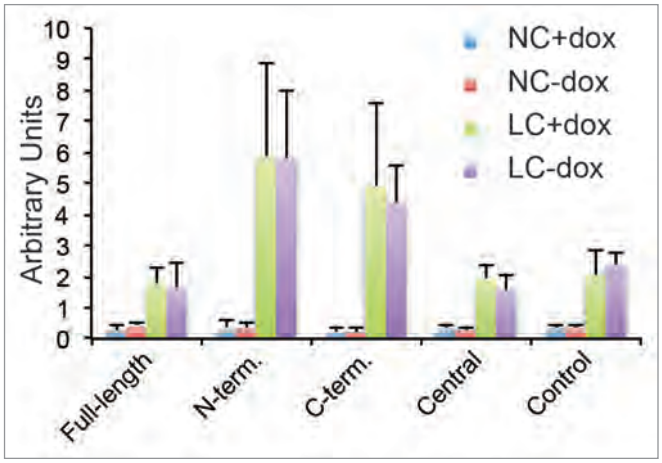

Figure 5. Exogenous expression of PLEKHA7 constructs does not affect paracellular permeability to large solutes. Histogram showing paracellular permeability to 3 kDa dextran of clonal MDCK lines expressing PLEKHA7 constructs, and control MDCK Tet-off cells, either at normal extracellular calcium concentration (NC, value at 2 h), or after extracellular calcium depletion (LC, value at 30 min after calcium depletion), either in the presence (+DOX, uninduced) or in the absence (-DOX, induced) of doxycycline.

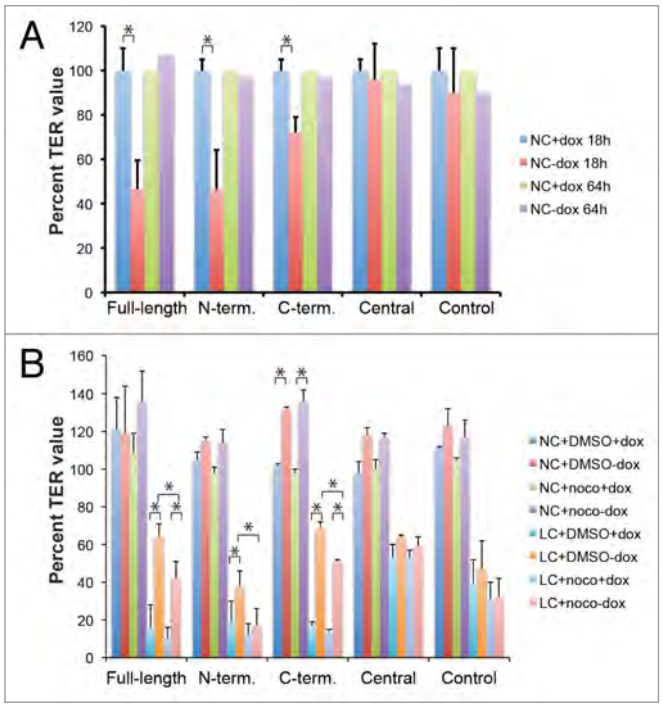

Figure 6. Exogenous expression of Full-length, N-terminal and C-terminal but not Central PLEKHA7 constructs attenuates barrier disruption by extracellular calcium removal, in a microtubule-dependent manner. (**A**) TER values (expressed as % of value of uninduced, +dox cultures) of clonal lines of MDCK cells after trypsinization and incubation of confluent monolayers at normal extracellular calcium for either 18 h (NC + dox 18hr, NC-dox 18hr) or 64 h (NC + dox 64hr, NC-dox 64hr). The values at 64 h were the average of two experiments. (**B**) TER values (expressed as % of value after overnight incubation in NC) of clonal lines of MDCK cells under different conditions: normal calcium (NC) or 30 min low calcium treatment (LC), uninduced or induced (+dox, -dox), treated or untreated with nocodazole (DMSO, noco). For cultures maintained at normal calcium, the TER values were expressed as % of the value before treatment with either DMSO or nocodazole. For cultures undergoing calcium depletion (only the 30 min time point is shown), the TER values were expressed as % of value at time 0, after treatment with either DMSO or nocodazole, and just prior to calcium removal. * = $P < 0.05$.

Exogenous expression of specific PLEKHA7 constructs affects the dynamics of TJ barrier establishment at normal calcium, and protects from disruption of the TJ barrier by extracellular calcium removal in a microtubule-dependent manner

When junctions are assembled during the calcium switch, assembly is rapid, because it occurs from a pool of pre-synthesized junctional proteins, which become stabilized at the cell membrane with fast kinetics, following calcium readdition. However, junction assembly can also be obtained following trypsinization of monolayers and assembly at normal calcium (NC). This assembly is slower, since it requires the synthesis and junctional delivery of protein components of junctions. To study the effect of exogenous expression of PLEKHA7 constructs on junction assembly at NC, clonal cell lines grown either in the presence, or in the absence of Dox were trypsinized, and seeded into transwells at confluent density in NC medium, and the TER was measured 18 h later. The TER value of clones expressing the full-length, N-terminal, and C-terminal constructs, but not the Central construct, was significantly lower than the values of uninduced cells (**Fig. 6A**), suggesting that expression of these exogenous proteins perturbs the development of the TJ barrier at normal calcium. When the TER was measured at steady-state, e.g., 48 h or later after the beginning of junction assembly at normal calcium, all clones showed a similar TER, and within each clone there was no difference between the uninduced and induced cells (**Fig. 6A**), confirming that exogenous expression of PLEKHA7 contructs does not affect TER at steady-state.

Next, we used the « calcium depletion » assay to examine whether exogenous expression of PLEKHA7 constructs can stabilize cadherin-based complexes, and thus partially protect the TJ barrier from disruption following extracellular calcium removal. Removal of extracellular calcium results in the inhibition of homophylic cadherin-mediated adhesion, and subsequent actomyosin cytoskeleton-mediated opening of the TJ.[14,20] To explore the role of microtubule integrity in this assay, we studied the behavior of monolayers treated either with nocodazole, or with vehicle (DMSO). Following this treatment, cultures were incubated for 30 min either in medium with normal calcium (NC, with either DMSO or nocodazole), or with low calcium medium (LC, with either DMSO or nocodazole), this latter to disassemble junctions. Incubation of uninduced cultures in LC medium and DMSO resulted in a fall in TER, to 10–20% of initial values (**Fig. 6B**, LC+DMSO+dox). However, in induced clones expressing either Full-length, N-terminal, or C-terminal constructs, the TER was significantly higher after calcium removal (**Fig. 6B**, LC+DMSO-dox). When nocodazole was added to the cultures, it did not modify significantly the size of the fall in TER in the presence of Dox (**Fig. 6B**, LC+noco+dox).

However, in the absence of Dox, where the TER was higher due to transgene expression, addition of nocodazole resulted in a significant fall in TER, down to levels similar to those of uninduced cultures, in cells expressing either the Full-length, N-terminal, or C-terminal constructs (**Fig. 6B**, LC+noco-dox). In contrast, lines expressing the Central construct did not display significant changes in the size of the fall in TER, with or without induction, or with or without nocodazole, when compared with Control cells. These results indicate that exogenous expression of PLEKHA7 constructs containing either all the N-terminal or all the C-terminal regions protects epithelial monolayers from TJ barrier disruption following extracellular calcium removal, and this protective effect is dependent upon the integrity of microtubules.

To further understand the cellular basis of the phenotype, we examined by immunofluorescence the effect of nocodazole on the organization of microtubules and the distribution of exogenous PLEKHA7 constructs. Microtubules were abundant in the apical plane of focus and scarce in the basal plane, and we could not detect any major change in their organization when comparing control cells, and cells expressing different levels of exogenous PLEKHA7 proteins (**Fig. S3**, see also **Fig. 1**). Nocodazole treatment resulted in an overall decrease in tubulin labeling, a decrease in the number of microtubules, and the appearance of fewer, more brightly stained microtubules, detectable especially in the apical plane of focus (**Fig. S3**). No significant difference could be observed between control cells, and cells expressing exogenous PLEKHA7 proteins. Treatment with nocodazole did not affect the junctional labeling for the exogenous PLEKHA7 constructs, except for a fragmentation of junctional labeling in the basal plane of focus, which was observed in cells expressing either the N-terminal or the Central constructs (arrow in **Fig. S3**, N-term). In the case of the Full-length and C-terminal constructs, we observed an increase in the number of cytoplasmic « dots » (circles in **Fig. S3**, Full-length), which could occasionally be imaged at microtubule ends (magnified inset in **Fig. S3**, C-term), suggesting that the exogenous proteins may be recruited to the minus ends of the microtubules generated following nocodazole treatment.

PLEKHA7 forms a microtubule-independent complex with TJ proteins

To explore whether PLEKHA7 might modulate TJ barrier function by an interaction with TJ proteins, we asked whether PLEKHA7 forms complexes with TJ proteins. PLEKHA7 is known to interact with paracingulin, which is not exclusively localized at TJ, but also at the ZA.[23] However, complex formation between PLEKHA7 and TJ proteins, such as cingulin and ZO-1, has not been reported so far. Immunoblot analysis of PLEKHA7 immunoprecipitates from lysates of intestinal epithelial cells showed that not only paracingulin, but also cingulin and ZO-1, are detected in PLEKHA7 immunoprecipitates (**Fig. 7A**). Next, we asked whether the integrity of microtubules is required for the formation of the complex between PLEKHA7 and TJ proteins, by carrying out immunoprecipitation from lysates of cells treated either with DMSO or nocodazole. We did not detect significant differences in the amount of ZO-1 (**Fig. 7B**) and cingulin (not shown) in PLEKHA7 immunoprecipitates, with or without nocodazole, indicating that the integrity of microtubules does not perturb the ability of PLEKHA7 to form a complex with TJ proteins.

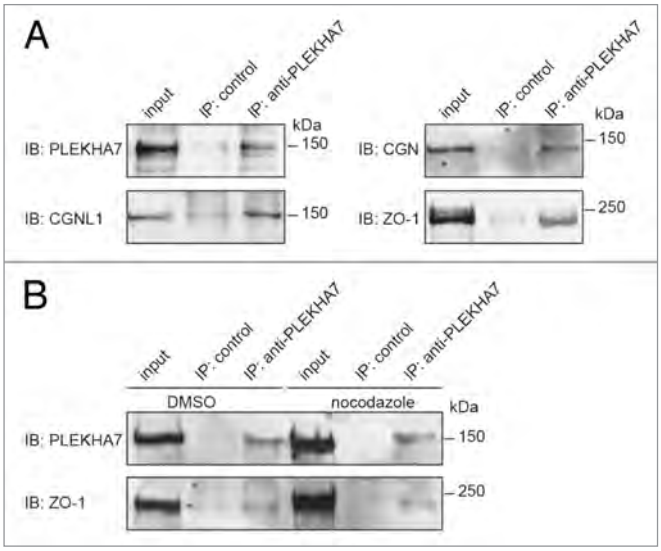

Figure 7. PLEKHA7 forms a complex with TJ proteins. (**A**) Immunoblot analysis of PLEKHA7 immunoprecipitates from lysates of confluent human intestinal colon carcinoma cells (Caco2) with antibodies against PLEKHA7, ZO-1, cingulin and paracingulin. (**B**) Immunoblot analysis of PLEKHA7 immunoprecipitates, with antibodies against either PLEKHA7 or ZO-1, from lysates of Caco2 cells treated with either DMSO or nocodazole for 1 h prior to lysis. Numbers on the right indicate migration of molecular size markers (kDa).

Discussion

Here we provide the first evidence for a role of the ZA protein PLEKHA7 in modulating epithelial TJ barrier function, through a mechanism which we propose to depend on the stabilization of the E-cadherin complex by microtubules. Although exogenous expression of PLEKHA7 constructs in MDCK monolayers did not affect either the development of the TJ barrier to ions during the calcium switch, or the steady-state TER, or the steady-state flux of large solutes, specific contructs slowed TER development at normal calcium, and attenuated the fall in TER of confluent monolayers following extracellular calcium depletion.

PLEKHA7 is a key component of the molecular complex that links the epithelial ZA to the minus ends of non-centrosomal microtubules.[21] Non-centrosomal microtubules are abundant in epithelial cells, and are stabilized by capture and anchoring at cortical sites.[32] In addition to PLEKHA7, several other junctional/cortical proteins, including desmoplakin, APC, and cingulin have been implicated in microtubule anchoring to epithelial junctions.[21,33-35] However, there is so far no evidence that any of the above proteins is involved in regulating the TJ permeability barrier. For example, cingulin depletion or exogenous expression in MDCK cells, and cingulin knockout, either in embryoid bodies

or mice, does not result in changes in either the development or the steady-state function of the TJ barrier, and does not affect the organization of the ZA.[30,36-38] Although previous studies have shown that a correct organization and anchoring of microtubules is required for the maturation of an efficient TJ barrier,[24-26,39] the molecular mechanisms of this regulation were unknown. Our observations identify PLEKHA7 as the first junctional protein, among those involved in microtubule anchoring, whose expression levels can modulate the TJ barrier function.

We observed a correlation between the ability of exogenous PLEKHA7 constructs to enhance the accumulation of E-cadherin complex proteins at the ZA and promote their clustering along lateral PA, with the ability of the same constructs to slow down the development of a normal TER at normal extracellular calcium, and attenuate the fall in TER induced by depletion of extracellular calcium. These observations point to a mechanistic implication of the E-cadherin complex in the phenotypes that we observed. Specifically, the observation that the fall in TER in the calcium depletion model in these clones was enhanced by disrupting microtubule integrity is consistent with the role of PLEKHA7 as a protein that stabilizes the E-cadherin protein complex, through connecting it to microtubules.[21] We propose that in cells that express specific exogenous contructs of PLEKHA7, the increase in the amount of E-cadherin complex proteins and PLEKHA7 at the ZA results in strengthened anchoring to the microtubule cytoskeleton, a more stable ZA, and a less dynamic remodeling, delivery and endocytic removal of ZA proteins.[26,40,41] Additional studies will be required to test these hypotheses.

Afadin has a key role in the proper formation and actin anchoring of the ZA,[42-44] and in TJ assembly and function.[45-47] However, since exogenous expression of PLEKHA7 constructs did not affect afadin recruitment at the ZA, we speculate that the effect of PLEKHA7 constructs on the TJ barrier does not occur through afadin. In contrast, the effect of PLEKHA7 constructs on the accumulation of paracingulin confirms the notion that paracingulin is a component of the complex that links microtubules to the ZA, and is recruited by PLEKHA7 to the ZA.[23] Finally, although we show that PLEKHA7 is detectable in a complex with specific TJ proteins such as cingulin and ZO-1, the apparent lack of effect of PLEKHA7 constructs on TJ protein organization argues against a direct role of PLEKHA7 in modulating TJ barrier function through actions on the cytoplasmic scaffolding complex of TJ. Therefore, the functional significance of PLEKHA7 interaction with afadin, cingulin, and ZO-1 in the regulation of TJ barrier function remains unclear.

There is an apparent discrepancy in our observation that exogenous expression of PLEKHA7 constructs slowed TER development when junction assembly was performed at normal extracellular calcium, but not when it was performed by the calcium switch. This could be due to the fact that junction assembly by the calcium switch is rapid, and relies on the fusion of endocytic vesicles containing the pre-assembled junctional complexes with the plasma membrane upon calcium re-addition.[48,49] Excess PLEKHA7 may not interfere with this process, since the junctional machineries are already pre-assembled, and the actin rather than the microtubule cytoskeleton plays a major role, as indicated by the role of Rac1 in TER development in this model.[31] In contrast, junction assembly at normal calcium after trypsinization has slower dynamics, involves de novo protein synthesis, and may require a precise spatial organization of microtubules, to correctly deliver newly synthesized ZA and TJ proteins to the plasma membrane.[13,50-52] Exogenous PLEKHA7 proteins appeared to be associated with microtubule minus ends, and future studies should address the role of PLEKHA7 in microtubule dynamics and trafficking. However, since at steady-state all clones showed a similar TER value, regardless of induction of exogenous protein expression, both in assembly by calcium switch and at normal calcium, we conclude that PLEKHA7 exogenous expression only subtly affects the dynamics of the establishment and disruption of the TJ barrier, but not its integrity at steady-state. Preliminary observations on intestinal epithelial cells also show that PLEKHA7 depletion has a modest inhibitory effect on the establishment and maintenance of the TJ barrier (our unpublished observations). The phenotype of PLEKHA7-depleted cells will be investigated in future studies.

Our results also provide new information about structure-function relationships in PLEKHA7. Although afadin was reported to be important for PLEKHA7 junctional recruitment,[29] we observed that the Central construct, lacking all of the putative afadin binding sequence, was still targeted to junctions. This would indicate that the interaction with p120ctn, which occurs in the central region, is sufficient for PLEKHA7 recruitment to both ZA and PA. Conversely, the observation that both the N-terminal and Central constructs displayed a cytoplasmic localization suggests that the presence of both afadin-binding and p120ctn/CGNL1/nezha binding regions is essential for a stable association of PLEKHA7 with the ZA. The association of the N-terminal construct with p120ctn is also, presumably, responsible for the E-cadherin enrichment at ZA and PA, since this construct is in principle lacking the CGNL1 and nezha interaction sequences. We cannot exclude that additional protein interactions may help endogenous PLEKHA7 or exogenous constructs to be targeted to ZA and PA, and future studies will address this question.

Our results, providing the first evidence for a role of PLEKHA7 in modulating the dynamics of the TJ barrier, may help to understand the molecular mechanisms through which PLEKHA7 participates in the pathogenesis of primary angle closure glaucoma[28,53] and hypertension.[54-56] For example, PLEKHA7 expression levels may influence the response of epithelial tissues to physiological or pathological stimuli that modulate the paracellular barrier. Similarly, mutations in the PLEKHA7 locus, which might affect the expression or interactions of PLEKHA7, could influence the barrier function of epithelial cells involved in these diseases, by interfering with the stabilizing role of the E-cadherin complex on the TJ barrier.

In summary, our results show that expression of specific exogenous PLEKHA7 constructs affects the dynamics of assembly and disassembly of the epithelial TJ barrier, and indicate that the E-cadherin protein complex and microtubules are mechanistically implicated in this modulation. These observations provide a framework for future studies on PLEKHA7 function in normal and diseased tissues.

Materials and Methods

Antibodies and plasmids

Antibodies were (species-antigen, dilution for immunofluorescence-IF with methanol fixation unless otherwise stated, and immunoblotting-IB): rabbit PLEKHA7 (1:10,000 IB[22]), rabbit cingulin (1:5000 IF-MeOH, 1:100 IF-PFA, 1:2000 IB[57]), rabbit paracingulin (1:250 IF, 1:10,000 IB[31]), mouse p120ctn (15D2, 1:250 IF, 1:2000 IB, from A. Reynolds), mouse E-cadherin (1:500 IF, 1:2000 IB, BD610181), rabbit α-catenin (1:100 IF, 1:1000 IB, BD610193), rabbit β-catenin (1:200 IF, Sigma C2206), mouse α-tubulin (1:150 IF, 1:1000 IB, Zymed 32–2500), rabbit anti-afadin (1:100 IF, Sigma A0224), rat ZO-1 (1:50 IF, a gift from D. Goodenough, Harvard University), rabbit occludin (1:50 IF, Zymed 71–1500), mouse myc (9E10 hybridoma culture supernatant, undiluted for IB). The constructs for inducible expression of YFP-PLEKHA7-myc were obtained by cloning either the full-length human PLEKHA7 sequence (residues 1–1121), or the truncated constructs (ΔCterm: 1–559, ΔNterm: 282–1121, Central: 351–820) into pBluescript (Xba-HindIII sites, except for Central, BamH1-EcoRI/XhoI), and subsequently into the NotI-ClaI sites of a previously prepared TRE2-Hyg vector[58] where NotI is downstream of a YFP cassette and ClaI upstream of a myc tag.

Cell culture, transfection, and other techniques

Culture of MDCKII (Madin-Darby Canine Kidney) Tet-off epithelial cells (Clontech) and Caco2 cells, transfection, selection, isolation of stable clones, immunoblotting and immunofluorescence (cold methanol fixation) were as described previously.[58,59] Stable clones of MDCK-tet-off cells full-length or truncated constructs of PLEKHA7 were incubated either in the presence or in the absence of doxycyclin (40 ng/ml) for 72 h, prior to experimental manipulations. Treatment with nocodazole 1 h at 37 °C was at final concentrations of either 0.2 μM (TER experiments) or 33 μM (immunofluorescence), by dilution from a concentrated stock, in DMSO. Three clonal lines were generated for each construct, and their behavior was similar. Representative examples of experiments performed with one of the three lines is shown.

Calcium switch assay

For the calcium switch assay, $2x10^4$ cells were plated into 6.5 mm Transwell filters (0.2 ml apical compartment, 0.7 ml basal compartment), and allowed to grow for 6 days, changing the medium every 2 days, to reach TER steady-state. The cells were then washed 3x with PBS without Ca, and the medium was replaced with Ca^{2+}-free medium (SMEM+EGTA[30]). Following overnight incubation (16–20 h), the Transepithelial Electrical Resistance (TER) was measured (t = 0), then the medium was replaced with normal calcium medium (calcium-switch), and the TER was measured at different times (1, 2, 3, 4, 8, 24, 30 h) after the switch. TER was meausred using a Millipore ERS-CELL voltohmeter.[14]

Assembly at normal calcium, and calcium depletion assays

Cells were incubated either with or without dox for 3 days, and then trypsinized and seeded on Transwells filters ($3x10^5$ cells per filter). The TER was measured after overnight (18 h) incubation, and at subsequent times (22 h, 26 h, 42 h, 64 h, 90 h), until the TER value reached steady-state (at around 50 h). The average values under induced conditions (-dox) were expressed as a percent of the values under uninduced conditions (+dox), that were taken as 100%. To test the effect of calcium depletion, cells after overnight assembly at normal calcium were incubated either with solvent (DMSO, final 0.01%) or nocodazole (0.2 μM, in DMSO) for 1 h. Next, the TER was measured again (time = 0), and expressed as percentage of the value before the treatment. Cells were then either left in NC medium (with either DMSO or nododazole), or washed 3x with PBS without Ca, and incubated with Ca^{2+}-free medium, containing either DMSO or nocodazole. The TER was then measured 30 min later, and expressed as a percent of the value before incubation with DMSO/nocodazole. The 30 min time point was chosen because at this time TER of MDCK monolayers is typically reduced by > 70% compared with the initial value.[14] The TER values at 30 min were ratioed to the TER values at time = 0, to express them as a percent of initial value.

Measurement of paracellular flux

For flux assays, confluent monolayers in duplicate 6.5 mm Transwell filters were cultured in normal medium for 24 h, washed with pre-warmed Hank's Buffer (Invitrogen 14025), and incubated in Hank's Buffer for 30 min at 37 °C. The Buffer in the apical chamber was aspirated, and the filter transferred into a new well, containing 0.7 ml Hanks' Buffer. 50 μl 3 kDa FITC-Dextran (Invitrogen D3305, stock 1 mg/ml) was added to the apical compartment. Cells were incubated at 37 °C for 2 h, and 0.1 ml of the basal compartment solution was removed, and replaced by 0.1 ml Hank's Buffer. For calcium depletion experiments, after aspiration cells were rinsed 3X with calcium-free PBS, and incubated in calcium-free PBS, containing the tracer. Fluorescence of the basal compartment sample was measured with a spectrophotometer, and the amount of dextran (ng/ml) in each sample was determined by interpolation with a standard curve. The apparent permeability was calculated using the formula: $Perm_{app}$ = (ng/ml basal) x 10^6/Area well x Initial concentration x Time (sec).

Immunofluorescence

For immunofluorescence analysis, we routinely used a cold methanol fixation protocol.[30] For labeling of microtubules, cells were washed twice with PBS, fixed in 4% paraformaldehyde (PFA), 1% Triton X-100 in Microtubule Stabilizing Buffer (MTSB, 1 mM EGTA, 4% PEG8000, 0.1M Pipes, pH 6.9) for 10 min at room temperature (RT), followed by incubation in 4% PFA in MTSB for 30 min RT, washing with PBS, blocking in 10 mM glycine, 1% bovine serum albumin (10 min RT), and washing with PBS. Incubation with primary and secondary antibodies (diluted in PBS) were performed either at 30 °C (45 min) or at 37° (30 min). Secondary antibodies (1:400, Jackson Laboratories) were labeled either with either Cy3 (anti-mouse or anti-rabbit) or Cy5 (anti-rat). Confocal images were acquired using a LSM-700 Zeiss confocal microscope.

Immunoprecipitation and immunoblotting

For immunoprecipitation, cells were lysed in IP lysis buffer (150 mM NaCl, 20 mM TRIS-HCl pH 7.5, 1% NP40, 1 mM EDTA),

lysates were clarified by centrifugation (13,000 rpm for 15 min), 20 μl of Dynabeads Protein G (Invitrogen) were washed three times with PBS containing 5% BSA and 1% NP40, antibodies (5 μl of rabbit either anti-PLEKHA7 or preimmune serum[22]) were incubated for 1 h at 4 °C with Dynabeads, subsequently lysates were incubated overnight at 4 °C and washed with IP lysis buffer. Proteins were separated on 8% polyacrylamide gels, transferred onto nitrocellulose (0. 45 μm) (100 V for 80 min at 4 °C), and blots were incubated with primary antibody, followed by secondary HRP-labeled antibody (1:10,000, Amersham), and chemiluminescence revelation.

Statistical analysis

Unless otherwise stated, TER and flux data represent the mean of at least three separate experiments, each with duplicate wells for each experimental condition. Data were analyzed for statistical significance ($P < 0.05$) using the Student's T-test, the comparisons being made each time either between the –Dox (induced) and +Dox (uninduced), or between DMSO vs. nocodazole condition.

Disclosure of Potential Conflicts of Interest

No potential conflicts of interest were disclosed.

Acknowledgments

This study was supported by grants from the Swiss Cancer League (KFS-2813-08-2011) and the Swiss National Science Foundation (31003A_135730/1), and by the State of Geneva. We are grateful to all colleagues who generously provided us with plasmids and reagents.

Supplementary Material

Supplementary materials may be found here: www.landesbioscience.com/tissuebarriers/article/28755

References

1. Powell DW. Barrier function of epithelia. Am J Physiol 1981; 241:G275-88; PMID:7032321
2. Farquhar MG, Palade GE. Junctional complexes in various epithelia. J Cell Biol 1963; 17:375-412; PMID:13944428; http://dx.doi.org/10.1083/jcb.17.2.375
3. Shin K, Fogg VC, Margolis B. Tight junctions and cell polarity. Annu Rev Cell Dev Biol 2006; 22:207-35; PMID:16771626; http://dx.doi.org/10.1146/annurev.cellbio.22.010305.104219
4. Guillemot L, Paschoud S, Pulimeno P, Foglia A, Citi S. The cytoplasmic plaque of tight junctions: a scaffolding and signalling center. Biochim Biophys Acta 2008; 1778:601-13; PMID:18339298; http://dx.doi.org/10.1016/j.bbamem.2007.09.032
5. Meng W, Takeichi M. Adherens junction: molecular architecture and regulation. Cold Spring Harb Perspect Biol 2009; 1:a002899; PMID:20457565; http://dx.doi.org/10.1101/cshperspect.a002899
6. Madara JL. Relationships between the tight junction and the cytoskeleton. In: Cereijido M, ed. Tight junctions. Boca Raton, FL: CRC Press, 1992:105-20.
7. Mooseker MS. Organization, chemistry, and assembly of the cytoskeletal apparatus of the intestinal brush border. Annu Rev Cell Biol 1985; 1:209-41; PMID:3916317; http://dx.doi.org/10.1146/annurev.cb.01.110185.001233
8. Van Itallie CM, Fanning AS, Bridges A, Anderson JM. ZO-1 stabilizes the tight junction solute barrier through coupling to the perijunctional cytoskeleton. Mol Biol Cell 2009; 20:3930-40; PMID:19605556; http://dx.doi.org/10.1091/mbc.E09-04-0320
9. Gumbiner B, Simons K. A functional assay for proteins involved in establishing an epithelial occluding barrier: identification of a uvomorulin-like polypeptide. J Cell Biol 1986; 102:457-68; PMID:3511070; http://dx.doi.org/10.1083/jcb.102.2.457
10. Tunggal JA, Helfrich I, Schmitz A, Schwarz H, Günzel D, Fromm M, Kemler R, Krieg T, Niessen CM. E-cadherin is essential for in vivo epidermal barrier function by regulating tight junctions. EMBO J 2005; 24:1146-56; PMID:15775979; http://dx.doi.org/10.1038/sj.emboj.7600605
11. Capaldo CT, Macara IG. Depletion of E-cadherin disrupts establishment but not maintenance of cell junctions in Madin-Darby canine kidney epithelial cells. Mol Biol Cell 2007; 18:189-200; PMID:17093058; http://dx.doi.org/10.1091/mbc.E06-05-0471
12. Martinez-Palomo A, Meza I, Beaty G, Cereijido M. Experimental modulation of occluding junctions in a cultured transporting epithelium. J Cell Biol 1980; 87:736-45; PMID:6780571; http://dx.doi.org/10.1083/jcb.87.3.736
13. Gonzalez-Mariscal L, Chávez de Ramírez B, Cereijido M. Tight junction formation in cultured epithelial cells (MDCK). J Membr Biol 1985; 86:113-25; PMID:4032460; http://dx.doi.org/10.1007/BF01870778
14. Citi S. Protein kinase inhibitors prevent junction dissociation induced by low extracellular calcium in MDCK epithelial cells. J Cell Biol 1992; 117:169-78; PMID:1556151; http://dx.doi.org/10.1083/jcb.117.1.169
15. Turner JR, Rill BK, Carlson SL, Carnes D, Kerner R, Mrsny RJ, Madara JL. Physiological regulation of epithelial tight junctions is associated with myosin light-chain phosphorylation. Am J Physiol 1997; 273:C1378-85; PMID:9357784
16. Turner JR, Angle JM, Black ED, Joyal JL, Sacks DB, Madara JL. PKC-dependent regulation of transepithelial resistance: roles of MLC and MLC kinase. Am J Physiol 1999; 277:C554-62; PMID:10484342
17. Hecht G, Pestic L, Nikcevic G, Koutsouris A, Tripuraneni J, Lorimer DD, Nowak G, Guerriero V Jr., Elson EL, Lanerolle PD. Expression of the catalytic domain of myosin light chain kinase increases paracellular permeability. Am J Physiol 1996; 271:C1678-84; PMID:8944652
18. Tinsley JH, De Lanerolle P, Wilson E, Ma W, Yuan SY. Myosin light chain kinase transference induces myosin light chain activation and endothelial hyperpermeability. Am J Physiol Cell Physiol 2000; 279:C1285-9; PMID:11003609
19. Clayburgh DR, Barrett TA, Tang Y, Meddings JB, Van Eldik LJ, Watterson DM, Clarke LL, Mrsny RJ, Turner JR. Epithelial myosin light chain kinase-dependent barrier dysfunction mediates T cell activation-induced diarrhea in vivo. J Clin Invest 2005; 115:2702-15; PMID:16184195; http://dx.doi.org/10.1172/JCI24970
20. Citi S, Volberg T, Bershadsky AD, Denisenko N, Geiger B. Cytoskeletal involvement in the modulation of cell-cell junctions by the protein kinase inhibitor H-7. J Cell Sci 1994; 107:683-92; PMID:8006081
21. Meng W, Mushika Y, Ichii T, Takeichi M. Anchorage of microtubule minus ends to adherens junctions regulates epithelial cell-cell contacts. Cell 2008; 135:948-59; PMID:19041755; http://dx.doi.org/10.1016/j.cell.2008.09.040
22. Pulimeno P, Bauer C, Stutz J, Citi S. PLEKHA7 is an adherens junction protein with a tissue distribution and subcellular localization distinct from ZO-1 and E-cadherin. PLoS One 2010; 5:e12207; PMID:20808826; http://dx.doi.org/10.1371/journal.pone.0012207
23. Pulimeno P, Paschoud S, Citi S. A role for ZO-1 and PLEKHA7 in recruiting paracingulin to tight and adherens junctions of epithelial cells. J Biol Chem 2011; 286:16743-50; PMID:21454477; http://dx.doi.org/10.1074/jbc.M111.230862
24. Yap AS, Stevenson BR, Abel KC, Cragoe EJ Jr., Manley SW. Microtubule integrity is necessary for the epithelial barrier function of cultured thyroid cell monolayers. Exp Cell Res 1995; 218:540-50; PMID:7796888; http://dx.doi.org/10.1006/excr.1995.1189
25. Birukova AA, Smurova K, Birukov KG, Usatyuk P, Liu F, Kaibuchi K, Ricks-Cord A, Natarajan V, Alieva I, Garcia JG, et al. Microtubule disassembly induces cytoskeletal remodeling and lung vascular barrier dysfunction: role of Rho-dependent mechanisms. J Cell Physiol 2004; 201:55-70; PMID:15281089; http://dx.doi.org/10.1002/jcp.20055
26. Ivanov AI, McCall IC, Babbin B, Samarin SN, Nusrat A, Parkos CA. Microtubules regulate disassembly of epithelial apical junctions. BMC Cell Biol 2006; 7:12; PMID:16509970; http://dx.doi.org/10.1186/1471-2121-7-12
27. Tomson FL, Viswanathan VK, Kanack KJ, Kanteti RP, Straub KV, Menet M, Kaper JB, Hecht G. Enteropathogenic Escherichia coli EspG disrupts microtubules and in conjunction with Orf3 enhances perturbation of the tight junction barrier. Mol Microbiol 2005; 56:447-64; PMID:15813736; http://dx.doi.org/10.1111/j.1365-2958.2005.04571.x
28. Vithana EN, Khor CC, Qiao C, Nongpiur ME, George R, Chen LJ, Do T, Abu-Amero K, Huang CK, Low S, et al. Genome-wide association analyses identify three new susceptibility loci for primary angle closure glaucoma. Nat Genet 2012; 44:1142-6; PMID:22922875; http://dx.doi.org/10.1038/ng.2390
29. Kurita S, Yamada T, Rikitsu E, Ikeda W, Takai Y. Binding between the junctional proteins afadin and PLEKHA7 and implication in the formation of adherens junction in epithelial cells. J Biol Chem 2013; 288:29356-68; PMID:23990464; http://dx.doi.org/10.1074/jbc.M113.453464
30. Guillemot L, Citi S. Cingulin regulates claudin-2 expression and cell proliferation through the small GTPase RhoA. Mol Biol Cell 2006; 17:3569-77; PMID:16723500; http://dx.doi.org/10.1091/mbc.E06-02-0122

31. Guillemot L, Paschoud S, Jond L, Foglia A, Citi S. Paracingulin regulates the activity of Rac1 and RhoA GTPases by recruiting Tiam1 and GEF-H1 to epithelial junctions. Mol Biol Cell 2008; 19:4442-53; PMID:18653465; http://dx.doi.org/10.1091/mbc.E08-06-0558
32. Bartolini F, Gundersen GG. Generation of noncentrosomal microtubule arrays. J Cell Sci 2006; 119:4155-63; PMID:17038542; http://dx.doi.org/10.1242/jcs.03227
33. Lechler T, Fuchs E. Desmoplakin: an unexpected regulator of microtubule organization in the epidermis. J Cell Biol 2007; 176:147-54; PMID:17227889; http://dx.doi.org/10.1083/jcb.200609109
34. McCartney BM, Näthke IS. Cell regulation by the Apc protein Apc as master regulator of epithelia. Curr Opin Cell Biol 2008; 20:186-93; PMID:18359618; http://dx.doi.org/10.1016/j.ceb.2008.02.001
35. Yano T, Matsui T, Tamura A, Uji M, Tsukita S. The association of microtubules with tight junctions is promoted by cingulin phosphorylation by AMPK. J Cell Biol 2013; 203:605-14; PMID:24385485; http://dx.doi.org/10.1083/jcb.201304194
36. Guillemot L, Hammar E, Kaister C, Ritz J, Caille D, Jond L, Bauer C, Meda P, Citi S. Disruption of the cingulin gene does not prevent tight junction formation but alters gene expression. J Cell Sci 2004; 117:5245-56; PMID:15454572; http://dx.doi.org/10.1242/jcs.01399
37. Guillemot L, Schneider Y, Brun P, Castagliuolo I, Pizzuti D, Martines D, Jond L, Bongiovanni M, Citi S. Cingulin is dispensable for epithelial barrier function and tight junction structure, and plays a role in the control of claudin-2 expression and response to duodenal mucosa injury. J Cell Sci 2012; 125:5005-14; PMID:22946046; http://dx.doi.org/10.1242/jcs.101261
38. Paschoud S, Citi S. Inducible overexpression of cingulin in stably transfected MDCK cells does not affect tight junction organization and gene expression. Mol Membr Biol 2008; 25:1-13; PMID:18097951; http://dx.doi.org/10.1080/09687680701474009
39. Yap AS, Manley SW. Microtubule integrity is essential for apical polarization and epithelial morphogenesis in the thyroid. Cell Motil Cytoskeleton 2001; 48:201-12; PMID:11223951; http://dx.doi.org/10.1002/1097-0169(200103)48:3<201::AID-CM1009>3.0.CO;2-C
40. Rodriguez OC, Schaefer AW, Mandato CA, Forscher P, Bement WM, Waterman-Storer CM. Conserved microtubule-actin interactions in cell movement and morphogenesis. Nat Cell Biol 2003; 5:599-609; PMID:12833063; http://dx.doi.org/10.1038/ncb0703-599
41. Birkenfeld J, Nalbant P, Yoon SH, Bokoch GM. Cellular functions of GEF-H1, a microtubule-regulated Rho-GEF: is altered GEF-H1 activity a crucial determinant of disease pathogenesis? Trends Cell Biol 2008; 18:210-9; PMID:18394899; http://dx.doi.org/10.1016/j.tcb.2008.02.006
42. Mandai K, Nakanishi H, Satoh A, Obaishi H, Wada M, Nishioka H, Itoh M, Mizoguchi A, Aoki T, Fujimoto T, et al. Afadin: A novel actin filament-binding protein with one PDZ domain localized at cadherin-based cell-to-cell adherens junction. J Cell Biol 1997; 139:517-28; PMID:9334353; http://dx.doi.org/10.1083/jcb.139.2.517
43. Ikeda W, Nakanishi H, Miyoshi J, Mandai K, Ishizaki H, Tanaka M, Togawa A, Takahashi K, Nishioka H, Yoshida H, et al. Afadin: A key molecule essential for structural organization of cell-cell junctions of polarized epithelia during embryogenesis. J Cell Biol 1999; 146:1117-32; PMID:10477764; http://dx.doi.org/10.1083/jcb.146.5.1117
44. Sawyer JK, Choi W, Jung KC, He L, Harris NJ, Peifer M. A contractile actomyosin network linked to adherens junctions by Canoe/afadin helps drive convergent extension. Mol Biol Cell 2011; 22:2491-508; PMID:21613546; http://dx.doi.org/10.1091/mbc.E11-05-0411
45. Ooshio T, Kobayashi R, Ikeda W, Miyata M, Fukumoto Y, Matsuzawa N, Ogita H, Takai Y. Involvement of the interaction of afadin with ZO-1 in the formation of tight junctions in Madin-Darby canine kidney cells. J Biol Chem 2010; 285:5003-12; PMID:20008323; http://dx.doi.org/10.1074/jbc.M109.043760
46. Tanaka-Okamoto M, Hori K, Ishizaki H, Itoh Y, Onishi S, Yonemura S, Takai Y, Miyoshi J. Involvement of afadin in barrier function and homeostasis of mouse intestinal epithelia. J Cell Sci 2011; 124:2231-40; PMID:21652626; http://dx.doi.org/10.1242/jcs.081000
47. Birukova AA, Tian X, Tian Y, Higginbotham K, Birukov KG. Rap-afadin axis in control of Rho signaling and endothelial barrier recovery. Mol Biol Cell 2013; 24:2678-88; PMID:23864716; http://dx.doi.org/10.1091/mbc.E13-02-0098
48. Kartenbeck J, Schmid E, Franke WW, Geiger B. Different modes of internalization of proteins associated with adhaerens junctions and desmosomes: experimental separation of lateral contacts induces endocytosis of desmosomal plaque material. EMBO J 1982; 1:725-32; PMID:6821357
49. Kartenbeck J, Schmelz M, Franke WW, Geiger B. Endocytosis of junctional cadherins in bovine kidney epithelial (MDBK) cells cultured in low Ca2+ ion medium. J Cell Biol 1991; 113:881-92; PMID:2026652; http://dx.doi.org/10.1083/jcb.113.4.881
50. Fesenko I, Kurth T, Sheth B, Fleming TP, Citi S, Hausen P. Tight junction biogenesis in the early Xenopus embryo. Mech Dev 2000; 96:51-65; PMID:10940624; http://dx.doi.org/10.1016/S0925-4773(00)00368-3
51. Ligon LA, Holzbaur EL. Microtubules tethered at epithelial cell junctions by dynein facilitate efficient junction assembly. Traffic 2007; 8:808-19; PMID:17550375; http://dx.doi.org/10.1111/j.1600-0854.2007.00574.x
52. Bellett G, Carter JM, Keynton J, Goldspink D, James C, Moss DK, Mogensen MM. Microtubule plus-end and minus-end capture at adherens junctions is involved in the assembly of apico-basal arrays in polarised epithelial cells. Cell Motil Cytoskeleton 2009; 66:893-908; PMID:19479825; http://dx.doi.org/10.1002/cm.20393
53. Day AC, Luben R, Khawaja AP, Low S, Hayat S, Dalzell N, Wareham NJ, Khaw KT, Foster PJ. Genotype-phenotype analysis of SNPs associated with primary angle closure glaucoma (rs1015213, rs3753841 and rs11024102) and ocular biometry in the EPIC-Norfolk Eye Study. Br J Ophthalmol 2013; 97:704-7; PMID:23505305; http://dx.doi.org/10.1136/bjophthalmol-2012-302969
54. Levy D, Ehret GB, Rice K, Verwoert GC, Launer LJ, Dehghan A, Glazer NL, Morrison AC, Johnson AD, Aspelund T, et al. Genome-wide association study of blood pressure and hypertension. Nat Genet 2009; 41:677-87; PMID:19430479; http://dx.doi.org/10.1038/ng.384
55. Hong KW, Jin HS, Lim JE, Kim S, Go MJ, Oh B. Recapitulation of two genomewide association studies on blood pressure and essential hypertension in the Korean population. J Hum Genet 2010; 55:336-41; PMID:20414254; http://dx.doi.org/10.1038/jhg.2010.31
56. Lin Y, Lai X, Chen B, Xu Y, Huang B, Chen Z, Zhu S, Yao J, Jiang Q, Huang H, et al. Genetic variations in CYP17A1, CACNB2 and PLEKHA7 are associated with blood pressure and/or hypertension in She ethnic minority of China. Atherosclerosis 2011; 219:709-14; PMID:21963141; http://dx.doi.org/10.1016/j.atherosclerosis.2011.09.006
57. Cardellini P, Davanzo G, Citi S. Tight junctions in early amphibian development: detection of junctional cingulin from the 2-cell stage and its localization at the boundary of distinct membrane domains in dividing blastomeres in low calcium. Dev Dyn 1996; 207:104-13; PMID:8875080; http://dx.doi.org/10.1002/(SICI)1097-0177(199609)207:1<104::AID-AJA10>3.0.CO;2-0
58. Paschoud S, Citi S. Inducible overexpression of cingulin in stably transfected MDCK cells does not affect tight junction organization and gene expression. Mol Membr Biol 2008; 25:1-13; PMID:18097951; http://dx.doi.org/10.1080/09687680701474009
59. Paschoud S, Guillemot L, Citi S. Distinct domains of paracingulin are involved in its targeting to the actin cytoskeleton and regulation of apical junction assembly. J Biol Chem 2012; 287:13159-69; PMID:22315225; http://dx.doi.org/10.1074/jbc.M111.315622

S1

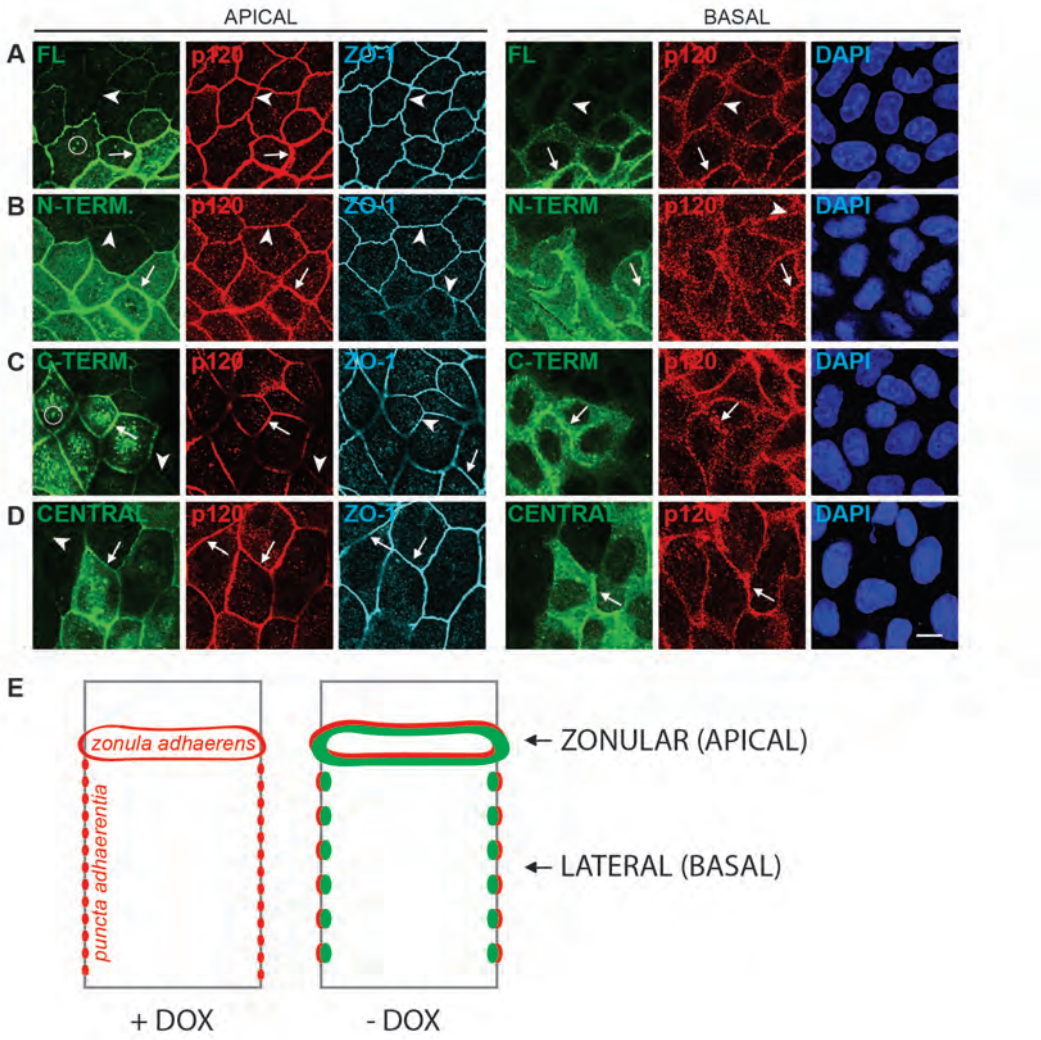

Supplementary Figure 1. Exogenous expression of full-length, N-terminal, C-terminal, but not Central PLEKHA7 constructs enhances ZA recruitment and PA clustering of p120-ctn. Confocal immunofluorescence analysis of clonal lines of MDCK cells showing labelling for exogenous constructs (green) in induced lines (-DOX) and p120-ctn, either in the apical plane of focus (ZO-1, gray, left panels), which contains ZA (zonula adhaerens), or in the basal plane (nuclei, blue DAPI, right panels), which contains PA (puncta adhaerentia). (A) Full-length; (B) N-terminal (N-TERM); (C) C-terminal (C-TERM); (D) Central. Matched arrows indicate matched normal/increased junctional labelling (using ZO-1 as a reference fore the apical plane), and arrowheads indicate decreased junctional labelling (B, C, D, apical plane) or diffuse lateral labelling (A and E, basal). Within each panel, arrows indicate stronger labelling than arrowheads. (E) Schematic diagram of polarized MDCK cells, showing the effect of exogenous expression of Full-length, N-terminal, and C-terminal constructs (green) on the localization of E-cadherin complex proteins (red). In the absence of exogenous protein (+DOX) the E-cadherin complex proteins are localized in the circumferential apical zonula adhaerens and on the lateral junctional surface, in finely distributed puncta adhaerentia. Upon exogenous protein expression, increased E-cadherin complex labelling is seen associated with PLEKHA7 constructs at the ZA, and lateral labelling is clustered in fewer, more brightly stained PA. Bar = 10 μm.

S2

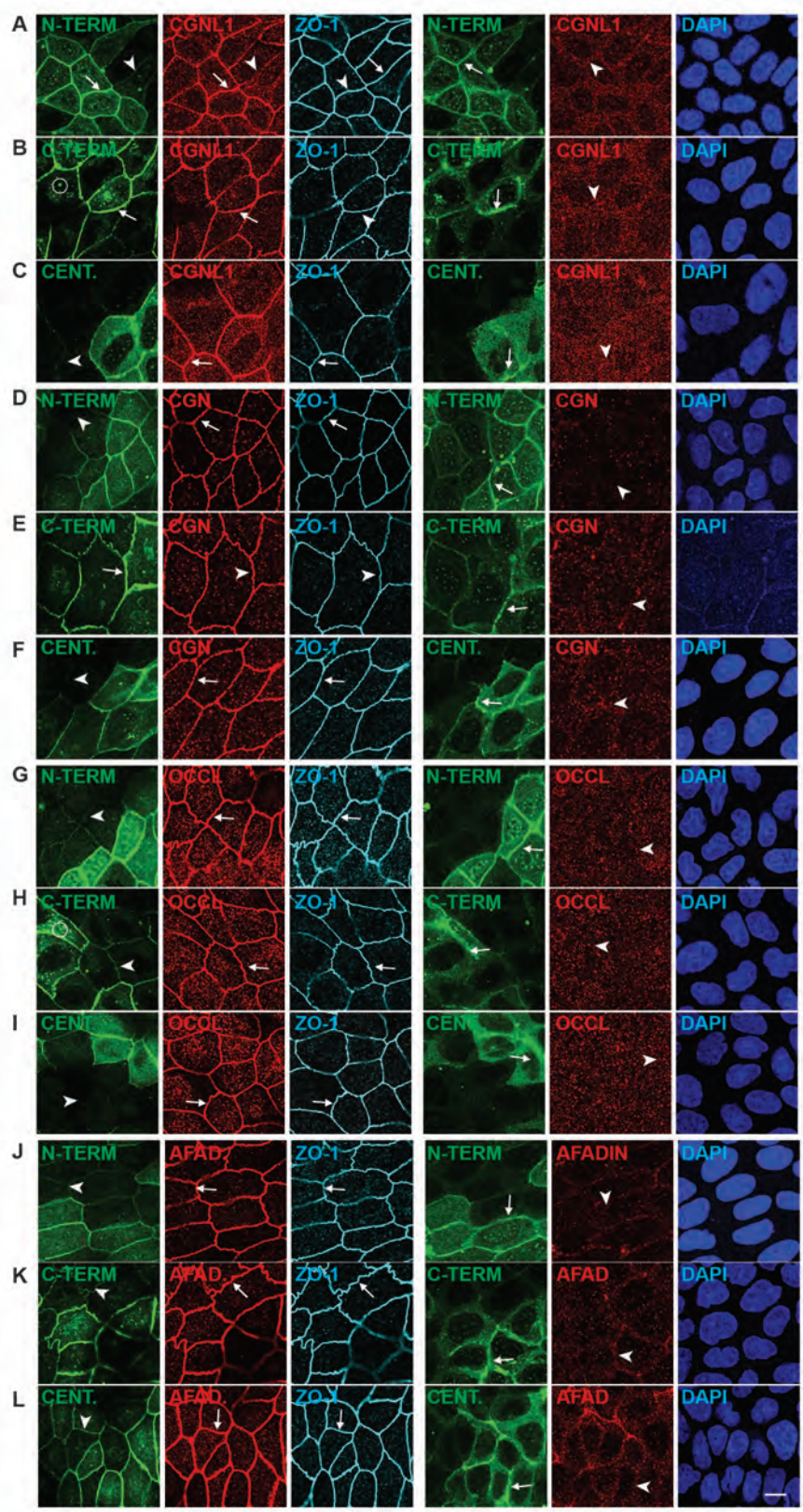

Supplementary Figure 2. The effect of exogenous expression of N-terminal, C-terminal and Central constructs of PLEKHA7 on the subcellular distribution of zonular apical junctional complex proteins. Confocal immunofluorescence analysis of MDCK cells expressing the indicated constructs (green), triple-labelled with antibodies against either paracingulin (CGNL1, (A-C)), cingulin (CGN, (D-F)) occludin (OCCL, (G-I)), or afadin (AFAD, (J-L)) in red, ZO-1 (gray in apical, left panels), and nuclei (DAPI, blue, basal plane). See legend to Fig. 1 for arrow/arrowheads significance. Bar = 10 μm.

S3

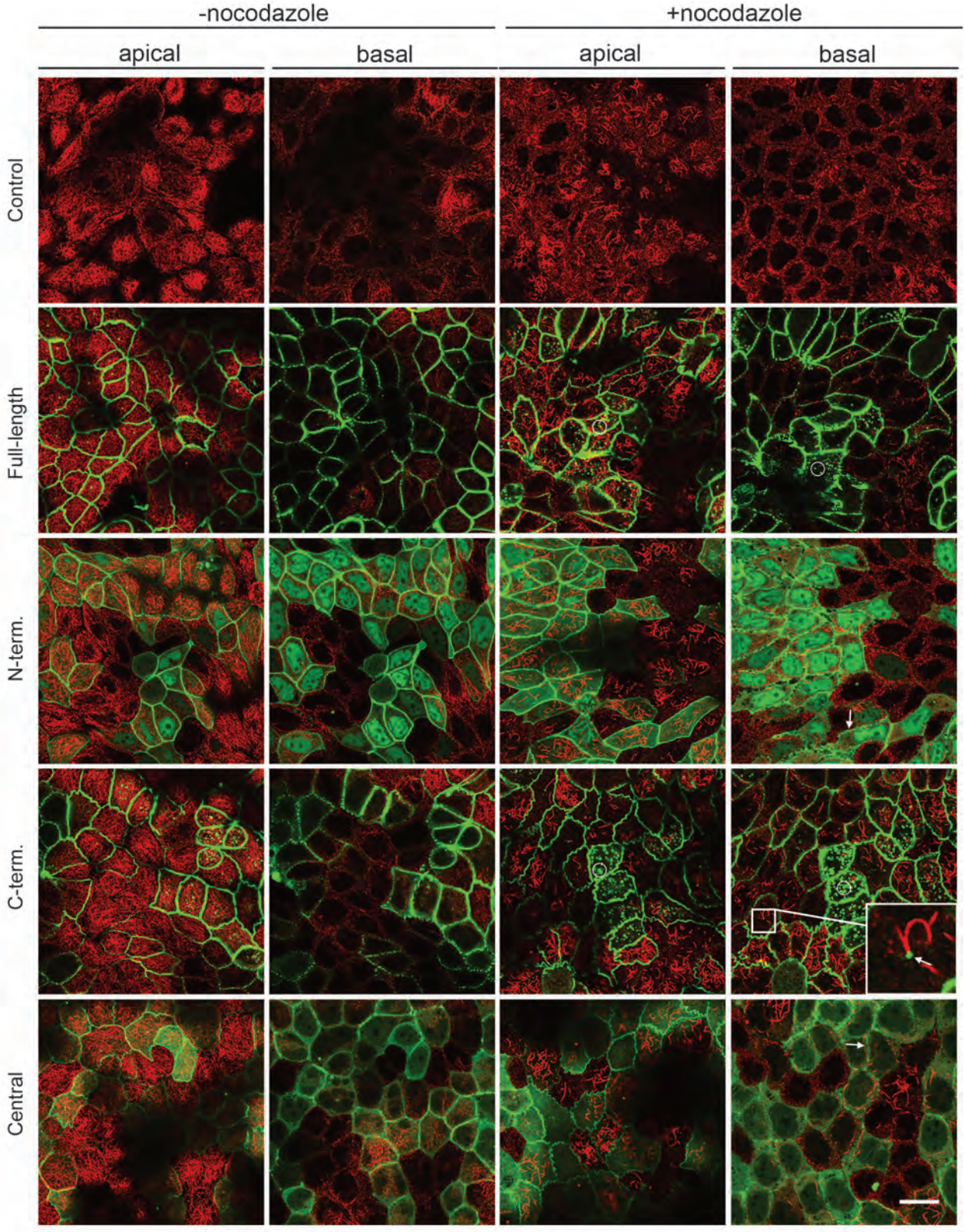

Supplementary Figure 3. The effect of nocodazole on the subcellular distribution of exogenous PLEKHA7 constructs. Confocal immunofluorescence analysis of MDCK cells expressing the indicated PLEKHA7 constructs (green), double-labelled with antibodies against α-tubulin (red) to visualize microtubules. Merge images of induced cells are shown, on apical and basal planes, respectively, without (-nocodazole) and with (+nocodazole) nocodazole. See legend to Fig. 1 for arrow/arrowheads significance. The arrow in the magnified inset in the C-term/+nocodazole/basal indicates exogenous PLEKHA7 associated with the end of a microtubule. Bar = 10 μm.

MgcRacGAP interacts with cingulin and paracingulin to regulate Rac1 activation and development of the tight junction barrier during epithelial junction assembly

The control of activation of Rho family GTPases is fundamental during the establishment and maintenance of cell-cell junctions. Cingulin and paracingulin are two structurally related proteins of TJ. Paracingulin is also present at AJ. Both these proteins regulate the activity of different GEFs, such as GEF-H1, and thus regulate the activity of RhoA in the cytoplasm [27, 75]. Additionally, cingulin can bind p114 RhoGEF at TJ and activate RhoA at junctions [77]. Paracingulin is important during junction assembly, through the junctional recruitment of the Rac1 GEF Tiam1 [27]. In this paper we show that cingulin and paracingulin can further modulate the activity of Rho family GTPases by recruiting at junction the Rac GAP MgcRacGAP. Cingulin and paracingulin can both bind in vitro and in vivo MgcRacGAP, and MDCK cells depleted of both cingulin and paracingulin show decreased levels and junctional accumulation of MgcRacGAP, providing the evidence that two pools of MgcRacGAP exist at junctions, one associated with ECT2 (another component of the centralspindlin complex) at E-cadherin juncitons, and one associated with cingulin and paracingulin at TJ. The results suggest that the dynamics of junction assembly and TER development result from a balance of the Rac1 activation mediated by Tiam1 and its inhibition mediated by MgcRacGAP, with cingulin and paracingulin playing a key role in this regulation.

My contribution to this publication was the analysis of cingulin and paracingulin interaction with MgcRacGAP in vivo through co-immunoprecipitation, and the molecular mapping of their sites of interaction (Figure 4 A, C, D).

MgcRacGAP interacts with cingulin and paracingulin to regulate Rac1 activation and development of the tight junction barrier during epithelial junction assembly

Laurent Guillemot[a], Diego Guerrera[a], Domenica Spadaro[a], Rocio Tapia[a], Lionel Jond[a], and Sandra Citi[a,b,c]

[a]Department of Molecular Biology, [b]Department of Cell Biology, and [c]Institute of Genetics and Genomics in Geneva, University of Geneva, CH-1211 Geneva, Switzerland

ABSTRACT **The regulation of Rho-family GTPases is crucial to direct the formation of cell–cell junctions and tissue barriers. Cingulin (CGN) and paracingulin (CGNL1) control RhoA activation in epithelial cells by interacting with RhoA guanidine exchange factors. CGNL1 depletion also inhibits Rac1 activation during junction assembly. Here we show that, unexpectedly, Madin–Darby canine kidney epithelial cells depleted of both CGN and CGNL1 (double-KD cells) display normal Rac1 activation and tight junction (TJ) formation, despite decreased junctional recruitment of the Rac1 activator Tiam1. The expression of the Rac1 inhibitor MgcRacGAP is decreased in double-KD cells, and the barrier development and Rac1 activation phenotypes are rescued by exogenous expression of MgcRacGAP. MgcRacGAP colocalizes with CGN and CGNL1 at TJs and forms a complex and interacts directly in vitro with CGN and CGNL1. Depletion of either CGN or CGNL1 in epithelial cells results in decreased junctional localization of MgcRacGAP but not of ECT2, a centralspindlin-interacting Rho GEF. These results provide new insight into coordination of Rho-family GTPase activities at junctions, since apical accumulation of CGN and CGNL1 at TJs during junction maturation provides a mechanism to spatially restrict down-regulation of Rac1 activation through the recruitment of MgcRacGAP.**

Monitoring Editor
Benjamin Margolis
University of Michigan Medical School

Received: Nov 20, 2013
Revised: Apr 16, 2014
Accepted: Apr 28, 2014

INTRODUCTION

The precise spatiotemporal control of the activity of Rho-family GTPases is essential in many cellular processes, including the establishment and maintenance of cell–cell junctions and the formation of epithelial barriers (Nusrat *et al.*, 1995; Braga *et al.*, 1997; Takaishi *et al.*, 1997; Jou *et al.*, 1998; Yamada and Nelson, 2007). Rho-family GTPases exist in active (GTP-bound) and inactive (GDP-bound) states, and the transition between these states depends on a finely tuned antagonism between activating guanine-nucleotide exchange factors (GEFs) and inhibitory GTPase-activating proteins (GAPs; Schmidt and Hall, 2002; Rossman *et al.*, 2005; Tcherkezian and Lamarche-Vane, 2007).

Tight junctions (TJs) form, together with the zonula adhaerens (ZA), a belt-like apical junctional complex (AJC) in epithelial cells, and are uniquely responsible for the barrier function of epithelia through the formation of claudin-based paracellular channels and pores (Furuse and Tsukita, 2006; Anderson and Van Itallie, 2009). The transmembrane proteins of TJ and ZA are clustered at the sites of cell–cell contact by distinct complexes of cytoplasmic adaptor proteins, some of which provide anchoring to the actin and microtubule cytoskeletons (Shin *et al.*, 2006; Meng and Takeichi, 2009). RhoA and Rac1 are the major GTPases of the Rho family, which are

This article was published online ahead of print in MBoC in Press (http://www.molbiolcell.org/cgi/doi/10.1091/mbc.E13-11-0680) on May 7, 2014.

The authors declare no commercial affiliation or conflict of interest.

Address correspondence to: Sandra Citi (sandra.citi@unige.ch).

Abbreviations used: AJC, apical junctional complex; Asef, APC-stimulated guanine nucleotide exchange factor; CGN, cingulin; CGNL1, paracingulin; ECT2, epithelial cell transforming sequence 2 oncogene; GAP, GTPase-activating protein; GEF, guanidine exchange factor; HA, hemagglutinin; KD, knockdown; KO, knockout; MDCK, Madin–Darby canine kidney; MgcRacGAP, male germ cell Rac GTPase-activating protein; MKLP1, mitotic kinesin-like protein; RICH1, RhoGAP interacting with CIP4 homologues protein 1; TER, transepithelial electrical resistance; Tiam1, T-cell lymphoma invasion and metastasis 1; TJ, tight junction; WT, wild type; ZA, zonula adhaerens.

Supplemental Material can be found at:
http://www.molbiolcell.org/content/suppl/2014/05/05/mbc.E13-11-0680v1.DC1.html

implicated in the regulation of TJs and the ZA through the dynamic reorganization and contractility of the actin cytoskeleton (Hall, 2012). However, the molecular mechanisms of their regulation are not completely understood. For example, although GEFs for RhoA and Rac1 have been found to interact with junctional proteins (reviewed in Citi *et al.*, 2011; McCormack *et al.*, 2013), little is known about the function of specific RhoA and Rac1 GAPs in modulating the establishment of the TJ barrier. Furthermore, it is not known whether any Rac-GAP protein interacts with specific components of the cytoplasmic plaque of the TJ. In contrast, GAPs for Cdc42 are required for TJ integrity and interact with junctional proteins (Wells *et al.*, 2006; Elbediwy *et al.*, 2012).

Two key players in the fine-tuning of RhoA activity in epithelial cells are cingulin (CGN), which is specifically localized in the cytoplasmic plaque region of TJs (Citi *et al.*, 1988), and paracingulin (CGNL1; also known as JACOP), which is localized to both the TJ and ZA (Ohnishi *et al.*, 2004; Guillemot and Citi, 2006b). CGN and CGNL1 are structurally related and recruit the Rho GEF GEF-H1 to junctions of Madin–Darby canine kidney (MDCK) cells and p114-RhoGEF to junctions of corneal cells (Citi *et al.*, 2000, 2009, 2012; Aijaz *et al.*, 2005; Guillemot and Citi, 2006a; Guillemot *et al.*, 2008; Terry *et al.*, 2011). CGNL1, unlike CGN, is also required for efficient junctional recruitment of the Rac1 GEF Tiam1 in MDCK cells, and depletion of CGNL1, but not of CGN, results in loss of the waves of increased Rac1 activation observed during junction assembly (Guillemot *et al.*, 2008). Here, by studying the junction assembly phenotype of MDCK cells depleted of both CGN and CGNL1 (double-KD cells), we find that MgcRacGAP (also known as RacGAP1, RacGAP50C, or Cyk-4; Toure *et al.*, 1998; Jantsch-Plunger *et al.*, 2000; Somers and Saint, 2003) plays a role in Rac1-dependent regulation of the dynamic establishment of the TJ barrier and interacts with both CGN and CGNL1.

RESULTS

In double-KD cells, Rac1 activation, junction assembly, and establishment of the TJ barrier are similar to those in wild-type cells, despite decreased junctional recruitment of Tiam1

Stable lines of MDCK epithelial cells depleted of both CGN and CGNL1 were reported previously (Guillemot *et al.*, 2013) and show increased RhoA activation at confluence, consistent with decreased junctional recruitment of GEF-H1, similar to cells depleted of either CGN alone (CGN-KD) or CGNL1 alone (CGNL1-KD; Guillemot and Citi, 2006a; Guillemot *et al.*, 2008). In addition, they show normal expression and localization of proteins of the zonula adhaerens and decreased expression of the transcription factor GATA-4 (Guillemot *et al.*, 2013). Here we investigate the dynamics of junction assembly of double-KD cells, starting from our previous observations that in CGNL1-KD cells Rac1 activation is decreased during junction assembly, junction assembly is delayed, and the peak in transepithelial electrical resistance (TER) observed during the calcium switch is abolished (Guillemot *et al.*, 2008).

In confluent monolayers, Rac1 activation in double-KD cells, as measured by a glutathione *S*-transferase (GST) pull-down assay, was the same as in wild-type (WT) cells (Figure 1A) and CGNL1-KD cells (Guillemot *et al.*, 2008). Rac1 activity as determined by GST-pull down on cell lysates is a reliable readout of junctional Rac1 activation during junction assembly because although Rac1 is necessary for maintenance of cell–cell contacts and protein traffic at steady state, during junction formation the zones of maximal Rac1 and lamellipodia activity are at the periphery of contacting membranes (Yamada and Nelson, 2007). So we examined Rac1 activation during junction formation in the calcium switch, an established experimental protocol to study the dynamic formation of the TJ barrier (Gonzalez-Mariscal *et al.*, 1985). Surprisingly, Rac1 activation in double-KD cells was indistinguishable from that in WT cells; for example, the peaks of Rac1 activity observed at the early (10–30 min) and late (3 h) time points were not abolished (Figure 1B and Supplemental Figure S1A), in contrast to CGNL1-depleted cells (Guillemot *et al.*, 2008) and similar to WT and CGN(–) cells (Supplemental Figure S1A). Instead, RhoA activity of double-KD cells during the calcium switch was high and remained high at 8 h after the beginning of the switch and in confluent monolayers (Figure 1B and Supplemental Figure S1A; Guillemot *et al.*, 2008), as previously shown for single-KD cells (Guillemot and Citi, 2006a; Supplemental Figure S1A).

As an alternative functional assay, we assessed TJ barrier function by examining the pattern of development of the ionic permeability barrier (TER) in double-KD cells. Whereas in CGNL1(–) cells the peak in TER is abolished (Guillemot *et al.*, 2008; Figure 1C), in double-KD cells it is similar to that observed in WT cells (Figure 1C). Distinct stable clones of double-KD cells behaved similarly (Supplemental Figure S1B).

As a third functional assay, we examined the kinetics of accumulation of the transmembrane TJ protein occludin at the junctions of double-KD cells. The behavior of double-KD cells was similar to that of WT cells and cells expressing control short hairpin RNA (shRNA; Figure 1D) and not delayed, as observed in CGNL1(–) cells (Guillemot *et al.*, 2008).

Because in CGNL1(–) cells decreased Rac1 activation and delayed junction assembly correlate with decreased junctional localization of Tiam1 (Guillemot *et al.*, 2008), we asked whether the unexpected phenotype of double-KD cells was due to a rescue in the junctional localization of Tiam1, which could account for the increased Rac1 activation, and normal TJ barrier development. Immunofluorescence analysis showed that in double-KD cells there was decreased junctional localization of Tiam1 compared with WT cells, similar to what observed in single-KD CGNL1(–) cells (Figure 1E; Guillemot *et al.*, 2008). In agreement, immunoblot analysis of soluble and insoluble fractions showed a decrease in the amount of insoluble, junction-associated Tiam1 (Figure 1F). Because this assay indicated that normal Rac1 activation and TJ barrier development in double-KD cells was not due to a rescue in Tiam1 localization, we conclude that Rac1 activation during junction assembly not only depends on Tiam1, but is influenced by additional activators and/or inhibitors of Rac1.

Expression of MgcRacGAP is decreased in double-KD cells, and rescue of normal levels of MgcRacGAP expression results in decreased Rac1 activation and delayed TJ barrier development

We postulated that rescue of Rac1 activation in double-KD cells could be due to either increased expression of a Rac1 GEF or decreased expression of a Rac1 GAP. So we examined the expression of Rac1 GEFs and GAPs, which are associated with junctional proteins such as Asef (Muroya *et al.*, 2007), RICH1 (Wells *et al.*, 2006), MgcRacGAP (Ratheesh *et al.*, 2012), and Vav2 (Noren *et al.*, 2000). By quantitative real-time (RT) PCR, the expression of Asef and RICH1 was not significantly altered in double-KD cells when compared with WT cells (Figure 2A and Supplemental Figure S1C). In contrast, expression of Vav2 and MgcRacGAP was significantly decreased in double-KD cells compared with WT cells (Figure 2A and Supplemental Figure S1C). Because decreased expression of Vav2 (an activator of Rac1) could not explain the increased Rac1

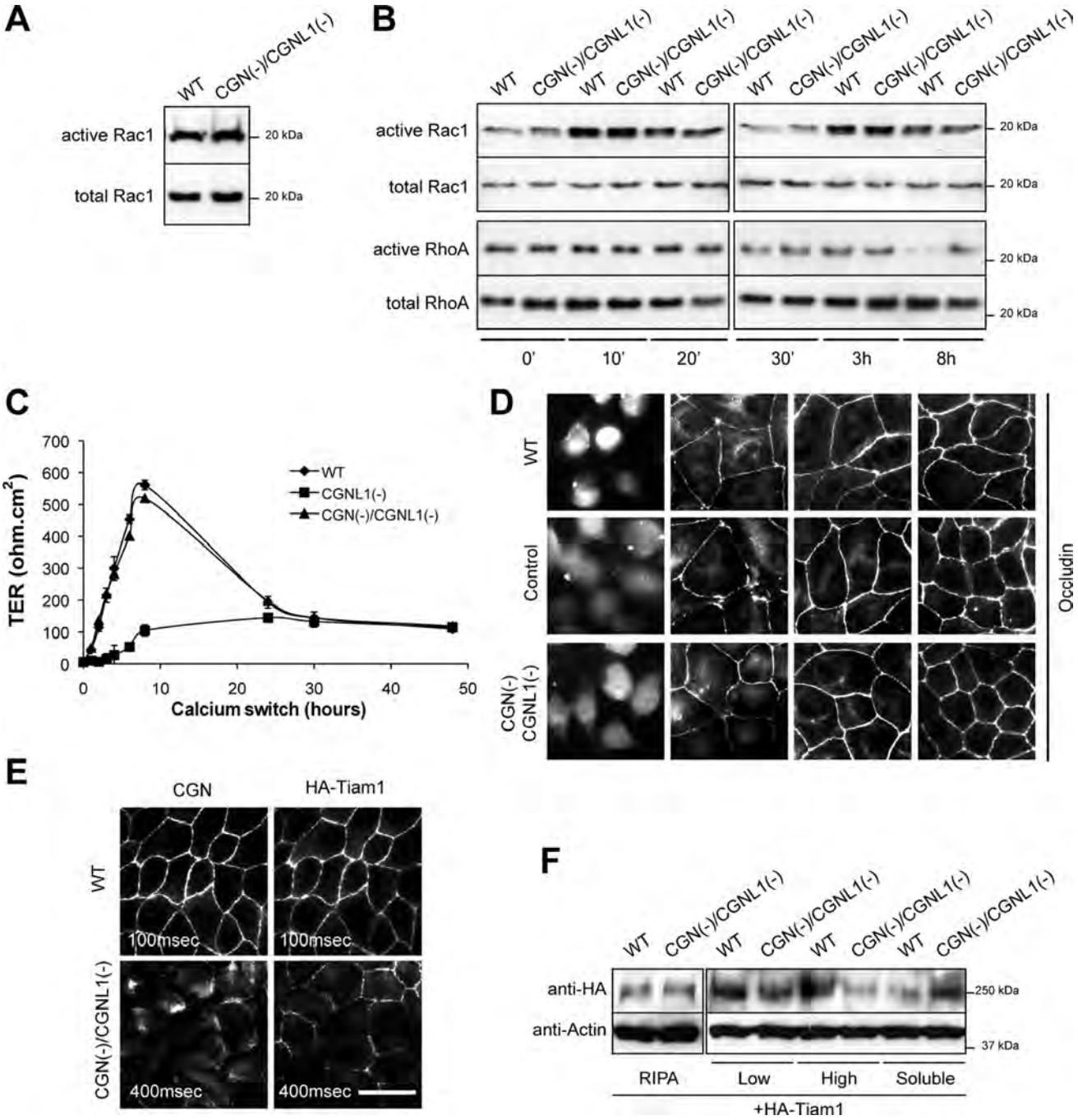

FIGURE 1: CGN(–)/CGNL1(–) (double-KD) cells show normal Rac1 activation and TJ assembly, despite reduced junctional Tiam1. (A, B) Rac1 activation at steady-state (A) and Rac1 and RhoA activation during the calcium switch (B), as determined by GST pull-down analysis. (C) TER (ohm·cm^2) of WT, single-KD (CGNL1(–)), and double-KD (CGN(–)/CGNL1(–)) cells during the calcium switch. (D) Occludin immunofluorescence, showing a similar pattern of occludin accumulation at junctions in WT, control, and double-KD cells during the calcium switch (for single-KD CGNL1(–), see Guillemot *et al.*, 2008). (E) Immunofluorescence analysis of exogenous hemagglutinin (HA)-tagged Tiam1 in WT and double-KD cells, showing reduced junctional recruitment of Tiam1 in double-KD cells (exposure time in double-KD cells increased fourfold; see key in each panel). Bar, 10 μm. (F) Immunoblotting with anti-HA (exogenous Tiam1) and anti-actin antibodies of fractionated lysates of WT and double-KD cells (Guillemot *et al.*, 2008). See Supplemental Figure S1 for additional data on single-KD cells.

activation in double-KD versus CGNL1(–) cells, we focused on MgcRacGAP, a GAP that is ~30-fold more active against Rac1 and Cdc42 than RhoA (Toure *et al.*, 1998). Immunoblotting analysis demonstrated that MgcRacGAP expression was decreased at both the mRNA and protein levels in double-KD cells compared with WT cells (Figure 2, B and C) and to either single-KD, CGN(–), or CGNL1(–) cells (Supplemental Figure S1D). Furthermore, analysis of fractionated lysates showed that the decrease in MgcRacGAP levels was observed only in the low-speed insoluble fraction (Figure 2B and Supplemental Figure S1D), suggesting decreased association with the cytoskeleton. The reduced mRNA and protein levels for MgcRacGAP in stable double-KD cells may be due to altered

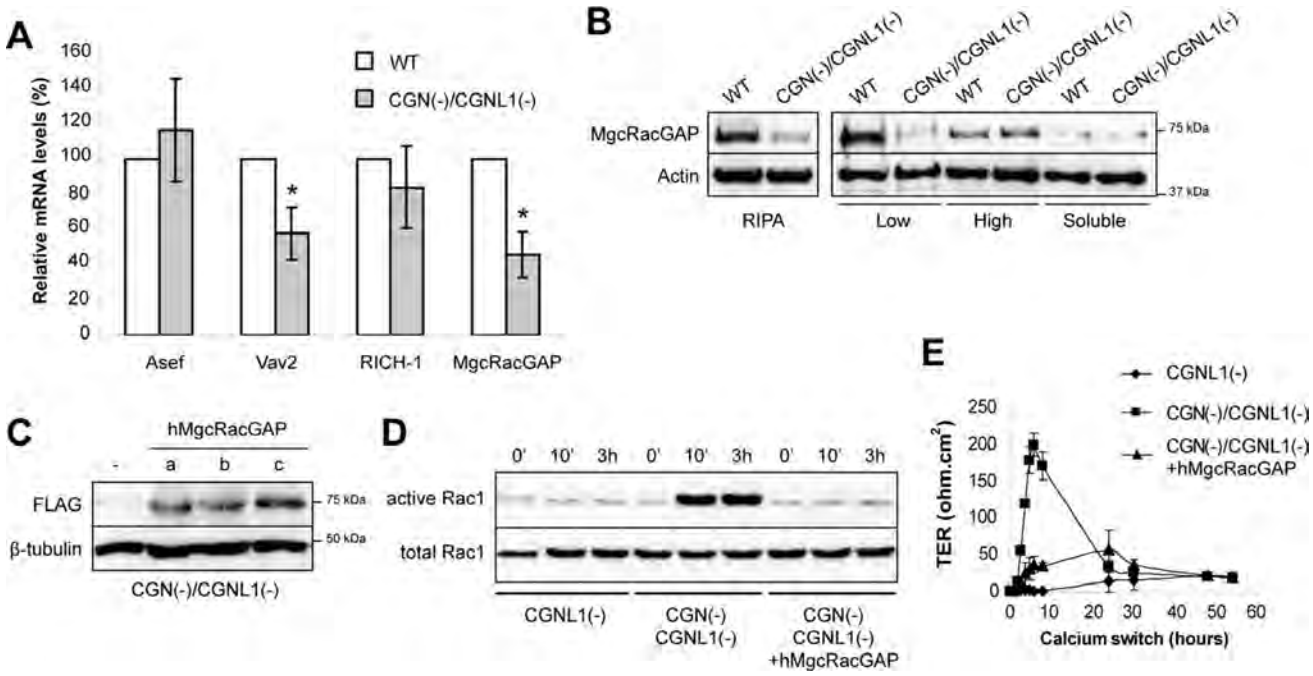

FIGURE 2: MgcRacGAP levels are reduced in double-KD MDCK cells, and rescue of MgcRacGAP expression inhibits Rac1 activation and the peak in TER during development of the TJ barrier. (A) Histogram showing the relative mRNA levels for Asef, Vav2, Rich-1, and MgcRacGAP in double-KD cells vs. WT cells, taking WT levels as 100, as determined by quantitative RT-PCR. (B) Immunoblotting analysis of either total lysates (RIPA) or fractionated lysates of WT and double-KD cells. Low, pellet after centrifugation at low speed (13,000 × *g*). High, pellet after high-speed (100,000 × *g*) centrifugation of the supernatant obtained after low-speed centrifugation. Soluble, Triton-soluble supernatant after centrifugation at 100,000 × *g* of the low-speed supernatant. (C) Immunoblotting of total (RIPA) lysates from three independent double-KD rescue clones (a–c) stably expressing or not (–) an exogenous human (h) FLAG-tagged MgcRacGAP. (D) Rac1 activation in either single-KD (CGNL1(–)) or double-KD cells expressing (clone a) or not the exogenous MgcRacGAP protein during the calcium switch. Clones b and c are shown in Supplemental Figure S1E. (E) TER profile in the calcium switch for the stable clones described in D. Clones b and c are shown in Supplemental Figure S1F.

transcriptional regulation (due to reduced GATA-4 levels; Guillemot *et al.*, 2013; our unpublished results) and additional mechanisms that regulate MgcRacGAP mRNA and/or protein stability, which remain to be investigated.

Next we tested the hypothesis that the decreased expression of MgcRacGAP plays a mechanistic role in the increased Rac1 activation and normal development of the epithelial paracellular permeability barrier of double-KD cells. We established stable lines expressing exogenous FLAG-tagged MgcRacGAP in the background of double-KD cells (Figure 2C) and asked whether the exogenous MgcRacGAP expression could revert the phenotype of double-KD cells to that of CGNL1(–), single-KD cells. GST pull-down analysis of activated Rac1 showed that when exogenous MgcRacGAP was expressed, the increased Rac1 activation detected at different time points during the calcium switch in double-KD cells was suppressed, thus reverting the phenotype to that of single-KD, CGNL1(–) cells (Figure 2D and Supplemental Figure S1E). Furthermore, Rac1 inactivation induced by exogenous MgcRacGAP expression correlated with a strong reduction in the peak of TER detected at 8 h after the calcium switch in double-KD cells, resulting in a phenotype that was similar to that of single-KD, CGNL1(–) cells (Figure 2E and Supplemental Figure S1F). We also attempted to generate stable lines depleted of MgcRacGAP through shRNA expression in order to test directly the role of MgcRacGAP in junction assembly in WT cells. However, such lines could not be isolated, probably due to the essential role of MgcRacGAP in cytokinesis (Glotzer, 2009).

Cingulin and paracingulin are required for efficient junctional recruitment of MgcRacGAP in different types of epithelial cells

Having established that modulating MgcRacGAP expression levels affects Rac1 activation and the dynamics of establishment of the TJ barrier to ions, we asked whether MgcRacGAP is localized at TJs through interaction with CGN, CGNL1, or both. To do this, we examined the localization of MgcRacGAP in epithelial cells in which CGN, CGNL1, or both were depleted through either shRNA or small interfering RNA (siRNA). In addition, we studied the localization of MgcRacGAP in mixed cultures of primary keratinocytes isolated from WT and CGN-KO mice (Figure 3).

In confluent WT MDCK cells, MgcRacGAP staining at junctions was continuous and largely colocalized with CGN (arrows in Figure 3, A, B, and D, and Supplemental Figure S2). However, in dividing cells, only MgcRacGAP and not CGN labeling was detected in the mitotic spindle (inset in Figure 3A, WT). In addition, unlike CGN and CGNL1, MgcRacGAP was also detected in the nucleus (marked "n" in Figure 3 and Supplemental Figure S2). In mixed cultures of WT MDCK cells, together with either CGN-KD or double-KD stable clonal cells (WT+dKD), MgcRacGAP labeling at junctions was reduced, albeit not abolished, in junctions between KD cells compared with junctions between WT cells (double arrowheads in Figure 3A). A similar reduction of junctional MgcRacGAP labeling was obtained by depleting CGN in MDCK cells, using siRNA instead of shRNA (Supplemental Figure S2A).

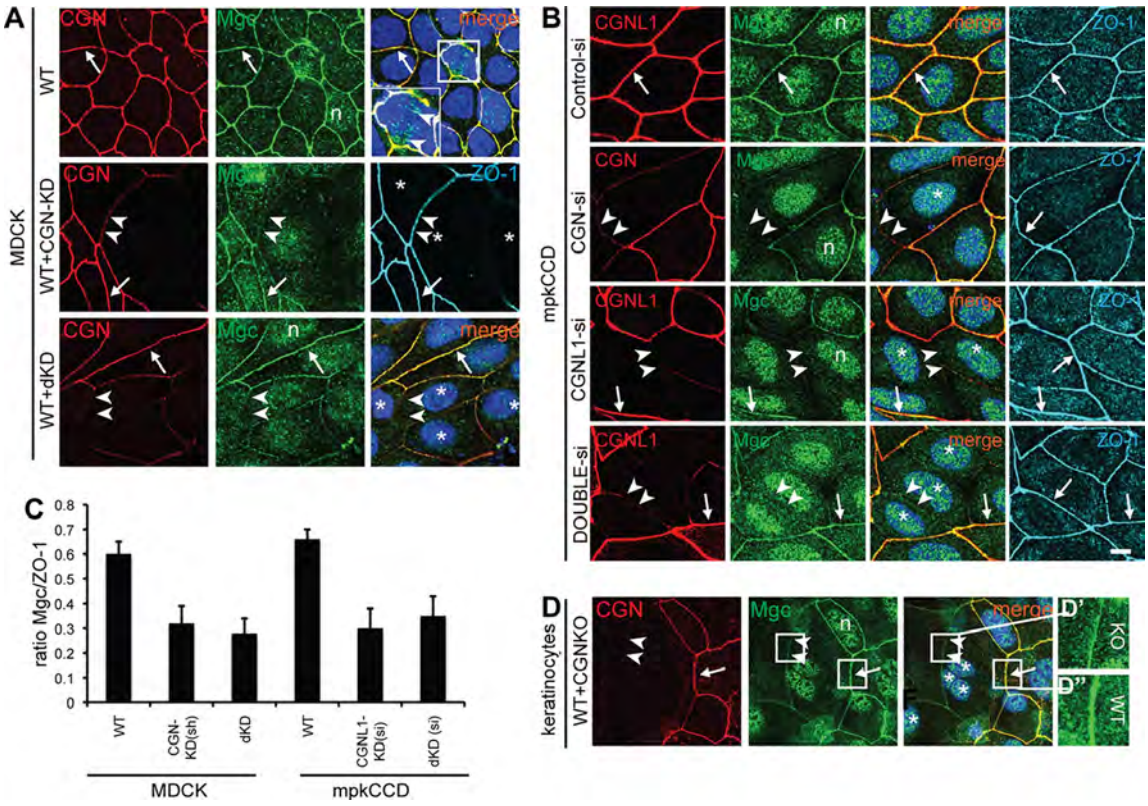

FIGURE 3: CGN and CGNL1 are required for the efficient recruitment of MgcRacGAP to epithelial junctions. (A, B) Double immunofluorescence of CGN and MgcRacGAP (Mgc) in WT MDCK cells in cocultures of WT and CGN-KD MDCK cells, WT and double-KD MDCK cells (A), or mouse kidney ($mpkCCD_{Cl4}$) cells, after siRNA control, si-CGN, si-CGNL1, and si-double (CGN and CGNL1) treatment. Cells were labeled also with rat anti–ZO-1 to identify junctions. Arrows, junctions labeled by both MgcRacGAP and CGN antibodies. Double arrowheads, junctions with decreased labeling for both CGN and MgcRacGAP and normal labeling for ZO-1. The square area in A and magnified inset shows labeling for MgcRacGAP (arrowheads) in the mitotic spindle. Asterisks, positions of nuclei of KD cells. Single arrowheads, junctions with reduced CGNL1 staining and normal MgcRacGAP staining. n, nuclear labeling for MgcRacGAP. (C) Semiquantitative analysis of junctional labeling intensity for MgcRacGAP (expressed as a ratio of MgcRacGAP to ZO-1 pixel intensity in the same junctional areas) in WT, CGN-KD, dKD junctions of MDCK clonal lines or WT, CGNL1-KD, dKD si-treated mouse kidney cells. (D) Double immunofluorescence of CGN and MgcRacGAP in cocultures of primary keratinocytes derived from either WT or CGN KO mice. Magnified insets in D′ and D″ show intensity-adjusted images of junctions, to show the lower levels (but not absence) of MgcRacGAP in junctional areas between KO cells (D′) vs. junctions between WT cells (D″). Bar, 5 μm.

To examine the effect of CGNL1 depletion on the junctional localization of MgcRacGAP, we used mouse kidney cells ($mpkCCD_{Cl4}$) because the mouse anti-CGNL1 antibody required for double immunofluorescence with rabbit anti-MgcRacGAP does not recognize canine CGNL1. In mouse kidney cells, depletion of CGN, CGNL1, or both by siRNA resulted in reduced but not absent junctional staining for MgcRacGAP (Figure 3B). Semiquantitative analysis of MgcRacGAP staining at junctions, expressed as a ratio to ZO-1 staining in the same junctional area, showed a similar decrease, by ~50%, in both single- and double-KD canine and mouse kidney cells (Figure 3C).

As a third cell model system, we examined differentiated keratinocytes isolated from WT and CGN-KO mice and grown in mixed cultures (Figure 3D). Both CGN and MgcRacGAP showed a continuous, linear (zonular), and mostly overlapping labeling of junctions in WT keratinocytes (arrow in Figure 3D). In contrast, in junctions between CGN-KO keratinocytes, MgcRacGAP labeling was decreased but not absent (arrowheads in Figure 3D and magnified insets in Figure 3, D′ and D″), indicating that even in the absence of any junctional CGN, a fraction of MgcRacGAP remains localized at junctions.

To extend our analysis to additional epithelial cell types, we also examined the effect of either CGN or CGNL1 depletion in human intestinal colon carcinoma cells (SKCO-15) and mouse mammary epithelial cells (Eph4). In both of these cell types (and also in MCF-7 cells; unpublished data) depletion of CGN, either alone or in combination with CGNL1 resulted in decreased junctional staining for MgcRacGAP (Supplemental Figure S2, B and C). In contrast, depletion of CGNL1 alone resulted in decreased junctional labeling for MgcRacGAP only in Eph4 (Supplemental Figure S2C) but not in SKCO-15 cells (single arrowhead in Supplemental Figure S2B, CGNL1-si) or human breast cancer (MCF-7) cells (unpublished data).

Taken together, these observations demonstrate that CGN, in all the epithelial cell types we tested, and CGNL1, in all the cell types we tested with the exception of SKCO-15 and MCF-7 cells, are required for the recruitment of MgcRacGAP to the AJC.

Cingulin and paracingulin interact with MgcRacGAP

To explore whether the requirement of CGN and CGNL1 for the junctional recruitment of MgcRacGAP depends on an interaction of MgcRacGAP with these proteins, we carried out immunoprecipitation and GST pull-down experiments. Immunoblot analysis of either

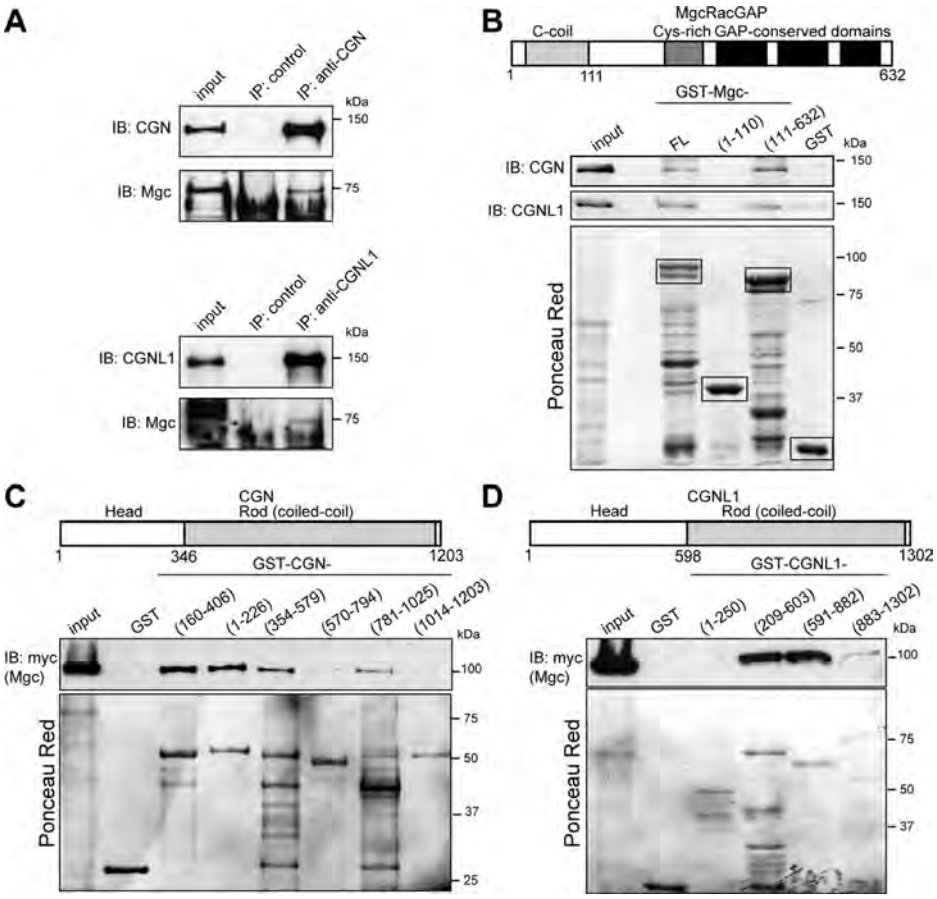

FIGURE 4: CGN and CGNL1 form a complex and interact directly with McRacGAP. (A) Immunoblotting of CGN (top, from MDCK cell lysates) or CGNL1 (bottom, from Eph4 cell lysates) immunoprecipitates, using antibodies against CGN/MgcRacGAP or CGNL1/MgcRacGAP, respectively. Input: 1/40 of volume used for immunoprecipitation. MgcRacGAP shows different mobility and forms in MDCK vs. Eph4 cells. (B) Domain organization of MgcRacGAP and immunoblotting analysis of CGN in GST pull downs of full-length CGN interacting with either full-length (FL) or truncated constructs (1–110, 111–632) of MgcRacGAP fused to GST. (C, D) Domain organization of CGN (C) and CGNL1 (D) and immunoblotting analysis of myc-tagged MgcRacGAP in GST pull downs of the indicated fragments of either CGN or CGNL1 fused to GST. Images of Ponceau red–labeled membranes below immunoblots show protein loadings for GST fusion proteins.

CGN or CGNL1 immunoprecipitates showed that endogenous MgcRacGAP is present in a complex with CGN and CGNL1 in epithelial cells (Figure 4A). Furthermore, specific coimmunoprecipitation was also detected between tagged, exogenously expressed MgcRacGAP, CGN, and CGNL1 in MDCK cells (Supplemental Figure S3).

Next we asked whether MgcRacGAP can interact directly with CGN and CGNL1, by incubating recombinant, bacterially expressed MgcRacGAP constructs with full-length CGN or CGNL1, the latter expressed in baculovirus-infected insect cells. Both CGN and CGNL1 were detected by immunoblotting when either full-length MgcRacGAP or an N-terminally truncated construct of MgcRacGAP (residues 111–632) were used as bait, but not when a fragment containing the coiled-coil domain of MgcRacGAP (1–111) was used (Figure 4B). Thus the region of MgcRacGAP that interacts with CGN and/or CGNL1 is distinct from the region (N-terminal 120 residues) that interacts with ECT2 and MKLP1 (Mishima *et al.*, 2002; Somers and Saint, 2003) and partially overlaps with the sites of interaction with anillin (D'Avino *et al.*, 2008; Gregory *et al.*, 2008) and PRC1 (Ban *et al.*, 2004).

To map the regions of CGN and CGNL1 that interact with MgcRacGAP, we incubated bacterially expressed constructs of either CGN or CGNL1 with myc-tagged MgcRacGAP. In the case of CGN, the strongest binding was observed with fragments of the CGN globular head domain (residues 160–406, 1–226), although fragments of the coiled-coil rod (residues 354–579, 781–1025) also interacted with MgcRacGAP (Figure 4C). In the case of CGNL1, the strongest interaction was observed with the C-terminal two-thirds of the globular head domain (residues 209–603) and the N-terminal one-third of the coiled-coil rod domain (residues 591–882; Figure 4D).

In summary, CGN and CGNL1 form a complex and interact directly with MgcRacGAP.

Cingulin and paracingulin are not required for junctional recruitment of the Rho GEF ECT2

MgcRacGAP interacts with and is required for the junctional recruitment of ECT2, a centralspindlin-associated Rho GEF, at cadherin-based junctions of human breast cancer cells (MCF-7; Ratheesh *et al.*, 2012). Because depletion of either CGN or CGNL1 reduced the junctional localization of MgcRacGAP, we asked whether ECT2 is also affected under these conditions.

The localization of ECT2 was investigated in different types of epithelial cells: canine and mouse kidney cells, mouse primary keratinocytes, human intestinal cells, and mouse mammary epithelial cells (Figure 5 and Supplemental Figure S4). In canine and mouse kidney cells, no junctional labeling for ECT2 could be detected (unpublished data). In keratinocytes, ECT2 labeling was detected at junctions, but it was not zonular like that of MgcRacGAP, and it only partially colocalized with CGN (arrows in Figure 5A, WT, and Supplemental Figure S4B), suggesting that it is associated with the ZA rather than the TJ. In addition, prominent ECT2 labeling was detected along lateral regions of cell–cell contact, clustered along aligned cable-like structures, some of which reached the zonular junctional region, where they apparently connected with continuing cables on the adjoining cells (double arrowheads in Figure 5A, WT, and Supplemental Figure S4A). These observations indicate that ECT2 is distributed along lateral spot-like adherens junctions associated with actomyosin bundles, which terminate at the zonula adhaerens and may be part of a transcellular network across neighboring cells that provides continuity across contractile units (Ebrahim and Kachar, 2013). Of importance, no decrease in ECT2 labeling was observed in CGN-KO keratinocytes (arrowhead in Figure 5A, WT+CGNKO) compared with junctions between WT keratinocytes (arrow in Figure 5A, WT+CGNKO). In SKCO-15 cells (Supplemental Figure S4) and Eph4 cells (unpublished data), labeling for ECT2 was highly heterogeneous in intensity and distribution in different cells, mostly detectable in the cytoplasm and nucleus in a pattern that suggested cell cycle–dependent

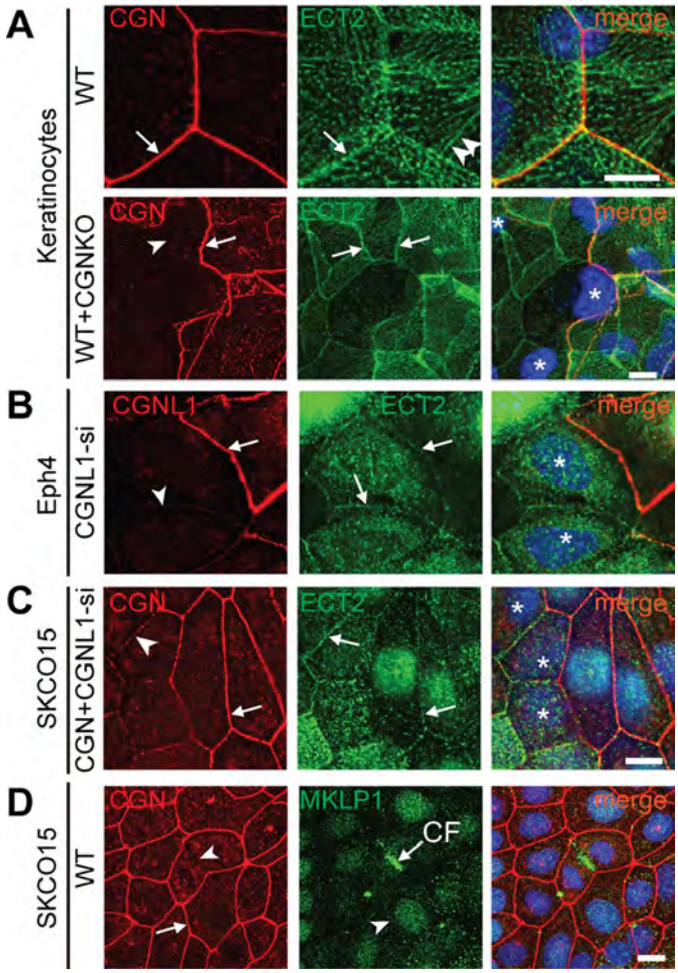

FIGURE 5: Depletion of CGN and CGNL1 does not affect the junctional recruitment of the Rho GEF ECT2. (A) Double immunofluorescence analysis (CGN, red; ECT2, green; 4′,6-diamidino-2-phenylindole [DAPI], blue; in merge images) of WT keratinocytes (top) or mixed cultures of WT and CGN-KO keratinocytes (bottom). Additional images are shown in Supplemental Figure S4A. Note the presence of ECT2 (arrow) in cells lacking CGN (arrowhead). (B, C) Double immunofluorescence analysis (CGN, red; ECT2, green; DAPI, blue; in merge images) of Eph4 cells treated with siRNA against CGNL1 or SKCO-15 cells treated with siRNA against both CGN and CGNL1 (C), showing both WT cells, containing junctional CGNL1/CGN (arrow) and CGNL1(CGN)-depleted cells (arrowhead). Note the presence of ECT2 (arrow) in cells lacking CGNL1/CGN. (D) Double immunofluorescence analysis (CGN, red; MKLP1, green) of confluent SKCO-15 cells, showing that MKLP1 is not detected at junctions (arrow), but only at the cleavage furrow (CF) of dividing cells. Asterisks, positions of nuclei of siRNA-CGN–depleted/KO cells. Single arrowheads, sites with reduced CGN/CGNL1 labeling (KD or KO) but detectable ECT2 labeling. Arrows, junctions between WT cells showing both CGN/CGNL1 and ECT2 labeling. Bar, 5 μm (B–D), 2 μm (A).

expression and localization (Liot *et al.*, 2011; Matthews *et al.*, 2012) and was more rarely detectable at junctions (Supplemental Figure S4). We found no correlation between intensity and distribution of ECT2 labeling and depletion of either CGN or CGNL1 in Eph4 or SKCO-15 cells (Figure 5, B and C, and Supplemental Figure S4B). In human mammary carcinoma cells (MCF-7), labeling for both ECT2 and MgcRacGAP was junctional, and CGN depletion decreased junctional MgcRacGAP, whereas ECT2 was not affected by depletion of either CGN or CGNL1 (unpublished data). These observations indicate that ECT2 distribution is highly variable depending on cell type, the decreased levels of junctional MgcRacGAP in CGN/CGNL1-depleted cells do not correlate with reduced junctional localization of ECT2, and neither CGN nor CGNL1 is required for junctional recruitment of ECT2. This is consistent with the observation that depletion of CGN, CGNL1, or both has no detectable effect on the organization of cadherin-based junctions (Guillemot *et al.*, 2008, 2013; Pulimeno *et al.*, 2011).

Finally, we examined the localization of the kinesin MKLP1 (KIF23), the second subunit of the centralspindlin complex, in SKCO-15 cells, and detected strong labeling only at the cleavage furrow of dividing cells but no junctional labeling in interphase cells (Figure 4D), suggesting that the centralspindlin complex dissociates upon completion of mitosis, and MKLP1 does not associate with junctions.

DISCUSSION

We provide evidence for a new molecular mechanism regulating the activity of Rac1 at epithelial junctions, based on observations on the phenotype of stable MDCK lines depleted of both CGN and CGNL1. Our data indicate that a component of the centralspindlin complex, MgcRacGAP, is involved in regulation of Rac1 activation and dynamics of TJ barrier formation during epithelial junction assembly, and is recruited to apical zonular junctions by CGN and CGNL1. We also provide evidence that the localization of MgcRacGAP in interphase epithelial cells is distinct from that of the second component of the centralspindlin complex, MKLP1, and of ECT2.

MgcRacGAP is a Rac-specific GAP (Toure *et al.*, 1998) fundamental for mammalian viability, since its deficiency in mouse embryos leads to preimplantation lethality (Van de Putte *et al.*, 2001). As a component of the centralspindlin complex, MgcRacGAP plays a critical role during cytokinesis, by regulating assembly of the central spindle, in part by affecting RhoA through the Rho GEF ECT2 (Mishima *et al.*, 2002; Yuce *et al.*, 2005; White and Glotzer, 2012) but mainly by inhibiting Rac1 activity (D'Avino *et al.*, 2004; D'Avino and Glover, 2009; Canman *et al.*, 2008; Bastos *et al.*, 2012). What role, if any, MgcRacGAP plays in Rac1 regulation at junctions of interphase cells has not been determined. A study reported that the centralspindlin complex is localized at the ZA of breast cancer (MCF-7) cells by anchoring with the N-terminus of α-catenin to support ECT2-controlled Rho signaling at junctions (Ratheesh *et al.*, 2012). Here we show that in interphase epithelial cells, MgcRacGAP colocalizes with CGN, a specific marker of TJ, whereas ECT2 is distributed heterogeneously at the ZA, along lateral contacts, and in the cytoplasm/nucleus in different cell types. In addition, whereas depletion of either CGN or CGNL1 results in decreased MgcRacGAP accumulation at junctions, we did not observe any decrease in the junctional localization of ECT2, in apparent disagreement with the idea that MgcRacGAP recruits ECT2 to junctions (Ratheesh *et al.*, 2012), and confirming the lack of effect of CGN/CGNL1 depletion on ZA organization (Guillemot *et al.*, 2004, 2008, 2012, 2013; Guillemot and Citi, 2006a; Pulimeno *et al.*, 2011). However, because even in double-KD kidney epithelial cells we observed residual junctional staining for MgcRacGAP, this discrepancy can be explained by the presence of two pools of MgcRacGAP, one at the TJ, which is recruited by CGN and CGNL1, and one at the ZA, recruited by the α-catenin/E-cadherin complex (Ratheesh *et al.*, 2012; Priya *et al.*, 2013). The proportion of MgcRacGAP that associates with TJ versus ZA, and hence its regulation, may be different in cancer cell lines versus spontaneously immortalized cell lines and may depend on the composition and degree of "maturation" of these junctions. Further studies should characterize the interactions of MgcRacGAP with components of the ZA, and its regulation at the apical junctional

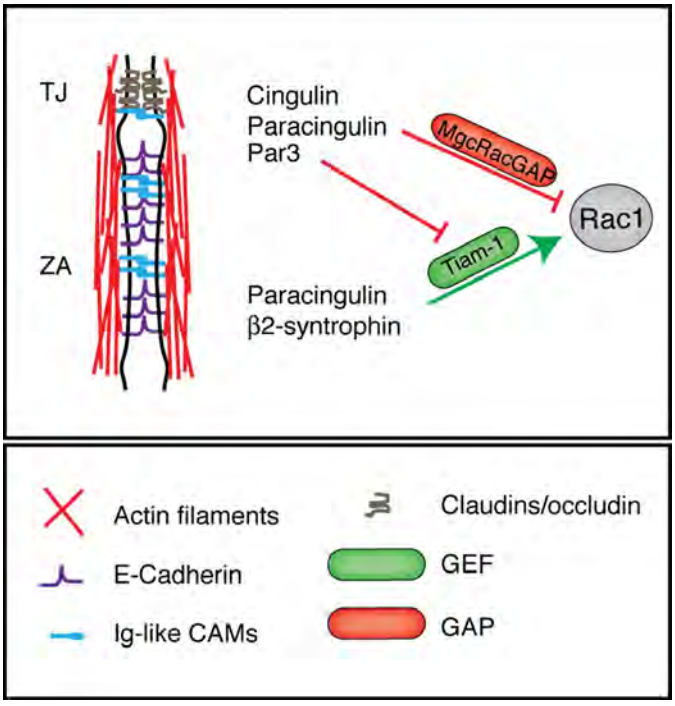

FIGURE 6: The control of Rac1 signaling at the apical junctional complex. Simplified scheme showing the AJC and the putative molecular interactions of GEFs and GAPs with CGN, CGNL1, and other junctional proteins. Green lines indicate activation; red lines indicate inhibition. A key for the graphical objects is shown at the bottom.

complex. On the other hand, our observations on different types of CGN/CGNL1-depleted cells, and the finding that MgcRacGAP forms a complex and interacts directly with CGN and CGNL1 strongly support the idea that CGN and CGNL1 play a major role in recruiting MgcRacGAP to the TJ.

Concerning the function of MgcRacGAP in interphase cells, we show that in double-KD MDCK cells, where MgcRacGAP levels are decreased, RhoA activation during the calcium switch is indistinguishable from WT and single-KD (CGNL1(–)) MDCK cells (Guillemot *et al.*, 2008; present study). In contrast, rescuing MgcRacGAP levels dramatically affects Rac1 signaling during junction assembly, supporting the notion that MgcRacGAP acts primarily on Rac1 and not RhoA signaling (D'Avino and Glover, 2009). The correlation between Rac1 activation and the pattern of TER development in the double-KD cell lines strengthens the idea that Rac1 activation regulates the development of the paracellular barrier to ions. The barrier to ions depends on claudins, which polymerize on a scaffold of cytoplasmic TJ proteins, which are linked directly or indirectly to the actin cytoskeleton (Umeda *et al.*, 2006; Fanning and Anderson, 2009; Citi *et al.*, 2012). Although the precise molecular mechanism that generates the peak in TER observed during junction assembly in MDCK cells is not known, it can be speculated that it is due to a transient, cytoskeleton-dependent "tightening" of the claudin-based barrier, the differential kinetics of assembly of "tight" (barrier) versus "leaky" (pore) claudin isoforms (Kolosov *et al.*, 2014), or a combination of these mechanisms. Because TER development is also modulated by Tiam1, a Rac1 GEF that interacts with Par3 and CGNL1 (Chen and Macara, 2005; Mertens *et al.*, 2005; Guillemot *et al.*, 2008); by RICH1, a Cdc42/Rac1 GAP that interacts with angiomotin (Wells *et al.*, 2006); and by β2-syntrophin, which modulates the localization of Tiam1 and Rac1 along the apicobasal axis (Mack *et al.*, 2012), we conclude that Rac1 is a key regulator of TER development, and we hypothesize that this regulation occurs primarily by controlling cytoskeletal organization and cytoskeletal anchoring of claudins. Of importance, the ability of MgcRacGAP to modulate TJ barrier development must depend on its spatially restricted activity at the cytoplasmic, cytoskeleton-linked "plaque" of the TJ, and our data indicate that this is through its interaction with CGN and CGNL1. Therefore, accumulation of CGN and CGNL1 at TJs during junction maturation provides a mechanism to spatially restrict down-regulation of Rac1 activation at TJs, through recruitment of MgcRacGAP.

Taken together, the results presented here and in previous studies (Aijaz *et al.*, 2005; Guillemot and Citi, 2006a; Guillemot *et al.*, 2008) suggest a working model in which CGN and CGNL1 have multiple functions in fine-tuning RhoA and Rac1 activation in MDCK cells (Figure 6). In confluent cells, they both inhibit RhoA activation by sequestering GEF-H1, whereas during junction assembly, CGNL1 promotes Rac1 activation by supporting junctional recruitment of Tiam1, whereas both CGN and CGNL1 inhibit Rac1 activation at TJ through recruitment of MgcRacGAP. So we propose that the dynamics of junction assembly and TER development result at least in part from a balance between Tiam1-mediated Rac1 activation and MgcRacGAP-mediated Rac1 inhibition. Changes in the levels of expression of either Tiam1 or MgcRacGAP or their interacting partners at junctions, and additional regulatory mechanisms, may affect such equilibrium, resulting in altered spatiotemporal dynamics of junction assembly. To further test this model, it will be necessary to explore in more detail the phenotype of CGN and CGNL1 KO model systems, and the regulation of the molecular interactions between different GEFs, GAPs, and cytoplasmic junctional proteins.

In summary, our data reveal a new mechanism of fine-tuning of junction assembly and development of the TJ barrier, by which MgcRacGAP controls Rac1 activation at apical junctions, where it is recruited through its interaction with CGN and CGNL1. Our results also support the idea that the spatiotemporal control of Rho GTPases is coordinated by the cell context–dependent makeup of GTPase activators and inhibitors and interacting junctional proteins.

MATERIALS AND METHODS

Antibodies and plasmids

Commercial antibodies were purchased against hemagglutinin (Covance, Meyrin, Switzerland), FLAG (M2; Sigma-Aldrich, Buchs, Switzerland), MgcRacGAP (rabbit sc-98617; Santa Cruz), ECT2 (07-1364; Millipore), MKLP1 (sc-867; Santa Cruz), and CGNL1 (mouse sc-162681; Santa Cruz, Muttenz, Switzerland). The mouse anti-CGNL1 antibody did not cross-react with canine CGNL1 and therefore could not be used to immunolocalize CGNL1 in double labeling of MDCK cells with rabbit anti-MgcRacGAP or for immunoprecipitations of CGNL1 from MDCK cells. The rat anti-ZO-1 monoclonal antibody (R40-76) was a kind gift of D. Goodenough (Harvard University, Cambridge, MA). Antibodies against MgcRacGAP (immunoblotting) and a plasmid (pMXs-neo) encoding FLAG-tagged human MgcRacGAP were kind gifts from T. Kitamura (Institute of Medical Science, University of Tokyo, Tokyo, Japan; Hirose *et al.*, 2001) and A. Touré (Institut Cochin, Paris, France; Toure *et al.*, 1998). Secondary antibodies for immunofluorescence (Jackson ImmunoResearch Europe, Newmarket, UK) were Alexa 488 anti-rabbit, Cy3 anti-mouse, and Cy5 anti-rat. Constructs for bacterial expression of MgcRacGAP GST fusion proteins (full-length and truncated) were produced by PCR amplification and subcloning into the pGEX4T1 vector. MgcRacGAP was subcloned into pcDNA3.1myc-His (*Eco*RI-*Not*I) for establishing stable MDCK cell lines. All new constructs were verified by sequencing. Polyclonal antiserum against CGN

(Cardellini *et al.*, 1996), other constructs, and antibodies were as previously described (Guillemot *et al.*, 2004, 2008; Guillemot and Citi, 2006a; Paschoud and Citi, 2008).

Cell culture, transfection, and other techniques

MDCK, SKCO-15 (human intestinal colon carcinoma; a kind gift from A. Nusrat, Emory University, Atlanta, GA; Ivanov *et al.*, 2010), and Eph4 cells (mouse mammary epithelial cells; a kind gift of E. Reichmann, University of Zurich, Zurich, Switzerland; Maschler *et al.*, 2005) were cultured in DMEM containing 10% fetal bovine serum (FBS), nonessential amino acids, and appropriate antibiotics for selection (Guillemot *et al.*, 2013). Mouse kidney collecting duct cells ($mpkCCD_{Cl4}$; a kind gift of E. Feraille, University of Geneva, Geneva, Switzerland; Gonin *et al.*, 2001) were cultured as described previously (Pulimeno *et al.*, 2010). Stable clones of MDCK cells expressing shRNAs to deplete CGN, CGNL1, or both CGN and CGNL1 (double-KD) or rescue MgcRacGAP constructs were obtained as described (Guillemot and Citi, 2006a; Guillemot *et al.*, 2008, 2013). For siRNA-mediated depletion, the following target sequences were used (sense): 1) CGN: GTGACCAGGAGGTGGAACA (human and mouse), AGCTCAGAAGGCTTCCAGA (canine); 2) CGNL1: AGTGGCTGAACTTCAGAGA (human), GACTTAAAGAGCCGGATTA (mouse). Transfections were carried out using Lipofectamine2000 (DNA) and RNAiMax (siRNA), and cells were analyzed by immunofluorescence 48–72 h after transfection. Calcium switch, measurement of TER, Rac1 and RhoA activation assays, immunoblotting, and immunofluorescence were as described (Citi *et al.*, 2001; Guillemot and Citi, 2006a; Guillemot *et al.*, 2008; Paschoud and Citi, 2008).

GST pull downs, immunoprecipitation, and cell fractionation

For GST pull downs, full-length CGN and CGNL1 were from baculovirus-infected insect cells and MgcRacGAP from HEK293 cells transfected with exogenous, myc-tagged MgcRacGAP (Citi *et al.*, 2001; Guillemot *et al.*, 2008). Coimmunoprecipitation experiments were carried out as described (Guillemot *et al.*, 2008), except that lysates were sonicated, and antibodies (2 µg) were incubated with Dynabeads Protein G (ReF. 1004D; Life Technologies Europe, Zug, Switzerland; 20 µl, prewashed three times with phosphate-buffered saline containing 5% skimmed milk) for 1 h at 4°C before incubation with cell lysates (overnight at 4°C) and washing with coimmunoprecipitation buffer. MDCK lysates were used for CGN-MgcRacGAP immunoprecipitations and Eph4 cell lysates for CGNL1-MgcRacGAP immunoprecipitation because the mouse anti-CGNL1 antibody does not cross-react with canine CGNL1. The anti-MgcRacGAP antibody did not work for immunoprecipitation. For fractionation, cells were lysed in cytoskeleton stabilizing buffer (CSK; 10 mM 4-(2-hydroxyethyl)-1-piperazineethanesulfonic acid, pH 6.8, 250 mM sucrose, 150 mM KCl, 1 mM ethylene glycol tetraacetic acid, 3 mM $MgCl_2$, 0.5% Triton X-100, 1 mM phenylmethylsulfonyl fluoride, and protease inhibitor cocktail). The CSK lysate was centrifuged for 15 min at 13,000 × *g*, and the pellet was resuspended, washed with CSK buffer, centrifuged again, and taken as the "low-speed" cytoskeleton fraction. The soluble fraction was centrifuged for 120 min at 100,000 × *g*, and the pellet was washed and taken as the "high-speed" Triton X-100 insoluble cytoskeleton fraction. The supernatant from high-speed centrifugation was taken as the "soluble" fraction. Equivalent protein loadings from each fraction were analyzed by SDS–PAGE and immunoblotting.

Primary keratinocyte cultures

Keratinocytes were isolated from WT and CGN KO (Guillemot *et al.*, 2012) newborn mice, following a protocol approved by the Ethics Committee of the University of Geneva and the Cantonal Veterinary Office (Authorization 1027/3853/53). Skins were dissected and incubated with dispase II (04942078001; Roche), 2.5 U/ml (3.1 mg/ml) at 37°C for 2 h, in low-calcium medium (DMEM/F12 3:1, pH 7.2, supplemented with 15% calcium-free FBS, 100 U/ml penicillin/streptomycin, 0.1 nM choleratoxin, 6×10^{-4} mg/ml hydrocortisone, 5×10^{-3} mg/ml insulin, 5×10^{-3} mg/ml transferrin, and 0.02 nM 3′,5-triiodo-L-thyronine). The epidermis was then separated from the dermis, minced into pieces, and incubated with trypsin 0.25%-1× EDTA (253000062; Invitrogen) for 15 min at 37°C. The cell suspension was filtered through a 70-µm cell strainer and centrifuged at 1500 rpm for 5 min. Cells were seeded at a density of 0.25×10^6 cells/cm^2 and incubated at 37°C in the presence of 5% CO_2. Immunofluorescence analysis of keratinocytes was performed after calcium-induced induction of differentiation, which promotes junction formation: $CaCl_2$ (0.25 M stock) was added to a final concentration of 1.2 mM, and keratinocytes were fixed (cold methanol) for immunofluorescence labeling at different times after calcium addition.

Quantitative RT-PCR

mRNA levels for GEFs and GAPs were analyzed by SYBR green–based RT-PCR (Guillemot and Citi, 2006a; Guillemot *et al.*, 2008, 2013), using the following primers: Asef (ARHGEF4) forward, 5′-GCGGACCAACGTCATCAAC-3′; reverse, 5′-CCCGCAGGTGCTTGATGTA-3′; Vav2 forward, 5′-AAGAACTCAATGACCCCCCTGA-3′; reverse, 5′-AGGTTGATGAAAATGGCTGCC-3′; RICH1 forward, 5′-TGGCAGCGGCTACCTCTG-3′; reverse, 5′-TCGGCGTGCTGAATGATG-3′; MgcRacGAP forward, 5′-TGAATTTGCGGAATCTGTTTGA-3′; reverse, 5′-TGGAGTTCATTTCCTTCACTGAGA-3′.

Confocal microscopy

Cells were observed using Zeiss conventional (Axiovert TV100) and confocal (LSM700) microscopes. For quantification of MgcRacGAP labeling in CGN-KD and double-KD cells, cells were triple labeled with mouse anti-CGN/CGNL1, rabbit anti-MgcRacGAP, and rat anti–ZO-1. ZO-1 was used as an internal reference for junction/plane of focus to exclude the possibility that reduced junctional labeling for MgcRacGAP could be due to shift of plane of focus. For quantifications using ImageJ (National Institutes of Health, Bethesda, MD), for each marker the cytoplasmic area (devoid of junctions) was taken as background and subtracted from the junctional labeling. The mean pixel intensity of MgcRacGAP junctional labeling was measured in junctional segments or representative images in WT, single-KD, and double-KD cells ($n = 5$) and ratioed to ZO-1 labeling in the corresponding junctions (Pulimeno *et al.*, 2011).

Statistical analysis

All experiments were carried out at least in triplicate, and histogram values show means ± SD. Values were considered statistically significant (*) when $p < 0.05$ between experiments (Student's *t* tests). For immunoblots and immunofluorescence data, one representative example is shown.

ACKNOWLEDGMENTS

This study was funded by the Swiss National Science Foundation (Grants31003A_116763,31003A_135730/1,and31003A_152899/1), the Swiss Cancer League (KFS-2813-08-2011), and the Canton and Republic of Geneva. We thank the colleagues cited in the text for kind gifts of reagents.

REFERENCES

Aijaz S, D'Atri F, Citi S, Balda MS, Matter K (2005). Binding of GEF-H1 to the tight junction-associated adaptor cingulin results in inhibition of Rho signaling and G1/S phase transition. Dev Cell 8, 777–786.

Anderson JM, Van Itallie CM (2009). Physiology and function of the tight junction. Cold Spring Harb Perspect Biol 1, a002584.

Ban R, Irino Y, Fukami K, Tanaka H (2004). Human mitotic spindle-associated protein PRC1 inhibits MgcRacGAP activity toward Cdc42 during the metaphase. J Biol Chem 279, 16394–16402.

Bastos RN, Penate X, Bates M, Hammond D, Barr FA (2012). CYK4 inhibits Rac1-dependent PAK1 and ARHGEF7 effector pathways during cytokinesis. J Cell Biol 198, 865–880.

Braga VM, Machesky LM, Hall A, Hotchin NA (1997). The small GTPases Rho and Rac are required for the establishment of cadherin-dependent cell-cell contacts. J Cell Biol 137, 1421–1431.

Canman JC, Lewellyn L, Laband K, Smerdon SJ, Desai A, Bowerman B, Oegema K (2008). Inhibition of Rac by the GAP activity of centralspindlin is essential for cytokinesis. Science 322, 1543–1546.

Cardellini P, Davanzo G, Citi S (1996). Tight junctions in early amphibian development: detection of junctional cingulin from the 2-cell stage and its localization at the boundary of distinct membrane domains in dividing blastomeres in low calcium. Dev Dyn 207, 104–113.

Chen X, Macara IG (2005). Par-3 controls tight junction assembly through the Rac exchange factor Tiam1. Nat Cell Biol 7, 262–269.

Citi S, D'Atri F, Cordenonsi M, Cardellini P (2001). Tight junction protein expression in early *Xenopus* development and protein interaction studies. In: Cell–Cell Interactions, Vol. 256, ed. TP Fleming, Oxford, UK: IRL Press, 153–176.

Citi S, D'Atri F, Parry DAD (2000). Human and *Xenopus* cingulin share a modular organization of the coiled-coil rod domain: predictions for intra- and intermolecular assembly. J Struct Biol 131, 135–145.

Citi S, Paschoud S, Pulimeno P, Timolati F, De Robertis F, Jond L, Guillemot L (2009). The tight junction protein cingulin regulates gene expression and RhoA signalling. Ann NY Acad Sci 1165, 88–98.

Citi S, Pulimeno P, Paschoud S (2012). Cingulin, paracingulin and PLEKHA7: signalling and cytoskeletal adaptors at the apical junctional complex. Ann NY Acad Sci 1257, 125–132.

Citi S, Sabanay H, Jakes R, Geiger B, Kendrick-Jones J (1988). Cingulin, a new peripheral component of tight junctions. Nature 333, 272–276.

Citi S, Spadaro D, Schneider Y, Stutz J, Pulimeno P (2011). Regulation of small GTPases at epithelial cell-cell junctions. Mol Membr Biol 28, 427–444.

D'Avino PP, Glover DM (2009). Cytokinesis: mind the GAP. Nat Cell Biol 11, 112–114.

D'Avino PP, Savoian MS, Glover DM (2004). Mutations in sticky lead to defective organization of the contractile ring during cytokinesis and are enhanced by Rho and suppressed by Rac. J Cell Biol 166, 61–71.

D'Avino PP, Takeda T, Capalbo L, Zhang W, Lilley KS, Laue ED, Glover DM (2008). Interaction between anillin and RacGAP50C connects the actomyosin contractile ring with spindle microtubules at the cell division site. J Cell Sci 121, 1151–1158.

Ebrahim S, Kachar B (2013). Myosin transcellular networks regulate epithelial apical geometry. Cell cycle 12, 2931–2932.

Elbediwy A, Zihni C, Terry SJ, Clark P, Matter K, Balda MS (2012). Epithelial junction formation requires confinement of Cdc42 activity by a novel SH3BP1 complex. J Cell Biol 198, 677–693.

Fanning AS, Anderson JM (2009). Zonula occludens-1 and -2 are cytosolic scaffolds that regulate the assembly of cellular junctions. Ann NY Acad Sci 1165, 113–120.

Furuse M, Tsukita S (2006). Claudins in occluding junctions of humans and flies. Trends Cell Biol 16, 181–188.

Glotzer M (2009). Cytokinesis: GAP gap. Curr Biol 19, R162–165.

Gonin S, Deschenes G, Roger F, Bens M, Martin PY, Carpentier JL, Vandewalle A, Doucet A, Feraille E (2001). Cyclic AMP increases cell surface expression of functional Na,K-ATPase units in mammalian cortical collecting duct principal cells. Mol Biol Cell 12, 255–264.

Gonzalez-Mariscal L, Chavez de Ramirez B, Cereijido M (1985). Tight junction formation in cultured epithelial cells (MDCK). J Membr Biol 86, 113–125.

Gregory SL, Ebrahimi S, Milverton J, Jones WM, Bejsovec A, Saint R (2008). Cell division requires a direct link between microtubule-bound RacGAP and Anillin in the contractile ring. Curr Biol 18, 25–29.

Guillemot L, Citi S (2006a). Cingulin regulates claudin-2 expression and cell proliferation through the small GTPase RhoA. Mol Biol Cell 17, 3569–3577.

Guillemot L, Citi S (2006b). Cingulin, a cytoskeleton-associated protein of the tight junction. In: Tight Junctions, ed. L Gonzalez-Mariscal, New York: Landes Bioscience-Springer Science, 54–63.

Guillemot L, Hammar E, Kaister C, Ritz J, Caille D, Jond L, Bauer C, Meda P, Citi S (2004). Disruption of the cingulin gene does not prevent tight junction formation but alters gene expression. J Cell Sci 117, 5245–5256.

Guillemot L, Paschoud S, Jond L, Foglia A, Citi S (2008). Paracingulin regulates the activity of Rac1 and RhoA GTPases by recruiting Tiam1 and GEF-H1 to epithelial junctions. Mol Biol Cell 19, 4442–4453.

Guillemot L, Schneider Y, Brun P, Castagliuolo I, Pizzuti D, Martines D, Jond L, Bongiovanni M, Citi S (2012). Cingulin is dispensable for epithelial barrier function and tight junction structure, and plays a role in the control of claudin-2 expression and response to duodenal mucosa injury. J Cell Sci 125, 5005–5014.

Guillemot L, Spadaro D, Citi S (2013). The junctional proteins cingulin and paracingulin modulate the expression of tight junction protein genes through GATA-4. PLoS One 8, e55873.

Hall A (2012). Rho family GTPases. Biochem Soc Trans 40, 1378–1382.

Hirose K, Kawashima T, Iwamoto I, Nosaka T, Kitamura T (2001). MgcRacGAP is involved in cytokinesis through associating with mitotic spindle and midbody. J Biol Chem 276, 5821–5828.

Ivanov AI, Young C, Den Beste K, Capaldo CT, Humbert PO, Brennwald P, Parkos CA, Nusrat A (2010). Tumor suppressor scribble regulates assembly of tight junctions in the intestinal epithelium. Am J Pathol 176, 134–145.

Jantsch-Plunger V, Gonczy P, Romano A, Schnabel H, Hamill D, Schnabel R, Hyman AA, Glotzer M (2000). CYK-4: A Rho family GTPase activating protein (GAP) required for central spindle formation and cytokinesis. J Cell Biol 149, 1391–1404.

Jou TS, Schneeberger EE, Nelson WJ (1998). Structural and functional regulation of tight junctions by RhoA and Rac1 small GTPases. J Cell Biol 142, 101–115.

Kolosov D, Chasiotis H, Kelly SP (2014). Tight junction protein gene expression patterns and changes in transcript abundance during development of model fish gill epithelia. J Exp Biol 217 (Pt 10), 1667–1681.

Liot C, Seguin L, Siret A, Crouin C, Schmidt S, Bertoglio J (2011). APC(cdh1) mediates degradation of the oncogenic Rho-GEF Ect2 after mitosis. PLoS One 6, e23676.

Mack NA, Porter AP, Whalley HJ, Schwarz JP, Jones RC, Khaja AS, Bjartell A, Anderson KI, Malliri A (2012). beta2-Syntrophin and Par-3 promote an apicobasal Rac activity gradient at cell-cell junctions by differentially regulating Tiam1 activity. Nat Cell Biol 14, 1169–1180.

Maschler S, Wirl G, Spring H, Bredow DV, Sordat I, Beug H, Reichmann E (2005). Tumor cell invasiveness correlates with changes in integrin expression and localization. Oncogene 24, 2032–2041.

Matthews HK, Delabre U, Rohn JL, Guck J, Kunda P, Baum B (2012). Changes in Ect2 localization couple actomyosin-dependent cell shape changes to mitotic progression. Dev Cell 23, 371–383.

McCormack J, Welsh NJ, Braga VM (2013). Cycling around cell-cell adhesion with Rho GTPase regulators. J Cell Sci 126, 379–391.

Meng W, Takeichi M (2009). Adherens junction: molecular architecture and regulation. Cold Spring Harbor Perspect Biol 1, a002899.

Mertens AE, Rygiel TP, Olivo C, van der Kammen R, Collard JG (2005). The Rac activator Tiam1 controls tight junction biogenesis in keratinocytes through binding to and activation of the Par polarity complex. J Cell Biol 170, 1029–1037.

Mishima M, Kaitna S, Glotzer M (2002). Central spindle assembly and cytokinesis require a kinesin-like protein/RhoGAP complex with microtubule bundling activity. Dev Cell 2, 41–54.

Muroya K, Kawasaki Y, Hayashi T, Ohwada S, Akiyama T (2007). PH domain-mediated membrane targeting of Asef. Biochem Biophys Res Commun 355, 85–88.

Noren NK, Liu BP, Burridge K, Kreft B (2000). p120 catenin regulates the actin cytoskeleton via Rho family GTPases. J Cell Biol 150, 567–580.

Nusrat A, Giry M, Turner JR, Colgan SP, Parkos CA, Carmes D, Lemichez E, Boquet P, Madara JL (1995). Rho protein regulates tight junctions and perijunctional actin organization in polarized epithelia. Proc Natl Acad Sci USA 92, 10629–10633.

Ohnishi H, Nakahara T, Furuse K, Sasaki H, Tsukita S, Furuse M (2004). JACOP, a novel plaque protein localizing at the apical junctional complex with sequence similarity to cingulin. J Biol Chem 279, 46014–46022.

Paschoud S, Citi S (2008). Inducible overexpression of cingulin in stably transfected MDCK cells does not affect tight junction organization and gene expression. Mol Membr Biol 25, 1–13.

Priya R, Yap AS, Gomez GA (2013). E-cadherin supports steady-state Rho signaling at the epithelial zonula adherens. Differentiation 86, 133–140.
Pulimeno P, Bauer C, Stutz J, Citi S (2010). PLEKHA7 is an adherens junction protein with a tissue distribution and subcellular localization distinct from ZO-1 and E-cadherin. PLoS One 5, e12207.
Pulimeno P, Paschoud S, Citi S (2011). A role for ZO-1 and PLEKHA7 in recruiting paracingulin to tight and adherens junctions of epithelial cells. J Biol Chem 286, 16743–16750.
Ratheesh A, Gomez GA, Priya R, Verma S, Kovacs EM, Jiang K, Brown NH, Akhmanova A, Stehbens SJ, Yap AS (2012). Centralspindlin and alpha-catenin regulate Rho signalling at the epithelial zonula adherens. Nat Cell Biol 14, 818–828.
Rossman KL, Der CJ, Sondek J (2005). GEF means go: turning on RHO GTPases with guanine nucleotide-exchange factors. Nat Rev Mol Cell Biol 6, 167–180.
Schmidt A, Hall A (2002). Guanine nucleotide exchange factors for Rho GTPases: turning on the switch. Genes Dev 16, 1587–1609.
Shin K, Fogg VC, Margolis B (2006). Tight junctions and cell polarity. Annu Rev Cell Dev Biol 22, 207–235.
Somers WG, Saint R (2003). A RhoGEF and Rho family GTPase-activating protein complex links the contractile ring to cortical microtubules at the onset of cytokinesis. Dev Cell 4, 29–39.
Takaishi K, Sasaki T, Kotani H, Nishioka H, Takai Y (1997). Regulation of cell-cell adhesion by Rac and Rho small G proteins in MDCK cells. J Cell Biol 139, 1047–1059.
Tcherkezian J, Lamarche-Vane N (2007). Current knowledge of the large RhoGAP family of proteins. Biol Cell 99, 67–86.
Terry SJ, Zihni C, Elbediwy A, Vitiello E, Leefa Chong San IV, Balda MS, Matter K (2011). Spatially restricted activation of RhoA signalling at epithelial junctions by p114RhoGEF drives junction formation and mvhogenesis. Nat Cell Biol 13, 159–166.
Toure A, Dorseuil O, Morin L, Timmons P, Jegou B, Reibel L, Gacon G (1998). MgcRacGAP, a new human GTPase-activating protein for Rac and Cdc42 similar to *Drosophila* rotundRacGAP gene product, is expressed in male germ cells. J Biol Chem 273, 6019–6023.
Umeda K, Ikenouchi J, Katahira-Tayama S, Furuse K, Sasaki H, Nakayama M, Matsui T, Tsukita S, Furuse M, Tsukita S (2006). ZO-1 and ZO-2 independently determine where claudins are polymerized in tight-junction strand formation. Cell 126, 741–754.
Van de Putte T, Zwijsen A, Lonnoy O, Rybin V, Cozijnsen M, Francis A, Baekelandt V, Kozak CA, Zerial M, Huylebroeck D (2001). Mice with a homozygous gene trap vector insertion in mgcRacGAP die during pre-implantation development. Mech Dev 102, 33–44.
Wells CD *et al.* (2006). A Rich1/Amot complex regulates the Cdc42 GTPase and apical-polarity proteins in epithelial cells. Cell 125, 535–548.
White EA, Glotzer M (2012). Centralspindlin: at the heart of cytokinesis. Cytoskeleton (Hoboken) 69, 882–892.
Yamada S, Nelson WJ (2007). Localized zones of Rho and Rac activities drive initiation and expansion of epithelial cell-cell adhesion. J Cell Biol 178, 517–527.
Yuce O, Piekny A, Glotzer M (2005). An ECT2-centralspindlin complex regulates the localization and function of RhoA. J Cell Biol 170, 571–582.

Supplemental Materials

Molecular Biology of the Cell

Guillemot et al.

Legends for Supplementary Figures

Figure S1. The expression of exogenous MgcRacGAP in double-KD cells reduces Rac1 activation and TJ formation during the calcium-switch. **(A):** Rac1 and RhoA activation assays of WT, single-KD (either CGN-KD or CGNL-KD) and double-KD cells at different times after the calcium switch. Note that peaks of Rac1 activation occur at 10', 20', and 3 hr in all cell lines except for CGNL-KD cells, and RhoA activity is down-regulated at 8 hr only in WT cells. **(B):** Transepithelial electrical resistance (TER, ohm.cm^2) of three different stable clones of double-KD CGN(-)/CGNL1(-) cells, showing a peak of TER during the calcium-switch. **(C):** Histogram showing the relative mRNA levels for Asef, Vav22, Rich-1 and MgcRacGAP in WT, single (CGN(-), CGNL1(-)), and double-KD cells, taking WT levels as 100%, as determined by qRT-PCR. **(D):** Immunoblotting analysis of either total lysates (RIPA) or fractionated lysates of WT, CGN(-), CGNL1(-), and double-KD cells with anti-MgcRacGAP. **(E)**: Rac1 activation assays in either single KD (CGNL1(-)) or three independent double-KD cell clones (a, b and c) stably expressing or not (-) an exogenous human (h) FLAG-tagged MgcRacGAP protein, during the calcium-switch assay (0, 10' and 3h time points). **(F):** Pattern of development of TER in three independent double-KD clones expressing (a, b, and c) or not the exogenous human (h) FLAG-tagged MgcRacGAP protein, during the calcium switch.

Figure S2. Effect of CGN and CGNL1 depletion on the localization of MgcRacGAP in different epithelial cell types. Immunofluorescence analysis (CGN/CGNL1-red, MgcRacGAP-green, ZO-1-gray, DAPI-blue) of **(A):** WT MDCK cells, and MDCK cells transfected with either CGN or control siRNA; **(B):** either WT SKCO-15 cells (WT), or a mix of WT cells and cells where either CGN (CGN-si) or both CGN and CGNL1 (CGN+CGNL1-si) were depleted through siRNA expression. The magnified square in the WT merge image shows the partial co-localization of CGN and MgcRacGAP labelling. Note that upon CGNL1 depletion MgcRacGAP is still detectable at junctions (arrow in CGNL1si, green). **(C):** mixes of WT Eph4 cells and Eph4 cells where either CGNL1 (CGNL1-si), CGN (CGN-si) or both CGN and CGNL1 (CGN+CGNL1-si) were depleted through siRNA expression. "n" = nuclear labelling for MgcRacGAP. Asterisks in merge images=siRNA-depleted cells. Double arrowheads= junctions with reduced CGN and MgcRacGAP labelling. Arrows= junctions between WT cells showing both CGN and MgcRacGAP labelling. Bar = 5 µm.

Figure S3. Exogenously expressed MgcRacGAP forms a complex with exogenously expressed CGN or CGNL1. **(A-B):** Immunoblotting analysis of immunoprecipitates of lysates of MDCK cells expressing (+) or not-expressing (-) exogenous myc-tagged MgcRacGAP, and either YFP-tagged CGNL1 ((A) or CGN (B), or YFP-myc (negative control). Immunoprecipitation was carried out using either anti-GFP antibodies, or anti-HA antibodies (negative control), and immunoblotting using anti-MgcRacGAP, to detect immunoprecipitated MgcRacGAP, or anti-myc, to detect exogenously expressed proteins (arrowheads) in IPs. The asterisk indicates a non-specific band, of size smaller than YFP-myc, recognized by the anti-myc antibodies. Note that MgcRacGAP is detected in both CGNL1 and CGN immunoprecipitates. **(C-D):** Immunoblotting analysis, with anti-myc antibodies, of the input of the lysates used for immunoprecipitation in panels A and B, respectively. Arrowheads indicate

migration of YFP-CGNL1 or YFP-CGN, MgcRacGAP-myc, and YFP-myc, from top to bottom. Migration of molecular size markers is indicated on the right (kDa).

Figure S4. Depletion of CGN and/or CGNL1 does not affect the localization of ECT2. Immunofluorescence analysis (CGN/CGNL1-red, ECT2-green, DAPI blue in merge images) of **(A):** mix of WT and CGN-KO keratinocytes, at different times (8 hr, 24 hr, 72 hr) after calcium-induced differentiation (the image WT+KO in Fig. 5 corresponds to the 48 hr time point, and the image WT in Fig. 5 is a magnification of a junction between WT cells in the 24 hr time point). **(B):** SKCO-15 cells: WT, or a mix of WT cells and cells where either CGN (CGN-si) or CGNL1 (CGNL1-si) are depleted through siRNA expression; Control-si was used as a negative control. Heterogeneous cellular labeling for ECT2 is indicated: CF= cleavage furrow; N = nuclear; Cyt = cytoplasmic; Neg= negative cell; Asterisks=KD/KO cells. Arrows= junctions between WT cells showing both CGN/CGNL1 and ECT2 labelling. Bar = 5 µm.

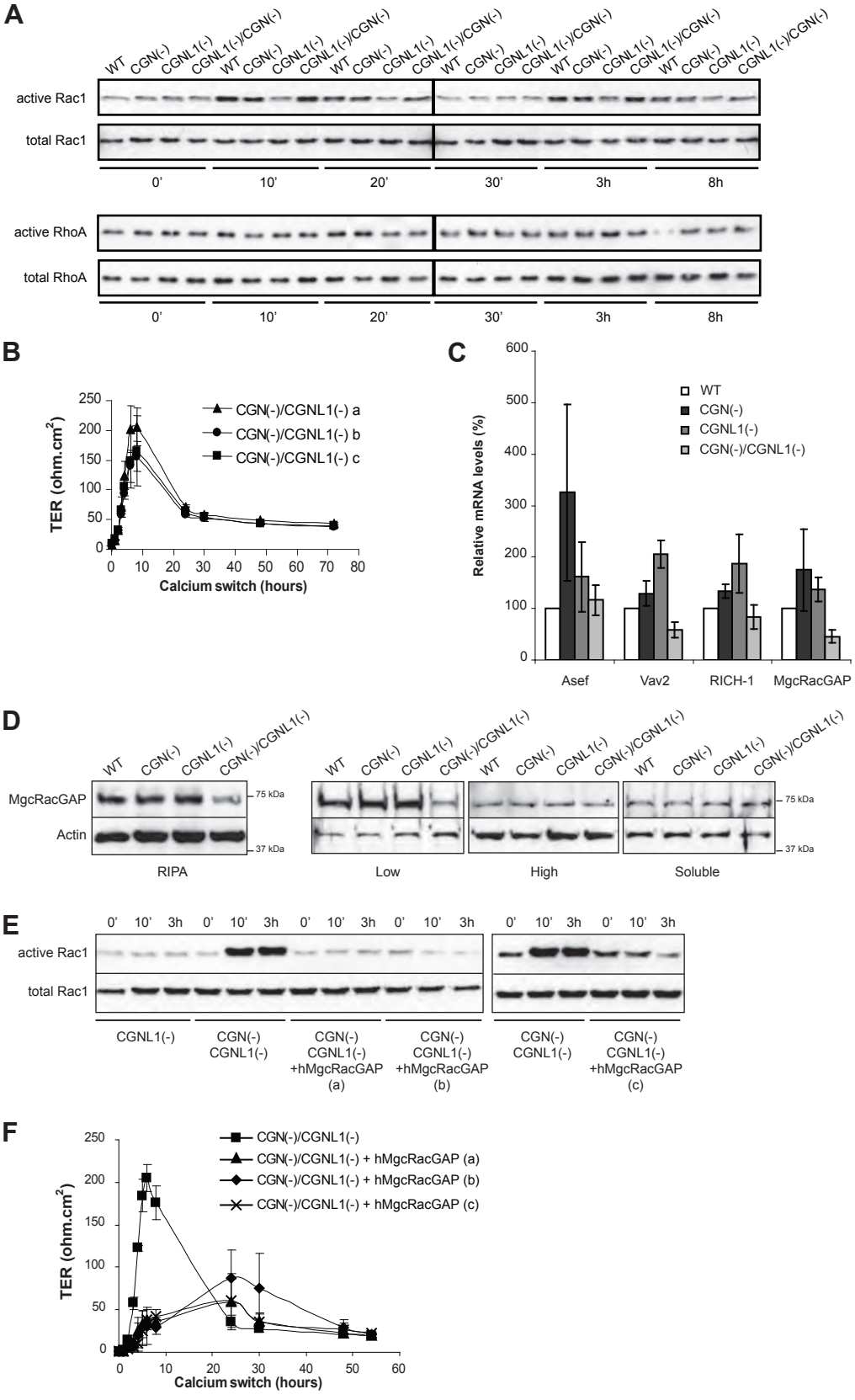

Supplementary Figure 1

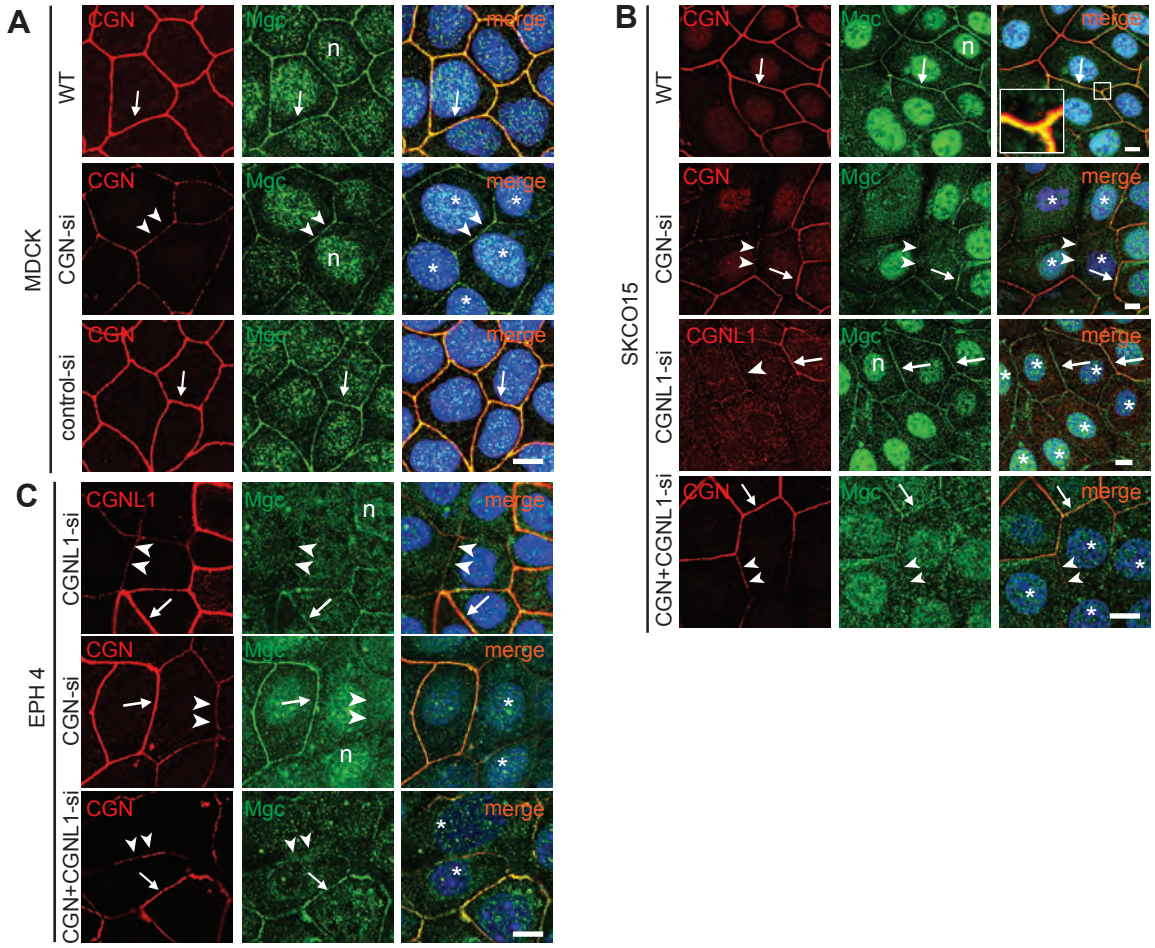

Supplementary Fig. 2

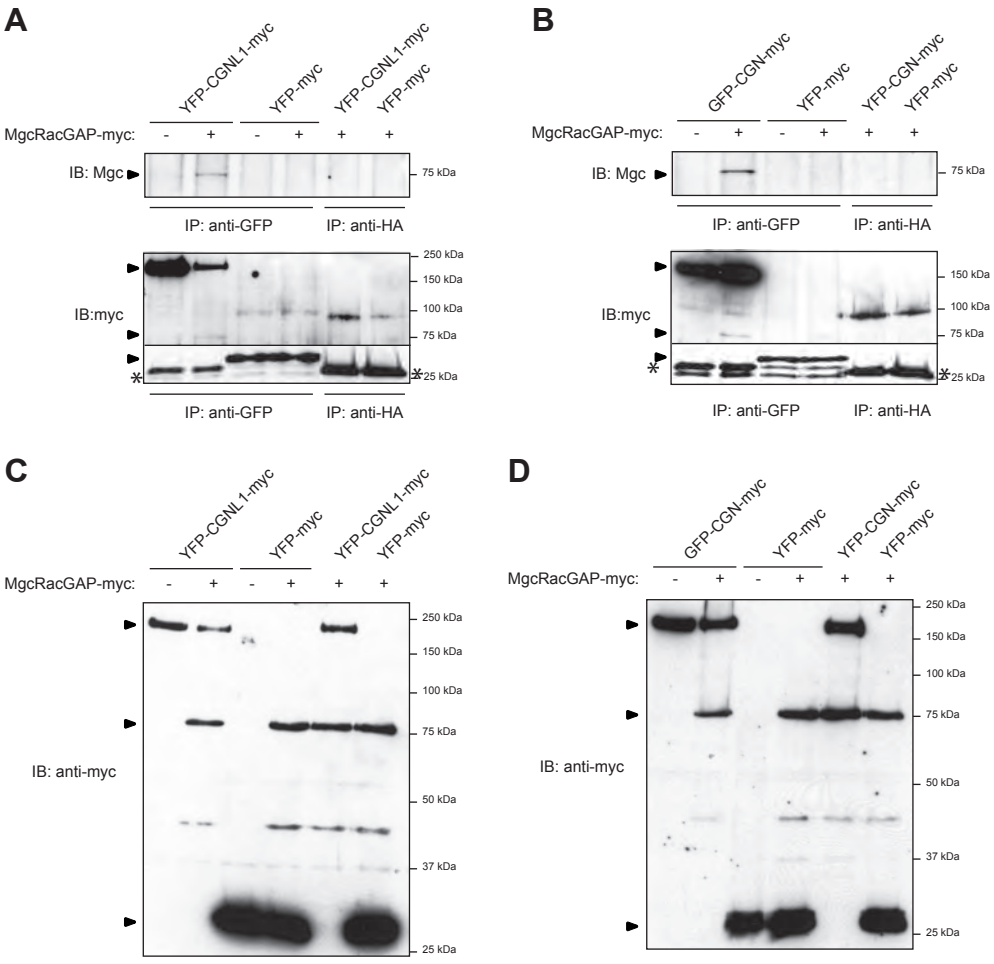

Supplementary Fig. 3

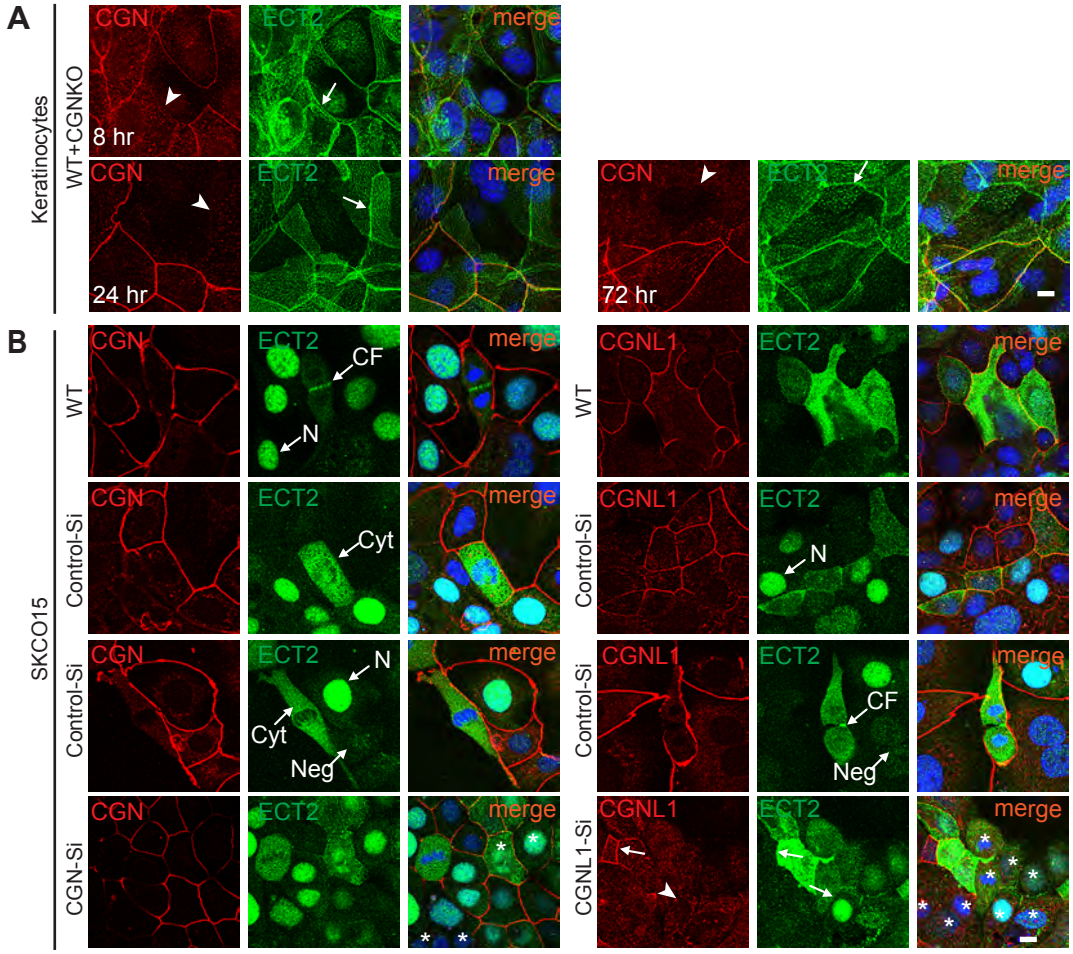

Supplementary Fig. 4

The adherens junctions control susceptibility to Staphylococcus aureus α-toxin

Staphylococcus aureus is a human pathogen, which colonizes the skin and is responsible for skin and soft tissue infections but can also access deeper tissue, causing for example pneumonia. The secretion of α-toxin, a protein that can form pores on the cell membrane and irreversibly injure the cells, leading to their death, mediates the pathogenicity of this bacterium. Through a high throughput genetic screening in human haploid cells (Hap1), several proteins involved in the cytotoxic effect of the α-toxin were identified by our collaborators at Stanford University. Along with the known receptor for the toxin ADAM10, PLEKHA7 and other proteins of adherens junction were found to be involved in the mechanism of action of the α-toxin. PLEKHA7 KO cells are more resistant to intoxication, undergoing cytopathic effects after intoxication that can gradually recover, showing an increased cell survival compared to WT cells. The N-terminal region of PLEKHA7 is sufficient to restore the cytotoxic effects of α-toxin in PLEKHA7 KO cells, the same region that mediates also the interaction with other junctional proteins found in the screening. The involvement of PLEKHA7 in the pathogenesis of *Staphylococcus aureus* infection in vivo was also shown through a PLEKHA7 KO mouse model. PLEKHA7 KO mice showed reduced pathology upon *Staphylococcus aureus* skin infection and an increased recovery and survival upon an acute lethal pneumonia. This study provides evidence that *Staphylococcus aureus* targets junctions and α-toxin acts through adherens junction proteins to mediate its cytotoxicity.

I contributed to this paper helping on the characterization of PLEKHA7 antibodies, reagents that were used to characterize KO cells and tissue models, and study the localization of PLEKHA7 in WT tissues and cells.

The adherens junctions control susceptibility to *Staphylococcus aureus* α-toxin

Lauren M. Popov[a], Caleb D. Marceau[a,1], Philipp M. Starkl[b,1], Jennifer H. Lumb[a], Jimit Shah[c], Diego Guerrera[c], Rachel L. Cooper[a], Christina Merakou[d], Donna M. Bouley[e], Wenxiang Meng[f,g], Hiroshi Kiyonari[h], Masatoshi Takeichi[g], Stephen J. Galli[a,b], Fabio Bagnoli[d], Sandra Citi[c], Jan E. Carette[a,2,3], and Manuel R. Amieva[a,i,2,3]

[a]Department of Microbiology and Immunology, Stanford University School of Medicine, Stanford, CA 94305; [b]Department of Pathology, Stanford University School of Medicine, Stanford, CA 94305; [c]Department of Cell Biology, University of Geneva, 1205 Geneva, Switzerland; [d]Glaxo Smith Kline Vaccines, Società a Responsabilità Limitata, 53100 Siena, Italy; [e]Department of Comparative Medicine, Stanford University School of Medicine, Stanford, CA 94305; [f]Institute of Genetics and Developmental Biology, Chinese Academy of Sciences, 100101 Beijing, China; [g]RIKEN Center for Developmental Biology, Kobe 650-0047, Japan; [h]Animal Resource Development Unit and Genetic Engineering Team, RIKEN Center for Life Science Technologies, Kobe 650-0047, Japan; and [i]Department of Pediatrics, Stanford University School of Medicine, Stanford, CA 94305

Edited by Richard P. Novick, New York University School of Medicine, New York, NY, and approved September 22, 2015 (received for review May 26, 2015)

***Staphylococcus aureus* is both a transient skin colonizer and a formidable human pathogen, ranking among the leading causes of skin and soft tissue infections as well as severe pneumonia. The secreted bacterial α-toxin is essential for *S. aureus* virulence in these epithelial diseases. To discover host cellular factors required for α-toxin cytotoxicity, we conducted a genetic screen using mutagenized haploid human cells. Our screen identified a cytoplasmic member of the adherens junctions, plekstrin-homology domain containing protein 7 (PLEKHA7), as the second most significantly enriched gene after the known α-toxin receptor, a disintegrin and metalloprotease 10 (ADAM10). Here we report a new, unexpected role for PLEKHA7 and several components of cellular adherens junctions in controlling susceptibility to *S. aureus* α-toxin. We find that despite being injured by α-toxin pore formation, PLEKHA7 knockout cells recover after intoxication. By infecting PLEKHA7$^{-/-}$ mice with methicillin-resistant *S. aureus* USA300 LAC strain, we demonstrate that this junctional protein controls disease severity in both skin infection and lethal *S. aureus* pneumonia. Our results suggest that adherens junctions actively control cellular responses to a potent pore-forming bacterial toxin and identify PLEKHA7 as a potential nonessential host target to reduce *S. aureus* virulence during epithelial infections.**

Staphylococcus aureus | α-toxin | adherens junctions | MRSA | PLEKHA7

The bacterium *Staphylococcus aureus* is not only one of the most important human pathogens resulting in considerable morbidity and mortality (1, 2) but also can be found as a transient skin resident, intermittently colonizing a sizable portion of the healthy population (3). *S. aureus* infections manifest in a diverse array of clinical presentations, but related to its transitory epithelial niche, *S. aureus* predominantly results in skin and soft tissue infections (4, 5). Through local infections bacteria can gain access to deeper tissue and disseminate hematogenously to cause invasive disease such as endocarditis, osteomyelitis, deep tissue abscesses, sepsis, and pneumonia (1). In the face of increasing antibiotic resistance, the widespread prevalence of methicillin-resistant *S. aureus* (MRSA) strains both in hospitals and communities across the globe presents a growing threat to human health worldwide (5, 6). Given the growing difficulty of treating these common and frequently life-threatening infections, understanding host–pathogen interactions that mediate *S. aureus* pathogenesis is imperative.

Chief among the arsenal of *S. aureus* virulence factors, α-toxin (or α-hemolysin) is a critical determinant for pathogenesis in a wide variety of experimental infections, particularly during epithelial infections such as skin abscesses and pneumonia (7–10). After secretion as a soluble monomer, α-toxin oligomerizes on the targeted host cell surface via interactions with its high-affinity metalloprotease receptor, a disintegrin and metalloprotease 10 (ADAM10), forming a 1–3-nm pore that spans the cellular membrane lipid bilayer (11, 12). Originally described solely for its ability to induce lysis of erythrocytes, it is now appreciated that α-toxin exerts pleiotropic effects on a diverse set of host cells (13). In addition to inducing cell death, at sublytic concentrations α-toxin has been described to alter a wide variety of cellular processes, including cell signaling, proliferation, immunomodulation, autophagy, and others (13–17).

Importantly, *S. aureus* uses α-toxin to remodel host epithelia and alter tissue integrity. Engagement of α-toxin with ADAM10 leads to intracellular ion flux across the toxin pore, which enhances the proteolytic activity of ADAM10 through an unknown mechanism (18). ADAM10 is essential for tissue morphogenesis and remodeling and acts on a multitude of extracellular substrates (19), one of which is the adherens junction protein E-cadherin (20). It has been proposed that α-toxin–enhanced ADAM10 cleavage of E-cadherin dismantles the adherens junctions to disrupt the integrity of cell–cell contacts in epithelial tissues during infection to contribute to *S. aureus* pathogenesis (18, 21). However, the molecular components that govern intracellular responses elicited by α-toxin in the targeted host cell remain largely undefined.

To advance understanding of how *S. aureus* α-toxin modulates host cell biology, we conducted a high-throughput genetic screen using human cells (22, 23) to discover novel host factors required

Significance

***Staphylococcus aureus* is a major cause of invasive bacterial infection. One prominent virulence factor is α-toxin, a protein that injures the cell by forming a damaging pore across the cell membrane. We conducted a genetic screen to identify host factors that control susceptibility to α-toxin. We discovered that several components of the adherens junction complex modulate α-toxin cytotoxicity. By eliminating expression of the junctional protein plekstrin-homology domain containing protein 7 (PLEKHA7), cells gained the ability to recover from α-toxin injury and mice lacking PLEKHA7 exhibited improved healing from *S. aureus* skin infection and enhanced survival of pneumonia. Our data suggest that targeting nonessential host epithelial junction components can reduce *S. aureus* morbidity by enhancing cellular resilience to α-toxin injury.**

Author contributions: L.M.P., J.E.C., and M.R.A. designed research; L.M.P., C.D.M., P.M.S., J.H.L., and R.L.C. performed research; J.S., D.G., C.M., W.M., H.K., M.T., F.B., S.C., J.E.C., and M.R.A. contributed new reagents/analytic tools; L.M.P., D.M.B., S.J.G., F.B., S.C., J.E.C., and M.R.A. analyzed data; and L.M.P., J.E.C., and M.R.A. wrote the paper.

The authors declare no conflict of interest.

This article is a PNAS Direct Submission.

See Commentary on page 14123.

[1]C.D.M. and P.M.S. contributed equally to this work.

[2]J.E.C. and M.R.A. contributed equally to this work.

[3]To whom correspondence may be addressed. Email: amieva@stanford.edu or carette@stanford.edu.

This article contains supporting information online at www.pnas.org/lookup/suppl/doi:10.1073/pnas.1510265112/-/DCSupplemental.

for α-toxin cytotoxicity. Our screen unexpectedly revealed that multiple components of the cellular adherens junctions modulate susceptibility to α-toxin, suggesting a previously unidentified role for the junctions as critical mediators of α-toxin cytotoxicity—not merely its target. The most significant hit following ADAM10 was plekstrin-homology domain containing protein 7 (PLEKHA7), a cytoplasmic accessory member of the adherens junction complex (24). In PLEKHA7-deficient cells, α-toxin pore formation occurs, but remarkably cells exhibit enhanced recovery from α-toxin injury. Furthermore, we establish the important contribution of PLEKHA7 for *S. aureus* pathogenesis in vivo using MRSA USA300 LAC mouse models of both a self-resolving skin and soft tissue infection and lethal pneumonia.

Results

Human Haploid Genetic Screen Reveals Novel Host Factors Required for α-Toxin Cytotoxicity. To discover host factors required for α-toxin cytotoxicity, we conducted a live/dead genetic screen by intoxicating haploid human cells (HAP1) carrying knockout alleles in essentially all genes through insertional mutagenesis (22, 23). A large-scale library of ∼100 million HAP1 mutagenized cells was treated with recombinant α-toxin, and gene-trap insertion sites were identified in the pool of surviving, toxin-resistant cells. The gene trap insertion sites in the toxin-selected population were compared with a control library that was not exposed to α-toxin (Dataset S1). We identified 46 genes that were significantly enriched in the toxin-treated library ($P < 0.05$) spanning several functional biological categories, suggesting that these genes are essential for α-toxin intoxication (Fig. 1*A* and Dataset S1).

The validity of our screen was confirmed by identification of ADAM10, the α-toxin cell surface metalloprotease receptor (12), which emerged as the most enriched gene in the toxin-selected library (Fig. 1*A*, $P = 7.36 \times 10^{-100}$). Moreover, the screen identified the chaperone protein TSPAN33 (25), which reportedly mediates surface localization of ADAM10 (Fig. 1*A*, $P = 1.09 \times 10^{-25}$). Lipid biogenesis genes, such as sterol response element binding proteins, were also enriched (Fig. 1*A*) and have been attributed roles in cellular innate immune responses against pore-forming toxins (26, 27).

Our screen discovered several genes not previously implicated in α-toxin cytotoxicity. PLEKHA7, the second most enriched gene in our screen (Fig. 1*A*, $P = 1.84 \times 10^{-81}$), is a cytoplasmic, accessory component of adherens junctions (24). PLEKHA7 localizes to the *zonula adhaerens* belt of the apical–junctional complex in epithelial cells, where it directly interacts with p120 catenin, paracingulin, and afadin (24, 28–31). Unlike E-cadherin or p120 catenin, PLEKHA7 is not required for adherens junctions formation, and previous studies suggest a role for PLEKHA7 in regulating the stability of the adherens junctions (24, 28–31). In accord with adherens junctions mediating α-toxin injury, our screen also identified several other junctional components including α-catenin, afadin, and

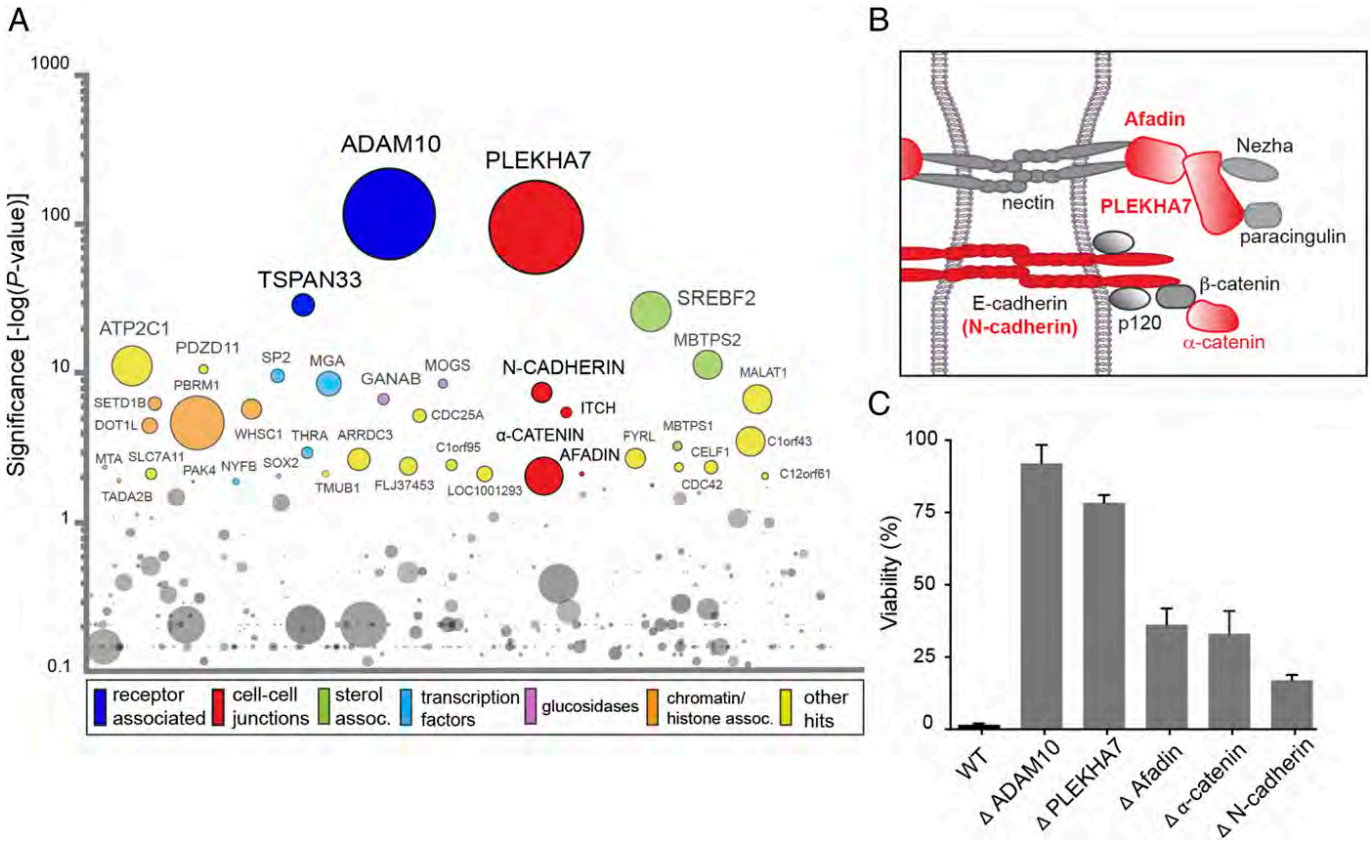

Fig. 1. A haploid genetic screen for cellular host factors required for α-toxin cytotoxicity identifies several components of the adherens junctions. (*A*) A haploid human cell genetic screen identified genes that confer resistance to α-toxin when inactivated by retroviral gene-trap insertion. Each bubble represents a gene, and bubble size corresponds to the number of independent gene-trap insertion events observed in the toxin-selected population. Genes are ranked on the *y* axis according to the significance of enrichment of gene-trap insertions in the α-toxin selected library compared with the nonselected control population (Fisher's exact test, corrected for false discovery rate). Functional groups of significant hits share a common color as indicated and are grouped together horizontally (with other genes in random order along the *x* axis). Gene names are displayed until $P = 0.05$. (*B*) An abridged diagram of the adherens junctional complex. Cell–cell adherens junction proteins found significantly enriched in our α-toxin screen are depicted in red, and associated proteins are shown in gray. (*C*) Viability of WT HAP1 cells or knockout (Δ) HAP1 clones for the indicated genes following treatment with α-toxin (indicated as percentage of nonintoxicated controls; data are mean + SEM; $n = 3$ biological replicates; all differences relative to WT cells are $P = <0.01$, unpaired *t* test).

N-cadherin (Fig. 1 *A* and *B*). Enrichment of inactivating insertions in multiple adherens junctions complex genes in the toxin-resistant library suggested the novel hypothesis that components of the cellular adherens junctions can control susceptibility to *S. aureus* α-toxin. To test this hypothesis, we used CRISPR/Cas9 gene editing to generate HAP1 knockout (Δ) subclone cell lines for multiple adherens junction genes revealed by our screen (Fig. S1). In accord with our screen results, we find that cells individually lacking the junctional proteins PLEKHA7, afadin, α-catenin, and *N*-cadherin are all significantly less susceptible to α-toxin cytotoxicity than WT controls (Fig. 1*C*). Given that PLEKHA7 was the most important junctional gene modulating susceptibility to α-toxin (Fig. 1*C*), we explored its role further.

The Adherens Junction Component PLEKHA7 Controls Susceptibility to α-Toxin. HAP1 cells lacking PLEKHA7 are markedly more resistant to α-toxin cytotoxicity than WT cells at a wide range of toxin concentrations (Fig. 2*A*). Furthermore, stable expression of a human PLEKHA7-FLAG construct *in trans* fully complements α-toxin cytotoxicity in ΔPLEKHA7 cells (Fig. 2*A*). To determine if PLEKHA7 deletion reduces susceptibility in the context of endogenously expressed levels of α-toxin, we treated WT and ΔPLEKHA7 cells with cell-free supernatants from MRSA strain USA300 LAC and an isogenic mutant MRSA strain lacking the α-toxin gene, USA300 LAC *hla::ermB*. This treatment confirmed that ΔPLEKHA7 cells are also more resistant to endogenous α-toxin (Fig. S2). We find that PLEKHA7 deletion does not confer a generalized injury resistance, as ΔPLEKHA7 cells are not more resistant to cytotoxicity caused by either bacterial pore-forming toxins (streptolysin O, perfringolysin O) or the potassium ionophore nigericin (Fig. S3). PLEKHA7's role in modulating α-toxin susceptibility on well-differentiated epithelial cells was further confirmed by testing the effect of α-toxin on a ΔPLEKHA7 cell line in the Madin–Darby Kidney (MDCK) background. MDCK cells are a widely used in vitro model of a simple epithelium and form a polarized monolayer when grown on transwell filters (32). Consistent with our observations made using HAP1 cells, we find that ΔPLEKHA7 MDCK epithelial monolayers are more resistant to α-toxin cytotoxicity than WT MDCK monolayers (Fig. S4).

Next, using PLEKHA7 deletion mutant constructs stably expressed in ΔPLEKHA7 cells (Fig. S5) and subsequently treated with α-toxin, we defined the PLEKHA7 residues necessary and sufficient for restoring α-toxin cytotoxicity to be restricted to the first 538 N-terminal amino acids (Fig. 2 *B* and *C*). This region of

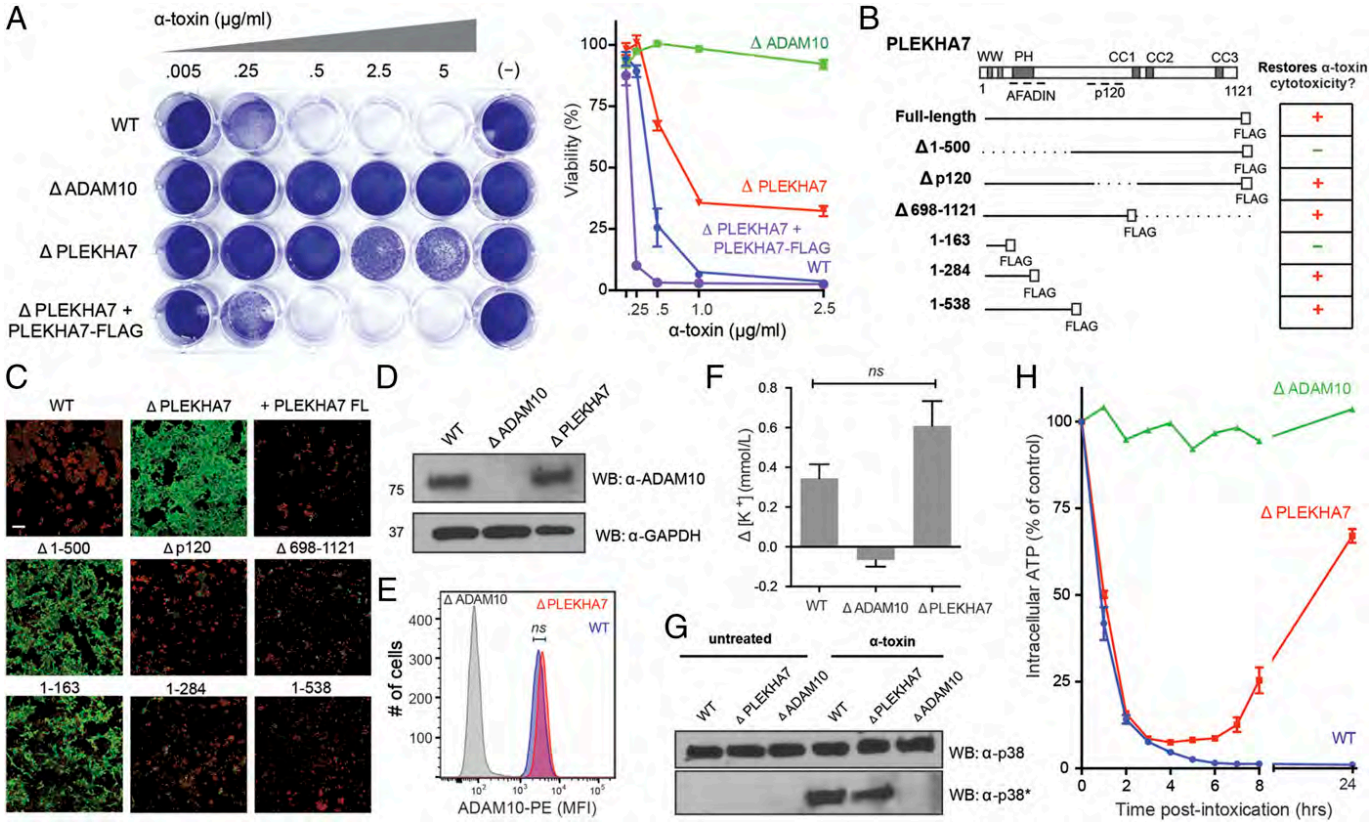

Fig. 2. The adherens junction protein PLEKHA7 controls susceptibility to α-toxin cytotoxicity despite pore formation and cellular injury. (*A*) WT HAP1 cells, knockout (Δ) HAP1 clones, and ΔPLEKHA7 cells stably expressing human PLEKHA7-FLAG were treated with indicated α-toxin concentrations or media only, then subsequently stained with crystal violet (*Left*), or viability was quantified after 24 h of α-toxin treatment (percentage viability shown relative to cell type-specific media controls; data are mean ± SEM; $n = 3$ biological replicates). (*B*) Diagram of deletion human PLEKHA7-FLAG constructs stably expressed by lentiviral transduction in ΔPLEKHA7 HAP1 cells. (*C*) ΔPLEKHA7 HAP1 cells stably expressing the indicated constructs in *B* were treated with α-toxin and 18 h later stained using a fluorescence-based LIVE/DEAD assay, where green fluorescence indicates live cells by esterase activity and red fluorescence demonstrates loss of plasma membrane integrity. (Scale bar, 70 μm.) (*D*) Western blot analysis of ADAM10 and GAPDH expression in whole-cell lysates from WT, ΔADAM10, and ΔPLEKHA7 HAP1 cells. (*E*) Cell surface expression of ADAM10 on WT, ΔADAM10, and ΔPLEKHA7 HAP1 cells as measured by flow cytometric analysis. Data are representative of three independent experiments. (*F*) Change in [K+] in extracellular media following α-toxin treatment of WT, ΔADAM10, and ΔPLEKHA7 HAP1 cells (shown relative to cell type-specific nonintoxicated controls; data are mean ± SEM; $n = 3$ biological replicates; comparison of WT and ΔPLEKHA7, $P = 0.069$, unpaired t test). (*G*) Western blot analysis of p38 and phosphorylated p38 in whole-cell lysates from left (nonintoxicated) and right (α-toxin treated) WT, ΔADAM10, and ΔPLEKHA7 HAP1 cells. Data are representative of three independent experiments. (*H*) Time course of intracellular [ATP] in WT, ΔADAM10, and ΔPLEKHA7 HAP1 cells following α-toxin treatment (shown as percentage of cell type-specific nonintoxicated controls; data are mean ± SEM; $n = 3$ biological replicates).

PLEKHA7 encompasses residues that mediate its interaction with afadin (29)—another junctional protein enriched in our screen (Fig. 1*A*) that modulates α-toxin susceptibility (Fig. 1*C*).

PLEKHA7-Deficient Cells Exhibit Enhanced Resilience to α-Toxin Injury. To interrogate the mechanism underlying PLEKHA7 modulation of α-toxin cytotoxicity, we first assessed whether PLEKHA7 deletion alters expression of the toxin receptor ADAM10. Western blot of whole-cell lysates demonstrates that ΔPLEKHA7 cells express comparable levels of ADAM10 as WT controls (Fig. 2*D*). To determine whether ADAM10 is localized at the plasma membrane in the absence of PLEKHA7, we quantified surface-available ADAM10 by flow cytometry and found no significant decrease in cell surface ADAM10 expression between WT and ΔPLEKHA7 cells (Fig. 2*E*). Consistent with these findings, time-lapse video microscopy reveals that WT and ΔPLEKHA7 cells, but not ΔADAM10 cells, develop cytopathic effects following intoxication. However, we observe that individual ΔPLEKHA7 cells recover from this initial injury and survive intoxication, in contrast to WT cells (Movie S1).

We next sought to determine whether ΔPLEKHA7 cells are more resistant to α-toxin cytotoxicity because of a defect in α-toxin pore formation spanning the targeted host cell surface. To do so, we assessed functional outcomes of pore formation and subsequent cellular injury in α-toxin–treated ΔPLEKHA7 cells using several distinct assays. Rapid efflux of intracellular potassium is an early effect of α-toxin pore formation (33). We observe an increase in extracellular potassium relative to nonintoxicated controls following intoxication of WT and ΔPLEKHA7 cells, but not ΔADAM10 cells (Fig. 2*F*). Another functional consequence of α-toxin injury known to be dependent on pore formation is the activating phosphorylation of the cellular stress response kinase p38 (34). Consistent with cellular injury occurring in the absence of PLEKHA7, we observe α-toxin–dependent p38 activation in WT and ΔPLEKHA7 cells but not ΔADAM10 cells (Fig. 2*G*). Because intracellular ATP depletion is a hallmark of α-toxin damage and ATP repletion is associated with enhanced recovery from α-toxin injury (16, 35), we quantified changes in intracellular ATP levels following intoxication. Shortly after α-toxin treatment, both WT and ΔPLEKHA7 cells quickly deplete intracellular ATP. At later time points, however, only ΔPLEKHA7 cells restore intracellular ATP (Fig. 2*H*). From these studies, we conclude that PLEKHA7 controls susceptibility to α-toxin in a step downstream of ADAM10 recognition and α-toxin pore formation. PLEKHA7 deletion does not strictly prevent damage caused by α-toxin, but rather cells lacking PLEKHA7 exhibit enhanced resilience to and recovery from α-toxin injury.

PLEKHA7 Contributes to the Severity of MRSA Skin and Pneumonia Infections in Vivo. Given α-toxin's critical role in *S. aureus* pathogenesis during skin and lung infections and the expression of PLEKHA7 in epithelial tissues at the adherens junctions, we hypothesized that PLEKHA7 may contribute to *S. aureus* pathogenesis during an in vivo infection. To test the role of PLEKHA7 during MRSA infection, we made use of previously unpublished PLEKHA7$^{-/-}$ whole-body transgenic mice (Fig. S6). Consistent with a recently described PLEKHA7-deficient rat (36), PLEKHA7$^{-/-}$ mice are viable and fecund, exhibiting no gross developmental defects.

We first examined the contribution of PLEKHA7 during a self-limiting MRSA skin and soft tissue infection. In this model, *S. aureus* is superficially introduced into the ear pinnae using a shallow needle, resulting in a necrotic, inflammatory lesion that resolves with tissue loss (37). Confirming the importance of α-toxin for this infection, USA300 LAC *hla::ermB* isogenic mutant infections result in significantly decreased lesion size compared with WT USA300 LAC (Fig. S7). To assess the contribution of PLEKHA7 to disease during a skin and soft tissue infection, we infected WT and PLEKHA7$^{-/-}$ mice with WT USA300 LAC and followed disease development in individual animals over time. We observe that both WT and PLEKHA7$^{-/-}$ mice developed similar-sized necrotic lesions at early time points (Fig. 3 *A* and *B*) indistinguishable by histopathology and bacterial burden (Figs. S8 and S9). However, despite an initial similarity between lesions in WT and PLEKHA7$^{-/-}$ mice, at day 14 postinfection, we found that PLEKHA7$^{-/-}$ mice had resolved the lesions with significantly less tissue loss than WT controls (Fig. 3*B* and Movie S2). Paralleling our in vitro observations at the cellular level, these data support an enhanced recovery phenotype for PLEKHA7$^{-/-}$ mice during a superficial MRSA skin infection.

Upon observing that a self-limiting MRSA skin infection in PLEKHA7$^{-/-}$ mice results in significantly reduced pathology, we sought to assess the importance of PLEKHA7 during an acute, lethal MRSA pneumonia (7, 8). Although both groups developed comparable hypothermia following infection, only PLEKHA7$^{-/-}$ animals showed an enhanced, significant recovery of core temperature by 24 h postinfection, and more animals fully recovered without antibiotic treatment (Fig. 3 *C* and *D*). We find that PLEKHA7$^{-/-}$ mice survived USA300 LAC pneumonia significantly better than WT controls (Fig. 3*D*). To explore the strength of this phenotype, we challenged mice with a threefold higher inoculum and measured similar bacterial loads in lung tissue homogenates at 6 h and 24 h postinfection in both groups (Fig. 3*E*). Despite this higher inoculum, PLEKHA7$^{-/-}$ mice exhibit an increased mean time to death relative to WT control animals (Fig. 3*F*), highlighting the contribution of PLEKHA7 to MRSA pneumonia virulence.

Discussion

S. aureus can transiently and asymptomatically colonize the human skin epithelium and also cause significant morbidity and mortality, predominantly through skin and soft tissue infections that can progress to dangerous systemic disease. Due to the critical importance of *S. aureus* α-toxin for both pathogenesis and its interface with host epithelia, we conducted a genetic screen to identify novel host mediators of α-toxin cytotoxicity. In addition to the toxin receptor ADAM10, our screen identified the intracellular junctional protein PLEKHA7 and several other members of the epithelial adherens junction complex as host factors that modulate α-toxin injury.

Our data suggest a previously unidentified biological role for the adherens junctions in controlling cellular injury caused by a potent bacterial cytotoxin. It is well established that many diverse pathogens and their virulence factors have evolved to target the cellular junctions to facilitate attachment, entry, and invasion across tissue barriers (38–40). Indeed, α-toxin has been shown to alter epithelial barrier integrity by enhancing ADAM10 cleavage of the ectodomain of E-cadherin (18, 21). It is increasingly appreciated, however, that microbial interactions with the host epithelium and cell–cell junctions are not restricted to mechanical disruption of barrier function (39, 41). Mounting evidence illustrates that bacteria can actively modulate other important aspects of junction function, such as altering cell polarity (42–44) and intracellular signals emanating from the junctions (45–47). Our findings build importantly on these observations, revealing not only that *S. aureus* α-toxin does target the junctions but also that α-toxin acts through adherens junctions components to mediate its cytotoxicity. Considering that *S. aureus* is an epithelial colonizer, our data suggest the likely existence of more subtle biological interplay between *S. aureus* and the host adherens junctions at sublytic concentrations of α-toxin to facilitate bacterial modification of its replicative niche during colonization.

Our in vitro studies demonstrate that PLEKHA7 modulates susceptibility to α-toxin in both a human cell line and an in vitro model of a simple, polarized epithelium. Surprisingly, further mechanistic investigations revealed that PLEKHA7 controls susceptibility to α-toxin downstream of functional pore formation, suggesting that pore formation by itself is not sufficient to cause cell death. Rather,

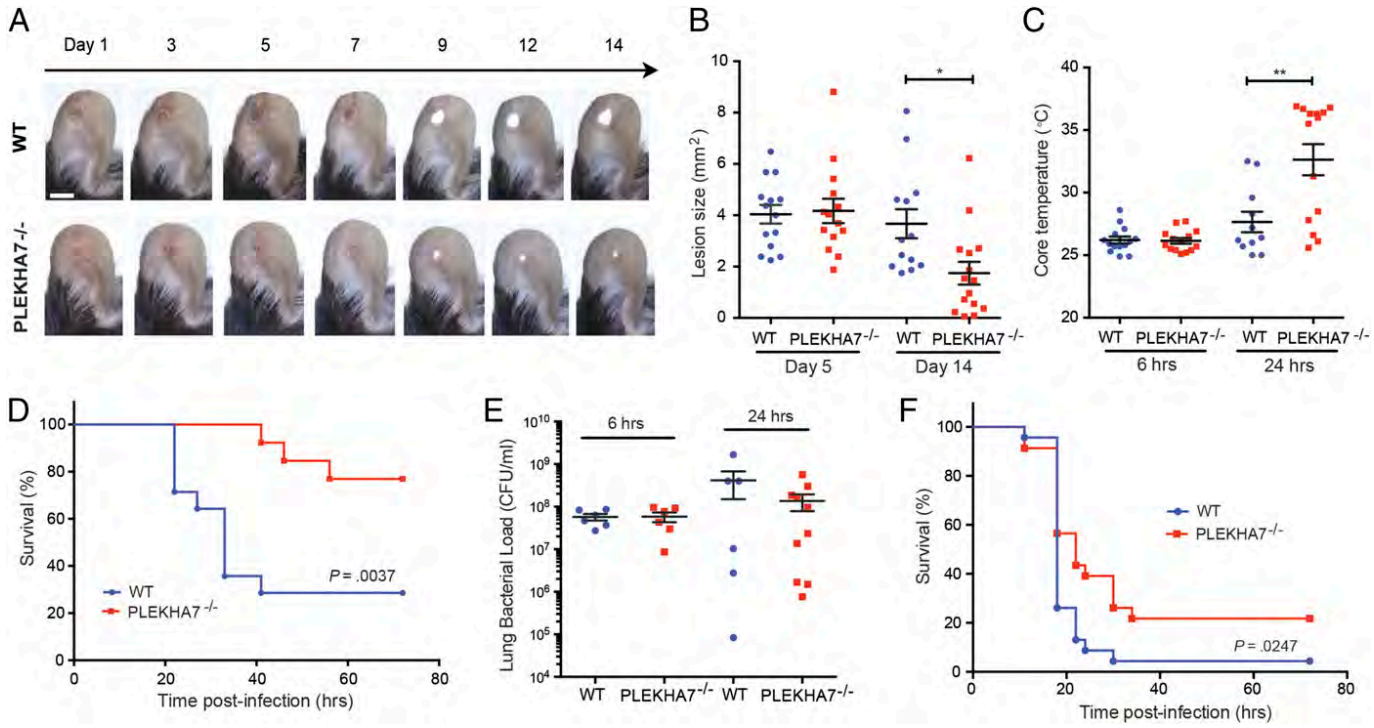

Fig. 3. PLEKHA7 contributes to the severity of MRSA skin and pneumonia infections in vivo. (*A*) Images of ear skin and soft tissue infection progression within individual animals over time from representative WT and PLEKHA7$^{-/-}$ mice following infection with MRSA strain USA300 LAC. (Scale bar, 5 mm for all panels.) (*B*) Lesion size (mm^2) in WT and PLEKHA7$^{-/-}$ mice at day 5 and day 14 in superficial ear infection with USA300 LAC. Data are mean ± SEM from two independent experiments, representing $n = 15$ animals in each group. $P = 0.0116$, unpaired t test. (*C*) Core body temperature of USA300 LAC-infected WT and PLEKHA7$^{-/-}$ mice as shown in *D* at 6 h and 24 h postinfection ($P = 0.0047$, unpaired t test). At 6 h, $n = 14$ animals in each group; at 24 h, $n = 11$ WT and $n = 14$ PLEKHA7$^{-/-}$ animals. (*D*) Survival analysis of PLEKHA7$^{-/-}$ mice and WT controls after infection with *S. aureus* USA300 LAC. $n = 14$ animals in each group; $P = 0.0037$, log-rank test. (*E*) USA300 LAC bacterial density measurements from infected lungs of WT and PLEKHA7$^{-/-}$ mice at 6 h ($n = 6$ animals per group) and 24 h postinfection ($n = 6$ WT animals and 10 PLEKHA7$^{-/-}$; data are mean ± SEM). (*F*) Survival analysis of PLEKHA7$^{-/-}$ mice and WT controls after infection with a threefold higher inoculum of *S. aureus* USA300 LAC than in *D*. $n = 23$ animals in each group; $P = 0.0247$, log-rank test.

we determined that PLEKHA7-deficient cells are more resilient than WT cells and better recover from injury caused by α-toxin, ultimately exhibiting enhanced survival from intoxication. This conclusion is supported by time-lapse video microscopy revealing individual cells recovering from intoxication, as well as population-level assays quantifying cellular viability and the kinetics of intracellular ATP repletion in α-toxin–treated PLEKHA7-deficient cells.

We speculate that adherens junctions may regulate cytotoxicity through controlling resolution of pores and cellular membrane repair, or alternatively may act to transmit prodeath intracellular signals or localize injury caused by pore-forming toxins. PLEKHA7 is known to link microtubules to the adherens junctions and regulate stability of the junctions (24, 30), which may serve to coordinate these hypothesized functions. Our data support a new biological role for intracellular components of the adherens junctions in regulating cellular injury in response to α-toxin, a paradigm that warrants future investigation.

The relevance of PLEKHA7 for determining the outcome of in vivo MRSA bacterial infections was demonstrated in two relevant infection models, a self-resolving skin infection (37) and a lethal pneumonia (7, 8). Some canonical adherens junctions proteins such as E-cadherin and p120 catenin are essential for junction formation, and systemic knockouts are embryonic lethal (48, 49). In contrast, our previously unpublished PLEKHA7$^{-/-}$ mice and a recently described PLEKHA7$^{-/-}$ rat model (36) are healthy and fecund, exhibiting no gross developmental or epithelial pathology. From this we infer that PLEKHA7 is not an essential junctional protein in vivo but rather may serve to regulate some previously unidentified aspect of junction function under specific conditions. We find that systemic PLEKHA7 deletion in vivo attenuates the pathogenicity of the clinically relevant MRSA USA300 LAC strain in mouse models of both a self-resolving skin infection as well as a lethal pneumonia. In both epithelial infection models, we observe an initial similarity in pathology between the WT- and PLEKHA7$^{-/-}$-infected animals; however, at later time points, PLEKHA7$^{-/-}$-infected animals recover better than WT-infected controls. These results suggest that targeting nonessential components of the host adherens junctions could potentially reduce MRSA morbidity by enhancing resilience to and recovery from α-toxin injury. The increasing prevalence of drug-resistant MRSA strains underscores the urgent need to develop host cellular targets of *S. aureus* virulence, which may have future utility as adjunctive therapy.

Materials and Methods

Haploid Human Cell Genetic Screen. HAP1 cells were mutagenized with a retroviral gene trap to cause inactivating mutations throughout the genome, and a haploid genetic screen was performed as previously described (22, 23). For a complete description of the haploid genetic screen, see *SI Materials and Methods*.

Genome Engineering and PLEKHA7 Cloning. Clustered regularly interspaced short palindromic repeats (CRISPR) sequence-targeting sequences were designed using the Zhang Lab CRISPR design tool (crispr.mit.edu), and oligos corresponding to the guide RNA sequences were directly cloned into the Zhang laboratory-generated Cas9-expressing plasmid px458 using the Gibson Assembly Reaction (NEB). A complete description of HAP1 and MDCK genome engineering, guide target sequence oligos, and PLEKHA7 construct cloning is presented in *SI Materials and Methods*.

Bacterial Strains and Culture. The MRSA strain USA300 LAC was kindly provided by Fabio Bagnoli. A detailed description of the generation of the α-toxin isogenic mutant strain *hla::ermB* and the complemented *hla::ermB-phla*

is provided in *SI Materials and Methods*. Bacteria were grown in tryptic soy broth at 37° and prepared as indicated for animal infections.

Generation and Validation of PLEKHA7$^{-/-}$ Transgenic Mice. A detailed description of the generation and validation of *Plekha7(LacZ)* mutant mice is provided in *SI Materials and Methods*.

Murine *S. aureus* Superficial Skin and Pneumonia Infection Models. Murine models of MRSA superficial skin and pneumonia infections were carried out as previously described (7, 8, 37) with minor modifications. Inoculum preparation, infection conditions, and postinfection procedures are fully presented in *SI Materials and Methods*.

Other Procedures. Detailed descriptions of all other procedures are available in *SI Materials and Methods*. Animal experiments were carried out with the approval of the Institutional Animal Care and Use Committees of Stanford University School of Medicine and the RIKEN Center for Developmental Biology.

ACKNOWLEDGMENTS. We thank Stanley Falkow, Denise Monack, and members of the J.E.C., M.R.A., and Monack laboratories for helpful discussion of these data. We thank Thijn Brummelkamp for valuable experimental reagents. This research was supported by a grant from the Child Health Research Institute at Stanford University (to M.R.A.), National Institute of Allergy and Infectious Diseases NIH Award F31AI118212 (to L.M.P.), and a National Science Foundation (NSF) Graduate Research Fellowship (to L.M.P.). J.E.C. is a David and Lucile Packard Foundation fellow and is funded by NIH Grant DP2 AI104557. P.M.S. is supported by a Max Kade Foundation Fellowship, the Austrian Academy of Sciences, and a Schroedinger Fellowship from the Austrian Science Fund (J3399-B21). S.C. is supported by the Swiss Cancer League (KFS-2813-08-2011) and NSF (31003A_135730/1).

1. Lowy FD (1998) Staphylococcus aureus infections. *N Engl J Med* 339(8):520–532.
2. Klein E, Smith DL, Laxminarayan R (2007) Hospitalizations and deaths caused by methicillin-resistant Staphylococcus aureus, United States, 1999-2005. *Emerg Infect Dis* 13(12):1840–1846.
3. Wertheim HFL, et al. (2005) The role of nasal carriage in Staphylococcus aureus infections. *Lancet Infect Dis* 5(12):751–762.
4. Moran GJ, et al.; EMERGEncy ID Net Study Group (2006) Methicillin-resistant S. aureus infections among patients in the emergency department. *N Engl J Med* 355(7): 666–674.
5. Klein EY, Sun L, Smith DL, Laxminarayan R (2013) The changing epidemiology of methicillin-resistant Staphylococcus aureus in the United States: A national observational study. *Am J Epidemiol* 177(7):666–674.
6. DeLeo FR, Otto M, Kreiswirth BN, Chambers HF (2010) Community-associated meticillin-resistant Staphylococcus aureus. *Lancet* 375(9725):1557–1568.
7. Bubeck Wardenburg J, Patel RJ, Schneewind O (2007) Surface proteins and exotoxins are required for the pathogenesis of Staphylococcus aureus pneumonia. *Infect Immun* 75(2):1040–1044.
8. Bubeck Wardenburg J, Bae T, Otto M, Deleo FR, Schneewind O (2007) Poring over pores: α-hemolysin and Panton-Valentine leukocidin in Staphylococcus aureus pneumonia. *Nat Med* 13(12):1405–1406.
9. Kennedy AD, et al. (2010) Targeting of alpha-hemolysin by active or passive immunization decreases severity of USA300 skin infection in a mouse model. *J Infect Dis* 202(7):1050–1058.
10. Kobayashi SD, et al. (2011) Comparative analysis of USA300 virulence determinants in a rabbit model of skin and soft tissue infection. *J Infect Dis* 204(6):937–941.
11. Song L, et al. (1996) Structure of staphylococcal alpha-hemolysin, a heptameric transmembrane pore. *Science* 274(5294):1859–1866.
12. Wilke GA, Bubeck Wardenburg J (2010) Role of a disintegrin and metalloprotease 10 in Staphylococcus aureus α-hemolysin-mediated cellular injury. *Proc Natl Acad Sci USA* 107(30):13473–13478.
13. Berube BJ, Bubeck Wardenburg J (2013) Staphylococcus aureus α-toxin: Nearly a century of intrigue. *Toxins (Basel)* 5(6):1140–1166.
14. Haugwitz U, et al. (2006) Pore-forming Staphylococcus aureus alpha-toxin triggers epidermal growth factor receptor-dependent proliferation. *Cell Microbiol* 8(10): 1591–1600.
15. Hruz P, et al. (2009) NOD2 contributes to cutaneous defense against Staphylococcus aureus through alpha-toxin-dependent innate immune activation. *Proc Natl Acad Sci USA* 106(31):12873–12878.
16. Lizak M, Yarovinsky TO (2012) Phospholipid scramblase 1 mediates type i interferon-induced protection against staphylococcal α-toxin. *Cell Host Microbe* 11(1):70–80.
17. Maurer K, et al. (2015) Autophagy mediates tolerance to Staphylococcus aureus alpha-toxin. *Cell Host Microbe* 17(4):429–440.
18. Inoshima I, et al. (2011) A Staphylococcus aureus pore-forming toxin subverts the activity of ADAM10 to cause lethal infection in mice. *Nat Med* 17(10):1310–1314.
19. Saftig P, Reiss K (2011) The "A Disintegrin and Metalloproteases" ADAM10 and ADAM17: Novel drug targets with therapeutic potential? *Eur J Cell Biol* 90(6-7): 527–535.
20. Maretzky T, et al. (2005) ADAM10 mediates E-cadherin shedding and regulates epithelial cell-cell adhesion, migration, and beta-catenin translocation. *Proc Natl Acad Sci USA* 102(26):9182–9187.
21. Inoshima N, Wang Y, Bubeck Wardenburg J (2012) Genetic requirement for ADAM10 in severe Staphylococcus aureus skin infection. *J Invest Dermatol* 132(5):1513–1516.
22. Carette JE, et al. (2009) Haploid genetic screens in human cells identify host factors used by pathogens. *Science* 326(5957):1231–1235.
23. Carette JE, et al. (2011) Global gene disruption in human cells to assign genes to phenotypes by deep sequencing. *Nat Biotechnol* 29(6):542–546.
24. Meng W, Mushika Y, Ichii T, Takeichi M (2008) Anchorage of microtubule minus ends to adherens junctions regulates epithelial cell-cell contacts. *Cell* 135(5):948–959.
25. Haining EJ, et al. (2012) The TspanC8 subgroup of tetraspanins interacts with A disintegrin and metalloprotease 10 (ADAM10) and regulates its maturation and cell surface expression. *J Biol Chem* 287(47):39753–39765.
26. Gurcel L, Abrami L, Girardin S, Tschopp J, van der Goot FG (2006) Caspase-1 activation of lipid metabolic pathways in response to bacterial pore-forming toxins promotes cell survival. *Cell* 126(6):1135–1145.
27. Im SS, Osborne TF (2012) Protection from bacterial-toxin-induced apoptosis in macrophages requires the lipogenic transcription factor sterol regulatory element binding protein 1a. *Mol Cell Biol* 32(12):2196–2202.
28. Pulimeno P, Bauer C, Stutz J, Citi S (2010) PLEKHA7 is an adherens junction protein with a tissue distribution and subcellular localization distinct from ZO-1 and E-cadherin. *PLoS One* 5(8):e12207.
29. Kurita S, Yamada T, Rikitsu E, Ikeda W, Takai Y (2013) Binding between the junctional proteins afadin and PLEKHA7 and implication in the formation of adherens junction in epithelial cells. *J Biol Chem* 288(41):29356–29368.
30. Citi S, Pulimeno P, Paschoud S (2012) Cingulin, paracingulin, and PLEKHA7: Signaling and cytoskeletal adaptors at the apical junctional complex. *Ann N Y Acad Sci* 1257: 125–132.
31. Paschoud S, Jond L, Guerrera D, Citi S (2014) PLEKHA7 modulates epithelial tight junction barrier function. *Tissue Barriers* 2(1):e28755.
32. Rodriguez-Boulan E, Nelson WJ (1989) Morphogenesis of the polarized epithelial cell phenotype. *Science* 245(4919):718–725.
33. Walev I, et al. (1993) Staphylococcal alpha-toxin kills human keratinocytes by permeabilizing the plasma membrane for monovalent ions. *Infect Immun* 61(12): 4972–4979.
34. Husmann M, et al. (2006) Differential role of p38 mitogen activated protein kinase for cellular recovery from attack by pore-forming S. aureus alpha-toxin or streptolysin O. *Biochem Biophys Res Commun* 344(4):1128–1134.
35. Walev I, et al. (1994) Recovery of human fibroblasts from attack by the pore-forming alpha-toxin of Staphylococcus aureus. *Microb Pathog* 17(3):187–201.
36. Endres BT, et al. (2014) Mutation of Plekha7 attenuates salt-sensitive hypertension in the rat. *Proc Natl Acad Sci USA* 111(35):12817–12822.
37. Prabhakara R, et al. (2013) Epicutaneous model of community-acquired Staphylococcus aureus skin infections. *Infect Immun* 81(4):1306–1315.
38. Vogelmann R, Amieva MR, Falkow S, Nelson WJ (2004) Breaking into the epithelial apical-junctional complex—News from pathogen hackers. *Curr Opin Cell Biol* 16(1): 86–93.
39. Sousa S, Lecuit M, Cossart P (2005) Microbial strategies to target, cross or disrupt epithelia. *Curr Opin Cell Biol* 17(5):489–498.
40. Nikitas G, Cossart P (2012) Adherens junctions and pathogen entry. *Subcell Biochem* 60:415–425.
41. Kim M, et al. (2010) Bacterial interactions with the host epithelium. *Cell Host Microbe* 8(1):20–35.
42. Tan S, Tompkins LS, Amieva MR (2009) Helicobacter pylori usurps cell polarity to turn the cell surface into a replicative niche. *PLoS Pathog* 5(5):e1000407.
43. Tan S, Noto JM, Romero-Gallo J, Peek RM, Jr, Amieva MR (2011) Helicobacter pylori perturbs iron trafficking in the epithelium to grow on the cell surface. *PLoS Pathog* 7(5):e1002050.
44. Tran CS, et al. (2014) Host cell polarity proteins participate in innate immunity to Pseudomonas aeruginosa infection. *Cell Host Microbe* 15(5):636–643.
45. Wu S, Morin PJ, Maouyo D, Sears CL (2003) Bacteroides fragilis enterotoxin induces c-Myc expression and cellular proliferation. *Gastroenterology* 124(2):392–400.
46. Pentecost M, Kumaran J, Ghosh P, Amieva MR (2010) Listeria monocytogenes internalin B activates junctional endocytosis to accelerate intestinal invasion. *PLoS Pathog* 6(5):e1000900.
47. Zihni C, Balda MS, Matter K (2014) Signalling at tight junctions during epithelial differentiation and microbial pathogenesis. *J Cell Sci* 127(Pt 16):3401–3413.
48. Larue L, Ohsugi M, Hirchenhain J, Kemler R (1994) E-cadherin null mutant embryos fail to form a trophectoderm epithelium. *Proc Natl Acad Sci USA* 91(17):8263–8267.
49. Davis MA, Reynolds AB (2006) Blocked acinar development, E-cadherin reduction, and intraepithelial neoplasia upon ablation of p120-catenin in the mouse salivary gland. *Dev Cell* 10(1):21–31.
50. Ran FA, et al. (2013) Genome engineering using the CRISPR-Cas9 system. *Nat Protoc* 8(11):2281–2308.
51. Campeau E, et al. (2009) A versatile viral system for expression and depletion of proteins in mammalian cells. *PLoS One* 4(8):e6529.
52. Bae T, et al. (2004) Staphylococcus aureus virulence genes identified by bursa aurealis mutagenesis and nematode killing. *Proc Natl Acad Sci USA* 101(33):12312–12317.
53. Foster TJ (1998) Genetic analysis of staphylococcal virulence. Methods in Microbiology, eds Williams P, Ketley J, Salmond, G (Academic, London), Vol 27, pp 433–454.

Supporting Information

Popov et al. 10.1073/pnas.1510265112

SI Materials and Methods

Eukaryotic Cell Culture. HAP1 cells and isogenic knockout subclone lines were grown in Iscove's modified Dulbecco's Medium (IMDM) (HyClone) supplemented with 10% (vol/vol) FCS, 1× penicillin/streptomycin (Gibco), and 2 mM L-glutamine. HEK-293T cells were used for lentivirus generation and cultured in DMEM (HyClone) supplemented with 10% FCS, 1× penicillin/streptomycin (Gibco), and 2 mM L-glutamine. MDCK II cells (kindly provided by W. James Nelson, Stanford University, Stanford, CA) were grown in DMEM (HyClone) supplemented with 10% FCS and 1× penicillin/streptomycin. Polarized MDCK monolayers were cultured by seeding cells at confluent density onto 12 mm, 0.4-μm pore polycarbonate tissue culture inserts (transwell filters; Corning Costar) and maintained as previously described (42).

Haploid Human Cell Genetic Screen. HAP1 cells were mutagenized with a retroviral gene trap to cause inactivating mutations throughout the genome, and a haploid genetic screen was performed as previously described (22, 23). Recombinant, purified *S. aureus* α-toxin was resuspended in PBS at 0.5 mg/mL (Sigma, lot 111M4048V). Approximately 10^8 gene-trap mutagenized cells were treated with 0.5 μg/mL α-toxin for 48 h. Following selection, surviving HAP1 colonies were expanded and pooled. Genomic DNA from the surviving, expanded cell population was isolated using the QIAamp DNA mini kit (Qiagen). Gene-trap insertion sites were recovered by linear amplification of genomic DNA sequences flanking the proviral DNA insertions and mapped to the human genome by deep sequencing. For each gene, enrichment of inactivating gene-trap insertions in the α-toxin selected pool over an unselected control dataset was determined by a one-sided Fisher's exact test and corrected for false discovery rate as previously described (23).

Genome Engineering. CRISPR sequence targeting oligos were designed using the Zhang Lab CRISPR design tool (crispr.mit.edu). Oligos corresponding to the guide RNA sequences in Table S1 were synthesized (Integrated DNA Technologies). Guide RNA oligos were directly cloned into Zhang laboratory-generated Cas9-expressing plasmid px458 as described (50), a gift from Feng Zhang, Broad Institute of Massachusetts Institute of Technology, Cambridge, MA (Addgene plasmid 48138), using the Gibson Assembly Reaction (New England BioLabs). HAP1 or MDCK cells were transfected with guide RNA encoding px458 plasmids as described in Table S1 using Lipofectamine 2000 according to the manufacturer's guidelines (Life Technologies). For the α-catenin CRISPR knockout cell line generation, the blasticidin resistance gene encoding plasmid pTIA (kindly provided by Thijn Brummelkamp, Netherlands Cancer Institute, Amsterdam, The Netherlands) was transfected along with the α-catenin guide containing px458 plasmid to allow for blasticidin screening-based selection of edited clones.

At 48 h posttransfection, cells were single-cell sorted using a BD InFlux cell sorter at the Stanford Shared FACS facility based on GFP expression into 96-well tissue plates containing cell culture growth media. Single-cell subclones were expanded and genomic DNA isolated for sequence-based genotyping of the targeted exonic sites using the sequencing primers listed in Table S1. Subclones containing frame-shift or large indels were selected for further experimentation, and when possible, gene knockout was confirmed by protein immunoblotting. ΔPLEKHA7 subclones in the diploid MDCK cell line were confirmed by TOPO cloning genomic DNA PCR products and sequencing multiple colonies to verify the editing events in each allele. Multiple independent subclones for each gene knockout were isolated and tested to confirm the reported phenotypes.

PLEKHA7 Cloning and Lentiviral Transduction of Cells. Using Gateway cloning and LR Clonase II (Life Technologies), human PLEKHA7 cDNA (Thermo Scientific, accession no. BC071599) was inserted into the pLenti CMV Puro DEST vector (w118-1). pLenti CMV Puro DEST (w118-1) was a gift from Eric Campeau, University of Massachusetts Medical School, Worcester, MA (Addgene plasmid 17452) and has been previously described (51). Lentivirus was produced and used to transduce the CRISPR/Cas9-generated ΔPLEKHA7 cell line. Two days posttransduction, stable cell lines were selected by treatment with 1 μg/mL puromycin (InvivoGen). To generate PLEKHA7 full-length and deletion mutant constructs, the following primers were used to generate PCR products from the human PLEKHA7 cDNA and then cloned directly into pLenti CMV Puro DEST using the Gibson Assembly Reaction (New England BioLabs). Reverse primers were designed to incorporate a C-terminal 1× FLAG tag sequence. Constructs were generated with the following primers to generate PLEKHA7 constructs: PLEKHA7 full-length, forward 5′ GACTCTAGTCCAGTGTGGTG 3′ and reverse 5′ ATCCAGAGGTTGATTGTCGAG 3′; PLEKHA7 Δ1–284, forward 5′ TGTGGTGGAATTCTGCAGATACCATGTCTCGATCG TCACTGAAGAG 3′ and reverse 5′ ATCCAGAGGTTGATTGTCGAG 3′; PLEKHA7 Δ1–500, forward 5′ TGTGGTGGAATTCTGCAGATACCATGCGAGCCAGCCACCTGAAG AT 3′ and reverse 5′ ATCCAGAGGTTGATTGTCGAG 3′; PLEKHA7 Δ800–1121, forward 5′ GACTCTAGTCCAGTGTGGTG 3′ and reverse 5′ CGGCCGCCACTG TGCTGGATTTACTTATCGTCGTCATCCTTGTAATCGGCTCTTCTGTGTTGCTCCT 3′; PLEKHA7 Δ698–1121, forward 5′ GACTCTAGTCCAGTGTGGTG 3′ and reverse 5′ CGGCCGCCACTGTGCTGGATTTACTTATCGTCGTCATCCTTGTAATCGATGCTCAGTTTGACGTCAG 3′; PLEKHA7 1–163, forward 5′ GACTCTAGTCCAGTGTGGTG 3′ and reverse 5′ CGGCCGCCACTGTGCTGGATTTACTTATCGTCGTCATCCTTGT AATCAACATTGGGGTTCCTCCGAA 3′; and PLEKHA7 1–284, forward 5′ GACTCTAGTC CAGTGTGGTG 3′ and reverse 5′ CGGCCGCCACTGTGCTGGATTTACTTATCGTC GTCATCCTTGTAATCCAGCACCTGTGCAGCCTGGT 3′. To generate the internal deletion construct PLEKHA7 Δp120 (538–696), two PCR products were generated and then assembled into pLenti CMV Puro DEST using the Gibson Assembly Reaction. The N-terminal fragment was generated using the following primers: forward 5′ GACTCTAGTCCAGTGT GGTG 3′ and reverse 5′ GGGGCTGCCGTGCCGGAACT 3′. The C-terminal fragment was generated using the following primers: forward 5′ AGTTCCGGCACGGCAGCCCCAT CTTCTGTGAACAAGACAG 3′ and reverse 5′ ATCCAGAGGTTGATTGTCGAG 3′.

Intoxication and Cell Viability Assays. HAP1 cells were seeded at 30,000 cells per well in 96-well tissue culture plates 1 d before intoxication with 0.5 μg/mL α-toxin. At 24 h postintoxication, viability was determined by CellTiter-Glo luminescent cell viability assay (Promega) according to the manufacturer's guidelines and read with a microplate reader (Tecan). Viability is plotted as a percentage compared with untreated control wells corresponding to each cell line. For macroscopic visualization of cellular viability following intoxication, HAP1 cells were seeded at 300,000 cells per well in 24-well tissue culture plates the day before intoxication and then treated with the indicated concentrations of α-toxin, other toxins (streptolysin O, kindly provided by Andres Lebensohn, Stanford University School of Medicine, Stanford, CA, and perfringolysin O, kindly provided by David Bewslow, Stanford University School of Medicine, Stanford, CA), or the ionophore

nigericin (Sigma). Two days after α-toxin treatment, viable, adherent cells were fixed with 4% (vol/vol) formaldehyde in PBS and stained with crystal violet. For microscopic visualization of cellular viability following intoxication, HAP1 cells were seeded at 50,000 cells per well onto Permanox chamber slides (LabTek) and treated the following day with 5 μg/mL α-toxin. At 24 h following intoxication, cells were washed 1× with PBS, then treated with the LIVE/DEAD viability/cytotoxicity kit according to the manufacturer's guidelines (Life Technologies), and visualized directly with a Zeiss LSM 700 confocal microscope.

WT and Δ PLEKHA7 MDCK cells were seeded onto 0.4 μm 12-well transwell filter cell culture inserts (Corning) at $1.0e^6$ cells per transwell insert and cultured under polarization conditions for 4 d (42). On day 5 postseeding, basolateral media was changed to media containing 2.5 μg/mL α-toxin, and apical media was replaced with plain DMEM containing 1 μm SYTOX 488 (Life Technologies). At 3 h postintoxication, the apical media was washed 5× with plain DMEM to remove excess SYTOX dye before fixation with 2% (vol/vol) paraformaldehyde in 100 mM phosphate buffer (pH 7.4) for 10 min at room temperature. Whole transwells filters were collected and monolayers counterstained with DAPI and 594 phalloidin (Life Technologies) in blocking buffer with PBS with 3% (wt/vol) BSA, 1% saponin, and 1% Triton X-100. Monolayers were imaged with a Zeiss LSM 700 confocal microscope.

Immunoblotting. Cell pellets were lysed with hot Lamelli SDS sample buffer containing 5% (vol/vol) β-mercaptoethanol and boiled for 10 min. To probe for secreted *S. aureus* α-toxin expression, WT USA300 LAC or isogenic mutant cultures were grown overnight to stationary phase, diluted to equivalent OD_{600}, and supernatants filtered before dilution in 2× hot Lamelli SDS sample buffer containing 5% β-mercaptoethanol.

To visualize total secreted bacterial exoproteins, stationary phase, cell-free supernatants from WT USA300 LAC and *hla::ermB* USA300 LAC were concentrated by trichloroacetic acid (TCA) precipitation. Cells were separated from 10 mL of equivalent density overnight cultures by centrifugation, the supernatants were passed through a 0.2-μm filter, and then one volume of 100% TCA (wt/vol) was added to four volumes of cell-free supernatant. After incubation for 10 min at 4 °C, total protein was pelleted by centrifugation and washed with 200 μL cold acetone and repeated for two acetone washes. Protein pellets were dried at room temperature for 30 min before resuspension in 2× Lamelli SDS sample buffer containing 5% β-mercaptoethanol and separation by SDS/PAGE as described below, and then total protein was visualized by Coomassie brilliant blue stain (Bio-Rad).

Lysates were separated by SDS/PAGE using the Mini-Protean system (Bio-Rad) on 4–15% (vol/vol) polyacrylamide gradient gels (Bio-Rad). Proteins were semiwet-transferred onto PVDF membranes (Bio-Rad) using the Bio-Rad Transblot protein transfer system. Membranes were blocked by incubating with PBS buffer containing 5% (wt/vol) nonfat milk and 0.01% Tween-20 for 1 h at room temperature. Membranes were incubated overnight at 4 °C with primary antibodies (from the following sources and dilutions) in blocking buffer as described below. Primary antibodies were detected using HRP-conjugated secondary antibodies, anti-mouse, and anti-rabbit (GeneTex) by incubating membranes with 1:5,000 in blocking buffer for 1 h at room temperature. Antibody-bound proteins were visualized by film using the West Pico and Extended Duration chemiluminescence peroxide solutions (Thermo).

Antibodies. ADAM10 was detected using a rabbit monoclonal antibody (GeneTex, EPR5622, 1:3,000). Human and murine PLEKHA7 was detected with previously described (28) rabbit polyclonal antibody against recombinant C-terminal fragments of PLEKHA7 (1:2,000 Western blot and 1:200 immunofluorescence). Canine PLEKHA7 was detected by Western blot with a polyclonal guinea pig antibody against recombinant C-terminal fragments of canine PLEKHA7 used at 1:1,000 (antibody a kind gift from Sandra Citi, University of Geneva, Geneva, Switzerland). Afadin was detected using a rabbit polyclonal antibody (Sigma, A0349, 1:2,000). *N*-cadherin was detected using a mouse monoclonal antibody (EMD Millipore, clone 13A9, 1;5,000). α-catenin was detected using a rabbit polyclonal antibody kindly provided by W. James Nelson, Stanford University, Stanford, CA, at 1:5,000. p38 MAPK was visualized with rabbit polyclonal antibody (Cell Signaling Technology, 9212, 1:1,000). Phosphorylated p38 MAPK (Thr180/Tyr182) was visualized using a rabbit polyclonal antibody (Cell Signaling Technology, 9211, 1:1,000). GAPDH was visualized with rabbit polyclonal antibody (Cell Signaling Technology, 5174, 1:5,000). *S. aureus* α-toxin was visualized with a rabbit antibody against H35L mutant α-toxin provided by Fabio Bagnoli at 1:1,000. Expression of FLAG-tagged PLEKHA7 constructs were visualized using rabbit polyclonal antibody anti-DYKDDDK (Cell Signaling Technology, 2368s, 1:2,500).

Live-Cell Time-Lapse Microscopy. WT or knockout HAP1 cells were seeded on Lab-TeK II two-chambered coverglass (Nalge Nunc International) slides for simultaneous imaging of two conditions. Imaging was performed using a Nikon TE2000E microscope equipped with high numerical aperture objectives for imaging at low light levels to minimize phototoxicity and a stage enclosed in an incubator system with temperature and CO_2 enrichment controls. A motorized, computer-controlled stage was used to sequentially monitor multiple sites of the same specimen over time by transmitted light differential interference contrast (DIC). For DIC imaging, a Hamamatsu high-resolution ORCA-285 digital camera was used. A z-stack of images was collected at each time point and processed with OpenLab software (Improvision), and the resulting movies were assembled in Quicktime Pro.

Flow Cytometry. HAP1 cells were harvested from tissue culture plates by incubating cells in PBS with 1 mM EDTA for 10 min at 37 °C. Live cells were suspended in 100 μL FACS buffer [5% (vol/vol) FCS, 0.1% Azide, and 1 mM EDTA in 1× PBS] and stained for 30 min on ice with ADAM10-PE conjugated antibody (anti-human CD156c, clone SHM14, BioLegend) according to the manufacturer's guidelines. Cells were analyzed using a BD LSRII cytometer with DIVA 6 acquisition software and gated using FlowJo vX.0.7. Events (at least 7,000 cells in the final gate) were gated on live cells and singlets. Cells were gated for PE-positive signal using unstained cells as a negative control.

Cellular Assays of α-Toxin Pore Formation. Efflux of intracellular potassium upon intoxication was assessed by seeding HAP1 cells at $2.0e^6$ cells per well in a six-well tissue culture plate 1 d before intoxication. Cells were either treated with media alone or with 5 μg/mL α-toxin in 500 μL total volume. At 30 min postintoxication, extracellular media was collected from α-toxin–treated cells and media control-treated cells, spun at 10,000 × *g* for 10 min, and passed through a 0.4-μm filter (Millipore) to remove any cellular debris. Potassium concentration in extracellular media was quantified using an Xpand Chemistry Analyzer (Siemens) by the Stanford University Veterinary Service Center diagnostic facility. Changes in extracellular potassium levels were normalized as change from media control potassium levels for each individual cell line tested.

Intracellular ATP concentration was assessed over a time-course postintoxication by seeding HAP1 at 30,000 cells per well in 96-well tissue culture plates 1 d before intoxication with 0.75 μg/mL α-toxin in complete media. Total intracellular [ATP] was determined at the indicated time points postintoxication by CellTiter-Glo luminescent cell viability assay (Promega) according to the manufacturer's guidelines and read with a microplate reader (Tecan). Cells were treated in a reverse time course of intoxication in technical quadruplicates, allowing for simultaneous lysis of all conditions at the end of the experiment to facilitate uniform luminescence

reading across multiple conditions. Intracellular ATP is plotted as a percentage compared with untreated control wells corresponding to each cell line and each time point posttreatment with α-toxin or media alone.

Generation and Validation of PLEKHA7$^{-/-}$ Transgenic Mice. The PLEKHA7(LacZ) mutant mice (accession no. CDB0750K, www.clst.riken.jp/arg/mutant%20mice%20list.html) were generated as described (www.clst.riken.jp/arg/Methods.html). The targeting vector of Plekha7 was cloned from a mouse genomic library (BACPAC). The fragment of eighth exon was replaced by the Neo selection cassette. Targeted ES clones were microinjected into ICR eight-cell stage embryos, and injected embryos were transferred into pseudopregnant ICR females. The resulting chimeras were bred with C57BL/6 mice, and heterozygous offspring were identified by PCR using the following primers: forward P1 5′ ACATGAACG-CCTGGGTCAGG 3′ and reverse P3 5′ GCCAGTGAGATGGT-CCAGTT 3′ for the WT allele, and forward P2 5′ ATGGAAG-GATTGGAGCTACG 3′ and reverse P3 for the targeted allele, yielding 627 bp and 811 bp products, respectively. PLEKHA7(LacZ) and WT mice (Jackson Laboratory) were maintained and bred in accordance with the protocols approved by the Institutional Animal Care and Use Committees of Stanford University School of Medicine and the RIKEN Center for Developmental Biology.

Tissue samples from WT and PLEKHA7$^{-/-}$ murine stomachs were processed for confocal immunofluorescence microscopy as previously described, with minor modification. Tissue samples were fixed in 2% paraformaldehyde in 100 mM phosphate buffer (pH 7.4) for 1 h. Tissue was embedded in 4% (wt/vol) agarose, and 100–200-μm sections were generated using a Vibratome (Leica). Tissue sections were permeabilized in PBS with 3% BSA, 1% saponin, and 1% Triton X-100 before staining with antibodies described above. Samples were imaged with a Zeiss LSM 700 confocal microscope.

Bacterial Strains and Culture. The WT MRSA strain USA300 LAC was kindly provided by Fabio Bagnoli. To generate *hla:ermB* mutant, an insertional lesion of the bursa aurealis minitransposon in the *hla* gene of *S. aureus* Newman was transduced to *S. aureus* USA300 LAC WT using bacteriophage 80 as previously described (52). For selection of the colonies harboring the trasposon mutation, tryptic soy agar (Sigma) plates containing 100 μg/mL erythromycin were used. The insertion was verified by DNA sequencing, and lack of *Hla* expression was checked by Western blotting. For plasmid complementation, full-length *hla* incorporating the endogenous promoter was cloned into *PstI* and *BamHI* sites of plasmid pOS1 (53) and transformed into *Escherichia coli* Dh5α. The resulting plasmid p*hla* was introduced into the *S. aureus* RN4220 strain by electroporation. Plasmid isolated from this RN4220 strain was then introduced by electroporation into the *hla::ermB* USA300 LAC mutant strain. Complementation of *hla* gene was verified by DNA sequencing, and *Hla* expression was checked by Western blotting. The complemented strain was named *hla::ermB-phla.* Bacteria was grown in tryptic soy broth (Sigma) at 37° and prepared as indicated below for animal infections.

Superficial Skin and Soft Tissue Murine Model of *S. aureus* Infection. We used a superficial skin and soft tissue murine infection model of MRSA infection as previously described (37). Briefly, 2 d before infection, *S. aureus* USA300 LAC or the USA300 LAC *hla::ermB* was streaked onto trypic soy agar (Sigma), and the following day an overnight culture in tryptic soy broth was initiated from a single bacterial colony. On the day of infection, overnight bacterial cultures were subcultured at 1:100 (vol/vol) in 50 mL of fresh tryptic soy broth on a shaker at 200 rpm for 2–3 h until an optical absorbance density (OD_{600}) of between 0.75 and 0.9 was reached. Bacteria were pelleted by centrifugation, washed 1× in sterile PBS, and resuspended in PBS at a density corresponding to 1.0×10^{11} cfu/mL. Inoculum density was determined by serial dilution on tryptic soy agar to enumerate viable staphylococci. We dispensed 10 μL of this inoculum onto the tip of a sterile allergy-testing needle (Morrow Brown Allergy Diagnostics) for infecting a single murine ear. WT PLEKHA7$^{+/+}$ and PLEKHA7$^{-/-}$ mice (males and females, 6–8 wk old, 6–12 per group) were lightly anesthetized by isoflurane inhalation before epicutaneous challenge. Before infection, mouse ears were cleansed with 70% (vol/vol) isoproponal, allowed to dry, and then the ventral epidermis of the ear was pricked 20 consecutive times at the same tissue site with a *S. aureus*-coated needle.

To enumerate bacterial density in infected ear tissues, animals were euthanized by CO_2 inhalation at the indicated time points, the infected ear pinna was excised and mechanically homogenized, and then homogenates were serially plated on tryptic soy agar. Disease progression was followed in individual animals over time by consecutively imaging isoflurane-anesthesized animals every 2 d postinfection for up to 14 d. A fixed camera position was used to standardize image size across animals and time points throughout multiple experiments, and an internal image ruler was used for validation and scaling. Lesion sizes were calculated from raw images by measuring the pixel area of the lesion area in ImageJ (NIH) to convert image pixel area to mm^2. For immunohistochemical analysis, infected ear tissue was gathered at indicated time points postinfection and fixed with 10% (vol/vol) neutral-buffered formalin. Samples were paraffin-embedded, sectioned, and stained with hematoxylin and eosin by the Department of Comparative Medicine at Stanford University. Blinded slides were interpreted by a veterinary pathologist (D.M.B.).

Pneumonia Model of *S. aureus* Infection. We used a murine model of *S. aureus* pneumonia as previously described (7, 8). Briefly, *S. aureus* USA300 LAC was grown as described above. After subculturing, bacteria were pelleted by centrifugation, washed 1× in sterile PBS, and the pellet was resuspended in PBS at a density corresponding to ca. 2.5×10^{11} cfu/mL. A total of 30 μL of this suspension was delivered by intranasal inoculation into the left nare of each infected animal, corresponding to a per animal inoculum of ca. $2–3 \times 10^8$ cfu. In a higher inoculum challenge shown in Fig. 3 *E* and *F*, an infectious dose of ca 8×10^8 cfu per animal was administered in a 30 μL PBS suspension. Inocula were determined by serial dilution plating on tryptic soy agar. Before infection, 6–8-wk-old male and female WT PLEKHA7$^{+/+}$ and PLEKHA7$^{-/-}$ mice (12–25 per group, per experiment) were anesthetized by i.p. injection of 100 mg/kg ketamine and 10 mg/kg xyazline in sterile PBS. Animals were held upright for 1 min postinfection. Animals were monitored every 6 h for 72 h and euthanized after 72 h or earlier if moribund. Core body temperature and weight of all animals was monitored before infection and every 6 h postinfection by use of a rectal thermometer. To enumerate bacterial density in infected lung tissues, infected animals were euthanized by CO_2 inhalation at the indicated time points, and the left lung was excised and mechanically homogenized, and homogenates were serially plated on tryptic soy agar.

Ethics Statement. All animal experiments were performed in accordance with NIH guidelines, the Animal Welfare Act, and US federal law. Animal experiments were carried out with the approval of the Institutional Animal Care and Use Committee of Stanford University. Animals were housed in Stanford University School of Medicine animal facilities, which are fully staffed with 24-h veterinary personnel and accredited by the Association of Assessment and Accreditation of Laboratory Animal Care International.

Statistical Analyses. Unless otherwise indicated, unpaired Student's *t* test was used for statistical calculations involving two group comparisons ($^*P < 0.05$, $^{**}P < 0.01$). Statistical significance of mouse mortality studies in the pneumonia model was assessed by the Mantel–Cox log-rank test.

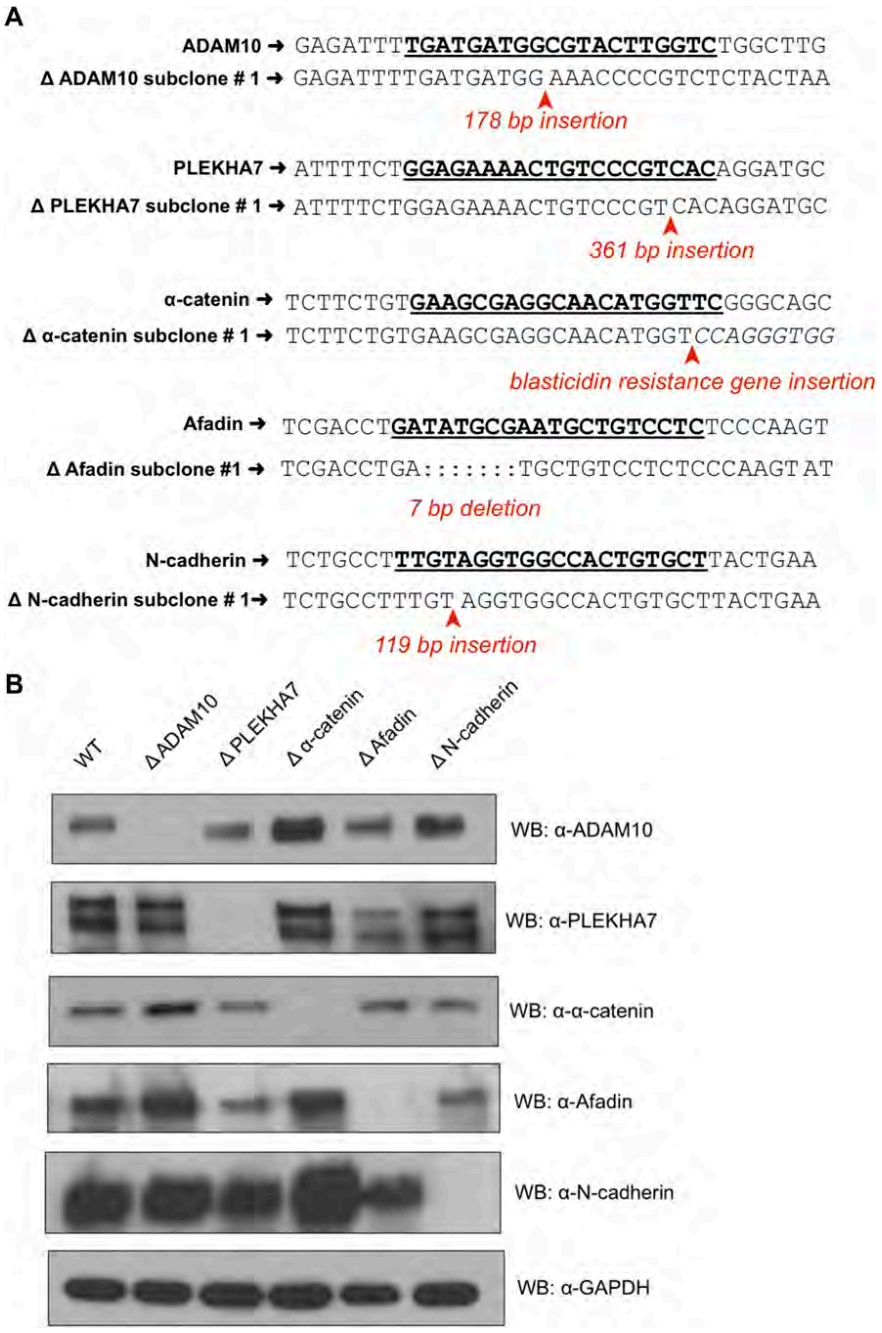

Fig. S1. Validation of HAP1 knockout subclone cell lines generated by CRISPR/Cas9 gene editing. (*A*) CRISPR/Cas9 target guide sites in HAP1 ΔADAM10, ΔPLEKHA7, Δα-catenin, ΔAfadin, and Δ*N*-cadherin HAP1 subclones were sequenced and compared with WT predicted sequence. CRISPR guide target sequences are indicated in bold, underlined text. Insertions and/or deletions caused by the observed editing event(s) are noted. (*B*) Western blot analysis of whole-cell lysates from WT, ΔADAM10, ΔPLEKHA7, Δα-catenin, ΔAfadin, and Δ*N*-cadherin HAP1 subclones as shown in *A* probed with the indicated antibodies.

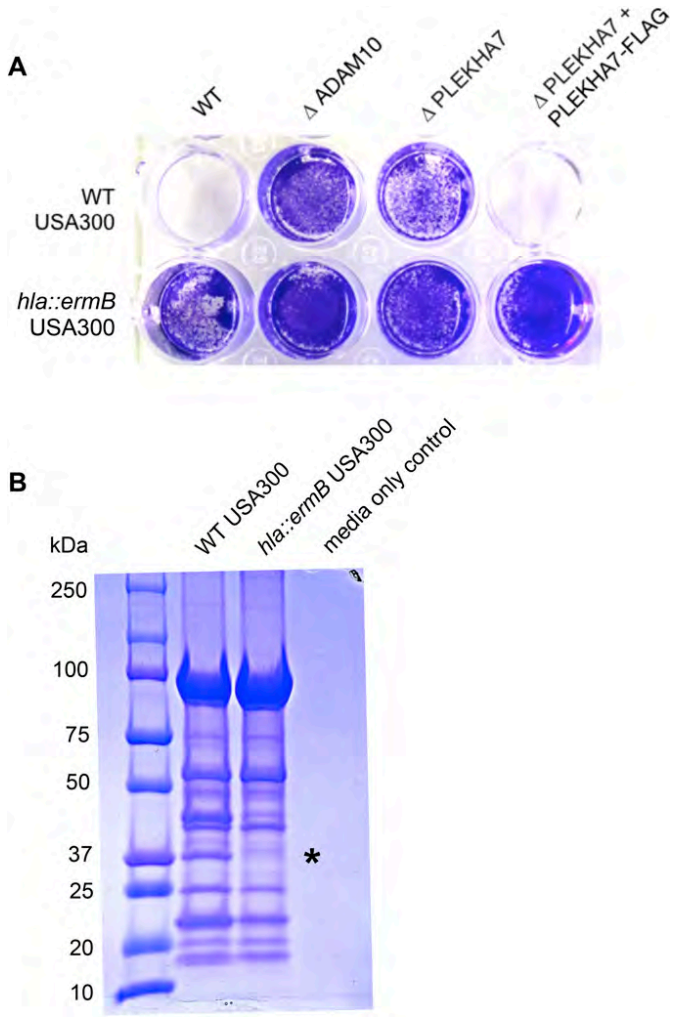

Fig. S2. ΔPLEKHA7 cells are more resistant to MRSA bacterial supernatants in an α-toxin–dependent manner. (*A*) WT, ΔADAM10, ΔPLEKHA7, and ΔPLEKHA7 HAP1 cells stably expressing human PLEKHA7-FLAG cell lines were incubated overnight with stationary phase bacterial cell-free supernatants derived from equivalent density cultures of WT USA300 LAC or the USA300 LAC *hla::ermB* α-toxin isogenic mutant. Two days after treatment, viable adherent cells were fixed and monolayers visualized by crystal violet stain. (*B*) Secreted proteins from stationary phase bacterial cell-free supernatants applied to cells as shown in *A* were concentrated by TCA precipitation, separated by SDS/PAGE, and total protein visualized by Coomassie blue staining to confirm similar exoprotein profiles for the two strains. The absence of a major band in the *hla::ermB* USA3000 LAC isogenic mutant strain at the predicted size of α-toxin is denoted by an asterisk.

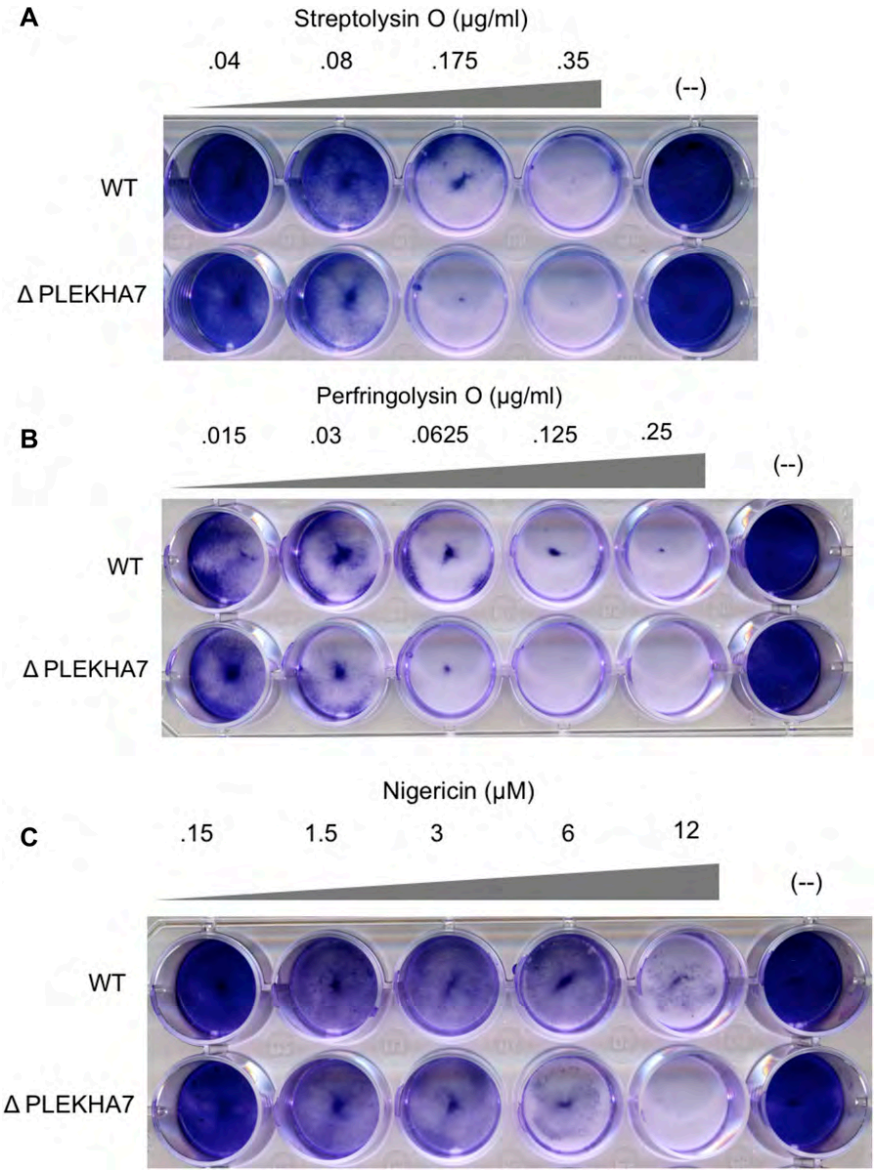

Fig. S3. PLEKHA7 deletion does not confer resistance to other bacterial pore-forming toxins or monovalent cation ionophores. (*A*–*C*) WT and ΔPLEKHA7 HAP1 cells were treated for 24 h with media as a control or the indicated concentrations of (*A*) Streptolysin O, (*B*) Perfringolysin O, and (*C*) nigericin. Two days after treatment, surviving cells were fixed and monolayers visualized by crystal violet stain.

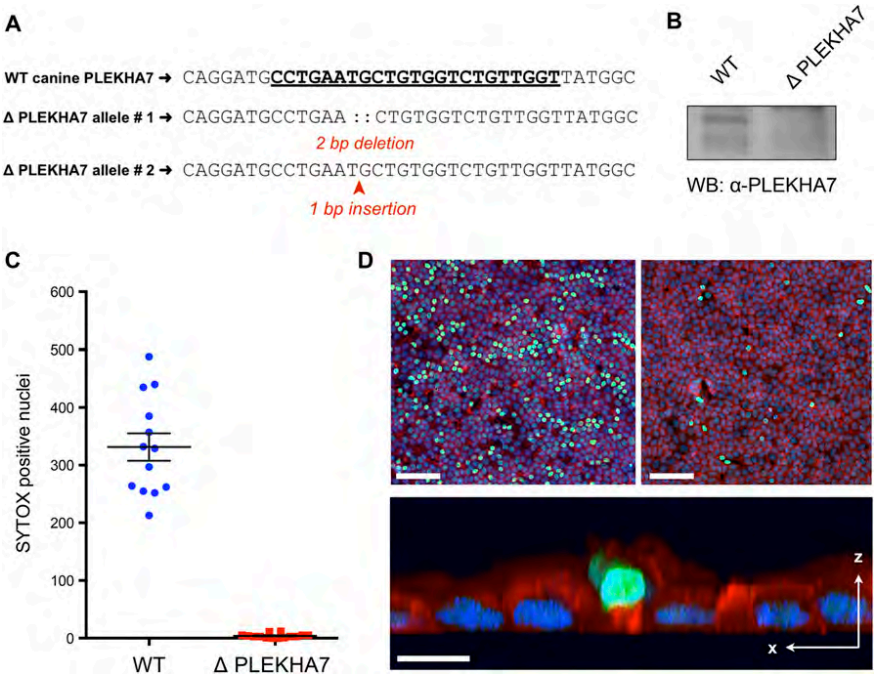

Fig. S4. PLEKHA7 modulates susceptibility to α-toxin cytotoxicity in a polarized, epithelial monolayer. (*A*) Sequencing reads from the CRISPR guide target site in ΔPLEKHA7 diploid canine MDCK subclone reveals inactivating CRISPR/Cas9 genome editing events in both PLEKHA7 alleles. CRISPR guide target site sequence is indicated in bold, underlined text. (*B*) Western blot analysis of PLEKHA7 expression in whole-cell lysates from WT and ΔPLEKHA7 MDCK cells. (*C*) Number of SYTOX-positive (dying or dead, membrane-compromised) nuclei observed per field of view following α-toxin treatment of WT MDCK polarized epithelial monolayers or ΔPLEKHA7 MDCK polarized epithelial monolayers. Data are mean ± SEM; $n = 13$ fields of view. Data shown are representative of three biological replicates. (*D*) Confocal microscopy images of WT (*Upper Left*) or ΔPLEKHA7 (*Upper Right*) MDCK epithelial monolayers treated with α-toxin. Filamentous actin, red; SYTOX-positive cells, green; nuclei stained with DAPI, blue. The *Lower* panel depicts a confocal microscopy 3D image reconstruction of a dying, extruding SYTOX-positive nucleus in a WT MDCK monolayer following α-toxin treatment. (Scale bars, 10 μm.)

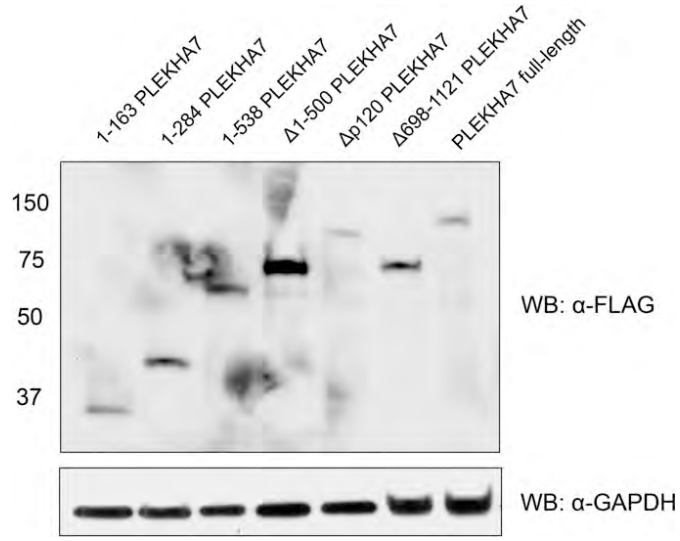

Fig. S5. Relative protein expression of PLEKHA7-FLAG truncation constructs. Western blot analysis of whole-cell lysates from PLEKHA7-FLAG constructs stably expressed by lentiviral transduction in ΔPLEKHA7 HAP1 cells, as shown in Fig. 2 *B* and *C*, probed with the indicated antibodies. Data are representative of three independent experiments.

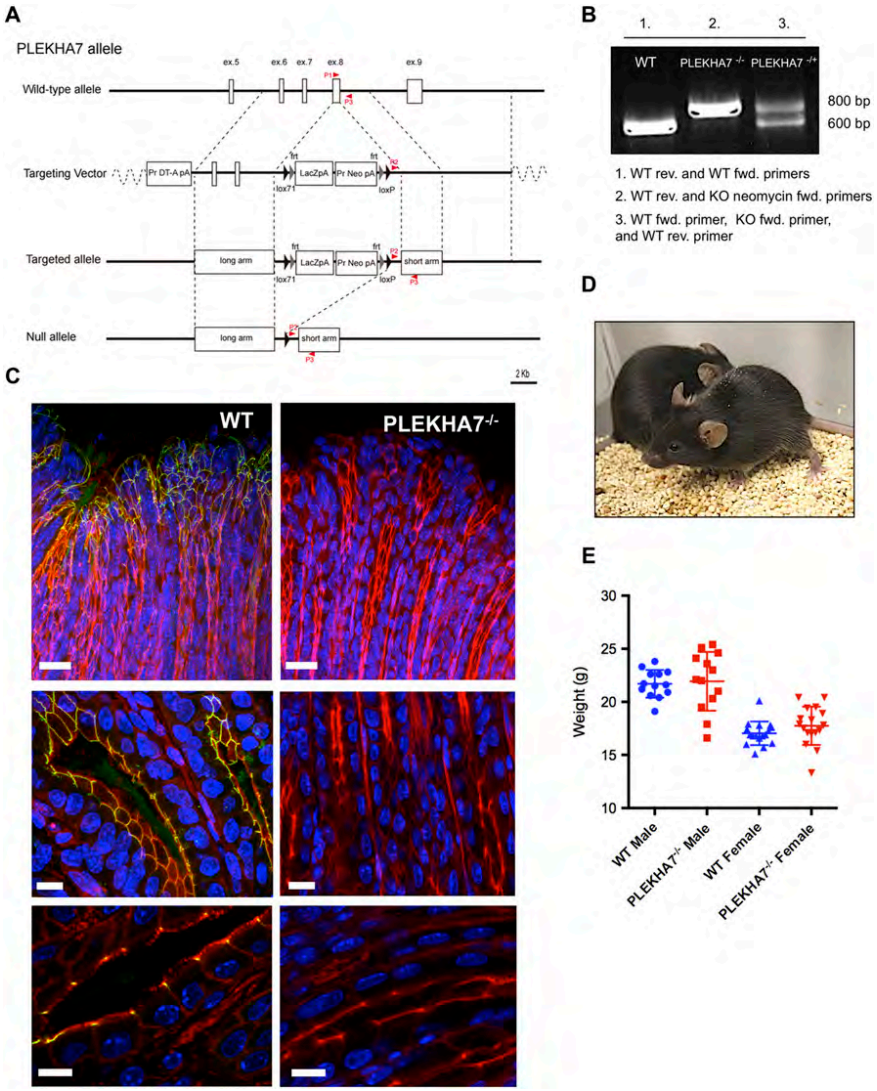

Fig. S6. Generation and validation of PLEKHA7$^{-/-}$ mice. (*A*) Diagram of the targeting vector used to generate PLEKHA7$^{-/-}$ mice. Genotyping primer binding sites are indicated in red. (*B*) Genotyping of PLEKHA7 $^{+/+}$ (WT), PLEKHA7$^{-/-}$, and PLEKHA7$^{-/+}$ heterozygous mice using a WT reverse primer, and either a WT forward primer or a forward primer complementary to the neomycin cassette, generating a 200 bp larger product. (*C*) Confocal microscopy images of PLEKHA7 expression in murine gastric epithelium of WT (*Left* panels) or PLEKHA7$^{-/-}$ (*Right* panels) animals. Filamentous actin, red; PLEKHA7, green; nuclei stained with DAPI, blue. (Scale bars, 25, 10, and 5 μm for the *Top*, *Middle*, and *Lower* panels, respectively.) (*D*) Photograph of 6-wk-old PLEKHA7$^{-/-}$ female mice. PLEKHA7$^{-/-}$ animals are healthy and fecund, with no gross developmental phenotypes. (*E*) Weight (in grams) of 6–8-wk-old WT and PLEKHA7$^{-/-}$ matched littermates; data are mean ± SEM; $n \geq 13$ animals in each group.

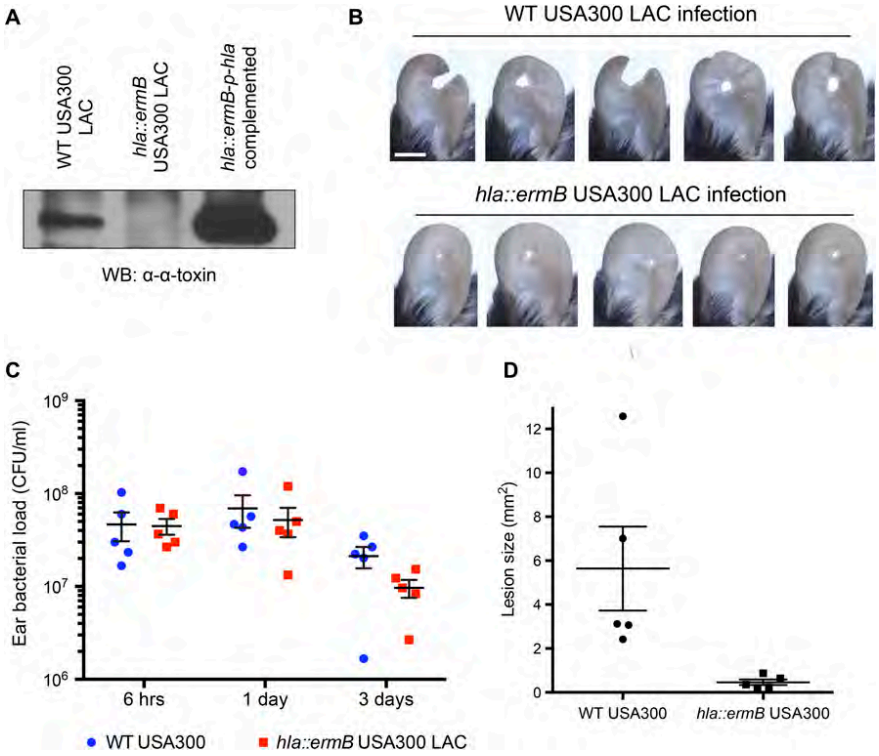

Fig. S7. α-toxin contributes to the severity of a self-resolving MRSA skin and soft tissue infection. (*A*) Western blot analysis of α-toxin expression in cell-free bacterial supernatant lysates from strains WT USA300 LAC, *hla::ermB* USA300 LAC, and *hla::ermB-phla* USA300 LAC complemented with α-toxin. (*B*) Representative images of WT USA300 LAC and *hla::ermB* USA300 LAC ear skin and soft tissue lesions within individual animals at day 14. (Scale bar, 5 mm for all panels.) (*C*) Bacterial density measurements from WT animals infected with WT USA300 LAC or *hla::ermB* USA300 LAC at the indicated time points. $n = 6$ animals per group, per time point. Data are mean ± SEM. (*D*) Lesion size (in mm^2) at day 14 in mice infected with WT or *hla::ermB* USA300 LAC. Data are mean ± SEM, representing $n = 5$ animals in each group, representative of two independent experiments.

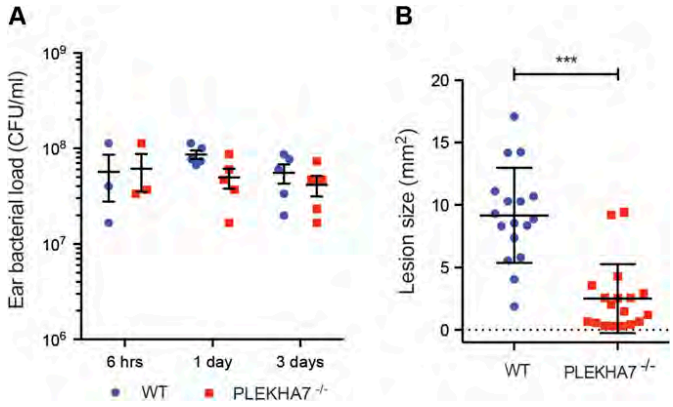

Fig. S8. USA300 LAC bacterial burden in self-resolving MRSA skin and soft tissue infections of WT and PLEKHA7$^{-/-}$ mice. (*A*) USA300 LAC bacterial density measurements from infected ear tissue of WT and PLEKHA7$^{-/-}$ animals at the indicated time points. At 6 h postinfection, $n = 3$ animals per group; at day 1 and day 3 postinfection, $n = 6$ animals per group. Data are mean ± SEM. (*B*) Lesion size (in mm^2) at day 14 postinfection of WT and PLEKHA7$^{-/-}$ animals in superficial ear infection model with USA300 LAC. Data are mean ± SEM pooled from two independent experiments, representing $n = 17$ WT and $n = 18$ PLEKHA7$^{-/-}$ matched littermates. $P < 0.001$, unpaired *t* test.

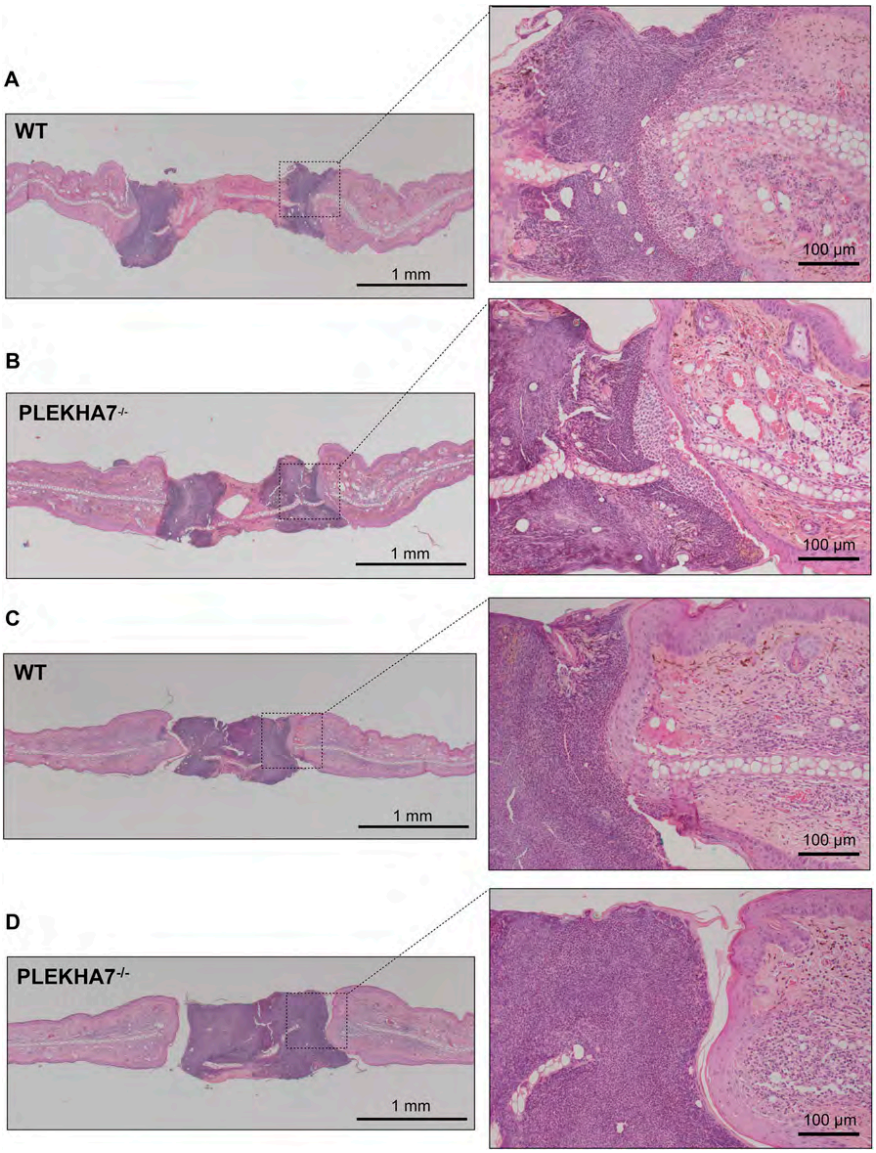

Fig. S9. Histopathology of MRSA skin infection in WT and PLEKHA7$^{-/-}$ mice. (*A*) Representative images of WT and PLEKHA7$^{-/-}$ animal MRSA ear skin and soft tissue lesions taken at day 3 (*A* and *B*) and day 5 (*C* and *D*) postinfection. Histopathology studies of USA300 LAC skin lesions reveal full-thickness lesions filled with serocellular material and a massive influx of degenerate neutrophils (*A*–*D*, *Insets*). Ear tissue edges adjacent to the necrotic, eosinophilic coagulum display moderate re-epithelialization with mild to moderate epidermal acanthosis and a moderate population of viable neutrophils. Lesions were uniformly indistinguishable when examined by a veterinary pathologist (D.M.B.) who was blinded to the experimental groups (n = 6 ears per time point per group).

Table S1. CRISPR/Cas9 genome editing guide sequences and primers

Gene	Guide RNA sequence	Genotyping sequencing primers
ADAM10	5′ TGATGATGGCGTACTTGGTC 3′	5′ GATCAGCTCAGGGATGTGG 3′ and 5′ CTGTAGTGAGATAAAGAGGAG 3′
PLEKHA7	5′ GGAGAAAACTGTCCCGTCAC 3′	5′ GACAATACCCATCATGCAC 3′ and 5′ CAACAGATATATGTGCCAGGG 3′
α-catenin	5′ GAACCATGTTGCCTCGCTTC 3′	5′ CCAGCAATATATGAAGGTGC 3′ and 5′ TTGGAATAGAGGAGTAAGTG 3′
Afadin	5′ GAGGACAGCATTCGCATATC 3′	5′ CATCTCTCTACATTAGTCTCAG 3′ and 5′ CGTTACTTATCTTTGGAGAAAT 3′
N-cadherin	5′ AGCACAGTGGCCACCTACAA 3′	5′ AGCTTTCTAATCCACAGTGTG 3′ and 5′ TTTCAGATACACAGTATAACCC 3′
PLEKHA7, canine	5′ ACCAACAGACCACAGCATTCAGG 3′	5′ CCACACTTCCACATCTTCCC 3′ and 5′ GTGGTCTCTTGCAGCCATTC 3′

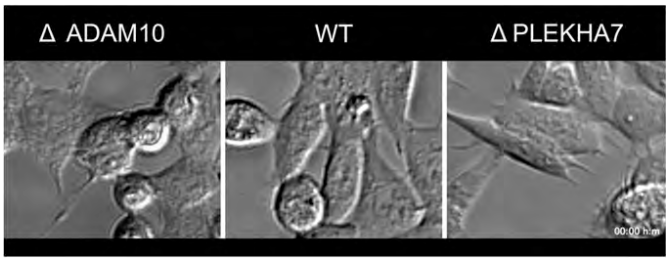

Movie S1. ΔPLEKHA7 cells develop cytopathic effects following treatment with α-toxin but recover and survive intoxication. WT, ΔADAM10, and ΔPLEKHA7 HAP1 cells were seeded at the same density onto coverglass and serially imaged following α-toxin treatment to visualize response to intoxication by time-lapse microscopy. Both WT and ΔPLEKHA7 cells, but not ΔADAM10 cells, develop cytopathic effects ∼1 h postintoxication, however individual ΔPLEKHA7 cells recover from this apparent injury, restoring normal cell morphology and ultimately surviving α-toxin treatment in contrast to WT cells.

Movie S1

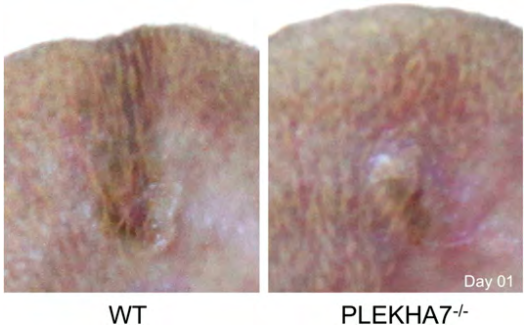

Movie S2. Comparative time-lapse visualization of MRSA skin and soft tissue infection reveals PLEKHA7$^{-/-}$ mice repair wounds with reduced tissue loss. WT and PLEKHA7$^{-/-}$ animals were serially imaged following USA300 ear skin and soft tissue infection for time-lapse visualization of lesion development and repair. PLEKHA7$^{-/-}$ mice resolve MRSA skin infection with significantly less tissue loss than WT animals.

Movie S2

Dataset S1. Inactivating gene-trap insertions mapped in an α-toxin–selected HAP1 cell population compared with gene-trap insertions mapped in a control, unselected HAP1 cell population

Dataset S1

PLEKHA7 recruits PDZD11 to adherens junctions to stabilize nectins

This article represents the main core of results of my PhD project. The aim of this study was to characterize novel interactors of PLEKHA7 to further elucidate its role in junction biology and to obtain new insights into its physiological and pathological role. As discussed above, PLEKHA7 is independently recruited by afadin and p120ctn at nectin based and E-cadherin based AJ. PLEKHA7 stabilizes the ZA by connecting the E-cadherin complex to the microtubule cytoskeleton. In this paper we report the identification by two-hybrid screening and mass spectrometry analysis of immunoprecipitates of PDZ domain-containing protein 11 (PDZD11) as the highest confidence PLEKHA7 interactor. PDZD11 was previously found to interact with several membrane ATPases, but never with a junctional protein. We confirmed that PLEKHA7 and PDZD11 interact in vitro and in vivo in epithelial and endothelial cells. This interaction is mediated by The N-terminal region of PDZD11, which binds the first WW domain in the N-terminal region of PLEKHA7. Furthermore, we show for the first time that PDZD11 is a new component of AJ, where it is recruited by PLEKHA7 through its WW domain; in fact, epithelial cells KO for PLEKHA7 lose the junctional accumulation of PDZD11, which is restored upon re-expression of PLEKHA7 but not of the PLEKHA7 mutant lacking the WW domain. Moreover, the analysis of epithelial cells KO for PDZD11 shows that PDZD11 is not required for TJ and AJ formation, but is important for the stabilization of nectin adhesion molecules at AJ. In fact, PDZD11 interacts with the nectin PDZ consensus motif through its PDZ domain. The PLEKHA7-PDZD11 complex is required to stabilize nectins

and prevent their proteasomal degradation. Finally, the PLEKHA7-PDZD11 complex, through its role in the stability of nectins, is required during the early steps of junction assembly, where PDZD11 KO cells show a delay in AJ/TJ formation.

My contribution to this publication was the generation of all the PDZD11 constructs and characterization of our own PDZD11 rabbit antiserum. I generated the PDZD11 CRISPR KO mCCD cells and rescue cell lines. I carried out most of the immunoprecipitation and pulldown experiments (except those in Fig. 1D, Fig. 2G and Fig. 5C). I performed most of the immunofluorescence analysis (except IHC on mouse tissues in Fig. 3A and IF on PLEKHA7 deletion mutants in Fig. 3F), and immunoblot analysis (except in Fig. 1A).

THE JOURNAL OF BIOLOGICAL CHEMISTRY VOL. 291, NO. 21, pp. 11016–11029, May 20, 2016

PLEKHA7 Recruits PDZD11 to Adherens Junctions to Stabilize Nectins*

Received for publication, December 27, 2015, and in revised form, April 1, 2016 Published, JBC Papers in Press, April 4, 2016, DOI 10.1074/jbc.M115.712935

Diego Guerrera[‡§], Jimit Shah[‡§], Ekaterina Vasileva[‡§], Sophie Sluysmans[‡§], Isabelle Méan[‡§], Lionel Jond[‡§], Ina Poser[¶1], Matthias Mann[‖], Anthony A. Hyman[¶1], and Sandra Citi[‡§2]

From the [‡]Department of Cell Biology and [§]Institute for Genetics and Genomics in Geneva (iGE3), University of Geneva, 1211-4 Geneva, Switzerland, the [¶]Max Planck Institute for Cell Biology and Genetics, 01307 Dresden, Germany, and the [‖]Max Planck Institute for Biochemistry, 82152 Martinsried, Germany

PLEKHA7 is a junctional protein implicated in stabilization of the cadherin protein complex, hypertension, cardiac contractility, glaucoma, microRNA processing, and susceptibility to bacterial toxins. To gain insight into the molecular basis for the functions of PLEKHA7, we looked for new PLEKHA7 interactors. Here, we report the identification of PDZ domain-containing protein 11 (PDZD11) as a new interactor of PLEKHA7 by yeast two-hybrid screening and by mass spectrometry analysis of PLEKHA7 immunoprecipitates. We show that PDZD11 (17 kDa) is expressed in epithelial and endothelial cells, where it forms a complex with PLEKHA7, as determined by co-immunoprecipitation analysis. The N-terminal Trp-Trp (WW) domain of PLEKHA7 interacts directly with the N-terminal 44 amino acids of PDZD11, as shown by GST-pulldown assays. Immunofluorescence analysis shows that PDZD11 is localized at adherens junctions in a PLEKHA7-dependent manner, because its junctional localization is abolished by knock-out of PLEKHA7, and is rescued by re-expression of exogenous PLEKHA7. The junctional recruitment of nectin-1 and nectin-3 and their protein levels are decreased via proteasome-mediated degradation in epithelial cells where either PDZD11 or PLEKHA7 have been knocked-out. PDZD11 forms a complex with nectin-1 and nectin-3, and its PDZ domain interacts directly with the PDZ-binding motif of nectin-1. PDZD11 is required for the efficient assembly of apical junctions of epithelial cells at early time points in the calcium-switch model. These results show that the PLEKHA7-PDZD11 complex stabilizes nectins to promote efficient early junction assembly and uncover a new molecular mechanism through which PLEKHA7 recruits PDZ-binding membrane proteins to epithelial adherens junctions.

The molecular organization of cell-cell contacts is of central importance in understanding the morphogenesis, architecture, and physiology of vertebrate organs, as well as the mechanisms underlying the pathogenesis of human disease. In epithelia, cell-cell junctions are essential to establish and maintain tissue integrity and barriers between tissue compartments, and they also play key roles in the transmission of signals to and from adjacent cells, and within tissues, to regulate proliferation and differentiation (1–4). The apical junctional complex includes two structurally and functionally distinct units, tight junctions (TJ)[3] and adherens junctions (AJ), whose canonical functions are paracellular barrier and intramembrane fence (TJ) (1) and cell-cell adhesion/mechanical tissue integrity (AJ), respectively (2, 3). AJ comprise cadherins and nectins as transmembrane adhesion molecules, both linked to the submembrane cortical cytoskeleton by cytoplasmic complexes of adaptor proteins: catenins (p120-catenin and β-catenin/α-catenin) for E-cadherin and afadin-ponsin for nectins (2, 5).

PLEKHA7 is a recently discovered cytoplasmic component of AJ, which was identified through its interaction with the AJ protein p120-catenin (6) and with the TJ/AJ protein paracingulin (CGNL1) (7–9). PLEKHA7 is specifically associated with the *zonula adhaerens* (ZA) (7), and it interacts with the microtubule-interacting protein nezha (CAMSAP3) to provide a molecular linkage between the cadherin-associated protein complex and the microtubule cytoskeleton (6). Genetic and genome-wide association studies have implicated PLEKHA7 in the regulation of cardiac contractility in a zebrafish model (10), in hypertension in human cohort studies (11–13) and in a rat model (14), and in primary angle closure glaucoma (15, 16). In addition, PLEKHA7 has recently been involved in the control of microRNA processing (17) and susceptibility to staphylococcal α-toxin (18). However, the molecular and cellular mechanisms through which PLEKHA7 is implicated in the above-mentioned diseases and in its cellular functions are still largely unknown.

To gain further insight into the biochemical basis for the functions of PLEKHA7, it is essential to identify and characterize new PLEKHA7 interacting partners. Toward this goal, we describe here the identification of PDZ domain-containing protein 11 (PDZD11) as a novel PLEKHA7 interactor. PDZD11 is recruited to AJ by PLEKHA7, contributing to the stabilization

* This work was supported in part by Swiss National Fund Grants 31003A103637 and 31003A116763 and the Swiss Cancer League Grant KFS-2813-08-2011 (to S. C.). The authors declare that they have no conflicts of interest with the contents of this article.
[1] Supported by the European Community's Seventh Framework Programme Grant FP7/2007-2013 under Grant Agreement 241548 (MitoSys Project).
[2] To whom correspondence should be addressed: Dept. of Cell Biology, 30 Quai Ernest Ansermet, 1211-4 Geneva, Switzerland. Tel.: 41-22-3796182; Fax: 41-22-3796868; E-mail: sandra.citi@unige.ch.

[3] The abbreviations used are: TJ, tight junction; AJ, adherens junction; Caco-2, colorectal carcinoma cell line-2; CFP, cyan fluorescent protein; mCCD, mouse kidney collecting duct; meEC, mouse embryonic aorta endothelial cell; MDCK, Madin-Darby canine kidney; PDZ, Psd95-Dlg1-ZO-1 domain; PDZD11, PDZ domain containing protein 11; PLA, proximity ligation assay; PLEKHA7, pleckstrin homology domain-containing family A member 7; Sf, *Spodoptera frugiperda*; ZA, *zonula adhaerens*; ZO-1, zonula occludens-1; IB, immunoblot; IF, immunofluorescence; PH, pleckstrin homology; qRT, quantitative RT.

of nectins at AJ and ensuring efficient early steps of junction assembly.

Experimental Procedures

Antibodies and Plasmids—Antibodies are annotated below with information on species-antigen and dilution for either immunoblotting (IB) or immunofluorescence (IF) (using fixation with methanol unless otherwise stated), or proximity ligation assay (PLA). The following are used: rabbit PDZD11 (immune and preimmune r29958, 1:1500 IB, 1:50 IF); mouse β-tubulin (1:1000 IB, Zymed Laboratories Inc., catalog no. 32-2500); mouse Myc (9E10 hybridoma culture supernatant, 1:2 IB); rabbit and guinea pig PLEKHA7 (1:10,000 IB, 1:1000 IF, in-house r30388, gp2737, these latter raised against GST fusion proteins of canine PLEKHA7 residues 936–1237 and 611–809, respectively); mouse PLEKHA7 (378F1, 1:10 PLA (7)); mouse His (Invitrogen, catalog no. 37-2900, 1:1500 IB); mouse HA (1:1000 IB, Zymed Laboratories Inc., catalog no. 32-6700); rabbit cingulin (1:5000 IF, in-house C532 (19)); mouse cingulin (1:1000 IF, in-house 22BD5A1); rabbit paracingulin (1:10,000 IB, 1:500 IF, in-house 20893); rabbit α-catenin (1:4000 IB, 1:100 IF, Sigma, catalog no. c-2081); rabbit β-catenin (1:10,000 IB, 1:500 IF, Sigma, catalog no. C2206); mouse p120-catenin (1:2000 IB, 1:250 IF, 15D2 monoclonal, a kind gift from Prof. A. Reynolds); mouse E-cadherin (1:2000 IB, 1:2000 IF, BD610181); rabbit ZO-1 (1:1000 IB, Zymed Laboratories Inc., catalog no. 61-7300); rat ZO-1 (R40-76, 1:50 IF); mouse occludin (1:3000 IB, 1:300 IF, Zymed Laboratories Inc., catalog no. 33-1500); rabbit nectin-1 (Abcam, catalog no. AB66-985, 1:3000 IB, 1:500 PLA); rat nectin-3 (MBL-D084-3, 1:100 IF); rabbit nectin-3 (Abcam, catalog no. AB-63931, 1:4000 IB, 1:500 IF and PLA); rabbit afadin (Sigma, catalog no. A0224, 1:4000 IB, 1:600 IF); and VeriBlot secondary HRP-labeled antibodies for IP experiments (Abcam, catalog no. ab131366, 1:4000). The rabbit polyclonal anti-PDZD11 antiserum (r29958) was generated by immunization with recombinant full-length PDZD11 and obtained by affinity purification and thrombin protease digestion of GST-PDZD11 expressed in BL21DE3 bacteria. The full-length human PDZD11 sequence was obtained from Kazusa DNA Research Institute (clone number PF1KB8215) and amplified by PCR with appropriate oligonucleotides for subsequent subcloning. PDZD11 sequences (either full-length or truncated) were cloned into pGEX4T1 for bacterial expression as GST fusion proteins (EcoRI-XhoI). GFP-PDZD11-Myc was obtained in pcDNA3.1GFP-Myc (vector generated by NotI-ClaI digestion of the GFP-cingulin-Myc construct (20) (NotI-ClaI)). YFP- and Myc-tagged N-terminal, central, and C-terminal fragments of PLEKHA7 were described previously (21). GST fusions of smaller fragments of PLEKHA7 (WW, 1–162), WWPH(1–284), PH(120–300), and proline-rich + coiled-coil region (PCC, 500–844) were generated by PCR and subcloned into pGEX4T1. Other GST fusions of PLEKHA7 were described previously (7, 8). The internal WW and WF domains within the larger WW region (1–162) were subsequently identified and subcloned into pGEX4T1 to make three GST fusion constructs: W1 (WW, 1–53), W2 (WF, 43–98), and W1 + 2 (WW-WF, 1–98). Constructs of YFP-tagged (N-terminal) PLEKHA7 were generated in pTre2-Hyg as follows: full length (21), ΔPH (1–165 fused to 285–1121), and ΔWW (90–1121). The human nectin-1 (PVRL1) cDNA was obtained from Promega (pF1KB0475) and used by PCR amplification to subclone into the BamHI-NotI sites of pcDNA3.1Myc/His, with an N-terminal Myc sequence and a stop codon before the vector's Myc tag. The Myc-nectin1-Δ4, lacking the C-terminal PDZ-binding four residues (EWYV), was similarly generated by PCR and subcloned into pcDNA3.1Myc/His. All new constructs were verified by sequencing.

Yeast Two-hybrid Screen and QUantitative BAC-Intera Ctomics (QUBIC)—For the yeast two-hybrid screen, the full-length sequence of human *PLEKHA7* (residues 1–1121) was fused C-terminally to LexA in the pB27 vector. This construct was used to screen a human placenta library, in the presence of 0.5 mM 3-amino-1,2,4-triazole (Hybrigenics, Paris, France). A very high confidence interaction (PBS Score "A", based on the PIM predicted global biological score) was detected with 24 distinct clones of PDZD11, all of which contained the full-length coding sequence of PDZD11. In addition, a PBS score A was also obtained with six clones of the known interactor paracingulin (CGNL1) (8), whereas no PLEKHA7-interacting clones were detected with scores "B" (high confidence) or "C" (good confidence). For affinity purification of PLEKHA7 prior to mass spectrometry, a BAC clone harboring the mouse *Plekha7* gene (RP23-350A9, BACPAC Resources Center) was recombined with an N-terminal GFP BAC tagging cassette (NFLAP: GFP_PreScission_S-peptide_TEV_FLAG) (22). Precise incorporation of the tagging cassette was confirmed by PCR and sequencing. Next, the GFP-tagged BAC was isolated from bacteria using the NucleoBond PC100 kit (Macherey-Nagel, Germany), and HeLa Kyoto cells were transfected using Effectene (Qiagen) and cultured in DMEM selection media containing 400 μg/ml geneticin (G418, Invitrogen). The pool of HeLa cells stably expressing the tagged *Plekha7* transgene was analyzed by Western blot and immunofluorescence using an anti-GFP antibody (Roche Applied Science) to verify correct protein size and localization of the tagged transgene. Affinity purification and mass spectrometry were carried out as described (23). PDZD11 (Target ID Q5EBL8-2) and PLEKHA7 (Target ID Q6IQ23-2) were identified in the immunoprecipitate with the highest identical score of 10.296 (three peptides).

Cell Culture, Preparation of Lysates, and Pharmacological Treatment—We previously described culture conditions for MDCKII (Madin-Darby canine kidney), MDCK-Tet-Off epithelial cells (Clontech), Caco-2 (human intestinal carcinoma cells), mCCD (mouse kidney collecting duct, mpkCCD, clone N64, a kind gift of Prof. Eric Feraille, University of Geneva), and Sf21 insect cells (24–28). Culture conditions for human keratinocytes (HaCaT, a kind gift from Dr. L. Fontao, University of Geneva), human lung carcinoma cells (A427 and A459, a kind gift of Prof. M. Paggi, Istituto Regina Elena, Roma, Italy), mouse microvascular endothelioma cells (bEnd.3, a kind gift from Prof. B. Imhof, University of Geneva), and mouse aortic endothelial cells (meEC, a kind gift from Prof. B. Kwak, University of Geneva) will be described elsewhere. Total lysates were obtained in RIPA buffer (150 mM NaCl, 40 mM Tris-HCl, pH 7.5, 2 mM EDTA, 10% glycerol, 1% Triton X-100, 0,5% sodium deoxycholate, 0.2% SDS) supplemented with protease inhibitor

mixture (Roche Applied Science) from 10-cm dishes, followed by sonication (8 s at 66% amplitude with a Branson sonifier). To inhibit proteasome-mediated degradation, cells were treated with 25 μM MG132 (C2211, Sigma) for 8 h at 37 °C prior to lysis.

Analysis of Dynamics of Junction Assembly by Calcium Switch—A modification of the classical protocol (29) was used here, because mCCD cells undergo complete junction disassembly upon removal of extracellular calcium much more rapidly than MDCK cells. mCCD cells (300,000 cells inoculated on each round coverslip in 24-well plates 24 h earlier) were rinsed twice with PBS and incubated for 30 min in S-MEM low calcium medium (Gibco catalog no. 11380-052), containing 10 mM Hepes, pH 7.4, 1× non-essential amino acids, 5% FBS, 2 mM L-glutamine, 2 μM EGTA, and 1× penicillin/streptomycin, to disassemble junctions. To initiate junction assembly, the S-MEM medium was replaced with normal medium, and cells were fixed for immunofluorescent labeling at 15 and 30 min and 1 and 4 h after the switch. Junctional assembly of E-cadherin and cingulin was evaluated by immunofluorescence as described below.

Generation of Knock-out (KO) mCCD Cells by CRISPR/Cas9 Genome Editing—A construct for the CRISPR/Cas9-mediated knock-out (KO) of PDZD11 KO in mouse mCCD cells was generated by cloning a guide-RNA targeting exon-1 of the mouse *Pdzd11* gene (sequence: GCCGGCCTATGAAAACCCTC) into the BbsI site of px458 CRISPR plasmid (Addgene catalog no. 48138, containing GFP). Cells were transfected by Lipofectamine2000, and isolated clones were obtained 2 days later by fluorescence-activated cell sorting (using a Beckman Coulter MoFlo Astrios sorter, Flow Cytometry Service, University of Geneva Medical School). Single PDZD11-KO clones were screened by immunoblotting, and the genomic sequence of the *Pdzd11* locus was determined in distinct KO clones by PCR amplification and subcloning of a fragment spanning a 1-kb region, from the 5′-untranslated region of the *Pdzd11* gene to exon-2. Clone 1B2 showed the insertion of a G in both alleles (resulting sequence: GCCGGGCCTATGAAAACCCTC). Clone 2C7 showed a 2-bp deletion in allele 1 (G-GGCCTATGAAAACCCTC) and a 164-bp insertion in allele 2 (GCC-164 bp-GGCCTATGAAAACCCTC). Clone 1C8 showed a 2-bp deletion in allele 1 (G-GGCCTATGAAAACCCTC) and a 1-bp insertion in allele 2 (GCCGGGCCTATGAAAACCCTC). Rescue clones were obtained by expression of either GFP or GFP-tagged PDZD11 (cloned in pTre-2Hyg), and selection of clones was made in hygromycin-containing medium. The three clones behaved similarly, but only data from one clone (2C7) are shown in Figs. 4 and 6 for the sake of space. The generation of PLEKHA7-KO mCCD cells by CRISPR-mediated genome editing, the generation of rescue clones, and their full characterization will be described elsewhere.[4] Transfection was carried out using either Lipofectamine 2000 (Invitrogen) or the calcium phosphate method (for HEK293T cells).

Immunofluorescence Microscopy, Immunohistochemistry, and Proximity Ligation Assay—Conventional fixation of cells for labeling of junctional proteins was with methanol (10 min at −20 °C), and incubations with antibodies were for 30 min at 37 °C. To detect cytoplasmic GFP in PLEKHA7-KO cells, cells were fixed with Triton X-100 and paraformaldehyde (26). Immunohistochemistry was carried out as described previously (7). Proximity ligation assay (Sigma, catalog no. DUO92101) was carried out according to the manufacturer's instructions, using rabbit anti-nectin1/3 and mouse anti-PLEKHA7. Coverslips were mounted with Vectashield (Reactolab) and imaged with a Zeiss LSM700 confocal microscope, equipped with ×63, 1.3NA objective (Zeiss LSM software). LSM 8-bit files were converted to TIFF files separately for each channel using ImageJ software and linearly adjusted and cropped using Adobe Photoshop. Quantification of immunofluorescent junctional labeling for nectin-3 was carried out with ImageJ software, as described previously (8), using either E-cadherin or cingulin as an internal reference standard for junctional labeling (E-cadherin is not affected by PDZD11-KO, and cingulin is not affected by PLEKHA7-KO). Quantification of junction assembly during the calcium switch was carried out by drawing the outline of the cell periphery of 20 cells/field (three fields for each sample) (each cell was identified by DAPI-labeled nuclei), and by measuring the length of the regions of cell-cell contact that were labeled by either anti-E-cadherin or anti-cingulin antibodies. The percentage of junction assembly was obtained by ratioing the labeled lengths over the total calculated lengths of the cell peripheries.

Immunoprecipitation, GST Pulldown, and Immunoblotting—Immunoprecipitation of endogenous proteins from Caco2, mCCD, and meEC cells was carried out by rinsing cells with cold PBS and incubating them in 0.5 ml (coIP) of buffer (150 mM NaCl, 20 mM Tris-HCl, pH 7.5, 1% Nonidet P-40, 1 mM EDTA, 5 mg/ml antipain, 5 mg/ml leupeptin, 5 mg/ml pepstatin, 1 mM PMSF) for 10 min at 4 °C. After sonication (8 s at 40% power, Branson sonifier), the lysate was centrifuged for 15 min at 13,000 rpm. The supernatant was kept (cytoskeleton-soluble fraction). The pellet (cytoskeleton-insoluble fraction) was resuspended in 50 μl of SDS-buffer (1% SDS, 10 mM Tris-HCl, pH 7.5, 2 mM EDTA, 0.5 mM DTT, 0.5 mM PMSF), sonicated 2 s at 10% power, incubated at 100 °C for 5 min, clarified by centrifugation, brought to a volume of 0.5 ml with co-IP buffer, and mixed with the cytoskeleton-soluble fraction to make a "total" IP lysate. Dynabeads protein-G or protein-A (Invitrogen) (20 μl) were coupled to antibodies (either 2 μl of serum or 2 μg of purified antibody) at 4 °C for 90 min, washed with PBS containing 5% bovine serum albumin and 1% Nonidet P-40, and incubated with 0.1–0.3 ml of total IP lysate for 16 h at 4 °C. After washing three times with coIP buffer, beads were incubated in 20 μl of SDS sample buffer at 100 °C for 5 min, and between 5 and 15 μl of eluate were loaded on SDS gels (12% polyacrylamide for PDZD11 and 8% for PLEKHA7). SDS-PAGE and immunoblotting were carried out as described previously (21, 27). Protein loadings were normalized by immunoblotting with anti-tubulin antibody. Detection of proteins after Western blotting was performed by Odyssey Imager (LI-COR). Quantification of nectin-1 and nectin-3 protein levels by immunoblotting in normalized samples was carried out using ImageJ software analysis of scanned blots. Sf21 cells expressing His-tagged PLEKHA7 were lysed in LBT buffer (150 mM NaCl, 20 mM

[4] J. Shah, D. Guerrera, and S. Citi, unpublished results.

Tris-HCl, 5 mM EDTA, 1% Triton X-100, 5 mg/ml antipain, 5 mg/ml leupeptin, 5 mg/ml pepstatin, 1 mM PMSF), sonicated four times for 30 s at 30% power and centrifuged for 20 min at 13,000 rpm (8). Purification of GST fusion proteins and GST pulldowns with full-length His-tagged PLEKHA7 expressed in baculovirus-infected insect cells was performed as described previously (24, 25).

RT-PCR—mRNA levels for nectin-1 and nectin-3 in PDZD11-KO and rescue clones were measured by qRT-PCR, as determined previously (28), using GAPDH as an internal reference. The primers were as follows: nectin-1, forward 5′-TGCACTGTAGCTTTGCCAAC-3′ and reverse 5′-ATGTACATGCCCTCGTCCTC-3′; nectin-3, forward 5′-TTGCCCTTTCCTTTGTCAAC-3′ and reverse 5′-GCATGTCTGATGGTGGAATG-3′.

Data Analysis—All experiments were carried out at least in triplicate, and similar results were obtained when using distinct clones of either PLEKHA7-KO or PDZD11-KO cells. For immunoblots and immunofluorescence data, one representative example out of three independent experiments is shown. Statistical significance of quantitative data was determined by Student's *t* test.

Results

PDZ Domain-containing Protein 11 Is a Novel Interactor of PLEKHA7—We sought to identify novel interactors of PLEKHA7 by yeast two-hybrid screen and by mass spectrometry analysis of affinity-purified PLEKHA7 immunoprecipitates. Both approaches identified PDZD11, also known as PISP (plasma membrane calcium ATPase-interacting single-PDZ protein) or AIPP1 (ATPase-interacting PDZ protein) (30–32) as the highest confidence interactor of PLEKHA7. We generated a rabbit polyclonal antiserum against PDZD11, which specifically labeled a polypeptide of 17 kDa in lysates of MDCK, mCCD, human keratinocytes (HaCaT), human lung carcinoma cells (A427 and A549), mouse endothelial cells (bEnd.3, meEC), human colon carcinoma cells (Caco-2), and mouse kidney tissue, consistent with the predicted size of PDZD11 (Fig. 1, *A* and *B*). The antiserum specifically immunoprecipitated exogenously expressed PDZD11, containing N-terminal GFP and C-terminal Myc tags, from MDCK cell lysates (Fig. 1*C*). To validate the findings of the two-hybrid screen and mass spectrometry analysis, we explored the PLEKHA7-PDZD11 interaction by co-immunoprecipitation and GST-pulldown experiments. First, PDZD11 was detected in PLEKHA7 immunoprecipitates from lysates of endothelial (aorta, meEC) and epithelial (kidney, mCCD) cells (Fig. 1*D*). Second, PLEKHA7 was detected in PDZD11 immunoprecipitates from lysates of Caco2 colon epithelial cells (Fig. 1*E*). Third, bacterially expressed full-length PDZD11 interacted with full-length His-tagged PLEKHA7, isolated from insect cells (Fig. 1*F*). Taken together, these results demonstrate that PDZD11 is expressed in epithelial and endothelial cells and tissues, where it forms a complex and directly interacts with PLEKHA7.

The First WW Domain of PLEKHA7 Interacts with the N-terminal 44 Residues of PDZD11 (P7-ID)—To identify the sequences involved in PLEKHA7-PDZD11 interaction, we generated mutated constructs of the proteins to use in GST-pull-down assays. PLEKHA7 comprises WW and PH domains in its N-terminal half and coiled-coil and proline-rich domains in its C-terminal half (Fig. 2*A*). PLEKHA7 prey (N- and C-terminal

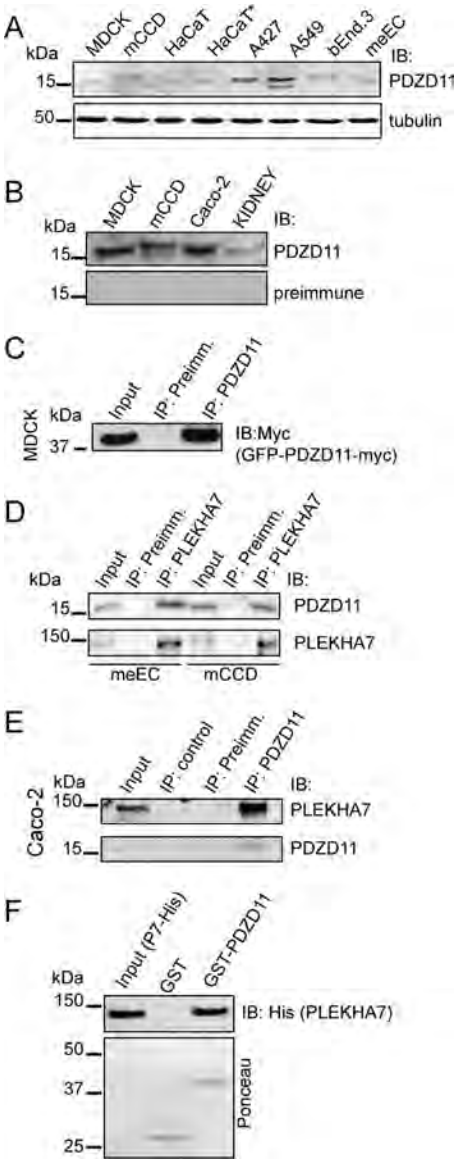

FIGURE 1. **PLEKHA7 forms a complex and interacts directly with PDZD11.** *A–C,* characterization of a rabbit anti-PDZD11 antiserum by immunoblotting analysis of the following. *A,* lysates of kidney epithelial (MDCK, mCCD) cells, human keratinocytes (HaCaT), human lung carcinoma cells (A427, A549), and mouse endothelial cells (bEnd.3, meEC) (tubulin levels for normalization of total protein loading is shown below). The *asterisk* near one lane of HaCaT lysates indicates overconfluent cells. *B,* lysates of MDCK, mCCD, and human colon carcinoma cells (Caco2) and mouse kidney with immune and pre-immune anti-PDZD11 antisera. *C,* immunoprecipitates of exogenously expressed GFP-PDZD11-Myc (in MDCK cells) with immune and pre-immune anti-PDZD11 antiserum. *D–F,* PDZD11 forms a complex and interacts directly with PLEKHA7. *D, top panel,* PDZD11 is detected by immunoblotting in PLEKHA7 immunoprecipitates from lysates of both meEC (*left lanes*) and mCCD cells (*right lanes*). *Bottom panel,* detection of PLEKHA7 in PLEKHA7 immunoprecipitate. Immunoprecipitates with pre-immune only are also shown. *E, top panel,* PLEKHA7 is detected in PDZD11 immunoprecipitates from lysates of Caco-2 cells. *Bottom panel,* detection of PDZD11 in the PDZD11 immunoprecipitate. Immunoprecipitates with pre-immune and immune sera and beads alone (control) are shown. *F,* GST pulldowns of lysates of insect cells expressing full-length His-tagged PLEKHA7, using either GST or GST-PDZD11 as baits, using anti-His antibodies. *Numbers* on the left indicate size (kDa) and migration of prestained markers. *Input lanes* = 0.1 of lysate volume used for immunoprecipitate.

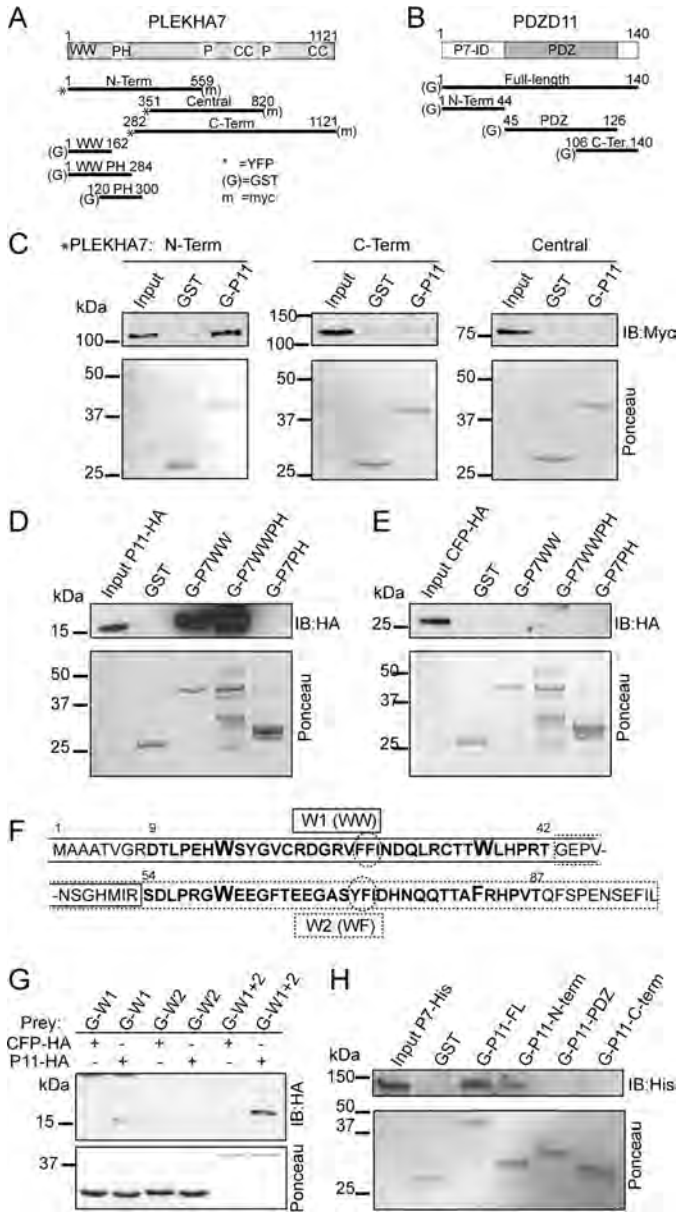

FIGURE 2. **The first WW domain of PLEKHA7 interacts with the N-terminal 44 residues of PDZD11.** *A* and *B,* schematic diagrams of PLEKHA7 (*A*) and PDZD11 (*B*), showing structural domains and amino acid boundaries of full-length and truncated constructs used in GST-pulldown assays. Note: the schemes of PLEKHA7 and PDZD11 are not size-scaled. **, m,* and *G* indicate GFP, Myc, and GST tags, respectively. *C,* immunoblot analysis, using anti-Myc antibodies, of GST pulldowns of lysates of MDCK cells expressing GFP-tagged constructs of PLEKHA7 (as schematically shown in *A*) (21) and either GST or GST-PDZD11 as baits. *D,* immunoblot analysis, using anti-HA antibodies, of GST pulldowns using GST (*G*-) fused to different domains (WW, WW and PH, and PH domain alone) of PLEKHA7 (see *A* for scheme) as baits and either HA-tagged PDZD11 (P11-HA) (*D*) or HA-tagged CFP (CFP-HA) (*E*) as preys. *F,* amino acid sequence of the first 98 residues of human PLEKHA7, and highlighted in *bold* are the W1 domain (WW domain, Trp = W residues are highlighted in larger size) and the W2 domain ("WF" domain, Trp = W and Phe = F residues are highlighted in larger size). The *boxes* show residues included in W1 construct (*continuous line,* residues 1–53) and in W2 construct (*dotted line,* residues 43–98). The cluster of aromatic amino acid at the center of each WW domain is highlighted by a *dotted circle*. *G,* immunoblot analysis, using anti-HA antibodies, of GST pulldowns using GST (*G*) fused either to the W1 sequence or the W2 sequence, or both (*W1 + 2*) (see *F* for residues), and either HA-tagged CFP (*CFP-HA*) or HA-tagged PDZD11 (*P11-HA*) as preys (+ or − indicate which prey is used in each lane). *H,* immunoblot analysis, using anti-His antibodies, of GST pulldowns of lysates of Sf21 insect cells expressing His-tagged full-length PLEKHA7 using GST fusion constructs of PDZD11, as schematically shown in *B*. Images of Ponceau-S-stained blots shows the amounts of recombinant proteins used as baits. Numbers on the *left* indicate size (kDa) and migration of prestained markers.

and central regions) containing N-terminal YFP and C-terminal Myc tags were obtained from lysates of stably transfected MDCK cell lines (Fig. 2, *A* and *C*) (21). Another PLEKHA7 prey consisted of His-tagged full-length PLEKHA7 obtained from lysates of insect cells infected with baculovirus (Fig. 2*H*) (8). PDZD11 consists of a 44-residue N-terminal peptide, followed by a 81-residue PDZ domain and a 14-residue C-terminal peptide (Fig. 2*B*). PDZD11 baits consisted of GST fused N-terminally to 1) full-length sequence, 2) N-terminal peptide, 3) PDZ domain, 4) the 21 C-terminal residues of the PDZ domain, followed by the 14-residue C-terminal peptide (Fig. 2, *B* and *H*). Immunoblot analysis of GST pulldowns showed that full-length PDZD11 interacts with the YFP-tagged N-terminal region of PLEKHA7, but not with C-terminal or central domains of PLEKHA7 (Fig. 2*C*), indicating that the PDZD11-interacting region in PLEKHA7 lies within residues 1–282 of PLEKHA7. This region includes Trp-Trp (WW) and PH domains (Fig. 2*A*). GST fusions of these domains, together or separately, were generated to prepare baits for pulldown assays (Fig. 2*A*). Pulldown experiments using HA-tagged PDZD11 as a prey showed that the N-terminal fragment of PLEKHA7 (residues 1–162) comprising the WW domains, either alone or in combination with the PH domain, but not the PH domain alone, specifically binds to PDZD11 (Fig. 2, *D* and *E,* for control pulldowns with CFP-HA). PLEKHA7 actually contains two WW domains (33). The first contains the canonical Trp-Trp signature, and the second contains a Trp and a Phe residue; the two domains are separated by a spacer region of 11 residues. We generated GST fusions comprising either the first WW (W1, Fig. 2*F*) or the second (W2, Fig. 2*F*), or both (W1 + 2), and we examined their interaction with full-length PDZD11 by pulldown assays (Fig. 2*G*). Only the first, but not the second, WW domain could interact, when isolated, with PDZD11. However, a stronger interaction was detected when both W1 and W2 domains were present in the fusion protein (Fig. 2*G*). Finally, GST fusion proteins were generated to map the region of PDZD11 involved in interaction with PLEKHA7 (Fig. 2, *B* and *H*). GST fusions of full-length PDZD11 and N-terminal peptide interacted with the full-length His-tagged PLEKHA7 in insect cell lysates, but no interaction of PLEKHA7 was detected with GST fusions of either the PDZ domain of PDZD11 or the C-terminal construct (Fig. 2*H*). Because its sequence is unique, and it binds specifically to PLEKHA7, we propose to name the 44-residue N-terminal sequence of PDZD11 P7-ID (PLEKHA7 interacting domain).

PLEKHA7 Recruits PDZD11 to Epithelial Adherens Junctions—Because PLEKHA7 is accumulated at the *zonula adhaerens* (7), the interaction between PLEKHA7 and PDZD11 predicts that PDZD11 should also be localized at AJ in epithelial cells and tissues. To test this, we first labeled epithelial cell lines and kidney tissue by immunofluorescence with the anti-PDZD11 antiserum. Junctional labeling for PDZD11 that co-localized with TJ and AJ markers was detected in MDCK, A427, meEC, and additional epithelial cell types and kidney tissue (Fig. 3*A*,

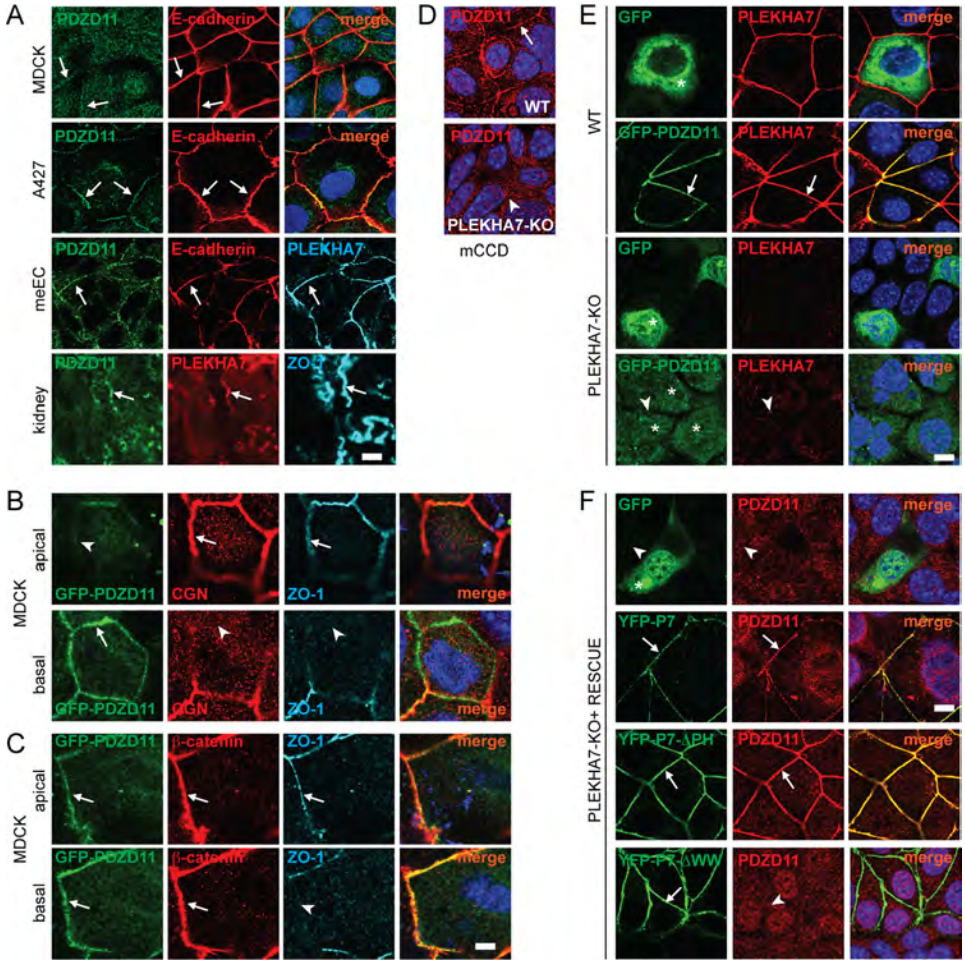

FIGURE 3. **PLEKHA7 recruits PDZD11 to adherens junctions.** *A,* PDZD11 is localized at cell-cell junctions in epithelial and endothelial cells and tissues as follows: immunofluorescent localization of endogenous PDZD11 at junctions of MDCK cells, A427 cells, meEC cells, and frozen sections of mouse kidney, using the anti-PDZD11 antiserum. MDCK and A427 cells were double-labeled with E-cadherin antibodies, and meEC cells were triple-labeled with E-cadherin and PLEKHA7 antibodies, to identify adherens junctions. The kidney section was triple-labeled with PLEKHA7 and ZO-1 to identify zonular junctions. *B* and *C,* exogenous PDZD11 co-localizes with AJ markers as follows: immunofluorescence analysis of serial z-sections of MDCK cells expressing exogenous GFP-tagged PDZD11, and double-stained for either cingulin and ZO-1 (*B*) or for β-catenin (*beta-cat*) and ZO-1 (*C*), as markers of TJ (cingulin and ZO-1) or AJ (β-catenin). *D–F,* PLEKHA7 recruits PDZD11 to epithelial AJ. *D,* immunofluorescence analysis of either WT or PLEKHA7-KO (P7-KO) mCCD cells, using anti-PDZD11 antiserum. Three distinct clones of PLEKHA7-KO cells gave identical results with regard to loss of junctional PDZD11. *E,* immunofluorescence analysis of either WT or PLEKHA7-KO mCCD cells, transiently expressing either GFP or GFP-PDZD11, using anti-PLEKHA7 antibodies (GFP fluorescence was visualized directly). *F,* immunofluorescence analysis of PLEKHA7-KO mCCD cells, transiently expressing either GFP or YFP-PLEKHA7 or YFP-PLEKHA7 with an internal deletion of the PH domain (YFP-P7-ΔPH), or PLEKHA7 with an N-terminal truncation of the WW domains (*YFP-P7-ΔWW*), using anti-PDZD11 antibodies (YFP green fluorescence was visualized directly). Merge images show nuclei in *blue* (DAPI). *Arrows* indicate junctional labeling, and *arrowheads* indicate lack of junctional labeling, and *asterisks i*ndicate cytoplasmic labeling. *Scale bar,* 10 μm (*A, B,* and *D–F*) and 5 μm (*C*).

data not shown). To establish more clearly the localization of PDZD11, we imaged serial apico-basal confocal z-sections of MDCK cells expressing GFP-tagged PDZD11 and double-labeled with markers of either TJ (cingulin and ZO-1) or AJ (β-catenin) (Fig. 3, *B* and *C*). Immunofluorescence analysis showed that GFP-PDZD11 labeling only partially overlapped with endogenous cingulin and ZO-1 labeling along apicolateral junctions (*arrow* and *arrowhead* in Fig. 3*B*), whereas it overlapped more precisely with endogenous labeling for junctional β-catenin (*arrows* in Fig. 3*C*). This is very similar to the localization of endogenous and exogenous PLEKHA7 in epithelial cells (8, 21). Next, we asked whether PDZD11 is recruited to adherens junctions by PLEKHA7, by examining the localization of endogenous PDZD11 in either wild-type (WT) mCCD or in cells where both PLEKHA7 alleles were targeted by CRISPR-mediated gene disruption, and which do not express PLEKHA7 (PLEKHA7-KO) (Fig. 3, *D–F*). Junctional labeling for PDZD11 was detected in WT cells but not in PLEKHA7-KO cells (*arrow* and *arrowhead* in Fig. 3*D*, respectively). Next, we transiently expressed either GFP or GFP-tagged PDZD11 in either WT or PLEKHA7-KO mCCD cells (Fig. 3*E*). Labeling for the GFP control protein was detected diffusely in the cytoplasm both in WT and in PLEKHA7-KO cells (*asterisks* in Fig. 3*E*). Importantly, exogenous GFP-tagged PDZD11 was detected exclusively at junctions in WT cells (*arrows* in Fig. 3*E, WT*), where it co-localized precisely with PLEKHA7. In contrast, exogenous GFP-tagged PDZD11 was localized exclusively in the cytoplasm in PLEKHA7-KO cells (*asterisks* and *arrowheads* in Fig. 3*E,* PLEKHA7-KO). PLEKHA7-KO mCCD cells form junctions similar to WT cells, as determined by labeling with most markers of TJ and AJ, and establish a normal TJ barrier.[4] This indicates that the lack of association of exogenous PDZD11 with

junctions in PLEKHA7-KO cells is specifically due to the absence of PLEKHA7, rather than to secondary effects on other components of zonular junctions. To confirm the role of PLEKHA7 in recruiting PDZD11, we carried out a rescue experiment by re-expressing either GFP- or YFP-tagged PLEKHA7 and either WT or mutant in PLEKHA7-KO mCCD cells (Fig. 3*F*). Immunofluorescence analysis showed that the junctional localization of PDZD11 was rescued in PLEKHA7-KO cells, upon exogenous expression of either full-length PLEKHA7 (*arrows* in Fig. 3*F*, *YFP-PLEKHA7*) or PLEKHA7 lacking the PH domain (*arrows* in Fig. 3*F*, *YFP-P7-ΔPH*), but not upon expression of PLEKHA7 lacking the N-terminal WW domains (*arrowhead* in Fig. 3*F*, *YFP-P7-ΔWW*). In addition, junctional labeling for endogenous PDZD11 was increased in WT cells that overexpressed exogenous PLEKHA7 (data not shown), supporting the idea that the accumulation of PDZD11 at junctions is promoted by PLEKHA7. Taken together, these results demonstrate that PLEKHA7 recruits PDZD11 to epithelial junctions through its WW domain-containing N-terminal region.

PDZD11 Is Required to Stabilize Nectin-1 and Nectin-3 at Epithelial Adherens Junctions—To determine the role of PDZD11 in the molecular architecture of epithelial junctions, we analyzed the localization and expression of zonular (ZO-1, afadin, paracingulin, cingulin, and PLEKHA7) and zonular/lateral (occludin, E-cadherin, α-catenin, β-catenin, and p120-catenin) junctional markers in cells where both alleles of *Pdzd11* were inactivated by CRISPR-mediated genome editing. When mixed cultures of WT and PDZD11-KO cells were analyzed by immunofluorescence (to identify better the differences between WT and KO cells in the same field), the localization of PLEKHA7 and ZO-1 was not detectably altered in PDZD11-KO cells, when compared with neighboring WT cells (Fig. 4*A*, *top row*). No labeling for PDZD11 was detected in KO cells by either immunofluorescence (Fig. 4*A*) or immunoblotting (Fig. 4*B*), confirming the specificity of the anti-PDZD11 antiserum. The immunofluorescent localization (Fig. 4*A* and data not shown) and the levels of expression (Fig. 4*B*), not only of PLEKHA7 but also of the other zonular and zonular/lateral tight and adherens junction markers (E-cadherin, cingulin, occludin, afadin, p120-catenin, α-catenin, β-catenin, and paracingulin), were not detectably altered in confluent PDZD11-KO cells (Fig. 4, *A* and *B*). Next, we examined the localization and expression of nectins, Ig-like cell adhesion molecules localized at adherens junctions, that display PDZ-binding motifs at their C-terminal cytoplasmic tail (34, 35). In three distinct PDZD11-KO clones, we observed a decrease in junctional labeling for nectin-3 (Fig. 4, *C, top row*, showing only clone 2C7, and quantification in *D*). The decreased junctional labeling for nectin-3 in PDZD11-KO cells was rescued by re-expression of GFP-tagged PDZD11 but not of GFP (*double arrows* in Fig. 4*C*, *2nd row*). By immunoblotting, we observed decreased levels of expression of both nectin-1 and nectin-3 in PDZD11-KO cells (Fig. 4*E* and quantification in *F*), with no significant changes in nectin mRNA levels, as determined by qRT-PCR (Fig. 4*G*). Nectin-1 and nectin-3 protein levels in PDZD11-KO cells were rescued by re-expression of GFP-tagged PDZD11, but not of GFP alone (Fig. 4*E* and quantifications in *F*). To ask whether the decreased levels of nectin-1 and nectin-3 in PDZD11 KO cells were due to decreased stability, *e.g.* increased degradation, we treated either WT or KO cells with the proteasome inhibitor MG132 (Fig. 4*H* and *I* for quantification). Immunoblot analysis showed that normal levels of nectin expression were rescued in PDZD11 KO cells upon treatment with MG132 (Fig. 4, *H* and *I*), revealing a proteasome-dependent degradation of nectin. Next, we tested the hypothesis that the junctional localization and expression of nectin-1 and nectin-3 should also be altered in PLEKHA7-KO cells, because PLEKHA7 recruits PDZD11 to junctions. Immunofluorescence (Fig. 4*C*, *3rd* and *4th rows*) and immunoblotting (Fig. 4*J* and quantifications in *K*) analyses showed that PLEKHA7-KO cells phenocopied PDZD11KO cells, because junctional nectin-3 labeling and nectin-1 and nectin-3 protein levels were reduced in PLEKHA7-KO cells and rescued upon re-expression of PLEKHA7. These data demonstrate that although PDZD11 is not required to maintain the molecular organization of either TJ or the E-cadherin-associated complex at steady state, the PLEKHA7-PDZD11 complex is required for the efficient recruitment and stabilization of nectins at AJ.

PDZD11 Binds Directly to Nectin-1—To examine the molecular basis for the regulation of nectin junctional accumulation and stability by the PDZD11-PLEKHA7 complex, we studied the physical interaction of PDZD11 and PLEKHA7 with nectins. Immunoprecipitation experiments show that endogenous nectin-1 and nectin-3 immunoprecipitate PDZD11 (Fig. 5*A*). In contrast, we were unable to detect PLEKHA7 in nectin immunoprecipitates. To determine whether PDZD11 or PLEKHA7 interacts directly with nectins, GST fusion constructs of PDZD11 and PLEKHA7 were used as baits to bind Myc-tagged nectin, expressed in HEK293T cells. Immunoblot analysis showed that full-length nectin-1 is detected specifically in GST pulldowns of PDZD11 but not in GST pulldown using fragments of PLEKHA7 from the N-terminal, central, or C-terminal domains (Fig. 5*B*). Next, we asked whether the interaction between nectin-1 and PDZD11 depends on the interaction between the PDZ domain of PDZD11 and the PDZ-binding motif of nectin-1. No binding to the PDZD11 GST fusion bait was observed when the four-residue PDZ-binding motif of nectin-1 was deleted (Myc-nectin1-Δ4 in Fig. 5*C*). Furthermore, only the PDZ fragment of PDZD11 could bind nectin-1 but not the N-terminal P7-ID nor the C-terminal fragments (Fig. 5*D*). Finally, we used the PLA to detect the physical association between PLEKHA7 and either nectin-1 or nectin-3. In both cases, a strong junctional accumulation of labeling was detected in WT cells (*double arrows* and *magnified insert* in Fig. 5*E*, *WT panels*). However, only background labeling was observed in PLEKHA7-KO cells (*arrowhead* and *magnified inset* in Fig. 5*E*, *PLEKHA7-KO panels*), demonstrating that the proximity between nectins and PLEKHA7 is specifically due to PLEKHA7. Importantly, in PDZD11 KO cells there was a strong reduction in junctional signal with respect to WT cells (*arrow* and *magnified inset* in Fig. 5*E*, *PDZD11-KO panels*). This indicates that PDZD11 is critical to ensure maximal physical proximity between PLEKHA7 and nectins and that residual association between nectins and PLEKHA7 may be indirect, through afadin. Taken together, the GST pulldown and PLA results demonstrate that a complex of PLEKHA7 and PDZD11 is required

for the efficient recruitment and stabilization of nectins at AJ, through the binding of the PDZ-binding motif of nectins to the PDZ domain of PDZD11.

PDZD11 Is Required for the Efficient Early Assembly of Apical Junctions in the Calcium-switch Experimental Model—To address the cellular functions of PDZD11, we hypothesized,

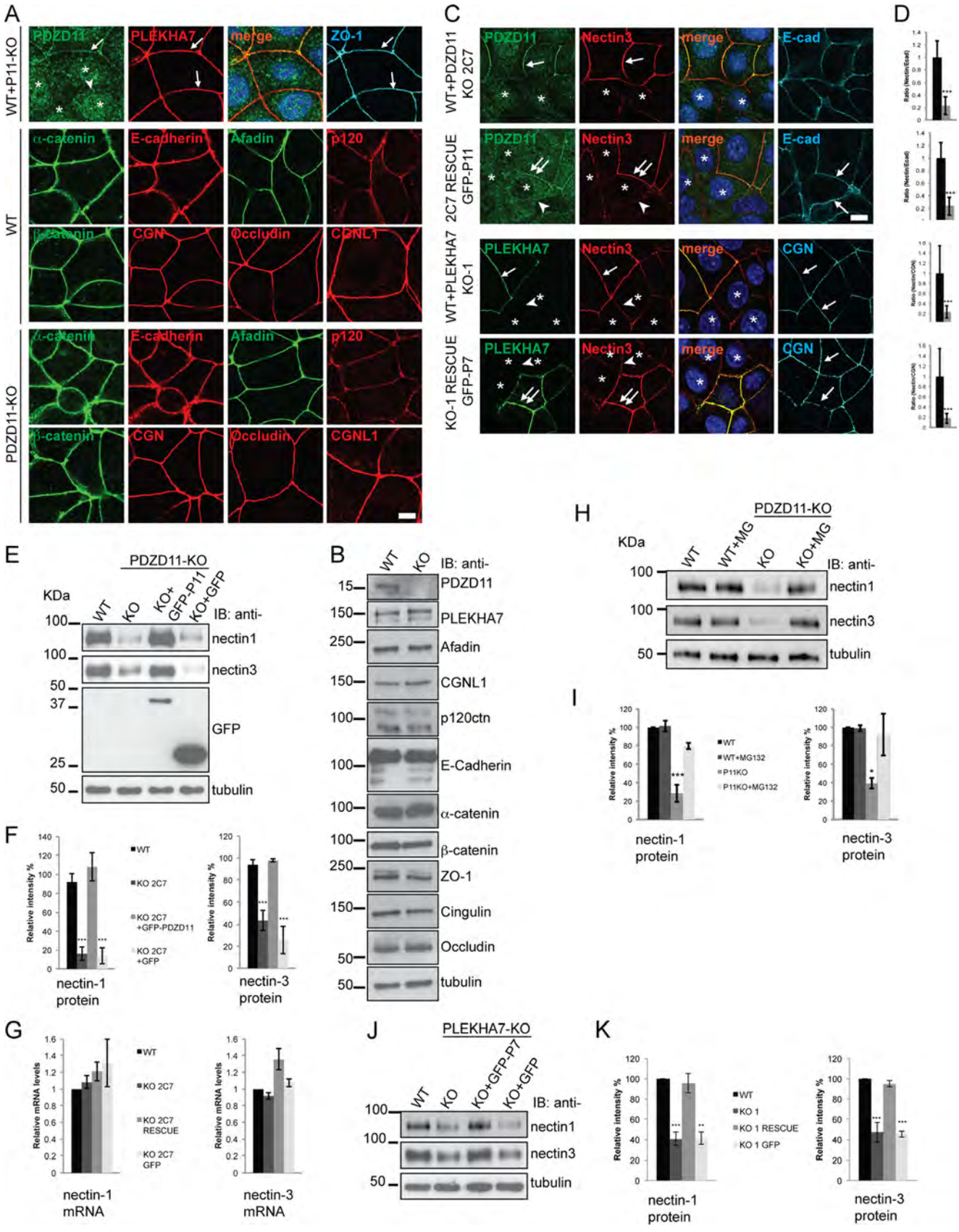

based on the effects of the PLEKHA7-PDZD11 complex on nectin junctional localization and stability, that we might detect a phenotype related to the function of nectins, which are implicated in early junction assembly (see under "Discussion") (5). Analysis of junctions at steady state showed that WT and PDZD11-KO cells are indistinguishable when examining a large number of markers (Fig. 4). Therefore, we examined the role of PDZD11 in the dynamic assembly of apical junctions, by using the calcium-switch protocol, which is the most commonly used experimental model to investigate the biogenesis of junctions in epithelial cells (29). Cells were immunofluorescently labeled with antibodies against cingulin (TJ marker) and E-cadherin (AJ marker) at different times after the start of junction assembly by the calcium switch (15 and 30 min and 1 and 4 h, Fig. 6, *A* and *D*). Junction assembly was scored by quantifying linear junctional labeling for each marker *versus* putative total junctional length (Fig. 6, *B, C, E,* and *F*). At 15 and 30 min after the calcium switch, WT cells showed 20 and 35% of junction assembly, respectively, corresponding to clearly identifiable segments of E-cadherin and cingulin labeling at the cell periphery (*arrows* in Fig. 6, *A, WT*, and quantifications in *B* and *C*). In contrast, in PDZD11 KO cells only 8 and 20% of junctions were assembled after 15 or 30 min, respectively, corresponding to fewer segments of the cell peripheries labeled by the cingulin and E-cadherin antibodies (*arrows* in Fig. 6, *A,* and quantifications in *B* and *C*). In PDZD11-KO cells, E-cadherin and cingulin labeling were detected mostly in a granular perinuclear pattern (*arrowheads* in Fig. 6*A*), suggesting an accumulation in endoplasmic reticulum/Golgi compartments. The differences between WT and PDZD11-KO cells were no longer observed at 1 and 4 h after the beginning of the calcium switch (WT and KO in Fig. 6*D* and quantifications in *E* and *F*). After 4 h, junctions were fully assembled (Fig. 6, *D* and *F*). The slight early delay in junction assembly observed in PDZD11-KO cells was specifically due to the lack of PDZD11 and not to clone-dependent variations, because the phenotype was rescued by the stable re-expression of GFP-PDZD11 but not by the re-expression GFP alone (*KO+GFP-PDZD11* and *KO+GFP* in Figs. 6, *A–C*, and see 4*E* for immunoblots of transgenes). Therefore, the absence of PDZD11 causes a slight delay in the very initial phases of junction assembly, but this delay is eventually overcome, allowing the formation of junctions with localization and expression of junctional proteins indistinguishable from that of WT cells.

Discussion

Here, we identify PDZD11 as a new interactor of PLEKHA7, and we show that PDZD11 is recruited by PLEKHA7 to AJ, to promote the efficient junctional recruitment and stabilization of nectins and the efficient early phases of assembly of apical junctions in epithelial cells. These results uncover a new function for PLEKHA7, in organizing the junctional clustering of PDZ-interacting proteins, through PDZD11. They also show that PLEKHA7 stabilizes both major adhesion transmembrane proteins of adherens junctions (cadherins and nectins), through binding to components of the respective cytoplasmically associated complexes: p120-catenin/paracingulin for E-cadherin and PDZD11-afadin for nectins (Fig. 7).

Considering the potentially critical role of PLEKHA7 in major human pathologies, such as hypertension and glaucoma, it is essential to learn more about its molecular interactors and its cellular functions. Here, we report that two different types of screening technologies identify PDZD11 as the top hit among PLEKHA7 interactors, and we confirm the relevance of the PLEKHA7-PDZD11 interaction, as well as of the interaction

FIGURE 4. **PDZD11 and PLEKHA7 are required for the efficient recruitment and stabilization of nectins at adherens junctions.** *A,* PDZD11 is not required for the integrity of adherens and tight junctions. *Top panel,* immunofluorescence analysis of mixed cultures of wild-type (*WT*) and PDZD11 knock-out (*KO*) cells with antibodies against PDZD11 (rabbit, Alexa488), PLEKHA7 (guinea pig, Cy3), and ZO-1 (rat, Cy5). *Merge* images show nuclei labeled in *blue* (DAPI). *Arrows* indicate junctional labeling; *arrowheads* indicate lack of junctional labeling; *asterisks* indicate KO cells. *Bottom panels,* individual cultures (not mixed) of either WT or PDZD11-KO cells were immunofluorescently labeled with antibodies against E-cadherin, afadin, α-catenin, β-catenin, p120-catenin, cingulin, paracingulin, and occludin. *B,* immunoblot analysis of lysates of wild-type (*WT*) and PDZD11-KO (*KO*) mCCD cells, using antibodies against PDZD11, PLEKHA7, afadin, paracingulin, p120-catenin (p120), E-cadherin, α-catenin, β-catenin, ZO-1, cingulin, occludin, and tubulin (for loading control). *C,* PDZD11 and PLEKHA7 are required for the junctional accumulation of nectin-3. Immunofluorescence analysis of (*from top to bottom*): *1st row*: mixed cultures of WT cells + 2C7 PDZD11-KO clone to identify differences in neighboring WT *versus* KO cells; *2nd row*: mixed cultures of the PDZD11-KO clone (2C7) rescued with GFP together with cells of the same clone rescued with GFP-PDZD11: again, to compare directly nectin-3 labeling in mock-rescued cells (GFP) or in cells rescued with the GFP-PDZD11 construct. *3rd row*: mixed cultures of WT cells + PLEKHA7-KO clone 1 (KO-1); *4th row*: mixed cultures of the PLEKHA7-KO-1 clone rescued with GFP together with cells of the same clone rescued with GFP-PLEKHA7. Cells were labeled with antibodies against either PDZD11 (*1st* and *2nd rows*) or PLEKHA7 (*3rd* and *4th rows*) to identify WT and KO cells (or cells expressing exogenous GFP-PDZD11 or GFP-PLEKHA7 rescue), with antibodies against nectin-3 to examine nectin-3 accumulation, and with either E-cadherin (*E-cad*) (*1st* and *2nd rows*) or cingulin (*CGN*) (*3rd* and *4th rows*) to identify junctional regions. The same results were obtained with additional clonal lines of PDZD11-KO cells (1B2 and 1C8) and PLEKHA7 (KO-5 and KO-7) (data not shown). *Arrows* and *arrowheads* indicate normal or decreased junctional labeling, respectively; *double arrows* indicate increased junctional labeling in cells expressing either the GFP-PDZD11 or GFP-PLEKHA7 constructs; *asterisks* identify the nuclei of either KO cells (*1st* and *3rd row*) or KO cells rescued with GFP alone (*2nd* and *4th rows*), which is not visible in the cytoplasm, due to methanol fixation. *D, histograms* showing the quantification of junctional labeling for nectin-3 in the corresponding panels, expressed as a ratio between nectin-3 and either E-cadherin (*rows 1* and *2*) or cingulin (*rows 3* and *4*) labeling in junctions between WT cells (*black*) or between KO cells (*gray*). *E,* immunoblot analysis of nectin-1 and nectin-3 levels in lysates from WT cells and from the PDZD11 2C7 clonal line, either without or with re-expression of exogenous GFP-PDZD11 (GFP-P11) (or GFP, as a control) for rescue. Immunoblotting with anti-GFP is also shown, to detect expression of rescuing proteins. *F, histograms* showing the quantification (based on densitometric scan of blots) of relative protein levels for nectin-1 (*left*) or nectin-3 (*right*), by considering protein levels in WT clones (*black*) as 100% and expressing protein levels in KO 2C7 clone (*dark gray*), KO 2C7 clone + GFP-PDZD11 rescue (*light gray*), KO 2C7 clone + GFP rescue (*very light gray*) as percentages of WT. *G, histograms* showing levels of either nectin-1 mRNA (*left*) or nectin-3 mRNA (*right*) in WT, PDZD11-KO (clone 2C7), and rescued clonal lines, as determined by qRT-PCR. See *F* for labeling of columns. *H,* PDZD11 stabilizes nectins by preventing their proteasome-mediated degradation. Immunoblot analysis of nectin-1 and nectin-3 levels in lysates from either WT or PDZD11KO cells (clone 2C7), either untreated (WT, KO) or treated with the proteasome inhibitor MG132 (*WT+MG* and *KO+MG*). *I, histograms* showing the quantification of relative protein levels for nectin-1 (*left*) or nectin-3 (*right*), in either WT cells (*black* and *dark gray columns*) or PDZD11 KO clone 2C7 (*light* and *very light grays*), either without (*black light gray*) or with (*dark* and *very light gray*) treatment with MG132. *J,* immunoblot analysis of nectin-1 and nectin-3 levels in lysates from WT cells and from the PLEKHA7-KO-1 clonal line, either without or with re-expression of exogenous GFP-PLEKHA7 (GFP-P7) (or GFP, as a control) for rescue. *K, histograms* showing the quantification of relative protein levels for nectin-1 (*left*) or nectin-3 (*right*) in WT cells (*black column*), PLEKHA7-KO-1 clone (*dark gray*), KO-1 clone + GFP-PLEKHA7 rescue (*light gray*), KO-1 clone + GFP rescue (*very light gray*) shown as percentages of WT. *Histograms* were obtained from three separate experiments. *Asterisks* above columns indicate statistical significance.

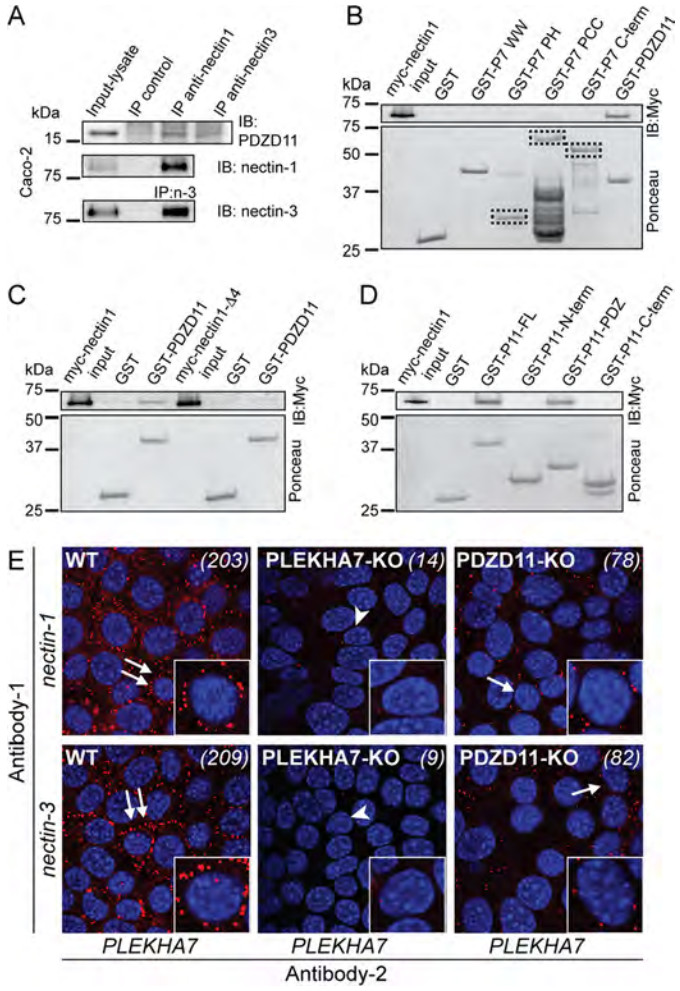

FIGURE 5. **Nectin forms a complex and interacts directly with PDZD11.** *A,* PDZD11 and nectins form a complex. Immunoblotting analysis of either nectin-1 or nectin-3 immunoprecipitates (from Caco2 whole cell lysates) with antibodies against PDZD11 (*top*), nectin-1 (*middle*), and nectin-3 (*bottom*). *B,* PDZD11 but not PLEKHA7 fragments interact directly with nectin-1. Immunoblotting analysis of GST pulldowns using either GST or GST fused to the following fragments of PLEKHA7: WW (residues 1–162, see Fig. 2); PH (residues 120–300); proline-rich and coiled-coil domains (PCC, residues 500–844); C-terminal (residues 821–1121 (7)), and Myc-tagged-nectin-1 as a prey. *Dotted boxes* indicate recombinant proteins stained by Ponceau-S. *C,* PDZD11 binds to the PDZ-binding motif of nectin-1. Immunoblotting analysis of GST pulldowns using either GST or GST-PDZD11 as baits and either Myc-tagged nectin-1 WT (Myc-nectin1) or the nectin-1 mutant lacking the last PDZ-binding motif 4 residues (Myc-nectin1-Δ4) (both expressed in HEK293T cells) as preys. The Ponceau-S-stained blot shows the amounts of recombinant proteins used as baits. *Numbers* on the *left* indicate size (kDa) and migration of prestained markers. *D,* PDZ domain of PDZD11 binds to nectin-1. Immunoblotting analysis of GST pulldowns using either GST or different fragments of PDZD11 (see Fig. 2) as baits, and Myc-tagged nectin-1 as a prey. *E,* detection of PDZD11-dependent PLEKHA7-nectin association by PLA. Cells were labeled with mouse anti-PLEKHA7 antibodies, and either rabbit anti-nectin-1 (*top panels*) or nectin-3 (*bottom panels*). Abundant brightly labeled dots along the regions of cell-cell contact are detected in WT cells (*double arrows* indicating WT cell shown in magnified *inset*); background labeling is detected in PLEKHA7-KO cells (*arrowhead* indicating PLEKHA7-KO cell shown in magnified *inset*), and decreased labeling (78 *versus* 203 dots for nectin-1 and 82 *versus* 209 dots for nectin-3) is detected in PDZD11-KO cells. Each panel is labeled with the cell genotype, and *numbers* in *italics* on the *top-right hand corner* of each image indicates number of fluorescent dots in the imaged field, for a semi-quantitative evaluation of assay results.

between PDZD11 and nectin, by biochemical direct *in vitro* binding assays. We show that the first WW domain of PLEKHA7 is sufficient for direct interaction with PDZD11 and that the 44-residue N-terminal sequence of PDZD11 interacts with PLEKHA7. Moreover, the PDZ-binding four-residue motif of nectin-1 mediates the interaction of nectin with the PDZ domain of PDZD11. The sequence of the P7-ID shows no homology to the N-terminal sequences of other single PDZ domain proteins and may function as a PDZ "supramodule," to allow higher specificity of interaction of PDZD11 with its target sequences (36). PLEKHA7 binding to this region may also modulate the affinity of binding of the PDZ domain of PDZD11 with its target sequences. Conversely, the P7-ID of PDZD11 comprises eight proline residues, including two PP (Pro-Pro) residues, but none of them shows a consensus ligand sequence belonging to any of the four previously identified WW-binding motif groups (37). Additional experiments are required to determine whether the proline motifs of PDZD11 define a new group of WW-interacting sequences and which residues of the WW1 domain of PLEKHA7 are implicated in its interaction with PDZD11. In summary, we assigned a specific protein-interaction function to the most N-terminal WW region of PLEKHA7, and we dissected the structure-function relationships in PDZD11.

PDZD11 was previously described as PISP, based on its binding to the cytoplasmic domain of all plasma membrane Ca^{2+}-ATPase b-splice variants (30). PDZD11 is also known as AIPP1 through its binding to the cytoplasmic tail of the Menkes copper ATPase ATP7A (31) and as an interactor of the sodium-dependent multivitamin transporter (32). The proposed function of PDZD11, a ubiquitously expressed protein, was to provide a scaffold for these transmembrane proteins, by binding through its PDZ domain, to the PDZ-binding motif at their C terminus. Supporting this idea, depletion of PDZD11 reduced the cell surface expression of the sodium-dependent multivitamin transporter, as assessed by cell surface biotinylation assay (32). Other single PDZ proteins, such as MALS (mammalian homolog of Lin-7), are implicated in intracellular transport and targeting of their partner proteins (38), and future studies should determine whether PDZD11 also plays this role, for example by promoting the efficient transport of PDZ-binding proteins such as nectins to the cell surface. Here, we discover a new role for PDZD11. It promotes the efficient recruitment and stabilization of nectins at AJ of epithelial cells. The C-terminal cytoplasmic domain of nectins interacts with the PDZ domains of several junctional partners as follows: afadin (35), which is important for the accumulation of nectin-1 at AJ (39), and depending on nectin isoform, also Par-3 (40), PICK-1 (41), MUPP1 (42), PATJ (42), and MPP3 (43). Therefore, redundant interactions can stabilize nectins at junctions (44). This is consistent with our observation that KO of PDZD11 in epithelial cells does not result in the complete loss of junctional nectins. PDZD11 may function not only through direct scaffolding of nectins but also indirectly by affecting the conformation of the N-terminal region of PLEKHA7, which interacts with afadin, hence affecting the PLEKHA7-afadin interaction and the ability of afadin to form an efficient scaffold for nectins.

Because PDZD11 promotes the efficient recruitment of nectins to ZA, we hypothesized that one cellular function of PDZD11 may be related to the function of nectins. Few studies have been carried out to address the function of nectins in cultured epithelial cells. Nectins independently initiate, subsequently followed by E-cadherin, the formation of AJ, by trans-

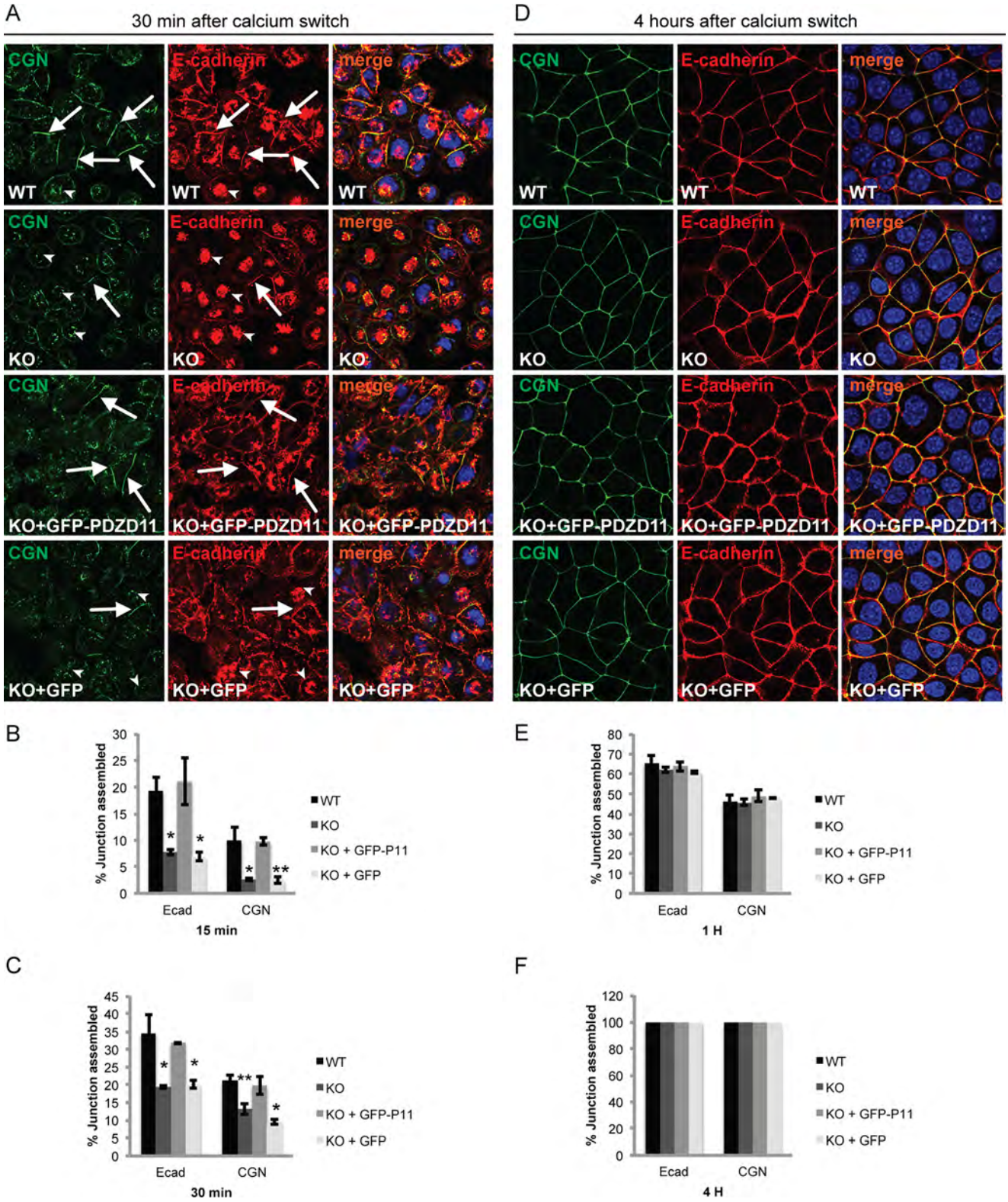

FIGURE 6. **PDZD11 is required for the efficient assembly of junctions at early time points after the calcium switch.** *A–C,* decreased junctional accumulation of E-cadherin and cingulin (*CGN*) at 15 and 30 min after the calcium switch. *A,* immunofluorescent localization of cingulin and E-cadherin in either WT cells (*1st row*), or PDZD11 KO cells (clone 2C7) (*2nd row*), or PDZD11 KO cells stably rescued with GFP-PDZD11 (*3rd row*), or PDZD11 KO cells stably rescued with GFP (*4th row*), 30 min after the calcium switch. *Arrows* indicate junctional labeling, and *arrowheads* indicate perinuclear granular labeling. *Merge* images show nuclei labeled in *blue* by DAPI. *B* and *C,* quantification of percent of junction assembly (see under "Experimental Procedures" for protocol) in WT cells (*black*), PDZD11 KO cells (*dark gray*), KO cells rescued with GFP-PDZD11 (*light gray*), KO cells rescued with GFP (*very light gray*), either 15 min (*B*) or 30 min (*C*) after the calcium switch. *D–F,* immunofluorescent localization of cingulin and E-cadherin 4 h after the calcium switch (*D*) and quantification of percent of junction assembly after either 1 h (*E*) or 4 h (*F*) after the calcium switch (see *A–C* for labeling). *Asterisks* indicate statistical significance (*, $p < 0.05$; **, $p < 0.01$).

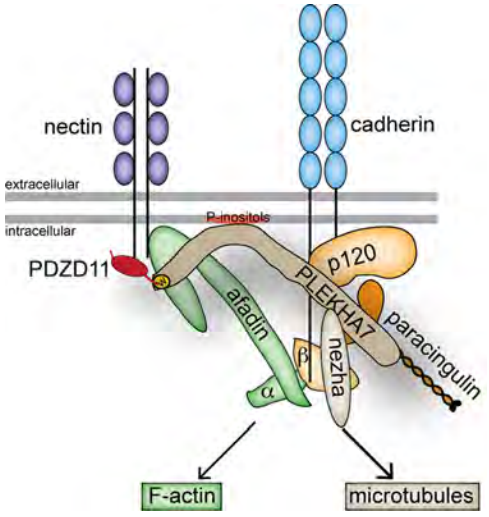

FIGURE 7. **New model of the molecular architecture of the *zonula adhaerens*.** This simplified scheme (depicting a half-junction) shows how PLEKHA7 may bridge nectin and cadherin complexes by binding through its N-terminal half to afadin and PDZD11, and through its C-terminal half to $p120^{Ctn}$ and paracingulin. The transmembrane ZA proteins nectin and E-cadherin are shown as dimers, with Ig-like and extracellular domains represented by *purple* and *blue ovals*, respectively. PLEKHA7 binds to its interactors $p120^{ctn}$ (6), paracingulin (CGNL1) (8), and nezha (6) through its central and C-terminal regions, to membrane-phosphorylated phosphatidylinositols (*orange patch*) through its PH domain (10), and to afadin (50) and PDZD11 through its N-terminal region. The *yellow circle* at the N terminus of PLEKHA7 indicates the WW1 domain (*w*) that is sufficient for PLEKHA7 interaction with PDZD11 *in vitro*. PDZD11 connects the C-terminal PDZ-binding motif of nectin to PLEKHA7. Afadin/α-catenin and nezha provide the linkage of the complexes to actin filaments and microtubules, respectively. The cytoplasmic domain of E-cadherin interacts with p120-catenin and β-catenin (which in turns binds to α-catenin).

interacting at protrusions of neighboring cells, giving rise to spot-like junctions that subsequently mature into belt-like AJ (45). Nectins and E-cadherin cooperatively organize AJ, by interacting through their cytoplasmic partners (46), although nectins can efficiently drive the formation of AJ and TJ even in the absence of E-cadherin (47). Nectin mutations that prevent their trans-interaction affect junction formation in MDCK cells, causing a delay in AJ formation (48). Consistent with the reduction of junctional nectin levels, and the role of nectins in initiating junction assembly, the KO of PDZD11 resulted in a reduction of the efficiency of assembly of zonular junctions, which was detectable at the 15- and 30-min time points in the calcium switch experimental model. Junction assembly resumed to normal kinetics at later time points in PDZD11-KO cells, probably due to the cooperative and redundant adhesive functions of E-cadherins and the residual nectin molecules.

We propose a new model for the architecture of the ZA (Fig. 7), based on the results presented here. By binding to p120-catenin and paracingulin on one side and to PDZD11 and afadin on the other side, PLEKHA7 establishes a molecular bridge between nectin- and cadherin-based protein complexes at the ZA (Fig. 7), distinct from the connection provided through the afadin-ponsin complex (49). Through PDZD11, PLEKHA7 contributes to recruiting nectins to the ZA. In addition, by binding both to afadin and to PDZD11, PLEKHA7 further strengthens the cytoplasmic scaffold for nectins, by bridging together these two cytoplasmic scaffolding proteins. Finally, by binding to actin filaments through afadin (and potentially other actin-binding proteins (17)), and to microtubules through nezha (6), PLEKHA7 contributes to reinforcing the cytoskeletal anchoring of both nectin and cadherin adhesion receptors.

The PLEKHA7-PDZD11 module that we describe provides a new type of molecular machinery that brings PDZ-binding membrane proteins to the AJ in epithelial and endothelial cells. This is important to explore new mechanistic hypotheses to understand at the molecular level the role of PLEKHA7 in tissue physiology and pathology. In fact, it has not escaped our attention that the interaction of PDZD11 with the plasma membrane Ca^{2+}-ATPase (30) may be relevant to the role of PLEKHA7 in the control of calcium homeostasis. Studies on zebrafish show that loss of the PLEKHA7 homologue *hadp1* leads to a reduced rate of extrusion of cytoplasmic Ca^{2+} during diastole (10). Furthermore, in a model of PLEKHA7-KO rats, increased endothelial NOS signaling and increased intracellular calcium detected in PLEKHA7-KO aortic endothelial cells suggest that reduced blood pressure in KO animals may depend on PLEKHA7- and calcium-mediated increase of endothelial NOS signaling to vascular smooth muscle, leading to its relaxation (14). Significantly, both PDZD11 and PLEKHA7 are localized at endothelial junctions (Fig. 3*A*). Thus, we are currently investigating whether PLEKHA7 regulates plasma membrane Ca^{2+}-ATPase, and hence calcium homeostasis, through PDZD11, to clarify mechanistically its role in the regulation of blood pressure, cardiac contractility, and glaucoma. It is also possible that altered calcium homeostasis in PLEKHA7-KO cells underlies the phenotype of decreased susceptibility and recovery after intoxication by staphylococcal α-toxin, shown by cells and mice lacking PLEKHA7 (18). Interestingly, PDZD11 was one of the proteins identified in the screen on Hap1 cells whose KO reduced the cytotoxic effects of α-toxin (18).

In summary, here we describe a new protein complex module comprising PDZD11 and PLEKHA7, whereby the single PDZ domain protein PDZD11 connects nectins to the cadherin- and cytoskeleton-associated protein complex, through its binding to PLEKHA7 (Fig. 7), to stabilize nectins at AJ and promote efficient early assembly of junctions. The results presented here also raise the hypothesis that PLEKHA7 orchestrates the membrane organization and function of proteins regulating calcium homeostasis, through PDZD11, providing a new potential molecular mechanism to explain the implication of PLEKHA7 in vascular and cardiac pathophysiology.

Author Contributions—D. G. characterized anti-PDZD11 antibodies, carried out immunofluorescence, immunoprecipitation, and pulldown analyses, and generated and characterized PDZD11-KO mCCD cells. J. S. generated PLEKHA7-KO mCCD cells and rescue cells and constructs, characterized anti-PLEKHA7 antibodies, and carried out immunofluorescence and pulldown analyses. E. V. and S. S. carried out immunoblotting, immunofluorescence, and immunoprecipitation analysis of additional cultured cell lines. I. M. and L. J. generated cDNA constructs and helped in recombinant protein expression, GST pulldown, and immunoblotting experiments. I. P., M. M., and A. A. H. conducted QUBIC experiments. S. C. initiated, organized, and supervised the project. D. G., J. S., and S. C. analyzed the data. S. C. wrote the paper.

Acknowledgments—We thank all the colleagues cited in the text for their kind gift of cell lines and reagents.

References

1. Anderson, J. M., and Van Itallie, C. M. (2009) Physiology and function of the tight junction. *Cold Spring Harb. Perspect. Biol.* **1,** a002584
2. Takeichi, M. (2014) Dynamic contacts: rearranging adherens junctions to drive epithelial remodelling. *Nat. Rev. Mol. Cell Biol.* **15,** 397–410
3. Harris, T. J., and Tepass, U. (2010) Adherens junctions: from molecules to morphogenesis. *Nat. Rev. Mol. Cell Biol.* **11,** 502–514
4. McCrea, P. D., Gu, D., and Balda, M. S. (2009) Junctional music that the nucleus hears: cell-cell contact signaling and the modulation of gene activity. *Cold Spring Harb. Perspect. Biol.* **1,** a002923
5. Mandai, K., Rikitake, Y., Mori, M., and Takai, Y. (2015) Nectins and nectin-like molecules in development and disease. *Curr. Top. Dev. Biol.* **112,** 197–231
6. Meng, W., Mushika, Y., Ichii, T., and Takeichi, M. (2008) Anchorage of microtubule minus ends to adherens junctions regulates epithelial cell-cell contacts. *Cell* **135,** 948–959
7. Pulimeno, P., Bauer, C., Stutz, J., and Citi, S. (2010) PLEKHA7 is an adherens junction protein with a tissue distribution and subcellular localization distinct from ZO-1 and E-cadherin. *PLoS ONE* **5,** e12207
8. Pulimeno, P., Paschoud, S., and Citi, S. (2011) A role for ZO-1 and PLEKHA7 in recruiting paracingulin to tight and adherens junctions of epithelial cells. *J. Biol. Chem.* **286,** 16743–16750
9. Citi, S., Pulimeno, P., and Paschoud, S. (2012) Cingulin, paracingulin, and PLEKHA7: signaling and cytoskeletal adaptors at the apical junctional complex. *Ann. N.Y. Acad. Sci.* **1257,** 125–132
10. Wythe, J. D., Jurynec, M. J., Urness, L. D., Jones, C. A., Sabeh, M. K., Werdich, A. A., Sato, M., Yost, H. J., Grunwald, D. J., Macrae, C. A., and Li, D. Y. (2011) Hadp1, a newly identified pleckstrin homology domain protein, is required for cardiac contractility in zebrafish. *Dis. Model. Mech.* **4,** 607–621
11. Levy, D., Ehret, G. B., Rice, K., Verwoert, G. C., Launer, L. J., Dehghan, A., Glazer, N. L., Morrison, A. C., Johnson, A. D., Aspelund, T., Aulchenko, Y., Lumley, T., Köttgen, A., Vasan, R. S., Rivadeneira, F., *et al.* (2009) Genome-wide association study of blood pressure and hypertension. *Nat. Genet.* **41,** 677–687
12. Hong, K. W., Jin, H. S., Lim, J. E., Kim, S., Go, M. J., and Oh, B. (2010) Recapitulation of two genome-wide association studies on blood pressure and essential hypertension in the Korean population. *J. Hum. Genet.* **55,** 336–341
13. Lin, Y., Lai, X., Chen, B., Xu, Y., Huang, B., Chen, Z., Zhu, S., Yao, J., Jiang, Q., Huang, H., Wen, J., and Chen, G. (2011) Genetic variations in CYP17A1, CACNB2 and PLEKHA7 are associated with blood pressure and/or hypertension in the ethnic minority of China. *Atherosclerosis* **219,** 709–714
14. Endres, B. T., Priestley, J. R., Palygin, O., Flister, M. J., Hoffman, M. J., Weinberg, B. D., Grzybowski, M., Lombard, J. H., Staruschenko, A., Moreno, C., Jacob, H. J., and Geurts, A. M. (2014) Mutation of Plekha7 attenuates salt-sensitive hypertension in the rat. *Proc. Natl. Acad. Sci. U.S.A.* **111,** 12817–12822
15. Vithana, E. N., Khor, C. C., Qiao, C., Nongpiur, M. E., George, R., Chen, L. J., Do, T., Abu-Amero, K., Huang, C. K., Low, S., Tajudin, L. S., Perera, S. A., Cheng, C. Y., Xu, L., Jia, H., *et al.* (2012) Genome-wide association analyses identify three new susceptibility loci for primary angle closure glaucoma. *Nat. Genet.* **44,** 1142–1146
16. Chen, Y., Chen, X., Wang, L., Hughes, G., Qian, S., and Sun, X. (2014) Extended association study of PLEKHA7 and COL11A1 with primary angle closure glaucoma in a Han Chinese population. *Invest. Ophthalmol. Vis. Sci.* **55,** 3797–3802
17. Kourtidis, A., Ngok, S. P., Pulimeno, P., Feathers, R. W., Carpio, L. R., Baker, T. R., Carr, J. M., Yan, I. K., Borges, S., Perez, E. A., Storz, P., Copland, J. A., Patel, T., Thompson, E. A., Citi, S., and Anastasiadis, P. Z. (2015) Distinct E-cadherin-based complexes regulate cell behaviour through miRNA processing or Src and p120 catenin activity. *Nat. Cell Biol.* **17,** 1145–1157
18. Popov, L. M., Marceau, C. D., Starkl, P. M., Lumb, J. H., Shah, J., Guerrera, D., Cooper, R. L., Merakou, C., Bouley, D. M., Meng, W., Kiyonari, H., Takeichi, M., Galli, S. J., Bagnoli, F., Citi, S., *et al.* (2015) The adherens junctions control susceptibility to *Staphylococcus aureus* α-toxin. *Proc. Natl. Acad. Sci. U.S.A.* **112,** 14337–14342
19. Cardellini, P., Davanzo, G., and Citi, S. (1996) Tight junctions in early amphibian development: detection of junctional cingulin from the 2-cell stage and its localization at the boundary of distinct membrane domains in dividing blastomeres in low calcium. *Dev. Dyn.* **207,** 104–113
20. Paschoud, S., Yu, D., Pulimeno, P., Jond, L., Turner, J. R., and Citi, S. (2011) Cingulin and paracingulin show similar dynamic behaviour, but are recruited independently to junctions. *Mol. Membr. Biol.* **28,** 123–135
21. Paschoud, S., Jond, L., Guerrera, D., and Citi, S. (2014) PLEKHA7 modulates epithelial tight junction barrier function. *Tissue Barriers* **2,** e28755
22. Poser, I., Sarov, M., Hutchins, J. R., Hériché, J. K., Toyoda, Y., Pozniakovsky, A., Weigl, D., Nitzsche, A., Hegemann, B., Bird, A. W., Pelletier, L., Kittler, R., Hua, S., Naumann, R., Augsburg, M., *et al.* (2008) BAC TransgeneOmics: a high-throughput method for exploration of protein function in mammals. *Nat. Methods* **5,** 409–415
23. Hubner, N. C., and Mann, M. (2011) Extracting gene function from protein-protein interactions using Quantitative BAC InteraCtomics (QUBIC). *Methods* **53,** 453–459
24. Cordenonsi, M., D'Atri, F., Hammar, E., Parry, D. A., Kendrick-Jones, J., Shore, D., and Citi, S. (1999) Cingulin contains globular and coiled-coil domains and interacts with ZO-1, ZO-2, ZO-3, and myosin. *J. Cell Biol.* **147,** 1569–1582
25. Citi, S., D'Atri, F., Cordenonsi, M., and Cardellini, P. (2001) in *Cell-Cell Interactions* (Fleming, T. P., ed) pp. 153–176, 2nd Ed., IRL Press, Oxford
26. Paschoud, S., and Citi, S. (2008) Inducible overexpression of cingulin in stably transfected MDCK cells does not affect tight junction organization and gene expression. *Mol. Membr. Biol.* **25,** 1–13
27. Guillemot, L., Guerrera, D., Spadaro, D., Tapia, R., Jond, L., and Citi, S. (2014) MgcRacGAP interacts with cingulin and paracingulin to regulate Rac1 activation and development of the tight junction barrier during epithelial junction assembly. *Mol. Biol. Cell* **25,** 1995–2005
28. Spadaro, D., Tapia, R., Jond, L., Sudol, M., Fanning, A. S., and Citi, S. (2014) ZO proteins redundantly regulate the transcription factor DbpA/ZONAB. *J. Biol. Chem.* **289,** 22500–22511
29. Martinez-Palomo, A., Meza, I., Beaty, G., and Cereijido, M. (1980) Experimental modulation of occluding junctions in a cultured transporting epithelium. *J. Cell Biol.* **87,** 736–745
30. Goellner, G. M., DeMarco, S. J., and Strehler, E. E. (2003) Characterization of PISP, a novel single-PDZ protein that binds to all plasma membrane Ca^{2+}-ATPase b-splice variants. *Ann. N.Y. Acad. Sci.* **986,** 461–471
31. Stephenson, S. E., Dubach, D., Lim, C. M., Mercer, J. F., and La Fontaine, S. (2005) A single PDZ domain protein interacts with the Menkes copper ATPase, ATP7A. A new protein implicated in copper homeostasis. *J. Biol. Chem.* **280,** 33270–33279
32. Nabokina, S. M., Subramanian, V. S., and Said, H. M. (2011) Association of PDZ-containing protein PDZD11 with the human sodium-dependent multivitamin transporter. *Am. J. Physiol. Gastrointest. Liver Physiol.* **300,** G561–G567
33. Shah, J., Guerrera, D., Vasileva, E., Sluysmans, S., Bertels, E., and Citi, S. (2016) PLEKHA7: cytoskeletal adaptor protein at center stage in junctional organization and signaling. *Int. J. Biochem. Cell Biol.* **75,** 112–116
34. Miyahara, M., Nakanishi, H., Takahashi, K., Satoh-Horikawa, K., Tachibana, K., and Takai, Y. (2000) Interaction of nectin with afadin is necessary for its clustering at cell-cell contact sites but not for its cis dimerization or trans interaction. *J. Biol. Chem.* **275,** 613–618
35. Takahashi, K., Nakanishi, H., Miyahara, M., Mandai, K., Satoh, K., Satoh, A., Nishioka, H., Aoki, J., Nomoto, A., Mizoguchi, A., and Takai, Y. (1999) Nectin/PRR: an immunoglobulin-like cell adhesion molecule recruited to cadherin-based adherens junctions through interaction with Afadin, a PDZ domain-containing protein. *J. Cell Biol.* **145,** 539–549
36. Ye, F., and Zhang, M. (2013) Structures and target recognition modes of PDZ domains: recurring themes and emerging pictures. *Biochem. J.* **455,** 1–14
37. Sudol, M., Sliwa, K., and Russo, T. (2001) Functions of WW domains in the nucleus. *FEBS Lett.* **490,** 190–195
38. Zhang, J., Yang, X., Wang, Z., Zhou, H., Xie, X., Shen, Y., and Long, J. (2012) Structure of an L27 domain heterotrimer from cell polarity com-

plex Patj/Pals1/Mals2 reveals mutually independent L27 domain assembly mode. *J. Biol. Chem.* **287,** 11132–11140
39. Ishiuchi, T., and Takeichi, M. (2012) Nectins localize Willin to cell-cell junctions. *Genes Cells* **17,** 387–397
40. Takekuni, K., Ikeda, W., Fujito, T., Morimoto, K., Takeuchi, M., Monden, M., and Takai, Y. (2003) Direct binding of cell polarity protein PAR-3 to cell-cell adhesion molecule nectin at neuroepithelial cells of developing mouse. *J. Biol. Chem.* **278,** 5497–5500
41. Reymond, N., Garrido-Urbani, S., Borg, J. P., Dubreuil, P., and Lopez, M. (2005) PICK-1: a scaffold protein that interacts with Nectins and JAMs at cell junctions. *FEBS Lett.* **579,** 2243–2249
42. Adachi, M., Hamazaki, Y., Kobayashi, Y., Itoh, M., Tsukita, S., Furuse, M., and Tsukita, S. (2009) Similar and distinct properties of MUPP1 and Patj, two homologous PDZ domain-containing tight-junction proteins. *Mol. Cell. Biol.* **29,** 2372–2389
43. Dudak, A., Kim, J., Cheong, B., Federoff, H. J., and Lim, S. T. (2011) Membrane palmitoylated proteins regulate trafficking and processing of nectins. *Eur. J. Cell Biol.* **90,** 365–375
44. Rikitake, Y., Mandai, K., and Takai, Y. (2012) The role of nectins in different types of cell-cell adhesion. *J. Cell Sci.* **125,** 3713–3722
45. Asakura, T., Nakanishi, H., Sakisaka, T., Takahashi, K., Mandai, K., Nishimura, M., Sasaki, T., and Takai, Y. (1999) Similar and differential behaviour between the nectin-afadin-ponsin and cadherin-catenin systems during the formation and disruption of the polarized junctional alignment in epithelial cells. *Genes Cells* **4,** 573–581
46. Tachibana, K., Nakanishi, H., Mandai, K., Ozaki, K., Ikeda, W., Yamamoto, Y., Nagafuchi, A., Tsukita, S., and Takai, Y. (2000) Two cell adhesion molecules, nectin and cadherin, interact through their cytoplasmic domain-associated proteins. *J. Cell Biol.* **150,** 1161–1176
47. Fukuhara, A., Irie, K., Yamada, A., Katata, T., Honda, T., Shimizu, K., Nakanishi, H., and Takai, Y. (2002) Role of nectin in organization of tight junctions in epithelial cells. *Genes Cells* **7,** 1059–1072
48. Hoshino, T., Shimizu, K., Honda, T., Kawakatsu, T., Fukuyama, T., Nakamura, T., Matsuda, M., and Takai, Y. (2004) A novel role of nectins in inhibition of the E-cadherin-induced activation of Rac and formation of cell-cell adherens junctions. *Mol. Biol. Cell* **15,** 1077–1088
49. Mandai, K., Nakanishi, H., Satoh, A., Takahashi, K., Satoh, K., Nishioka, H., Mizoguchi, A., and Takai, Y. (1999) Ponsin/SH3P12: an l-afadin- and vinculin-binding protein localized at cell-cell and cell-matrix adherens junctions. *J. Cell Biol.* **144,** 1001–1017
50. Kurita, S., Yamada, T., Rikitsu, E., Ikeda, W., and Takai, Y. (2013) Binding between the junctional proteins afadin and PLEKHA7 and implication in the formation of adherens junction in epithelial cells. *J. Biol. Chem.* **288,** 29356–29368

Epithelial junctions and Rho family GTPases: the zonular signalosome

The formation and maintenance of cell-cell junctions is fundamental for epithelial cells to regulate adhesion, polarity and motility, and to build epithelial organs. Junctions are supported and regulated by the actin cytoskeleton, whose organization and dynamics are in turn regulated by small GTPases of the Rho family. In this review we summarized current knowledge about the role of the Rho GTPases RhoA, Rac1 and Cdc42 in the assembly of apical junctional complexes and in the regulation of actin cytoskeleton organization and contractility. Furthermore, we describe the role of junctional proteins in this regulation, through the junctional recruitment and modulation of the regulator of Rho family GTPases, GEFs and GAPs. The fine tuning of Rho family GTPases activity is required for proper junction assembly and maintenance, and this is achieved through the zonular signalosome, including zonular junctional proteins functioning as adaptors for GEFs and GAPs, transcription factors and signaling proteins, cytoskeletal proteins, and RhoGTPases which act in feedback loops supporting the assembly and disassembly of this signalosome.

I contributed in this publication writing the section about the regulation of GAPs.

REVIEW

Small GTPases 5:4, e973760; November 1, 2014; Published with license by Taylor & Francis Group, LLC

Epithelial junctions and Rho family GTPases: the zonular signalosome

Sandra Citi[1,2,*], Diego Guerrera[1], Domenica Spadaro[1], and Jimit Shah[1]

[1]Department of Cell Biology; University of Geneva; Geneva, Switzerland; [2]Institute of Genetics and Genomics of Geneva; University of Geneva; Switzerland

Keywords: junctions, Rho, Rac, Cdc42, cytoseleton, epithelium

Abbreviations: AJ, adherens junction; AMOT, angiomotin; AMPK, Adenosine Monophosphate-Activated Protein Kinase; APC, adenomatous poliposis coli; Cdc42, cell division cycle 42; CD2AP, CD2-associated protein; CGN, cingulin; CGNL1, paracingulin; Dbl, diffuse B-cell lymphoma; DLC, deleted in liver cancer; EPLIN, epithelial protein lost in neoplasm; ERK, extracellular regulated kinase; FERM, four.point.one, ezrin, radixin, moesin; FGD5, FYVE, RhoGEF and PH domain containing 5; GEF, guanine nucleotide exchange factor; GAP, GTPase activating protein; GST, glutathione -S- transferase; JAM = junctional adhesion molecule; MCF-7, Michigan Cancer Foundation - 7; MDCK, Madin Darby Canine Kidney; MgcRacGAP, male germ cell racGAP; MKLP1, mitotic kinesin-like protein-1; MRCK, myotonic dystrophy-related Cdc42-binding kinase; PA, puncta adhaerentia; PAK, p21-activated kinase; PATJ, Pals1 associated tight junction protein; PCNA, proliferating cell nuclear antigen; PDZ, Post synaptic density protein (PSD95), Drosophila, disc large tumour suppressor (DlgA), and zonula occludens-1; PLEKHA7, pleckstrin homology domain containing, family A member 7; RICH-1, RhoGAP interacting with CIP4 homologues; ROCK, Rho-associated protein kinase; SH3BP1, (SH3 domain 490 binding protein-1); Tbx-3, T-box-3; Tiam, Tumor invasion and metastasis; TJ, tight junction; WASP, Wiskott-Aldrich Syndrome Protein; WAVE, WASP family Verprolin-homologous protein; ZA, zonula adhaerens; ZO, zonula occludens; ZONAB, (ZO-1)–associated nucleic acid binding protein.

The establishment and maintenance of epithelial cell-cell junctions is crucially important to regulate adhesion, apicobasal polarity and motility of epithelial cells, and ultimately controls the architecture and physiology of epithelial organs. Junctions are supported, shaped and regulated by cytoskeletal filaments, whose dynamic organization and contractility are finely tuned by GTPases of the Rho family, primarily RhoA, Rac1 and Cdc42. Recent research has identified new molecular mechanisms underlying the cross-talk between these GTPases and epithelial junctions. Here we briefly summarize the current knowledge about the organization, molecular evolution and cytoskeletal anchoring of cell-cell junctions, and we comment on the most recent advances in the characterization of the interactions between Rho GTPases and junctional proteins, and their consequences with regards to junction assembly and regulation of cell behavior in vertebrate model systems. The concept of "zonular signalosome" is proposed, which highlights the close functional relationship between proteins of zonular junctions (*zonulae occludentes* and *adhaerentes*) and the control of cytoskeletal organization and signaling through Rho GTPases, transcription factors, and their effectors.

*Correspondence to: Sandra Citi; Email: sandra.citi@unige.ch
Submitted: 11/06/2013; Revised: 06/02/2014; Accepted: 09/05/2014
http://dx.doi.org/10.4161/21541248.2014.973760

Introduction

Cell-cell junctions provide epithelial tissues with mechanical and functional integrity, by playing an essential role in cell-cell adhesion and formation of barriers between distinct body compartments. One key feature of junctions is their association with highly ordered cytoskeletal networks of actin, microtubules and intermediate filaments. Since Rho GTPases are major regulators of the polymerization, organization and mechanics of the cytoskeleton, the interplay between Rho GTPase activity and the organization of junctions is of fundamental importance in epithelial morphogenesis and physiology. In this review we attempt to address the complexity of this regulation, going from basic concepts about the organization, evolution and cytoskeletal anchoring of cell-cell junctions, to the most recent exciting findings about the role of GEFs and GAPs at junctions, and their mechanisms of regulation.

The Organization and Molecular Evolution of the Epithelial Apical Junctional Complex

Epithelial tissues are at the boundary between the organism and the external environment, and form the first barrier to the entry of pathogens and toxins.[1,2] In addition, they separate internal body compartments, thus allowing the maintenance of homeostatic specialized functions, which depend on polarized secretion and absorption, and maintenance of gradients across epithelia.

To form efficient barriers, epithelial tissues must display specific architectural characteristics, such as being formed by at least one continuous layer of closely packed cells, and show a

topological asymmetry, paralleled in the structural and functional apico-basal polarity of their individual units. Furthermore, they must ensure the maintenance of a strong adhesion between cells, to prevent their mechanical separation when tensile forces are applied. Finally, they must establish and maintain continuous seals, to prevent the free diffusion of solutes, molecules and pathogens through the paracellular space. The adhesion and barrier functions in vertebrate epithelia are carried out by specialized intercellular junctions: tight junction (TJ), *zonula adhaerens* (ZA), and desmosomes. Tight junctions (TJ, also called *zonulae occludentes*) (**Fig. 1**) provide the paracellular permeability seal, through 4-pass membrane proteins such as occludin and claudins, which are anchored to the actin cytoskeleton via scaffolding complexes of PDZ-containing proteins.[3,4] ZAs can be viewed as a highly specialized and topologically unique form of adherens junction (AJ): a continuous, linear circumferential belt (zonula) around the apex of polarized epithelial cells. AJ are present both in non-epithelial cells (e.g., intercalated disks of cardiac myocites, sites of adhesion between fibroblasts, neurons and others), and epithelial and endothelial cells, and are characterized by the presence of a member of the classical cadherin family (E-cadherin for epithelia, VE-cadherin for endothelia, and so on).[5,6] The epithelial ZA is located immediately below the TJ, and contains not only E-cadherin, α-catenin, β-catenin, and p120ctn, but also PLEKHA7 and afadin, whereas lateral contacts with spot-like adhesions (*puncta adhaerentia*) lack PLEKHA7 and afadin.[7] Transmembrane Ig-like adhesion molecules such as JAM and nectin are also present both in TJ and AJ, where they perform adhesion and signaling functions. Desmosomes are essential to provide tissue integrity and strength to the cell-cell junctions, and they contain, as transmembrane proteins, desmocollin and desmoglein, which belong to the cadherin superfamily of proteins. Although there is evidence for a cross-talk between desmosomes and Rho GTPases,[8-11] here we will focus primarily on Rho GTPase regulation at the apical, zonular junctional complex of vertebrates (ZA and TJ). The structure, function, and molecular composition of vertebrate cell-cell junctions have been described in several excellent reviews.[3,4,6,12,13]

Morphological and genomic analyses show that during evolution from lower Eukaryotes to Metazoans, and from invertebrates to vertebrates, junctions have undergone dramatic changes with regards to architectural organization, molecular composition, regulatory mechanisms, and, in some cases, the functions of individual molecular constituents (**Fig. 1**). For example, the barrier function in vertebrates is fulfilled by TJ, which are located immediately apical to the cadherin-based *zonula adhaerens* (**Fig. 1**). In contrast, the barrier function in invertebrates is carried out by septate junctions, which are located basally, with respect to cadherin-based adherens junctions.[14] Ultrastructurally, vertebrate TJ are characterized by the intimate apposition of claudins on adjoining plasma membranes, which appear as a network of fibrils upon freeze

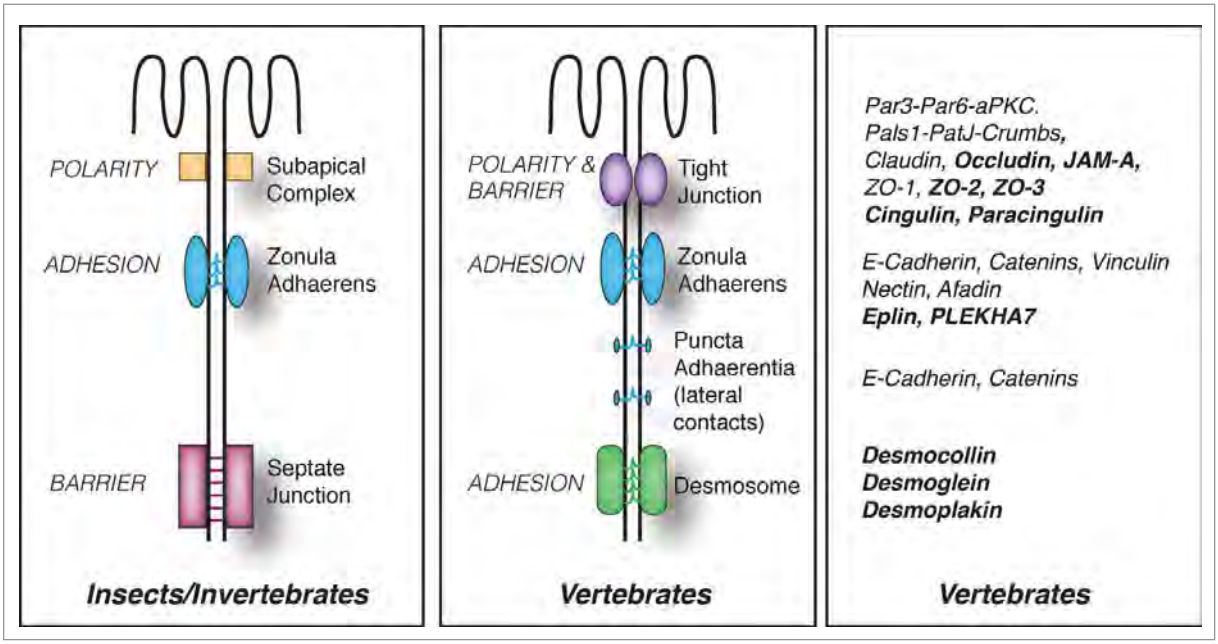

Figure 1. Evolution of junctional architecture, and the molecular complexity of vertebrate junctions. Simplified schemes showing the organization of the apical junctional complexes of polarized epithelial cells in insects (as an example of invertebrates) and vertebrate organisms. The canonical functions (polarity, barrier, adhesion) of each type of junction (SAC = sub-apical complex/marginal zone, *zonula adhaerens* (ZA), septate junction, tight junction, desmosome) are indicated on the left of the respective junction. E-cadherin based junctions along the lateral contacts of epithelial cells (*puncta adhaerentia*) have a composition similar to that of punctate junctions between filopodial tips, e.g they contain a classical cadherin, and catenins (p120ctn, β-catenin, α-catenin), but not PLEKHA7 and afadin. On the right, a non-exhaustive list of proteins associated with vertebrate junctions is shown. Proteins, which have so far been identified exclusively in vertebrate organisms, are highlighted in bold character.

fracture. Insect septate junctions show extracellular electron-dense "septa" bridging the opposite plasma membranes, rather than claudin-based fibrils.[14] In vertebrates, TJ correspond topologically to the physical "fence" separating apical from lateral plasma membrane domains, which maintains apico-basal polarity (**Fig. 1**). Instead, the fence in invertebrates is not the septate junction, but the subapical complex (SAC)/marginal zone, which is apical to the ZA, and morphologically distinct from TJ (**Fig. 1**). Evolutionarily conserved polarity complexes confer either apical identity (Par3-Par6-apKC and Crumbs-Pals1-PatJ complexes), or basolateral identity (Scribble-Dlg-Lgl complex) to the plasma membrane, and are segregated at the level of the TJ in vertebrates and the subapical complex (SAC)/marginal zone in invertebrates (**Fig. 1**).[3,14,15] At the molecular level, the number of isoforms and/or family members for most junctional proteins is considerably larger in vertebrates, providing for increased molecular complexity and redundancy. For example, although cadherin and catenins are shared between insect and vertebrate AJ, invertebrates do not express many classical cadherin isoforms, and lack desmosomal cadherins, desmosomes and intermediate filaments.[15,16] Strikingly, epithelial cells of lower Eukaryotes, such as the amoeba *Dyctiostelium discoideum*, achieve adhesion and polarity in the absence of any cadherin, whereas in metazoans E-cadherin is critically required for cell-adhesion, embryonic development, and the generation of apico-basal polarity.[17,18] Claudins, the transmembrane proteins responsible for the barrier of TJ to ions, are highly divergent in their sequence from invertebrates to vertebrates, and the family includes over 20 members in vertebrates, whereas only 5 and 3 members, respectively, have been described so far in *C. elegans* or *Drosophila*.[14] A ZO-1 homolog has been identified in *Drosophila*, but the ZO family in vertebrates comprises also ZO-2 and ZO-3, which have partially redundant functions with ZO-1.[19,20] Knock-out of the components of the Par3-Par6-aPKC complex in invertebrates has dramatic consequences on epithelial and neuronal morphogenesis, but can have only tissue-specific and more subtle effects in mice.[21] The lateral polarity protein Lgl acts as a canonical tumor suppressor protein in *Drosophila*, but not in mice.[22] Over 70 GEFs and 60 GAPs have been described in Vertebrates, whereas only about 10 Rho GEFs and GAPs combined have so far been identified in *Drosophila*.[23] In summary, although invertebrate model systems are useful to establish some general principles, vertebrate cells and organisms are required to understand the remarkably more complex organization of vertebrate junctions and their signaling and regulatory mechanisms. In this review, we focus on vertebrate model systems.

Assembly and Anchoring of the Cytoskeleton at Epithelial Apical Junctional Complexes

To understand the relationships between Rho GTPase regulation and assembly of vertebrate junctions, it is necessary to examine how the actomyosin and microtubule cytoskeletons, which are major targets of Rho GTPase effectors, functionally and structurally interact with AJ and TJ.

The circumferential, junction-associated bundle of actin microfilaments and nonmuscle myosin in the brush border of polarized epithelial cells was described three decades ago.[24] The actomyosin cytoskeleton regulates the distribution, stability, clustering and endocytosis of cadherin at the cell membrane,[25] and the thickness of the bundle is related to the greater mechanical tensions applied to the ZA, compared to weaker forces applied to lateral AJ complexes.[26] Contraction of the ZA-associated actomyosin ring causes apical constriction, which is crucial to support morphogenetic changes in developing embryos.[27] In addition, the contractile apical actomyosin ring is critical for the regulation of TJ integrity and barrier function.[28]

How actin and myosin are structurally connected to junctions, and how they are regulated in their polymerization, assembly and activities by junctional molecules are crucial questions. Several actin-binding proteins are localized at AJ and TJ (**Fig. 2**).[12,29] E-cadherin, although not directly binding to actin, acts as a scaffold for cytoskeleton-associated protein complexes, and plays an instructive role by marking the sites of de novo actin filament polymerization.[30,31] E-cadherin directly interacts with cortactin, which in the presence of N-WASP can recruit Arp2/3 and its activator WAVE2 to the ZA, thus promoting actin nucleation at junctions.[30,32] This process also requires α-actinin.[33] The WAVE2-Arp2/3 complex is activated by Rac1, and is necessary for junctional integrity and contractile tension at the ZA.[34] At the ZA, N-WASP is also involved in a putative "non-canonical," Arp2/3-independent pathway, to stabilize newly formed actin filaments, and promote their incorporation into apical rings.[35]

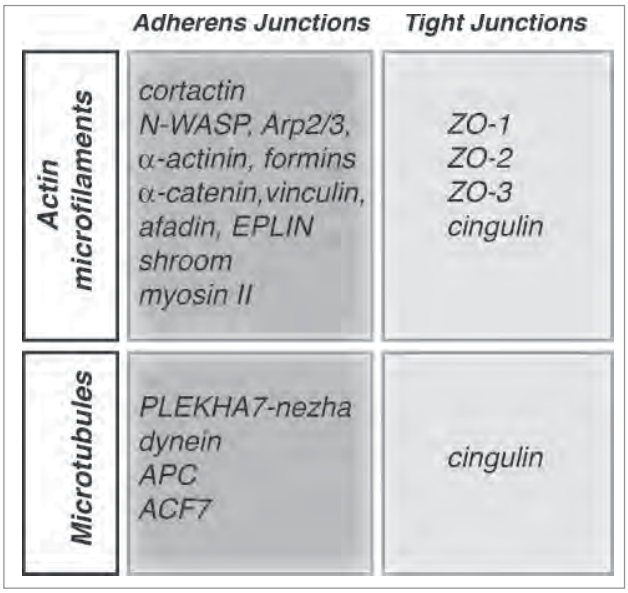

Figure 2. Proteins implicated in the organization and junctional anchoring of cytoskeletal filaments. For each type of cytoskeletal filament (actin and microtubules) the proteins shown are involved either in their polymerization, bundling, and anchoring to junctions, based on biochemical and/or cell biological evidence.

This is an example of a new role played at zonular junctions by a protein, beyond its classical activity. Nucleation of actin filaments by the Arp2/3 complex gives rise to an extensive array of branched actin filaments, but mature apical junctions are characterized by the presence of bundled actin filaments. Several actin-binding proteins can influence microfilament organization and dynamics at the ZA. Formins, for example, have been implicated in the formation of junctional actin bundles in some cell types.[36,37] α-catenin, which has an evolutionarily conserved role in organizing the cortical actin cytoskeleton,[17,38,39] suppresses actin polymerization by the Arp2/3 complex, while stabilizing and bundling actin filaments. The affinities of interaction of monomeric α-catenin with actin and vinculin are dramatically increased when tensile forces are applied to junctions, through a molecular stretching mechanism, indicating that monomeric α-catenin bound to β-catenin can directly link F-actin to the cadherin complex in vivo,[40,41] although this is not observed in vitro.[42] EPLIN (Epithelial Protein Lost In Neoplasm) is recruited to junctions by α-catenin, and it inhibits actin depolymerization, and crosslinks actin filaments.[43,44] Afadin associates with the cytoplasmic domain of nectins and JAM,[45] is recruited to the ZA through an interaction with α-catenin, and directly interacts with actin filaments.[46] Afadin is a major organizer of the apical junctional complex, and is essential for the development of apico-basal polarity in vertebrate embryogenesis.[47,48] Finally, myosin II is an essential component of the contractile bundle associated with the ZA, and its positioning is regulated by Shroom, and actin-binding protein which interacts with the Rho effector kinase ROCK,[49] and is regulated by the FERM domain protein Lulu.[50] Recent studies have addressed the role of different actin and myosin isoforms at epithelial junctions. Depletion studies show that both β- and γ- actin isoforms, though differently distributed, are essential for TJ barrier function and junction assembly, whereas β-actin is selectively involved in the establishment of apico-basal cell polarity.[51] Concerning myosins, myosin IIA is the most important in regulating cell morphology and cell-cell adhesion, whereas myosin IIB has more subtle roles in actin filament dynamics.[52,53]

Besides AJ, TJ are also structurally and functionally linked to the actin cytoskeleton (**Fig. 2**). Actin has multiple potential partners at TJ, including the ZO proteins (ZO-1, ZO-2, ZO-3), occludin and cingulin (**Fig. 2**).[54-56] Cells depleted of ZO-1 show defects in the barrier to larger solutes, and changes in the junction-associated actin, indicating that ZO-1 forms a stabilizing link between the barrier and the junctional actomyosin.[57,58] In contrast, depletion of ZO-2 does not lead to either actin reorganization or altered permeability to larger molecules,[59] whereas depletion of both ZO-1 and ZO-2 leads to a dramatic expansion of the actomyosin belt associated with AJ.[60] Since ZO-1 interacts directly or indirectly with several actin-binding proteins, including α-catenin and cortactin,[19,61,62] and with GEFs for Rac1 and RhoA,[63,64] some of the phenotypes of these knock-down models may be dependent on these interactions, although this remains to be determined. Cingulin is so far the only TJ protein for which an actin-bundling activity has been described in vitro.[56] However, cingulin depletion or overexpression in MDCK cells does not result in dramatic changes in actin organization or barrier function,[65-67] suggesting functional redundancies with other proteins.

Microtubules show a polarized distribution in epithelial cells, and associate with the apical junctional complex.[68] Recent studies show that E-cadherin is connected to the minus ends of microtubules through a complex containing p120ctn, PLEKHA7, paracingulin and nezha (CAMSAP3)[69,70] (**Fig. 2**). Microtubule anchoring confers stability to apical junctions,[69,71] and also indirectly stabilizes TJ barrier function, by enhancing the accumulation of E-cadherin and associated proteins at the ZA.[72] Exogenous PLEKHA7 can accumulate at lateral contacts *puncta adhaerentia*, probably through its interaction with p120ctn, but this does not result in increased recruitment of microtubule minus ends, suggesting that microtubule anchoring requires a specialized molecular environment that occurs only at the ZA.[72] Interaction of microtubule plus ends with cadherin-based junctions involves dynein, which interacts with β-catenin,[73] APC,[74] and the spectroplakin ACF7.[75] Recent experiments indicate that a planar apical network of microtubules is anchored to TJ through cingulin, and this interaction is regulated by adenosine monophosphate protein kinase (AMPK)-mediated phosphorylation of cingulin [76] (**Fig. 2**). There is an important cross-talk between the actin and microtubule cytoskeletons. For example, the formin mDia is involved both in linear actin polymerization and microtubule stabilization,[77] and microtubules can both sequester Rho GEFs that control actin organization,[78,79] and associate with the centralspindlin complex, which plays roles not only in mitotic spindle organization and cytokinesis, but also in the control of Rho and Rac activity at junctions.[29,80] In summary, cell-cell junctions are critical sites of anchoring and organization of cytoskeletal filaments, through specific adaptor and regulatory molecules.

The Involvement of RhoA, Rac1 and Cdc42 in Epithelial Junction Assembly and Regulation

The cytoskeleton is essential for the establishment, maintenance, remodeling and disassembly of apical junctions, and this process is regulated by Rho family GTPases and their effectors. The first studies addressed the role of Rho GTPases in junction regulation by exogenously expressing either the Rho inhibitor C3 transferase, or dominant negative (DN) or constitutively active (CA) mutants of Rho GTPases. This lead to loss of barrier and fence functions of TJ, inhibition or perturbation of junction assembly, and was in some cases associated with disrupted localization of junctional proteins, depending on expression levels of mutant proteins.[81-85] The observation that DN and CA mutants have similar effects is consistent with the notion that catalytic cycling between active and inactive states, rather than a permanent "on" or "off" state, is essential for the proper functioning of Rho GTPases. Thus, mutant phenotypes may similarly affect the Rho GTPases functional output, by binding to and sequestering targets and effectors. In summary, correct junction assembly and function requires a finely tuned balance in the activities of RhoA, Rac1 and Cdc42.

Rac1 and Cdc42 are essential in the initial formation of junctions, following engagement of adhesion receptors at primordial junctions,[31,86,87] by promoting the polymerization of actin filaments in lamellipodia and filopodia, through activation of the Arp2/3 complex by WAVE2.[29] A second crucial role of Cdc42 is to promote the formation of the Par6-aPKC-Par3 complex, thus allowing the establishment of apico-basal polarity and segregation of apical TJ.[3] The role of Cdc42 in polarity was first discovered in the yeast *Saccharomyces cerevisiae*, where a Cdc42 mutation resulted in inhibition of polarized budding.[88] In vertebrate cells, aPKC activity is required for the establishment of TJ, but not for their maintenance, whereas the role of Cdc42 in the regulation of mature TJ appears to depend on cell type. For example, in endothelial cells Cdc42 does not play a significant role in regulating junctional actin organization and barrier function,[89] but in other, non-endothelial cells, regulation of Cdc42 is necessary for TJ maintenance.[90,91] Evidence from invertebrate models indicates that at steady state the Cdc42-Par6-aPKC axis acts by limiting RhoA activity, and thus junctional tension at AJ.[92] The role of N-WASP, a target of Cdc42 and Rac1, in regulating junction architecture and cortical tension has also been demonstrated in vertebrate model systems.[63] N-WASP can also be targeted by pathogens, to promote cell-to-cell spreading.[93]

RhoA plays a fundamental role both in the establishment and maintenance of AJ and TJ through 2 major effectors: Rho-associated protein kinase (ROCK) and Diaphanous-related formin-1 (Dia).[94] mDia nucleates linear actin polymerization at the AJ,[36] and can sense and generate mechanical forces on actin filaments,[95] whereas ROCK promotes the bundling of actin filaments and the contractility of actomyosin, by enhancing the phosphorylation of nonmuscle myosin light chains.[96] These functions are critical to maintain tension at apical junctions, inhibit cadherin endocytosis, and establish and maintain TJ barriers.[92,97,98] A physiological balance between mDia and ROCK activities is required to maintain ZAs, since decreased Dia or increased ROCK activation can induce the transition from belt-like ZA to punctate PA.[94,99] Indeed, ROCK activation can also be a major mechanism of junction disruption, triggered by cytokines and other exogenous stimuli.[100] Therefore the fine-tuning of the activation of RhoA effectors in space and time is a critical factor in the regulation of junction assembly and stability.

New Insights Into the Molecular Mechanisms Underlying the Spatio-temporal Regulation of Rho Family GTPases at Junctions

The biological impact of Rho family GTPases critically depends on the precise site and timing of their activation. Thus, understanding how Rho GTPases control junction assembly requires the identification of the molecular mechanisms that regulate Rho GTPase activity at junctions.

The spatial and temporal control of Rho GTPases is coordinated by GEFs and GAPs, which activate and deactivate Rho GTPases by promoting either the exchange of GDP for GTP, or GTP hydrolysis, respectively. GEFs and GAPs interact with adaptor proteins, which recruit them to defined subcellular sites, and/or modulate their activity, for example by phosphorylation (see section on "Regulation of regulators"). In a previous review, we summarized the interactions of vertebrate junctional proteins with GEFs and GAPs implicated in the regulation of RhoA, Rac1, Rap1 and Cdc42.[101] Here, we will focus on more recent studies, which have provided additional insights into the cross-talk between junctional proteins and Rho family GTPases, and frame them into a dynamic view of the involvement of GEFs and GAPs in the different steps of junction formation.

RhoA

New roles in the regulation of RhoA activation at junctions have recently been identified for both TJ and ZA proteins. ARHGEF11 (also known as PDZ-RhoGEF), a Rho-GEF containing a regulator of G protein signaling (RGS) domain, was found to interact with ZO-1, and to be important for the efficient assembly and remodeling of apical junctions [64] (**Fig. 3**). Genomic studies identify ARHGEF11 as a susceptibility locus for intracranial aneurysms [102] and kidney injury in the Dahl salt-sensitive rat model,[103] suggesting that ARHGEF11 is also involved in cardiovascular and renal physiology and pathology, possibly through its activity at endothelial and/or epithelial junctions. Two additional RhoGEFs were recently found to be associated with the E-cadherin-catenin junctional complex. TEM4 (ARHGEF17, also known as p164-RhoGEF) localizes at stress fibers in sparse cells, and at junctions in confluent epithelial cells.[104] TEM4 depletion leads to decreased RhoA activation, decreased myosin light chain phosphorylation, defective endothelial junctions, and attenuated angiogenesis.[104] Second, the E-cadherin-α-catenin complex was found to mediate the retention of the RhoGEF ECT2 (Epithelial Cell Transforming gene 2, also known as ARHGEF31) at the ZA in breast cancer (MCF7) cells, resulting in spatially restricted RhoA activation, and generation of junctional tension, to maintain junction integrity [29,105] (**Fig. 3**). During cytokinesis ECT2 plays an important regulatory role in furrow contractility, and is associated with the centralspindin complex, which comprises MgcRacGAP (RACGAP1), and the kinesin family member MKLP1 (KIF23).[106] Centralspindin not only regulates ECT2-Rho signaling at junctions, but also inhibits the junctional recruitment of p190RhoGAP (ARHGAP35),[29] which functionally interacts with p120-catenin.[107,108] In addition to TEM4 and ECT2, a new junctional RhoA GEF which has been identified is p114RhoGEF (ARHGEF18), which interacts with cingulin to promote junctional tension in some, but not all types of epithelial cells[98] (**Fig. 3**). Recently it was found that p114RhoGEF also binds to the FERM domain protein Lulu2, the polarity protein PatJ,[109] and the Ser/Thr kinase LKB [110] (**Fig. 3**), suggesting that different adaptor proteins can recruit p114RhoGEF to cellular sites where it must be localized. GEF-H1 is another prominent junctional Rho GEF, which interacts with cingulin and paracingulin, resulting in its inactivation, and thus decreased RhoA activation and stress fiber formation in the cytoplasm (reviewed in [101]). GEF-H1 has been implicated in diverse cellular activities, and recently it was also shown to regulate apical constriction and cell intercalation to regulate neural tube closure in *Xenopus* development.[111] Additional

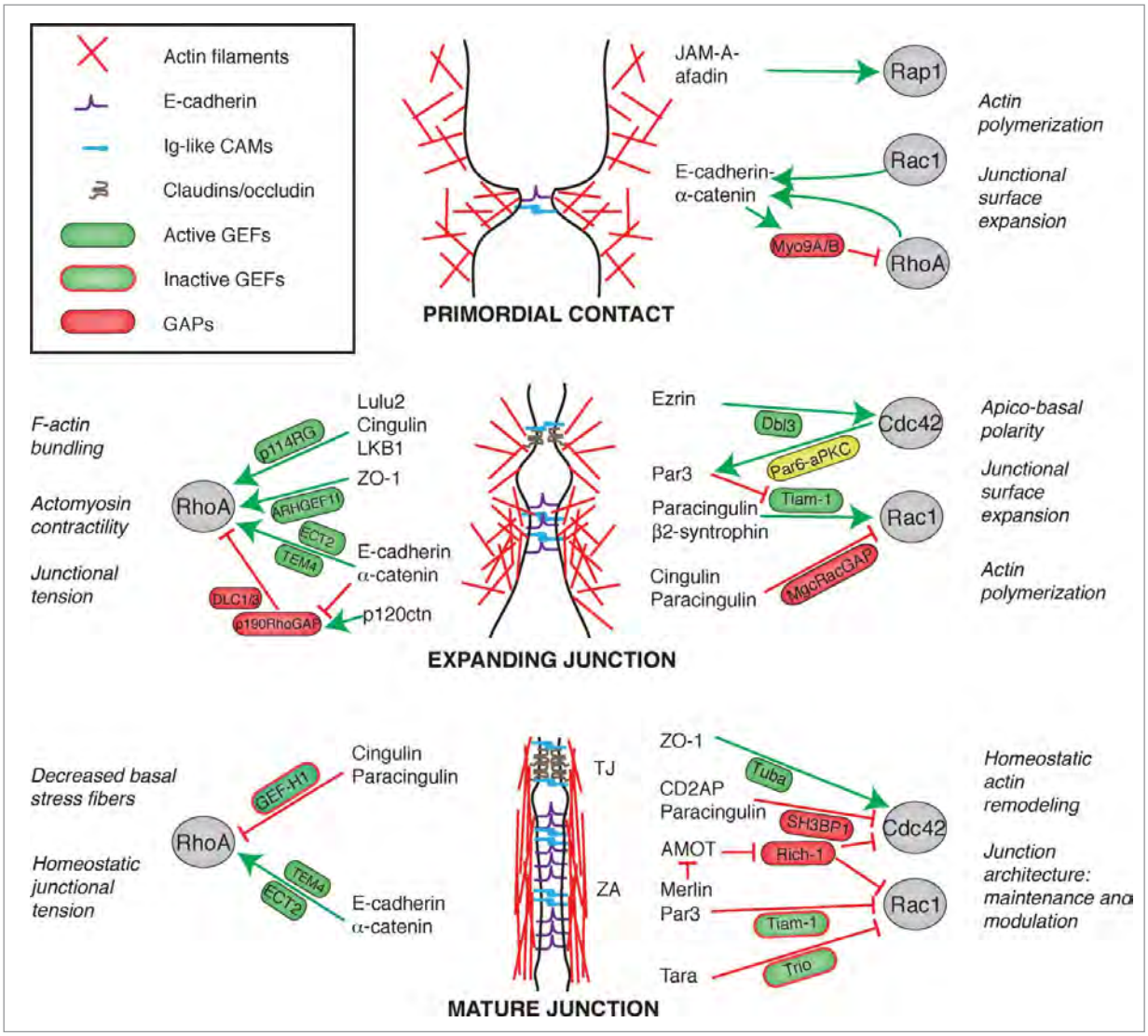

Figure 3. Crosstalk between junctions and Rho GTPases during the biogenesis of epithelial junctions. Simplified schemes showing sequential steps in the formation and maturation of the apical junctional complex (TJ and ZA) in epithelial cells, from primordial contact (top) to mature junction (bottom), and the proteins involved. Legends for graphical objects are shown in box (top left). Green and red arrows/lines indicate activation and inhibition, respectively. The main effects of Rho GTPase regulation on cytoskeletal organization and function are summarized on the sides of each scheme. Proteins and protein interactions depicted here are derived from studies on different model systems, so they do not necessarily occur together, but are grouped in one scheme for the sake of summarizing them. See text for additional details.

RhoGEFs which have been implicated in epithelial apical constriction during morphogenesis are Trio,[112] and ARHGEF11.[113]

Regarding Rho GAPs, indirect roles in regulating junctions have been found for the unconventional myosins Myo9a and Myo9b, large single-headed motor molecules that comprise a N-terminal actin binding domain, and a tail with a Rho GAP domain.[114,115] Depletion and overexpression studies show that both Myo9a and Myo9b regulate collective epithelial cell migration and wound healing, by down-regulating RhoA activity, and thus reducing localized cytoskeletal tension at the leading edge of lamellipodia, thus stabilizing nascent cell-cell contacts. However, assembly of junctions in non-migrating cells is not affected by Myo9a-depletion, suggesting that this myosin may be important only for dynamic junctions.[114] In another study, knockdown of Myo9a was reported to disrupt TJ,[116] similarly to what observed following Myo9b depletion in Caco2 intestinal cells.[115] Interestingly, polymorphisms in the gene encoding the Myo9b heavy chain are linked to several forms of inflammatory bowel disease,[117,118] and Myo9b function may be implicated in pathogenesis both through defective cell migration of sub-mucosal immune cells, and a leaky TJ barrier. Another Rho GAP that has recently been implicated in the maintenance of cell adhesion is DLC1 (Deleted in Liver Cancer 1), which acts as a GAP for RhoA, RhoC, and, to a lesser extent, for Cdc42. Exogenous

DLC1 interacts with α-catenin at AJ, and suppresses invasion and metastasis by up-regulating E-cadherin expression, in a Rho-dependent manner.[119] Another member of the DLC family of RhoGAP proteins, DLC3, is localized at AJ in breast cancer cells when exogenously expressed, and is essential for E-cadherin-mediated maintenance of cell-cell contacts[120] (**Fig. 3**).

Rac1

A key regulator of Rac1 activity at epithelial junctions is Tiam1, which is required for the efficient formation of TJ, and is inhibited in confluent cells by Par3,[121] suggesting a negative feedback mechanism upon junction maturation. The junctional adaptor paracingulin interacts with Tiam1 and is involved in its recruitment to junctions in MDCK cells,[122] whereas β2-syntrophin regulates apico-basal positioning of Rac1 activity at junctions, by counteracting the Par3-Tiam1 inhibitory interaction[123] (**Fig. 3**). A new E-cadherin associated Rac GEF, Trio, was recently localized at AJ, and its Rac1-activating activity is down-regulated by the F-actin binding protein Tara in confluent epithelial monolayers [124] (**Fig. 3**). Interestingly, the regulation of Rac1 activity by Tara is implicated in the modulation of expression of E-cadherin, through a pathway involving the transcription factor Tbx3,[124] highlighting the link between junction assembly and Rho family GTPase-mediated regulation of gene expression.[125] A new functional interaction of AMOT with merlin was reported to regulate Rac signaling, through the Cdc42/Rac1 GAP RICH1 (ARHGAP17).[126] Merlin is a FERM-domain protein encoded by the NF2 (neurofibromatosis-2) tumor suppressor gene, and it regulates cell proliferation in response to adhesive signaling.[127] In confluent cells, junctionally localized merlin relieves the inhibition of AMOT over Rich-1, thereby allowing Rich-1 to inhibit Rac1, and thus inhibit downstream MAPK and PAK signaling.[126] Thus merlin functions to block mitogenic signaling, by inhibiting Rac1 activity at TJ. Recent studies also demonstrate that Rac1 activity during junction assembly is regulated by the centralspindlin complex protein MgcRacGAP, which is recruited to TJ by cingulin and paracingulin.[80] Since cingulin and paracingulin do not affect the localization of the RhoGEF ECT2, it appears that there are 2 pools of MgcRacGAP at apical junctions, one which is recruited by cingulin and paracingulin (at TJ), and a second one which is recruited by the E-cadherin/ α-catenin complex, and interacts with ECT2, at least in MCF7 cells.[29,80]

It should be emphasized that not all GEFs and GAPs act locally at junctions, but they may contribute to junction assembly through their action on different steps of junctions biogenesis, as shown in the case of the Rac1/Cdc42 GAP PX-RICS (ARHGAP32), which is involved in the transport of N-cadherin and β-catenin from the endoplasmic reticulum to the junctional surface, but is not localized at junctions.[128]

Cdc42

Cdc42 is a third Rho family GTPase member that has been implicated in regulation of junctions, albeit not in all cell types.[129] In MDCK cells, for example, activation of Cdc42 is crucial for regulation of membrane traffic, biogenesis of cell polarity, and formation of junctions, primarily through the activation of the Par6-aPKC-Par3 apical polarity complex.[3] In addition to the previously characterized regulation by the Cdc42 GAP Rich-1,[101] a new protein complex, comprising paracingulin and CD2AP (CD2-associated protein), was found to regulate Cdc42 activity at junctions of intestinal carcinoma cells, through its interaction with the Cdc42 GAP SH3BP1 (SH3 domain binding protein-1).[130] SH3BP1 is implicated both in the maturation of cell-cell junctions, and in homeostatic actin remodeling at mature junctions.[130] CD2AP is a scaffolding protein that has been implicated in the maintenance of cell-cell contacts in the slit diaphragms of glomerular podocytes, as well as the function of cortactin and actin-capping proteins.[131,132] Regarding specific Cdc42 GEFs, genetic experiments in *Drosophila* embryos indicate that multiple GEFs, including the Rho GEF ECT2, contribute to cortical activation of Cdc42 during contact-induced cell polarization.[133] However in mammalian epithelia only the ZO-1-interacting Cdc42 GEF Tuba has so far been implicated in the maintenance of junctional architecture, but not in junction assembly.[63,93] Recently, it was shown that the Cdc42 GEF Dbl (MCF2, also known as ARHGEF21) regulates apical differentiation and apical junction positioning, but not junction assembly, through enhancing the accumulation and activity the Par6-aPKC complex, and the expansion of the apical membrane.[134]

Importantly, Cdc42 and RhoA activities can also be modulated by the cross-talk with Rap1, a member of the Ras family of GTPases, which is associated with cadherin-, JAM- and nectin-based complexes in epithelial and endothelial cells.[101,135] In endothelial cells the physiological restoration of the TJ barrier requires the activation of the Rap1-afadin axis, through phosphorylation of the Rap1 GEF C3G (RAPGEF1), and leads to the down-regulation of RhoA signaling, and enhanced AJ assembly.[136] In addition, Rap1 induces FGD5 (FYVE, RhoGEF and PH domain containing 5)-dependent Cdc42 activation, leading to MRCK (myotonic dystrophy-related Cdc42-binding kinase)-dependent circumferential accumulation of nonmuscle myosin II at junctions, while at the same time suppressing the Rho-ROCK pathway, leading to dissolution of radial stress fibers.[137] In summary, different molecular pathways are employed, in a cell-context-dependent manner, to orchestrate junction assembly/disassembly through Rho GTPase-dependent modulation of the actomyosin cytoskeleton. Moreover, the finely tuned antagonism between different Rho GTPases (typically Rac1/Cdc42 versus RhoA) sets the position of the border between apical and lateral plasma membrane domain, and thus apico-basal polarity, through the spatially restricted accumulation of cytoskeletal and polarity complex proteins.

Regulation of Regulators

Several mechanisms have been characterized, which regulate the activity and stability of GEFs and GAPs, including phosphorylation, lipid binding, intra-molecular auto-inhibition, and protein-protein interactions.

The Rho GEF GEF-H1 can be sequestered either by binding to microtubules in the cytoplasm,[78,138] or by binding to cingulin and paracingulin at epithelial junctions.[66,122,139] Phosphorylation of GEF-H1 occurs at several different sites and has multiple effects on GEF-H1 activity. In Jurkat cells, phosphorylation by the Rac1 effector PAK1 leads to GEF-H1 binding to 14-3-3, and association of the complex with microtubules, resulting in inhibition of GEF-H1 activity.[140] Another member of the PAK kinase family, PAK4, induces dissociation of GEF-H1 from microtubules in fibroblasts, and switching of substrate specificity, from Rho to Rac1.[141] In COS cells, phosphorylation by Par1b, a member of the conserved Par/MARK serine/threonine kinase family, leads to dissociation of GEF-H1 from microtubules, and microtubule destabilization.[142,143] GEF-H1 phosphorylation can be cell-cycle dependent, since at early stages of mitosis in Hela cells GEF-H1 is phosphorylated by Aurora A kinase, whereas at telophase it is dephosphorylated, to allow RhoA activation, cleavage furrow formation, and ingression during cytokinesis.[144] In HT1080 (fibrosarcoma) and LK2 (lung squamous cell carcinoma) cells phosphorylation by ERK enhances the guanidine exchange activity of GEF-H1.[145] In LLC-PK1 kidney tubular cells, GEF-H1 is involved in the sequential activation of Rac1 and RhoA, through TNF-α induced phosphorylation, which activates Rac1, followed by a signaling cascade that results in ERK phosphorylating GEF-H1, leading to RhoA activation.[146] ERK signaling also leads to inhibition of GEF-H1 through phosphorylation in MDA-MB-231 breast cancer cells, thus regulating cell motility and invasiveness.[147] In summary, the specific mechanisms of GEF-H1 regulation appear largely determined by the cell context-dependent expression of interacting partners.

The Rho activator ECT2 is a key regulator of cytokinesis, and is subjected to cell-cycle-dependent regulation. ECT2 first becomes active in prophase, when it is phosphorylated by Cdk1, and exported from the nucleus into the cytoplasm, to activate RhoA and induce the formation of a mechanically stiff and rounded metaphase cortex.[148] Phosphorylation on a different site is required for catalytic activity and interaction with polo-like kinase, leading to stimulation of RhoA activity and SRE-regulated transcription.[149] In anaphase ECT2 associates with the centralspindlin complex, and is targeted to the equatorial membrane through a mechanism that requires a pleckstrin homology domain and a polybasic cluster that bind to phosphoinositide lipids.[150] Targeting of ECT2 to the equatorial membrane is the key step to initiate cleavage furrow formation during cytokinesis. Upon completion of mitosis, ECT2 undergoes ubiquitin-dependent degradation, indicating that ECT2 is a bona fide cell-cycle-regulated protein.[151]

Another GEF for which a putative phosphoinositide lipid-mediated recruitment to the membrane has been proposed is Tiam1, a Rac1-specific GEF.[152] The guanine nucleotide exchange activity of Tiam1 is enhanced by different inositol phospholipids and other lipids.[153,154] Tiam1 is a substrate for the Src kinase, and phosphorylation of residue Y384 of Tiam1, which occurs preferentially at AJ, triggers its degradation, leading to AJ disruption and increased cell migration.[155] Tiam1 also interacts with 14-3-3 proteins when phosphorylated on serine residues, and although phosphorylation does not affect Tiam1 activity, it is required for Tiam1 proteolytic degradation.[155,156] Tiam1 phosphorylation by protein kinase C and by calcium-calmodulin kinase II have been described in activated fibroblasts, this latter leading to increased guanidine exchange activity toward Rac1 in vitro.[157] Finally, protein kinase-D-mediated phosphorylation of the Rho GEF Syx reduces its junctional targeting, through binding to 14-3-3 proteins.[158]

Phosphorylation also regulates GAPs, to activate or inhibit their activity, or affect their stability. p190RhoGAP is regulated by phosphorylation on Tyr, Ser and Thr residues, and by binding to phospholipids. Activation of Src by different pathways (EGF, integrin, PKC, and cadherin engagement) leads to phosphorylation of p190RhoGAP on Y1105, resulting in enhanced GAP activity, inhibition of RhoA and stress fiber disassembly.[159,160] Recruitment of active p190RhoGAP to cadherin through p120ctn leads to local suppression of RhoA activity, which is essential for AJ formation.[107,161] ERK mediated phosphorylation on different Ser and Thr residues in the C-terminal part of the protein suppresses the GAP activity of p190RhoGAP during focal adhesion formation.[162] Interaction of a polybasic region (PBR) of p190RhoGAP with phospholipids can switch substrate specificity of p190RhoGAP, from RhoA to Rac1, and this interaction is antagonized by phosphorylation on Ser1221 and Thr1226.[163] Substrate specificity of RICH-1 is regulated in platelets by Src-mediated phosphorylation, either to inhibit activity on Rho/Rac or to activate GAP activity toward Cdc42.[164] MgcRacGAP is regulated by binding to PRC1, which inhibits GAP activity toward Cdc42, thus allowing spindle formation during mitosis, and by Aurora B-mediated phosphorylation and PP2A-mediated dephosphorylation, which affect substrate specificity and interaction with ECT2.[165-167] The Rho GAP activity of DLC1 can be inhibited either by phosphorylation, which favors interaction with 14-3-3 and exclusion from focal adhesions,[168] or by intramolecular autoinhibition, which is mediated by a SAM domain, and modulated by EGF signaling, through tensin3.[169]

A Dynamic View of the Cross-talk Between Rho GTPases and Junction Assembly

The process that leads to the formation of epithelial cell-cell junctions is highly regulated in space and time, and results from the coordinated interactions between Rho GTPases, their GEF and GAP regulators, and junctional molecules (**Fig. 3**). Upon formation of primordial contacts, accumulation of E-cadherin and Ig-like adhesion molecules (JAMs, nectins) is driven by and, at the same time, stimulates Rac1-dependent actin polymerization at the submembrane cortex, in positive feedback loop that further promotes the accumulation of adhesion molecules at new junctions (**Fig. 3**). In this initial phase, the activities of Rac1/Cdc42, and the Ras-like GTPase Rap1 play a key role, both to generate the cytoskeletal scaffold upon which to build the new junction, and to expand the junctional surface, through cortactin/N-WASP/WAVE2/Arp2/3-mediated actin polymerization, and directed targeting of membrane vesicles. In order for

junctions to be expanded and stabilized, RhoA must also be deactivated at sites of cell-substratum interaction, for example through the Rho GAP activity of myosin-9, and activated at junctions (**Fig. 3**). Junctional RhoA activation is stimulated by GEFs such as p114RhoGEF, ARHGEF11 and ECT2, which interact with different ZA and TJ molecules (**Fig. 3**), and lead to positioning, assembly and contractility of myosin filaments. Actomyosin contraction at junctions generates the tension required to strengthen adhesion, and helps to cluster and stabilize adhesion molecules (**Fig. 3**). Since excessive RhoA activation can lead to junction disruption, a process which occurs also during epithelial-mesenchymal transition or in response to pathogens and injury, RhoA activity must also be downregulated, a process which depends at least in part on the p120-dependent recruitment of p190RhoGAP to AJ, and on the antagonism between RhoA and Rac1. Activation of the Rac1/Cdc42 axis of Rho GTPases is essential both for junction expansion, through actin polymerization, and to set apico-basal polarity, through the precise segregation of apical from basolateral determinants at TJ. This is achieved through ezrinDbl3-mediated localized activation of Cdc42, which in turns activates the Par6-aPKC complex, to expand the apical membrane.[134] In developing embryos most junctional proteins are targeted to the new junctional membrane through incorporation of membrane vesicles along the basal/lateral plasma membrane, whereas some junctional proteins are recruited to new junctions from a cortical, apical pool.[170-174] Once junctions are mature, the dynamic remodelling and functional modulation of the actin and microtubule cytoskeletons is supported by the steady-state equilibrium between activation and inhibition of GEFs, which maintains homeostatic junction architecture and tension (**Fig. 3**).

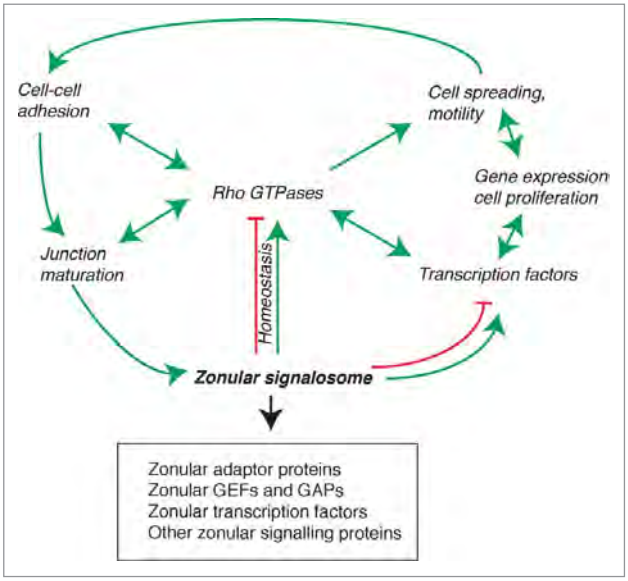

Figure 4. The zonular signalosome. The zonular signalosome is composed of zonular adaptor proteins, GEFs and GAPs, transcription factors and other signaling proteins (see text). Rho GTPases which functionally interact with the signalosome are at the center of a regulatory network that controls adhesion, junction assembly and maturation, regulation of gene expression, cell differentiation and survival, and motile behavior of cells. Transcription factors and other signaling molecules can either exist as part of the signalosome, or are cytoplasmic and regulated indirectly by the signalosome (for example, through RhoA regulation). Arrows indicate functional interactions (unidirectional or reciprocal activation, inhibition, homeostatic balance). See text for additional details.

A Zonular Signalosome at the Crossroads of Junction Assembly, Rho GTPase Activities, Cytoskeletal Organization, and Nuclear Signaling

Junction assembly and maturation is a dynamic process where different inter-related events are coordinated in space and time: a) accumulation and stabilization of transmembrane adhesion proteins at TJ and ZA; b) accumulation of cytoplasmic plaque proteins of ZA and TJ in the submembrane cortical cytoplasm, and their linkage to cytoskeletal filaments; c) actin polymerization, actin filament bundling and actomyosin contractility; d) microtubule reorganization; e) spatial segregation of junctional protein complexes into apical zonular TJ, subapical zonular ZA, and lateral adherens junction (puncta adhaerentia). This process is mediated by and culminates in the formation of a "zonular signalosome" (**Fig. 4**), defined as a complex of apical adaptor and signaling proteins associated with zonular (circumferential, belt-like) epithelial junctions (TJ and ZA). The zonular signalosome therefore includes: 1) zonular junctional proteins which function as adaptors for GEFs, GAPs (see **Fig. 3**), transcription factors and other signaling molecules (for example ZO proteins, cingulin, paracingulin, AMOT, Par3, afadin, etc); 2) the interacting zonular signaling partners of zonular adaptors (GEFs, GAPs, transcription factors, and other signaling molecules); 3) potentially, additional zonular structural proteins for which no or little direct role in regulation of signaling has yet been described (PLEKHA7, for example), and their interacting signaling partners. The targets and/or effectors of the zonular signalosome are: 1) RhoGTPases and their effectors (kinases and phosphatases for example), which in turn affect signalosome assembly and disassembly, through feedback loops (**Fig. 4**); 2) genes whose expression is modulated by zonular signalosome-regulated pathways; 3) cytoskeletal proteins (actins, myosins, microtubules and associated proteins): 4) transmembrane and adaptor proteins which are clustered at zonulae through interactions with signalosome adaptors, but can also be distributed at lateral contacts (claudins, occludin, Ig-like CAMs, E-cadherin, catenins, and others). Zonular clustering creates a molecular environment which may confer new or different functions to these proteins, for example only at TJ claudins assemble into continuous fibrils, and are thus able to form ionic pores or barriers.

The composition and properties of the zonular signalosome depend on cell and tissue type, as well as on cell-cycle stages. For example, the Rho GEF ECT2 is zonular in cultured MCF7 mammalian carcinoma cells,[29] partially zonular in keratinocytes, not zonular in intestinal carcinoma cells, and not detectable in kidney cells.[80] MgcRacGAP is zonular in interphase kidney cells, and excluded from junctions during mitosis.[80] Different

members of the large GEFs and GAPs families probably show cell- and tissue-type specific expression, however we are far from a precise immunohistochemical mapping of their distribution in different normal and diseased tissues. Similarly, structural adaptor proteins are not identically distributed in all cell types. For example paracingulin is not detected in differentiated intestinal epithelial cells,[175] and ZO-3 shows a narrower tissue distribution than ZO-1,[176] and is not expressed in cultured mammary epithelial cells.[20]

What are the functions of the zonular signalosome? One is to fine-tune in space and time the activation of Rho family GTPases, and thus the organization of the cytoskeleton, during the dynamic processes of junction assembly and disassembly, and at steady-state, to ensure the correct remodelling and turnover of cytoskeletal and junctional proteins (**Fig. 4**). This equilibrium can be perturbed by mechanical stresses, and pathological cues (cytokines, pathogens, toxins), leading to junction disruption, perturbation of the signalosome complex, and hence dramatically altered spatio-temporal regulation of Rho GTPases. As such, the signalosome can be viewed as a sensor, or signal transducer, of extra- and intra-cellular signals, to control cell behavior, including adhesion, motility, and junctional membrane integrity and dynamics. By sequestering and/or stabilizing at junctions GEFs and GAPs, the zonular signalosome also indirectly controls activation of signaling at cell-substratum adhesions, and thus cell spreading and motility, for example through the Par3-Tiam1,[177,178] p114RhoGEF,[179] and GEF-H1 [139] modules. At the tissue and organ level, perturbation of the zonular signalosome can elicit dramatic consequences on epithelial or endothelial cell cell-adhesion and barrier functions, resulting for example in loss of skin or mucosal barrier integrity, jaundice, edema, and loss of proteins or ions across tissue barriers.

A second important function of the zonular signalosome is to regulate transcription factors, cell-cycle regulators, and other signaling molecules, thus controlling gene expression, proliferation, differentiation, and survival. One mechanism of this regulation involves the direct or indirect sequestration of the signaling molecules at junctions, as shown for example by the role of ZO proteins in the junctional retention and stability of the transcription factor DbpA/ZONAB,[20,180] and the cell cycle regulator cyclinD1.[181] Moreover, ZO-2, α-catenin and AMOT control the nucleo-cytoplasmic shuttling of YAP/TAZ transcription factors by different mechanisms, including direct or indirect interaction, stabilization at junctions, and cytoplasmic retention through modulation of phosphorylation (reviewed in [125]). Another mechanism involves the modulation of RhoA activation, by zonular GEFs, and interacting adaptor proteins. For example GEF-H1 activation is critical in Dbpa/ZONAB activation and nuclear shuttling [182] and RhoA activation is also critically involved in the mechanotransduction-dependent regulation of the activity of YAP transcription factors.[183] RhoA is a central molecule in the cross-talk between cytoskeletal organization and nuclear signaling, and the integrity of the zonular signalosome, by regulating not only Rho, but also Rac and Cdc42 activities, is crucial to coordinate regulation of cytoskeletal organization with cell-cell adhesion, motility and nuclear signaling.

Concluding Remarks

In the past decade there have been striking advances in clarifying the identity of junctional proteins, GEFs and GAPs, and their functional interactions. The general picture that has emerged is one whereby epithelial morphogenesis and physiology are regulated by the carefully tuned balance between the activities of antagonistic Rho GTPases, through modulation of the expression, subcellular localization and activities of GEFs and GAPs. However, many important questions remain open. First of all, the majority of studies have been carried out on only one or a few experimental models (cells, tissues, species), and should be validated on additional vertebrate models. Junctions are remarkably heterogeneous in architecture, composition and function,[12] and each cell type is thus likely to be characterized by a unique configuration of junctional adaptors and Rho GTPase regulating molecules. So, results obtained in one model system cannot be extrapolated to other cells and tissues. Systematic transcriptomic and proteomic approaches, and the generation of new and improved reagents for the subcellular localization of GEFs and GAPs will be critical to map sets of regulatory modules in their correct context. In addition, detailed characterization of vertebrate knockout models will be essential to understand the role of GEFs and GAPs, and their interacting partners, in tissue and organ physiology and pathology. Special attention should be devoted to elucidating the 3-dimensional structures and affinities of interaction between the adaptor molecules, GEFs and GAPs, and how post-translational modifications can modulate them. Addressing these questions will help to define the composition and functions of zonular signalosomes in different epithelial and endothelial cells and tissues, and develop strategies for their experimental and therapeutic modulation.

Disclosure of Potential Conflicts of Interest

No potential conflicts of interest were disclosed.

Funding

The authors gratefully acknowledge the funding agencies that sponsor research in the Citi laboratory: the Swiss National Foundation, the Swiss Cancer League, and the State of Geneva.

References

1. Gonzalez-Mariscal L, Garay E, Lechuga S. Virus interaction with the apical junctional complex. Front Biosci 2009; 14:731-68; http://dx.doi.org/10.2741/3276
2. Vogelmann R, Amieva MR, Falkow S, Nelson WJ. Breaking into the epithelial apical-junctional complex–news from pathogen hackers. Curr Opin Cell Biol 2004; 16:86-93; PMID:15037310; http://dx.doi.org/10.1016/j.ceb.2003.12.002
3. Shin K, Fogg VC, Margolis B. Tight junctions and cell polarity. Annu Rev Cell Dev Biol 2006; 22: 207-35; PMID:16771626; http://dx.doi.org/10.1146/annurev.cellbio.22.010305.104219
4. Anderson JM, Van Itallie CM. Physiology and function of the tight junction. Cold Spring Harb Perspect Biol 2009; 1:a002584:1-16; PMID:20066090; http://dx.doi.org/10.1101/cshperspect.a002584
5. Franke WW, Rickelt S, Barth M, Pieperhoff S. The junctions that don't fit the scheme: special symmetrical cell-cell junctions of their own kind. Cell Tissue

Res 2009; 338:1-17; PMID:19680692; http://dx.doi.org/10.1007/s00441-009-0849-z
6. Takeichi M. Dynamic contacts: rearranging adherens junctions to drive epithelial remodelling. Nat Rev Mol Cell Biol 2014; 15:397-410; PMID:24824068; http://dx.doi.org/10.1038/nrm3802
7. Pulimeno P, Bauer C, Stutz J, Citi S. PLEKHA7 is an adherens junction protein with a tissue distribution and subcellular localization distinct from ZO-1 and E-cadherin. PLoS One 2010; 5:10.1371journal.pone.0012207; PMID:20808826; http://dx.doi.org/10.1371/journal.pone.0012207
8. Goto H, Tanabe K, Manser E, Lim L, Yasui Y, Inagaki M. Phosphorylation and reorganization of vimentin by p21-activated kinase (PAK). Genes Cells 2002; 7:91-7; PMID:11895474; http://dx.doi.org/10.1046/j.1356-9597.2001.00504.x
9. Spindler V, Waschke J. Role of Rho GTPases in desmosomal adhesion and pemphigus pathogenesis. Ann Anat = Anat Anz: Off Organ Anat Ges 2011; 193:177-80; PMID:21441018; http://dx.doi.org/10.1016/j.aanat.2011.02.003
10. Tsang SM, Brown L, Gadmor H, Gammon L, Fortune F, Wheeler A, Wan H. Desmoglein 3 acting as an upstream regulator of Rho GTPases, Rac-1Cdc42 in the regulation of actin organisation and dynamics. Exp Cell Res 2012; 318:2269-83; PMID:22796473; http://dx.doi.org/10.1016/j.yexcr.2012.07.002
11. Koetsier JL, Amargo EV, Todorovic V, Green KJ, Godsel LM. Plakophilin 2 affects cell migration by modulating focal adhesion dynamics and integrin protein expression. J Invest Dermatol 2014; 134:112-22; PMID:23884246; http://dx.doi.org/10.1038/jid.2013.266
12. Franke WW. Discovering the molecular components of intercellular junctions-a historical view. Cold Spring Harbor Perspect Biol 2009; 1:a003061; PMID:20066111; http://dx.doi.org/10.1101/cshperspect.a003061
13. Garrod D, Chidgey M. Desmosome structure, composition and function. Biochim Biophys Acta 2008; 1778:572-87; PMID:17854763; http://dx.doi.org/10.1016/j.bbamem.2007.07.014
14. Simske JS. Claudins reign: the claudinEMPPMP22-gamma channel protein family in C. elegans. Tissue Barriers 2013; 1:e25502; PMID:24665403; http://dx.doi.org/10.4161/tisb.25502
15. Harris TJ, Tepass U. Adherens junctions: from molecules to morphogenesis. Nat Rev Mol Cell Biol 2010; 11:502-14; PMID:20571587; http://dx.doi.org/10.1038/nrm2927
16. Hulpiau P, Gul IS, van Roy F. New insights into the evolution of metazoan cadherins and catenins. Prog Mol Biol Translational Sci 2013; 116:71-94; PMID:23481191; http://dx.doi.org/10.1016/B978-0-12-394311-8.00004-2
17. Dickinson DJ, Nelson WJ, Weis WI. A polarized epithelium organized by beta- and alpha-catenin predates cadherin and metazoan origins. Science 2011; 331:1336-9; PMID:21393547; http://dx.doi.org/10.1126/science.1199633
18. Capaldo CT, Macara IG. Depletion of E-cadherin disrupts establishment but not maintenance of cell junctions in Madin-Darby canine kidney epithelial cells. Mol Biol Cell 2007; 18:189-200; PMID:17093058; http://dx.doi.org/10.1091/mbc.E06-05-0471
19. Fanning AS, Anderson JM. Zonula occludens-1 and -2 are cytosolic scaffolds that regulate the assembly of cellular junctions. Ann N Y Acad Sci 2009; 1165:113-20; PMID:19538295; http://dx.doi.org/10.1111/j.1749-6632.2009.04440.x
20. Spadaro D, Tapia R, Jond L, Sudol M, Fanning AS, Citi S. ZO proteins redundantly regulate the transcription factor DbpAZONAB. J Biol Chem 2014; 289:22500-11; PMID:24986862; http://dx.doi.org/10.1074/jbc.M114.556449
21. Yamanaka T, Tosaki A, Kurosawa M, Akimoto K, Hirose T, Ohno S, Hattori N, Nukina N. Loss of aPKClambda in differentiated neurons disrupts the polarity complex but does not induce obvious neuronal loss or disorientation in mouse brains. PLoS One 2013; 8:e84036; PMID:24391875; http://dx.doi.org/10.1371/journal.pone.0084036
22. Sripathy S, Lee M, Vasioukhin V. Mammalian Llgl2 is necessary for proper branching morphogenesis during placental development. Mol Cell Biol 2011; 31:2920-33; PMID:21606200; http://dx.doi.org/10.1128/MCB.05431-11
23. Bernards A. GAPs galore! A survey of putative Ras superfamily GTPase activating proteins in man and Drosophila. Biochim Biophys Acta 2003; 1603:47-82; PMID:12618308
24. Mooseker MS. Organisation, chemistry and assembly of the cytoskeletal apparatus of the intestinal brush border. Annu Rev Cell Biol 1985; 1:209-41; PMID:3916317; http://dx.doi.org/10.1146/annurev.cb.01.110185.001233
25. Akhtar N, Hotchin NA. RAC1 regulates adherens junctions through endocytosis of E-cadherin. Mol Biol Cell 2001; 12:847-62; PMID:11294891; http://dx.doi.org/10.1091/mbc.12.4.847
26. Budnar S, Yap AS. A mechanobiological perspective on cadherins and the actin-myosin cytoskeleton. F1000prime Rep 2013; 5:35; PMID:24049639; http://dx.doi.org/10.12703/P5-35
27. Pilot F, Lecuit T. Compartmentalized morphogenesis in epithelia: from cell to tissue shape. Dev Dyn 2005; 232:685-94; PMID:15712202; http://dx.doi.org/10.1002/dvdy.20334
28. Turner JR. 'Putting the squeeze' on the tight junction: understanding cytoskeletal regulation. Semin Cell Dev Biol 2000; 11:301-8; PMID:10966864; http://dx.doi.org/10.1006/scdb.2000.0180
29. Ratheesh A, Gomez GA, Priya R, Verma S, Kovacs EM, Jiang K, Brown NH, Akhmanova A, Stehbens SJ, Yap AS. Centralspindlin and alpha-catenin regulate Rho signalling at the epithelial zonula adherens. Nat Cell Biol 2012; 14:818-28; PMID:22750944; http://dx.doi.org/10.1038/ncb2532
30. Kovacs EM, Goodwin M, Ali RG, Paterson AD, Yap AS. Cadherin-directed actin assembly: e-cadherin physically associates with the Arp23 complex to direct actin assembly in nascent adhesive contacts. Curr Biol 2002; 12:379-82; PMID:11882288; http://dx.doi.org/10.1016/S0960-9822(02)00661-9
31. Ehrlich JS, Hansen MD, Nelson WJ. Spatio-temporal regulation of Rac1 localization and lamellipodia dynamics during epithelial cell-cell adhesion. Dev Cell 2002; 3:259-70; PMID:12194856; http://dx.doi.org/10.1016/S1534-5807(02)00216-2
32. Han SP, Gambin Y, Gomez GA, Verma S, Giles N, Michael M, Wu SK, Guo Z, Johnston W, Sierecki E, et al. Cortactin scaffolds Arp23 and WAVE2 at the epithelial zonula adherens. J Biol Chem 2014; 289:7764-75; PMID:24469447; http://dx.doi.org/10.1074/jbc.M113.544478
33. Tang VW, Brieher WM. alpha-Actinin-4FSGS1 is required for Arp23-dependent actin assembly at the adherens junction. J Cell Biol 2012; 196:115-30; PMID:22232703; http://dx.doi.org/10.1083/jcb.201103116
34. Verma S, Han SP, Michael M, Gomez GA, Yang Z, Teasdale RD, Ratheesh A, Kovacs EM, Ali RG, Yap AS. A WAVE2-Arp23 actin nucleator apparatus supports junctional tension at the epithelial zonula adherens. Mol Biol Cell 2012; 23:4601-10; PMID:23051739; http://dx.doi.org/10.1091/mbc.E12-08-0574
35. Kovacs EM, Verma S, Ali RG, Ratheesh A, Hamilton NA, Akhmanova A, Yap AS. N-WASP regulates the epithelial junctional actin cytoskeleton through a non-canonical post-nucleation pathway. Nat Cell Biol 2011; 13:934-43; PMID:21785420; http://dx.doi.org/10.1038/ncb2290
36. Kobielak A, Pasolli HA, Fuchs E. Mammalian formin-1 participates in adherens junctions and polymerization of linear actin cables. Nat Cell Biol 2004; 6:21-30; PMID:14647292; http://dx.doi.org/10.1038/ncb1075
37. Carramusa L, Ballestrem C, Zilberman Y, Bershadsky AD. Mammalian diaphanous-related formin Dia1 controls the organization of E-cadherin-mediated cell-cell junctions. J Cell Sci 2007; 120:3870-82; PMID:17940061; http://dx.doi.org/10.1242/jcs.014365
38. Ozono K, Komiya S, Shimamura K, Ito T, Nagafuchi A. Defining the roles of alpha-catenin in cell adhesion and cytoskeleton organization: isolation of F9 cells completely lacking cadherin-catenin complex. Cell Struct Funct 2011; 36:131-43; PMID:21685705; http://dx.doi.org/10.1247/csf.11009
39. Desai R, Sarpal R, Ishiyama N, Pellikka M, Ikura M, Tepass U. Monomeric alpha-catenin links cadherin to the actin cytoskeleton. Nat Cell Biol 2013; 15:261-73; PMID:23417122; http://dx.doi.org/10.1038/ncb2685
40. Yonemura S, Wada Y, Watanabe T, Nagafuchi A, Shibata M. Alpha-catenin as a tension transducer that induces adherens junction development. Nat Cell Biol 2010; 12:533-42; PMID:20453849; http://dx.doi.org/10.1038/ncb2055
41. le Duc Q, Shi Q, Blonk I, Sonnenberg A, Wang N, Leckband D, de Rooij J. Vinculin potentiates E-cadherin mechanosensing and is recruited to actin-anchored sites within adherens junctions in a myosin II-dependent manner. J Cell Biol 2010; 189:1107-15; PMID:20584916; http://dx.doi.org/10.1083/jcb.201001149
42. Drees F, Pokutta S, Yamada S, Nelson WJ, Weis WI. Alpha-catenin is a molecular switch that binds E-cadherin-beta-catenin and regulates actin-filament assembly. Cell 2005; 123:903-15; PMID:16325583; http://dx.doi.org/10.1016/j.cell.2005.09.021
43. Abe K, Takeichi M. EPLIN mediates linkage of the cadherin catenin complex to F-actin and stabilizes the circumferential actin belt. Proc Natl Acad Sci U S A 2008; 105:13-9; PMID:18093941; http://dx.doi.org/10.1073/pnas.0710504105
44. Maul RS, Song Y, Amann KJ, Gerbin SC, Pollard TD, Chang DD. EPLIN regulates actin dynamics by cross-linking and stabilizing filaments. J Cell Biol 2003; 160:399-407; PMID:12566430; http://dx.doi.org/10.1083/jcb.200212057
45. Mandai K, Nakanishi H, Satoh A, Obaishi H, Wada M, Nishioka H, Itoh M, Mizoguchi A, Aoki T, Fujimoto T, et al. Afadin: a novel actin filament-binding protein with one PDZ domain localized at cadherin-based cell-to-cell adherens junction. J Cell Biol 1997; 139:517-28; PMID:9334353; http://dx.doi.org/10.1083/jcb.139.2.517
46. Tachibana K, Nakanishi H, Mandai K, Ozaki K, Ikeda W, Yamamoto Y, Nagafuchi A, Tsukita S, Takai Y. Two cell adhesion molecules, nectin and cadherin, interact through their cytoplasmic domain-associated proteins. J Cell Biol 2000; 150:1161-76; PMID:10974003; http://dx.doi.org/10.1083/jcb.150.5.1161
47. Zhadanov AB, Provance DW, Speer CA, Coffin JD, Goss D, Blixt JA, Reichert CM, Mercer JA. Absence of the tight junctional protein AF-6 disrupts epithelial cell- cell junctions and cell polarity during mouse development. Curr Biol 1999; 9:880-8; PMID:10469590; http://dx.doi.org/10.1016/S0960-9822(99)80392-3
48. Ikeda W, Nakanishi H, Miyoshi J, Mandai K, Ishizaki H, Tanaka M, Togawa A, Takahashi K, Nishioka H, Yoshida H, et al. Afadin: a key molecule essential for structural organization of cell-cell junctions of polarized epithelia during embryogenesis. J Cell Biol 1999; 146:1117-32; PMID:10477764; http://dx.doi.org/10.1083/jcb.146.5.1117
49. Simoes Sde M, Mainieri A, Zallen JA. Rho GTPase and Shroom direct planar polarized actomyosin contractility during convergent extension. J Cell Biol

2014; 204:575-89; PMID:24535826; http://dx.doi.org/10.1083/jcb.201307070
50. Chu CW, Gerstenzang E, Ossipova O, Sokol SY. Lulu regulates Shroom-induced apical constriction during neural tube closure. PLoS One 2013; 8:e81854; PMID:24282618; http://dx.doi.org/10.1371/journal.pone.0081854
51. Baranwal S, Naydenov NG, Harris G, Dugina V, Morgan KG, Chaponnier C, Ivanov AI. Nonredundant roles of cytoplasmic beta- and gamma-actin isoforms in regulation of epithelial apical junctions. Mol Biol Cell 2012; 23:3542-53; PMID:22855531; http://dx.doi.org/10.1091/mbc.E12-02-0162
52. Ivanov AI, Bachar M, Babbin BA, Adelstein RS, Nusrat A, Parkos CA. A unique role for nonmuscle myosin heavy chain IIA in regulation of epithelial apical junctions. PLoS One 2007; 2:e658; PMID:17668046; http://dx.doi.org/10.1371/journal.pone.0000658
53. Smutny M, Cox HL, Leerberg JM, Kovacs EM, Conti MA, Ferguson C, Hamilton NA, Parton RG, Adelstein RS, Yap AS. Myosin II isoforms identify distinct functional modules that support integrity of the epithelial zonula adherens. Nat Cell Biol 2010; 12:696-702; PMID:20543839; http://dx.doi.org/10.1038/ncb2072
54. Fanning AS, Jameson BJ, Jesaitis LA, Anderson JM. The tight junction protein ZO-1 establishes a link between the transmembrane protein occludin and the actin cytoskeleton. J Biol Chem 1998; 273:29745-53; PMID:9792688; http://dx.doi.org/10.1074/jbc.273.45.29745
55. Wittchen ES, Haskins J, Stevenson BR. Protein interactions at the tight junction. Actin has multiple binding partners, and zo-1 forms independent complexes with zo-2 and zo-3. J Biol Chem 1999; 274:35179-85; PMID:10575001; http://dx.doi.org/10.1074/jbc.274.49.35179
56. D'Atri F, Citi S. Cingulin interacts with F-actin in vitro. FEBS Lett 2001; 507:21-4; PMID:11682052; http://dx.doi.org/10.1016/S0014-5793(01)02936-2
57. Van Itallie CM, Fanning AS, Bridges A, Anderson JM. ZO-1 stabilizes the tight junction solute barrier through coupling to the perijunctional cytoskeleton. Mol Biol Cell 2009; 20:3930-40; PMID:19605556; http://dx.doi.org/10.1091/mbc.E09-04-0320
58. Tokuda S, Higashi T, Furuse M. ZO-1 knockout by TALEN-mediated gene targeting in MDCK cells: involvement of ZO-1 in the regulation of cytoskeleton and cell shape. PLoS One 2014; 9:e104994; PMID:25157572; http://dx.doi.org/10.1371/journal.pone.0104994
59. Fanning AS, Van Itallie C, Anderson JM. Zonula occludens (ZO)-1 and -2 regulate apical cell structure and the zonula adherens cytoskeleton in polarized epithelia. Mol Biol Cell 2011; 23:577-90; PMID:22190737; http://dx.doi.org/10.1091/mbc.E11-09-0791
60. Fanning AS, Van Itallie CM, Anderson JM. Zonula occludens-1 and -2 regulate apical cell structure and the zonula adherens cytoskeleton in polarized epithelia. Mol Biol Cell 2012; 23:577-90; PMID:22190737; http://dx.doi.org/10.1091/mbc.E11-09-0791
61. Maiers JL, Peng X, Fanning AS, DeMali KA. ZO-1 recruitment to alpha-catenin–a novel mechanism for coupling the assembly of tight junctions to adherens junctions. J Cell Sci 2013; 126:3904-15; PMID:23813953; http://dx.doi.org/10.1242/jcs.126565
62. Ooshio T, Kobayashi R, Ikeda W, Miyata M, Fukumoto Y, Matsuzawa N, Ogita H, Takai Y. Involvement of the interaction of afadin with ZO-1 in the formation of tight junctions in Madin-Darby canine kidney cells. J Biol Chem 2010; 285:5003-12; PMID:20008323; http://dx.doi.org/10.1074/jbc.M109.043760
63. Otani T, Ichii T, Aono S, Takeichi M. Cdc42 GEF Tuba regulates the junctional configuration of simple epithelial cells. J Cell Biol 2006; 175:135-46; PMID:17015620; http://dx.doi.org/10.1083/jcb.200605012
64. Itoh M, Tsukita S, Yamazaki Y, Sugimoto H. Rho GTP exchange factor ARHGEF11 regulates the integrity of epithelial junctions by connecting ZO-1 and RhoA-myosin II signaling. Proc Natl Acad Sci U S A 2012; 109:9905-10; PMID:22665792; http://dx.doi.org/10.1073/pnas.1115063109
65. Paschoud S, Citi S. Inducible overexpression of cingulin in stably transfected MDCK cells does not affect tight junction organization and gene expression. Mol Membr Biol 2008; 25:1-13; PMID:18097951; http://dx.doi.org/10.1080/09687680701474009
66. Guillemot L, Citi S. Cingulin regulates claudin-2 expression and cell proliferation through the small GTPase RhoA. Mol Biol Cell 2006; 17:3569-77; PMID:16723500; http://dx.doi.org/10.1091/mbc.E06-02-0122
67. Guillemot L, Schneider Y, Brun P, Castagliuolo I, Pizzuti D, Martines D, Jond L, Bongiovanni M, Citi S. Cingulin is dispensable for epithelial barrier function and tight junction structure, and plays a role in the control of claudin-2 expression and response to duodenal mucosa injury. J Cell Sci 2012; 125:5005-14; in press; PMID:22946046; http://dx.doi.org/10.1242/jcs.101261
68. Meng W, Takeichi M. Adherens junction: molecular architecture and regulation. Cold Spring Harbor Perspect Biol 2009; 1:a002899; PMID:20457565; http://dx.doi.org10.1101cshperspect.a002899
69. Meng W, Mushika Y, Ichii T, Takeichi M. Anchorage of microtubule minus ends to adherens junctions regulates epithelial cell-cell contacts. Cell 2008; 135:948-59; PMID:19041755; http://dx.doi.org/10.1016/j.cell.2008.09.040
70. Pulimeno P, Paschoud S, Citi S. A role for ZO-1 and PLEKHA7 in recruiting paracingulin to tight and adherens junctions of epithelial cells. J Biol Chem 2011; 286:16743-50; PMID:21454477; http://dx.doi.org/10.1074/jbc.M111.230862
71. Ivanov AI, McCall IC, Babbin B, Samarin SN, Nusrat A, Parkos CA. Microtubules regulate disassembly of epithelial apical junctions. BMC Cell Biol 2006; 7:12; PMID:16509970; http://dx.doi.org/10.1186/1471-2121-7-12
72. Paschoud S, Jond L, Guerrera D, Citi S. PLEKHA7 modulates epithelial tight junction barrier function. Tissue Barriers 2014; 2:e28755; PMID:24843844; http://dx.doi.org/10.4161/tisb.28755
73. Ligon LA, Holzbaur EL. Microtubules tethered at epithelial cell junctions by dynein facilitate efficient junction assembly. Traffic 2007; 8:808-19; PMID:17550375; http://dx.doi.org/10.1111/j.1600-0854.2007.00574.x
74. Rosin-Arbesfeld R, Ihrke G, Bienz M. Actin-dependent membrane association of the APC tumour suppressor in polarized mammalian epithelial cells. EMBO J 2001; 20:5929-39; PMID:11689433; http://dx.doi.org/10.1093/emboj/20.21.5929
75. Karakesisoglou I, Yang Y, Fuchs E. An epidermal plakin that integrates actin and microtubule networks at cellular junctions. J Cell Biol 2000; 149:195-208; PMID:10747097; http://dx.doi.org/10.1083/jcb.149.1.195
76. Yano T, Matsui T, Tamura A, Uji M, Tsukita S. The association of microtubules with tight junctions is promoted by cingulin phosphorylation by AMPK. J Cell Biol 2013; 203:605-14; PMID:24385485; http://dx.doi.org/10.1083/jcb.201304194
77. Bartolini F, Ramalingam N, Gundersen GG. Actin-capping protein promotes microtubule stability by antagonizing the actin activity of mDia1. Mol Biol Cell 2012; 23:4032-40; PMID:22918941; http://dx.doi.org/10.1091/mbc.E12-05-0338
78. Krendel M, Zenke FT, Bokoch GM. Nucleotide exchange factor GEF-H1 mediates cross-talk between microtubules and the actin cytoskeleton. Nat Cell Biol 2002; 4:294-301; PMID:11912491; http://dx.doi.org/10.1038/ncb773
79. Nagae S, Meng W, Takeichi M. Non-centrosomal microtubules regulate F-actin organization through the suppression of GEF-H1 activity. Genes Cells 2013; 18:387-96; PMID:23432781; http://dx.doi.org/10.1111/gtc.12044
80. Guillemot L, Guerrera D, Spadaro D, Tapia R, Jond L, Citi S. MgcRacGAP interacts with cingulin and paracingulin to regulate Rac1 activation and development of the tight junction barrier during epithelial junction assembly. Mol Biol Cell 2014; 25:1995-2005; PMID:24807907; http://dx.doi.org/10.1091/mbc.E13-11-0680
81. Nusrat A, Giry M, Turner JR, Colgan SP, Parkos CA, Carmes D, Lemichez E, Boquet P, Madara JL. Rho protein regulates tight junctions and perijunctional actin organization in polarized epithelia. Proc Natl Acad Sci USA 1995; 92:10629-33; PMID:7479854; http://dx.doi.org/10.1073/pnas.92.23.10629
82. Braga VM, Machesky LM, Hall A, Hotchin NA. The small GTPases Rho and Rac are required for the establishment of cadherin-dependent cell-cell contacts. J Cell Biol 1997; 137:1421-31; PMID:9182672; http://dx.doi.org/10.1083/jcb.137.6.1421
83. Takaishi K, Sasaki T, Kotani H, Nishioka H, Takai Y. Regulation of cell-cell adhesion by rac and rho small G proteins in MDCK cells. J Cell Biol 1997; 139:1047-59; PMID:9362522; http://dx.doi.org/10.1083/jcb.139.4.1047
84. Jou TS, Nelson WJ. Effects of regulated expression of mutant RhoA and Rac1 small GTPases on the development of epithelial (MDCK) cell polarity. J Cell Biol 1998; 142:85-100; PMID:9660865; http://dx.doi.org/10.1083/jcb.142.1.85
85. Jou TS, Schneeberger EE, Nelson WJ. Structural and functional regulation of tight junctions by RhoA and Rac1 small GTPases. J Cell Biol 1998; 142:101-15; PMID:9660866; http://dx.doi.org/10.1083/jcb.142.1.101
86. Kovacs EM, Ali RG, McCormack AJ, Yap AS. E-cadherin homophilic ligation directly signals through Rac and phosphatidylinositol 3-kinase to regulate adhesive contacts. J Biol Chem 2002; 277:6708-18; PMID:11744701; http://dx.doi.org/10.1074/jbc.M109640200
87. Vasioukhin V, Fuchs E. Actin dynamics and cell-cell adhesion in epithelia. Curr Opin Cell Biol 2001; 13:76-84; PMID:11163137; http://dx.doi.org/10.1016/S0955-0674(00)00177-0
88. Adams AE, Johnson DI, Longnecker RM, Sloat BF, Pringle JR. CDC42 and CDC43, two additional genes involved in budding and the establishment of cell polarity in the yeast Saccharomyces cerevisiae. J Cell Biol 1990; 111:131-42; PMID:2195038; http://dx.doi.org/10.1083/jcb.111.1.131
89. Wojciak-Stothard B, Tsang LY, Haworth SG. Rac and Rho play opposing roles in the regulation of hypoxiar-eoxygenation-induced permeability changes in pulmonary artery endothelial cells. Am J Physiol Lung Cell Mol Physiol 2005; 288:L749-60; PMID:15591411; http://dx.doi.org/10.1152/ajplung.00361.2004
90. Fukuhara A, Shimizu K, Kawakatsu T, Fukuhara T, Takai Y. Involvement of nectin-activated Cdc42 small G protein in organization of adherens and tight junctions in Madin-Darby canine kidney cells. J Biol Chem 2003; 278:51885-93; PMID:14530286; http://dx.doi.org/10.1074/jbc.M308015200
91. Wells CD, Fawcett JP, Traweger A, Yamanaka Y, Goudreault M, Elder K, Kulkarni S, Gish G, Virag C, Lim C, et al. A Rich1Amot complex regulates the Cdc42 GTPase and apical-polarity proteins in epithelial cells. Cell 2006; 125:535-48; PMID:16678097; http://dx.doi.org/10.1016/j.cell.2006.02.045
92. Warner SJ, Longmore GD. Cdc42 antagonizes Rho1 activity at adherens junctions to limit epithelial cell apical tension. J Cell Biol 2009; 187:119-33; PMID:19805632; http://dx.doi.org/10.1083/jcb.200906047

93. Rajabian T, Gavicherla B, Heisig M, Muller-Altrock S, Goebel W, Gray-Owen SD, Ireton K. The bacterial virulence factor InlC perturbs apical cell junctions and promotes cell-to-cell spread of Listeria. Nat Cell Biol 2009; 11:1212-8; PMID:19767742; http://dx.doi.org/10.1038/ncb1964
94. Sahai E, Marshall CJ. ROCK and Dia have opposing effects on adherens junctions downstream of Rho. Nat Cell Biol 2002; 4:408-15; PMID:11992112; http://dx.doi.org/10.1038/ncb796
95. Jegou A, Carlier MF, Romet-Lemonne G. Formin mDia1 senses and generates mechanical forces on actin filaments. Nat Commun 2013; 4:1883; PMID:23695677; http://dx.doi.org/10.1038/ncomms2888
96. Amano M, Nakayama M, Kaibuchi K. Rho-kinase/ROCK: a key regulator of the cytoskeleton and cell polarity. Cytoskel (Hoboken) 2010; 67:545-54; PMID:20803696; http://dx.doi.org/10.1002/cm.20472
97. Levayer R, Pelissier-Monier A, Lecuit T. Spatial regulation of Dia and Myosin-II by RhoGEF2 controls initiation of E-cadherin endocytosis during epithelial morphogenesis. Nat Cell Biol 2011; 13:529-40; PMID:21516109; http://dx.doi.org/10.1038/ncb2224
98. Terry SJ, Zihni C, Elbediwy A, Vitiello E, Leefa Chong San IV, Balda MS, Matter K. Spatially restricted activation of RhoA signalling at epithelial junctions by p114RhoGEF drives junction formation and morphogenesis. Nat Cell Biol 2011; 13:159-66; PMID:21258369; http://dx.doi.org/10.1038/ncb2156
99. Ngok SP, Anastasiadis PZ. Rho GEFs in endothelial junctions: effector selectivity and signaling integration determine junctional response. Tissue Barriers 2013; 1:e27132; PMID:24790803; http://dx.doi.org/10.4161/tisb.27132
100. Capaldo CT, Nusrat A. Cytokine regulation of tight junctions. Biochim Biophys Acta 2009; 1788:864-71; PMID:18952050; http://dx.doi.org/10.1016/j.bbamem.2008.08.027
101. Citi S, Spadaro D, Schneider Y, Stutz J, Pulimeno P. Regulation of small GTPases at epithelial cell-cell junctions. Mol Membr Biol 2011; 28:427-44; PMID:21781017; http://dx.doi.org/10.3109/09687688.2011.603101
102. Akiyama K, Narita A, Nakaoka H, Cui T, Takahashi T, Yasuno K, Tajima A, Krischek B, Yamamoto K, Kasuya H, et al. Genome-wide association study to identify genetic variants present in Japanese patients harboring intracranial aneurysms. J Hum Genet 2010; 55:656-61; PMID:20613766; http://dx.doi.org/10.1038/jhg.2010.82
103. Williams JM, Johnson AC, Stelloh C, Dreisbach AW, Franceschini N, Regner KR, Townsend RR, Roman RJ, Garrett MR. Genetic variants in Arhgef11 are associated with kidney injury in the Dahl salt-sensitive rat. Hypertension 2012; 60:1157-68; PMID:22987919; http://dx.doi.org/10.1161/HYPERTENSIONAHA.112.199240
104. Ngok SP, Geyer R, Kourtidis A, Mitin N, Feathers R, Der C, Anastasiadis PZ. TEM4 is a junctional Rho GEF required for cell-cell adhesion, monolayer integrity and barrier function. J Cell Sci 2013; 126:3271-7; PMID:23729734; http://dx.doi.org/10.1242/jcs.123869
105. Priya R, Yap AS, Gomez GA. E-cadherin supports steady-state Rho signaling at the epithelial zonula adherens. Differ; Res Biol Divers 2013; 86:133-40; PMID:23643492; http://dx.doi.org/10.1016/j.diff.2013.01.002
106. Yuce O, Piekny A, Glotzer M. An ECT2-centralspindlin complex regulates the localization and function of RhoA. J Cell Biol 2005; 170:571-82; PMID:16103226; http://dx.doi.org/10.1083/jcb.200501097
107. Wildenberg GA, Dohn MR, Carnahan RH, Davis MA, Lobdell NA, Settleman J, Reynolds AB. p120-catenin and p190RhoGAP regulate cell-cell adhesion by coordinating antagonism between Rac and Rho. Cell 2006; 127:1027-39; PMID:17129786; http://dx.doi.org/10.1016/j.cell.2006.09.046
108. Birukova AA, Zebda N, Cokic I, Fu P, Wu T, Dubrovskyi O, Birukov KG. p190RhoGAP mediates protective effects of oxidized phospholipids in the models of ventilator-induced lung injury. Exp Cell Res 2011; 317:859-72; PMID:21111731; http://dx.doi.org/10.1016/j.yexcr.2010.11.011
109. Nakajima H, Tanoue T. Lulu2 regulates the circumferential actomyosin tensile system in epithelial cells through p114RhoGEF. J Cell Biol 2011; 195:245-61; PMID:22006950; http://dx.doi.org/10.1083/jcb.201104118
110. Nongpiur ME, Wei X, Xu L, Perera SA, Wu RY, Zheng Y, Li Y, Wang YX, Cheng CY, Jonas JB, et al. Lack of association between primary angle-closure glaucoma susceptibility loci and the ocular biometric parameters anterior chamber depth and axial length. Invest Ophthalmol Vis Sci 2013; 54:5824-8; PMID:23920366; http://dx.doi.org/10.1167/iovs.13-11901
111. Itoh K, Ossipova O, Sokol SY. GEF-H1 functions in apical constriction and cell intercalations and is essential for vertebrate neural tube closure. J Cell Sci 2014; 127:2542-53; PMID:24681784; http://dx.doi.org/10.1242/jcs.146811
112. Plageman TF Jr, Chauhan BK, Yang C, Jaudon F, Shang X, Zheng Y, Lou M, Debant A, Hildebrand JD, Lang RA. A Trio-RhoA-Shroom3 pathway is required for apical constriction and epithelial invagination. Development 2011; 138:5177-88; PMID:22031541; http://dx.doi.org/10.1242/dev.067868
113. Nishimura T, Honda H, Takeichi M. Planar cell polarity links axes of spatial dynamics in neural-tube closure. Cell 2012; 149:1084-97; PMID:22632972; http://dx.doi.org/10.1016/j.cell.2012.04.021
114. Omelchenko T, Hall A. Myosin-IXA regulates collective epithelial cell migration by targeting RhoGAP activity to cell-cell junctions. Curr Biol 2012; 22:278-88; PMID:22305756; http://dx.doi.org/10.1016/j.cub.2012.01.014
115. Chandhoke SK, Mooseker MS. A role for myosin IXb, a motor-RhoGAP chimera, in epithelial wound healing and tight junction regulation. Mol Biol Cell 2012; 23:2468-80; PMID:22573889; http://dx.doi.org/10.1091/mbc.E11-09-0803
116. Abouhamed M, Grobe K, San IV, Thelen S, Honnert U, Balda MS, Matter K, Bahler M. Myosin IXa regulates epithelial differentiation and its deficiency results in hydrocephalus. Mol Biol Cell 2009; 20:5074-85; PMID:19828736; http://dx.doi.org/10.1091/mbc.E09-04-0291
117. van Bodegraven AA, Curley CR, Hunt KA, Monsuur AJ, Linskens RK, Onnie CM, Crusius JB, Annese V, Latiano A, Silverberg MS, et al. Genetic variation in myosin IXB is associated with ulcerative colitis. Gastroenterology 2006; 131:1768-74; PMID:17087940; http://dx.doi.org/10.1053/j.gastro.2006.09.011
118. Monsuur AJ, de Bakker PI, Alizadeh BZ, Zhernakova A, Bevova MR, Strengman E, Franke L, van't Slot R, van Belzen MJ, Lavrijsen IC, et al. Myosin IXB variant increases the risk of celiac disease and points toward a primary intestinal barrier defect. Nat Genet 2005; 37:1341-4; PMID:16282976; http://dx.doi.org/10.1038/ng1680
119. Tripathi V, Popescu NC, Zimonjic DB. DLC1 induces expression of E-cadherin in prostate cancer cells through Rho pathway and suppresses invasion. Oncogene 2014; 33:724-33; PMID:23376848; http://dx.doi.org/10.1038/onc.2013.7
120. Holeiter G, Bischoff A, Braun AC, Huck B, Erlmann P, Schmid S, Herr R, Brummer T, Olayioye MA. The RhoGAP protein Deleted in Liver Cancer 3 (DLC3) is essential for adherens junctions integrity. Oncogenesis 2012; 1:e13; PMID:23552697; http://dx.doi.org/10.1038/oncsis.2012.13
121. Chen X, Macara IG. Par-3 controls tight junction assembly through the Rac exchange factor Tiam1. Nat Cell Biol 2005; 7:262-9; PMID:15723052; http://dx.doi.org/10.1038/ncb1226
122. Guillemot L, Paschoud S, Jond L, Foglia A, Citi S. Paracingulin regulates the activity of Rac1 and RhoA GTPases by recruiting Tiam1 and GEF-H1 to epithelial junctions. Mol Biol Cell 2008; 19:4442-53; PMID:18653465; http://dx.doi.org/10.1091/mbc.E08-06-0558
123. Mack NA, Porter AP, Whalley HJ, Schwarz JP, Jones RC, Khaja AS, Bjartell A, Anderson KI, Malliri A. beta2-syntrophin and Par-3 promote an apicobasal Rac activity gradient at cell-cell junctions by differentially regulating Tiam1 activity. Nat Cell Biol 2012; 14:1169-80; PMID:23103911; http://dx.doi.org/10.1038/ncb2608
124. Yano T, Yamazaki Y, Adachi M, Okawa K, Fort P, Uji M, Tsukita S, Tsukita S. Tara up-regulates E-cadherin transcription by binding to the Trio RhoGEF and inhibiting Rac signaling. J Cell Biol 2011; 193:319-32; PMID:21482718; http://dx.doi.org/10.1083/jcb.201009100
125. Spadaro D, Tapia R, Pulimeno P, Citi S. The control of gene expression and cell proliferation by the epithelial apical junctional complex. Essays Biochem 2012; 53:83-93; PMID:22928510; http://dx.doi.org/10.1042/bse0530083
126. Yi C, Troutman S, Fera D, Stemmer-Rachamimov A, Avila JL, Christian N, Persson NL, Shimono A, Speicher DW, Marmorstein R, et al. A tight junction-associated Merlin-angiomotin complex mediates Merlin's regulation of mitogenic signaling and tumor suppressive functions. Cancer Cell 2011; 19:527-40; PMID:21481793; http://dx.doi.org/10.1016/j.ccr.2011.02.017
127. Cooper J, Giancotti FG. Molecular insights into NF2/Merlin tumor suppressor function. FEBS Lett 2014; 588:2743-52; PMID:24726726; http://dx.doi.org/10.1016/j.febslet.2014.04.001
128. Nakamura T, Hayashi T, Mimori-Kiyosue Y, Sakaue F, Matsuura K, Iemura S, Natsume T, Akiyama T. The PX-RICS-14-3-3zetatheta complex couples N-cadherin-beta-catenin with dynein-dynactin to mediate its export from the endoplasmic reticulum. J Biol Chem 2010; 285:16145-54; PMID:20308060; http://dx.doi.org/10.1074/jbc.M109.081315
129. Erasmus J, Aresta S, Nola S, Caron E, Braga VM. Newly formed E-cadherin contacts do not activate Cdc42 or induce filopodia protrusion in human keratinocytes. Biol Cell 2010; 102:13-24; http://dx.doi.org/10.1042/BC20090048
130. Elbediwy A, Zihni C, Terry SJ, Clark P, Matter K, Balda MS. Epithelial junction formation requires confinement of Cdc42 activity by a novel SH3BP1 complex. J Cell Biol 2012; 198:677-93; PMID:22891260; http://dx.doi.org/10.1083/jcb.201202094
131. Zhao J, Bruck S, Cemerski S, Zhang L, Butler B, Dani A, Cooper JA, Shaw AS. CD2AP links cortactin and capping protein at the cell periphery to facilitate formation of lamellipodia. Mol Cell Biol 2013; 33:38-47; PMID:23090967; http://dx.doi.org/10.1128/MCB.00734-12
132. van Duijn TJ, Anthony EC, Hensbergen PJ, Deelder AM, Hordijk PL. Rac1 recruits the adapter protein CMSCD2AP to cell-cell contacts. J Biol Chem 2010; 285:20137-46; PMID:20404345; http://dx.doi.org/10.1074/jbc.M109.099481
133. Chan E, Nance J. Mechanisms of CDC-42 activation during contact-induced cell polarization. J Cell Sci 2013; 126:1692-702; PMID:23424200; http://dx.doi.org/10.1242/jcs.124594
134. Zihni C, Munro PM, Elbediwy A, Keep NH, Terry SJ, Harris J, Balda MS, Matter K. Dbl3 drives Cdc42 signaling at the apical margin to regulate junction position and apical differentiation. J Cell Biol 2014; 204:111-27; PMID:24379416; http://dx.doi.org/10.1083/jcb.201304064
135. Kooistra MR, Dube N, Bos JL. Rap1: a key regulator in cell-cell junction formation. J Cell Sci 2007; 120:17-22; PMID:17182900; http://dx.doi.org/10.1242/jcs.03306
136. Birukova AA, Tian X, Tian Y, Higginbotham K, Birukov KG. Rap-afadin axis in control of Rho signaling

and endothelial barrier recovery. Mol Biol Cell 2013; 24:2678-88; PMID:23864716; http://dx.doi.org/10.1091/mbc.E13-02-0098
137. Ando K, Fukuhara S, Moriya T, Obara Y, Nakahata N, Mochizuki N. Rap1 potentiates endothelial cell junctions by spatially controlling myosin II activity and actin organization. J Cell Biol 2013; 202:901-16; PMID:24019534; http://dx.doi.org/10.1083/jcb.201301115
138. Birkenfeld J, Nalbant P, Yoon SH, Bokoch GM. Cellular functions of GEF-H1, a microtubule-regulated Rho-GEF: is altered GEF-H1 activity a crucial determinant of disease pathogenesis? Trends Cell Biol 2008; 18:210-9; PMID:18394899; http://dx.doi.org/10.1016/j.tcb.2008.02.006
139. Aijaz S, D'Atri F, Citi S, Balda MS, Matter K. Binding of GEF-H1 to the tight junction-associated adaptor cingulin results in inhibition of Rho signaling and G1S phase transition. Dev Cell 2005; 8:777-86; PMID:15866167; http://dx.doi.org/10.1016/j.devcel.2005.03.003
140. Zenke FT, Krendel M, DerMardirossian C, King CC, Bohl BP, Bokoch GM. p21-activated kinase 1 phosphorylates and regulates 14-3-3 binding to GEF-H1, a microtubule-localized Rho exchange factor. J Biol Chem 2004; 279:18392-400; PMID:14970201; http://dx.doi.org/10.1074/jbc.M400084200
141. Callow MG, Zozulya S, Gishizky ML, Jallal B, Smeal T. PAK4 mediates morphological changes through the regulation of GEF-H1. J Cell Sci 2005; 118:1861-72; PMID:15827085; http://dx.doi.org/10.1242/jcs.02313
142. Yoshimura Y, Miki H. Dynamic regulation of GEF-H1 localization at microtubules by Par1bMARK2. Biochem Biophys Res Commun 2011; 408:322-8; PMID:21513698; http://dx.doi.org/10.1016/j.bbrc.2011.04.032
143. Yamahashi Y, Saito Y, Murata-Kamiya N, Hatakeyama M. Polarity-regulating kinase partitioning-defective 1b (PAR1b) phosphorylates guanine nucleotide exchange factor H1 (GEF-H1) to regulate RhoA-dependent actin cytoskeletal reorganization. J Biol Chem 2011; 286:44576-84; PMID:22072711; http://dx.doi.org/10.1074/jbc.M111.267021
144. Birkenfeld J, Nalbant P, Bohl BP, Pertz O, Hahn KM, Bokoch GM. GEF-H1 modulates localized RhoA activation during cytokinesis under the control of mitotic kinases. Dev Cell 2007; 12:699-712; PMID:17488622; http://dx.doi.org/10.1016/j.devcel.2007.03.014
145. Fujishiro SH, Tanimura S, Mure S, Kashimoto Y, Watanabe K, Kohno M. ERK12 phosphorylate GEF-H1 to enhance its guanine nucleotide exchange activity toward RhoA. Biochem Biophys Res Commun 2008; 368:162-7; PMID:18211802; http://dx.doi.org/10.1016/j.bbrc.2008.01.066
146. Waheed F, Dan Q, Amoozadeh Y, Zhang Y, Tanimura S, Speight P, Kapus A, Szaszi K. Central role of the exchange factor GEF-H1 in TNF-alpha-induced sequential activation of Rac, ADAM17TACE, and RhoA in tubular epithelial cells. Mol Biol Cell 2013; 24:1068-82; PMID:23389627; http://dx.doi.org/10.1091/mbc.E12-09-0661
147. von Thun A, Preisinger C, Rath O, Schwarz JP, Ward C, Monsefi N, Rodriguez J, Garcia-Munoz A, Birtwistle M, Bienvenut W, et al. Extracellular signal-regulated kinase regulates RhoA activation and tumor cell plasticity by inhibiting guanine exchange factor H1 activity. Mol Cell Biol 2013; 33:4526-37; PMID:24043311; http://dx.doi.org/10.1128/MCB.00585-13
148. Matthews HK, Delabre U, Rohn JL, Guck J, Kunda P, Baum B. Changes in Ect2 localization couple actomyosin-dependent cell shape changes to mitotic progression. Dev Cell 2012; 23:371-83; PMID:22898780; http://dx.doi.org/10.1016/j.devcel.2012.06.003
149. Niiya F, Tatsumoto T, Lee KS, Miki T. Phosphorylation of the cytokinesis regulator ECT2 at G2M phase stimulates association of the mitotic kinase Plk1 and accumulation of GTP-bound RhoA. Oncogene 2006; 25:827-37; PMID:16247472; http://dx.doi.org/10.1038/sj.onc.1209124
150. Su KC, Takaki T, Petronczki M. Targeting of the RhoGEF Ect2 to the equatorial membrane controls cleavage furrow formation during cytokinesis. Dev Cell 2011; 21:1104-15; PMID:22172673; http://dx.doi.org/10.1016/j.devcel.2011.11.003
151. Liot C, Seguin L, Siret A, Crouin C, Schmidt S, Bertoglio J. APC(cdh1) mediates degradation of the oncogenic Rho-GEF Ect2 after mitosis. PLoS One 2011; 6:e23676; PMID:21886810; http://dx.doi.org/10.1371/journal.pone.0023676
152. Michiels F, Stam JC, Hordijk PL, van der Kammen RA, Ruuls-Van Stalle L, Feltkamp CA, Collard JG. Regulated membrane localization of Tiam1, mediated by the NH2-terminal pleckstrin homology domain, is required for Rac-dependent membrane ruffling and C-Jun NH2-terminal kinase activation. J Cell Biol 1997; 137:387-98; PMID:9128250; http://dx.doi.org/10.1083/jcb.137.2.387
153. Fleming IN, Gray A, Downes CP. Regulation of the Rac1-specific exchange factor Tiam1 involves both phosphoinositide 3-kinase-dependent and -independent components. Biochem J 2000; 351:173-82; PMID:10998360; http://dx.doi.org/10.1042/0264-6021:3510173
154. Baumeister MA, Martinu L, Rossman KL, Sondek J, Lemmon MA, Chou MM. Loss of phosphatidylinositol 3-phosphate binding by the C-terminal Tiam-1 pleckstrin homology domain prevents in vivo Rac1 activation without affecting membrane targeting. J Biol Chem 2003; 278:11457-64; PMID:12525493; http://dx.doi.org/10.1074/jbc.M211901200
155. Woodcock SA, Rooney C, Liontos M, Connolly Y, Zoumpourlis V, Whetton AD, Gorgoulis VG, Malliri A. SRC-induced disassembly of adherens junctions requires localized phosphorylation and degradation of the rac activator tiam1. Mol Cell 2009; 33:639-53; PMID:19285946; http://dx.doi.org/10.1016/j.molcel.2009.02.012
156. Woodcock SA, Jones RC, Edmondson RD, Malliri A. A modified tandem affinity purification technique identifies that 14-3-3 proteins interact with Tiam1, an interaction which controls Tiam1 stability. J Proteome Res 2009; 8:5629-41; PMID:19899799; http://dx.doi.org/10.1021/pr900716e
157. Fleming IN, Elliott CM, Buchanan FG, Downes CP, Exton JH. Ca2+calmodulin-dependent protein kinase II regulates Tiam1 by reversible protein phosphorylation. J Biol Chem 1999; 274:12753-8; PMID:10212259; http://dx.doi.org/10.1074/jbc.274.18.12753
158. Ngok SP, Geyer R, Kourtidis A, Storz P, Anastasiadis PZ. Phosphorylation-mediated 14-3-3 protein binding regulates the function of the rho-specific guanine nucleotide exchange factor (RhoGEF) Syx. J Biol Chem 2013; 288:6640-50; PMID:23335514; http://dx.doi.org/10.1074/jbc.M112.432682
159. Haskell MD, Nickles AL, Agati JM, Su L, Dukes BD, Parsons SJ. Phosphorylation of p190 on Tyr1105 by c-Src is necessary but not sufficient for EGF-induced actin disassembly in C3H10T12 fibroblasts. J Cell Sci 2001; 114:1699-708; PMID:11309200
160. Arthur WT, Petch LA, Burridge K. Integrin engagement suppresses RhoA activity via a c-Src-dependent mechanism. Curr Biol 2000; 10:719-22; PMID:10873807; http://dx.doi.org/10.1016/S0960-9822(00)00537-6
161. Noren NK, Liu BP, Burridge K, Kreft B. p120 catenin regulates the actin cytoskeleton via Rho family GTPases. J Cell Biol 2000; 150:567-80; PMID:10931868; http://dx.doi.org/10.1083/jcb.150.3.567
162. Pullikuth AK, Catling AD. Extracellular signal-regulated kinase promotes Rho-dependent focal adhesion formation by suppressing p190A RhoGAP. Mol Cell Biol 2010; 30:3233-48; PMID:20439493; http://dx.doi.org/10.1128/MCB.01178-09
163. Levay M, Bartos B, Ligeti E. p190RhoGAP has cellular RacGAP activity regulated by a polybasic region. Cell Signal 2013; 25:1388-94; PMID:23499677; http://dx.doi.org/10.1016/j.cellsig.2013.03.004
164. Beck S, Fotinos A, Lang F, Gawaz M, Elvers M. Isoform-specific roles of the GTPase activating protein Nadrin in cytoskeletal reorganization of platelets. Cell Signal 2013; 25:236-46; PMID:22975681; http://dx.doi.org/10.1016/j.cellsig.2012.09.005
165. Minoshima Y, Kawashima T, Hirose K, Tonozuka Y, Kawajiri A, Bao YC, Deng X, Tatsuka M, Narumiya S, May WS Jr, et al. Phosphorylation by aurora B converts MgcRacGAP to a RhoGAP during cytokinesis. Dev Cell 2003; 4:549-60; PMID:12689593; http://dx.doi.org/10.1016/S1534-5807(03)00089-3
166. Ban R, Irino Y, Fukami K, Tanaka H. Human mitotic spindle-associated protein PRC1 inhibits MgcRacGAP activity toward Cdc42 during the metaphase. J Biol Chem 2004; 279:16394-402; PMID:14744859; http://dx.doi.org/10.1074/jbc.M313257200
167. Toure A, Mzali R, Liot C, Seguin L, Morin L, Crouin C, Chen-Yang I, Tsay YG, Dorseuil O, Gacon G, et al. Phosphoregulation of MgcRacGAP in mitosis involves Aurora B and Cdk1 protein kinases and the PP2A phosphatase. FEBS Lett 2008; 582:1182-8; PMID:18201571; http://dx.doi.org/10.1016/j.febslet.2007.12.036
168. Scholz RP, Regner J, Theil A, Erlmann P, Holeiter G, Jahne R, Schmid S, Hausser A, Olayioye MA. DLC1 interacts with 14-3-3 proteins to inhibit RhoGAP activity and block nucleocytoplasmic shuttling. J Cell Sci 2009; 122:92-102; PMID:19066281; http://dx.doi.org/10.1242/jcs.036251
169. Cao X, Voss C, Zhao B, Kaneko T, Li SS. Differential regulation of the activity of deleted in liver cancer 1 (DLC1) by tensins controls cell migration and transformation. Proc Natl Acad Sci U S A 2012; 109:1455-60; PMID:22307599; http://dx.doi.org/10.1073/pnas.1114368109
170. Fesenko I, Kurth T, Sheth B, Fleming TP, Citi S, Hausen P. Tight junction biogenesis in the early Xenopus embryo. Mech Dev 2000; 96:51-65; PMID:10940624; http://dx.doi.org/10.1016/S0925-4773(00)00368-3
171. Cardellini P, Davanzo G, Citi S. Tight junctions in early amphibian development: detection of junctional cingulin from the 2-cell stage and its localization at the boundary of distinct membrane domains in dividing blastomeres in low calcium. Dev Dyn 1996; 207:104-13; PMID:8875080; http://dx.doi.org/10.1002/(SICI)1097-0177(199609)207:1%3c104::AID-AJA10%3e3.0.CO;2-0
172. Javed Q, Fleming TP, Hay M, Citi S. Tight junction protein cingulin is expressed by maternal and embryonic genomes during early mouse development. Development 1993; 117:1145-51; PMID:8325239
173. Fleming TP, Hay M, Javed Q, Citi S. Localisation of tight junction protein cingulin is temporally and spatially regulated during early mouse development. Development 1993; 117:1135-44; PMID:8325238
174. Chalmers AD, Strauss B, Papalopulu N. Oriented cell divisions asymmetrically segregate aPKC and generate cell fate diversity in the early Xenopus embryo. Development 2003; 130:2657-68; PMID:12736210; http://dx.doi.org/10.1242/dev.00490
175. Ohnishi H, Nakahara T, Furuse K, Sasaki H, Tsukita S, Furuse M. JACOP, a novel plaque protein localizing at the apical junctional complex with sequence similarity to cingulin. J Biol Chem 2004; 279:46014-22; PMID:15292197; http://dx.doi.org/10.1074/jbc.M402616200
176. Inoko A, Itoh M, Tamura A, Matsuda M, Furuse M, Tsukita S. Expression and distribution of ZO-3, a tight junction MAGUK protein, in mouse tissues. Genes Cells 2003; 8:837-45; PMID:14622136; http://dx.doi.org/10.1046/j.1365-2443.2003.00681.x

177. Pegtel DM, Ellenbroek SI, Mertens AE, van der Kammen RA, de Rooij J, Collard JG. The Par-Tiam1 complex controls persistent migration by stabilizing microtubule-dependent front-rear polarity. Curr Biol 2007; 17:1623-34; PMID:17825562; http://dx.doi.org/10.1016/j.cub.2007.08.035
178. Wang S, Watanabe T, Matsuzawa K, Katsumi A, Kakeno M, Matsui T, Ye F, Sato K, Murase K, Sugiyama I, et al. Tiam1 interaction with the PAR complex promotes talin-mediated Rac1 activation during polarized cell migration. J Cell Biol 2012; 199:331-45; PMID:23071154; http://dx.doi.org/10.1083/jcb.201202041
179. Terry SJ, Elbediwy A, Zihni C, Harris AR, Bailly M, Charras GT, Balda MS, Matter K. Stimulation of cortical myosin phosphorylation by p114RhoGEF drives cell migration and tumor cell invasion. PLoS One 2012; 7:e50188; PMID:23185572; http://dx.doi.org/10.1371/journal.pone.0050188
180. Balda MS, Matter K. The tight junction protein ZO-1 and an interacting transcription factor regulate ErbB-2 expression. Embo J 2000; 19:2024-33; PMID:10790369; http://dx.doi.org/10.1093/emboj/19.9.2024
181. Capaldo CT, Koch S, Kwon M, Laur O, Parkos CA, Nusrat A. Tight function zonula occludens-3 regulates cyclin D1-dependent cell proliferation. Mol Biol Cell 2011; 22:1677-85; PMID:21411630; http://dx.doi.org/10.1091/mbc.E10-08-0677
182. Nie M, Aijaz S, Leefa Chong San IV, Balda MS, Matter K. The Y-box factor ZONABDbpA associates with GEF-H1Lfc and mediates Rho-stimulated transcription. EMBO Rep 2009; 10:1125-31; PMID:19730435; http://dx.doi.org/10.1038/embor.2009.182
183. Dupont S, Morsut L, Aragona M, Enzo E, Giulitti S, Cordenonsi M, Zanconato F, Le Digabel J, Forcato M, Bicciato S, et al. Role of YAPTAZ in mechanotransduction. Nature 2011; 474:179-83; PMID:21654799; http://dx.doi.org/10.1038/nature10137

PLEKHA7: Cytoskeletal adaptor protein at center stage in junctional organization and signaling

Several studies have been published in the last year, showing the importance of PLEKHA7 in junctional organization and signaling, and in pathology. For example, genome-wide analysis and genetic studies indicate its implication in cardiac morphogenesis and contractility, blood pressure regulation and primary angle closure glaucoma. More recent studies showed its role in micro RNA processing and cell response to alpha-toxin. In this review we summarize the current knowledge about PLEKHA7, describing its domain organization, molecular interactors and reviewing studies that highlight its importance in junction organization, signaling, and diseases. We also discuss possible therapeutic strategies involving PLEKHA7.

My role in this publication was writing the part about PLEKHA7 role in miRNA processing and related possible therapeutic strategies.

The International Journal of Biochemistry & Cell Biology 75 (2016) 112–116

Contents lists available at ScienceDirect

The International Journal of Biochemistry & Cell Biology

journal homepage: www.elsevier.com/locate/biocel

Molecules in focus

PLEKHA7: Cytoskeletal adaptor protein at center stage in junctional organization and signaling

Jimit Shah[a,b], Diego Guerrera[a,b], Ekaterina Vasileva[a,b], Sophie Sluysmans[a,b], Eva Bertels[a,b], Sandra Citi[a,b,*]

[a] Department of Cell Biology, University of Geneva, Geneva, Switzerland
[b] The Institute for Genetics and Genomics in Geneva (iGE3), University of Geneva, Geneva, Switzerland

ARTICLE INFO

Article history:
Received 4 March 2016
Received in revised form 4 April 2016
Accepted 5 April 2016
Available online 9 April 2016

Keywords:
PLEKHA7
p120catenin
Afadin
Paracingulin
PDZD11
Adherens junctions
Microtubules

ABSTRACT

PLEKHA7 is a recently characterized component of the cytoplasmic region of epithelial adherens junctions (AJ). It comprises two WW domains, a pleckstrin-homology domain, and proline-rich and coiled-coil domains. PLEKHA7 interacts with cytoplasmic components of the AJ (p120-catenin, paracingulin, afadin), stabilizes the E-cadherin complex by linking it to the minus ends of noncentrosomal microtubules, and stabilizes junctional nectins through the newly identified interactor PDZD11. Similarly to afadin, and unlike E-cadherin and p120-catenin, the localization of PLEKHA7 at AJ is strictly zonular (in the *zonula adhaerens* subdomain of AJ), and does not extend along the basolateral contacts. Genome-wide association studies and experiments on animal and cellular models show that although PLEKHA7 is not required for organism viability, it is implicated in cardiovascular physiology, hypertension, primary angle closure glaucoma, susceptibility to staphylococcal α-toxin, and epithelial morphogenesis and growth. Thus, PLEKHA7 is a cytoskeletal adaptor protein important for AJ organization, and at the center of junction-associated signaling pathways which fine-tune important pathophysiological processes.

1. Introduction

PLEKHA7 stands for Pleckstrin Homology Domain Containing, Family A Member 7, and was discovered as a new AJ protein independently by the Takeichi laboratory through its interaction with the N-terminal region of p120-catenin (Meng et al., 2008), and by the Citi laboratory as an interactor of the N-terminal region of paracingulin (CGNL1) (Pulimeno et al., 2010; Pulimeno et al., 2011). Genomic and genetic studies also identified PLEKHA7 as a protein associated with human hypertension (Levy et al., 2009), and implicated in cardiac development and contractility (Wythe et al., 2011). PLEKHA7 is involved not only in stabilizing the two main transmembrane components of AJ, e.g. E-cadherin (Meng et al., 2008) and nectins (Guerrera et al., 2016), but also in a wider array of signaling functions, which are relevant to its role in tissue physiology and pathology.

2. Gene and protein structure

PLEKHA7 is coded by the *plekha7* gene, which is found only in vertebrate organisms, although other members of Pleckstrin Homology Domain Containing Family A of genes are expressed in lower metazoa. In the human genome the *plekha7* gene maps to chromosome 11 and spans a 237 kB region. In the mouse the *plekha7* gene maps to chromosome 7 and spans a 185 kB region.

The amino acid sequence of the PLEKHA7 protein is well conserved throughout vertebrate species: the sequence identity between the human protein sequence and those of dog, mouse, chicken, *Xenopus laevis* and *Danio rerio* are 94%, 89%, 73%, 61% and 64%, respectively.

Human PLEKHA7 is predicted to exist in two isoforms, comprising either 1121 or 1271 amino acids, and PLEKHA7 is detected as polypeptides with apparent sizes of 135–145 kDa in lysates of mammalian cells and tissues (Pulimeno et al., 2010). The functional differences between the isoforms are not known. The N-terminal half of PLEKHA7 contains a pleckstrin-homology (PH) domain (residues 166–281) (Fig. 1A), which allows PLEKHA7 to interact in vitro with phosphorylated phosphatidyinositol lipids (Wythe et al., 2011) (PI in Fig. 2B). A region of PLEKHA7 comprising the PH domain, but lacking the WW domain (residues 120–374) is

* Corresponding author at: Department of Cell Biology, 4 Boulevard d'Yvoy, 1211-4 Geneva, Switzerland.
E-mail address: sandra.citi@unige.ch (S. Citi).

http://dx.doi.org/10.1016/j.biocel.2016.04.001
1357-2725/

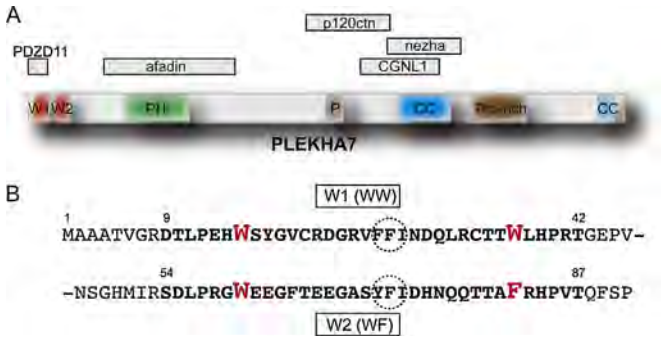

Fig. 1. The structure and molecular interactors of PLEKHA7. (A) Scheme of human PLEKHA7, with domains highlighted in: red (the two WW domains); green (PH); brown (proline-rich); blue (coiled-coil). The regions of interaction with PDZD11, afadin, p120-catenin, paracingulin (CGNL1) and nezha, based on in vitro binding studies, are indicated. (B) Alignement of the two WW domains of PLEKHA7 (highlighted in bold type): the first (W1) containing two Trp residues, and the second (W2) containin a Trp and a Phe residue. Signature Trp and Phe are highlighted in bold, red and larger size. Dotted circles outline the hydophobic residues at the core of the structure.

involved in PLEKHA7 interaction with the scaffold protein afadin (Kurita et al., 2013) (Fig. 1A). Although in some studies only one WW domain was annotated (Meng et al., 2008; Kurita et al., 2013), PLEKHA7 comprises two WW domains in its N-terminal region (Pulimeno et al., 2011; Wythe et al., 2011; Endres et al., 2014; Popov et al., 2015): one canonical class 1 WW domain (with the two signature Trp residues) and a second WW domain, comprising a Trp and a Phe residue, a feature detected in other class-I WW domains (Kasanov et al., 2001), separated by a spacer region of 11 residues (Fig. 1B). Both domains are 33-residue long, and contain a cluster of aromatic residues in the second β-sheet strand (dotted circle in Fig. 1B), which are implicated in the stabilization of the hydrophobic core of the structure (Martinez-Rodriguez et al., 2015). We showed that the region of PLEKHA7 comprising the WW domains specifically interacts with the small PDZ protein PDZD11, and is required for the recruitment of PDZD11 to AJ (Guerrera et al., 2016) (Fig. 1A). The C-terminal half of PLEKHA7 comprises coiled-coil (CC) and proline-rich (Pro) domains (Fig. 1A). p120-catenin binds to a central region of PLEKHA7, that includes the first proline-rich region but lacks the coiled-coil region. Paracingulin and nezha (calmodulin-regulated spectrin-associated protein 3, CAMSAP3) interact with overlapping C-terminal regions of PLEKHA7, comprising the larger coiled-coil domain (Fig. 1A). The recruitment of PLEKHA7 to AJ probably depends on its redundant interactions with phospholipids, p120-catenin and afadin (Meng et al., 2008; Wythe et al., 2011; Kurita et al., 2013; Pulimeno et al., 2010). Additional interactors of PLEKHA7, for which no direct in vitro binding validation is yet available, have been identified through mass spectrometry analysis of PLEKHA7 immunoprecipitates (Kourtidis et al., 2015; Kourtidis and Anastasiadis, 2016).

3. Expression and localization

Immunofluorescence (Meng et al., 2008; Pulimeno et al., 2010) and immuno-electron microscopy (Pulimeno et al., 2010) analyses show that PLEKHA7 is localized at adherens junctions (AJ) of epithelial cells, and specifically in its zonular subdomain (*zonula adhaerens*) (Fig. 2A), which has important signaling functions (Citi et al., 2014). The distance of PLEKHA7 from the junctional membrane, as determined by immuno-electron microscopy, is 25 nm (Pulimeno et al., 2010). Similarly to afadin and differently from E-cadherin, α-catenin, β-catenin and p120-catenin, PLEKHA7 is not detected along lateral contacts of epithelial cells (Pulimeno et al., 2010), thereby defining two pools of p120-catenin, belonging to two distinct E-cadherin complexes, one comprising and one lacking PLEKHA7 (Kourtidis et al., 2015) (Fig. 2A). However, exogenously expressed PLEKHA7 localizes at lateral contacts (Paschoud et al., 2014), suggesting different affinities for zonular and lateral complexes. PLEKHA7 is detected at zonular junctions in all epithelial tissues investigated so far, and in endothelial cells and tissues (Pulimeno et al., 2010; Guerrera et al., 2016; Lee et al., 2014). In human eye tissues expression of PLEKHA7 was detected in epithelial, smooth muscle and endothelial cells, and within anterior cavity structures, such as iris and ciliary body (Lee et al., 2014). The expression of the PLEKHA7 homolog in zebrafish, Hadp1, was determined only by mRNA in situ hybridization in the embryonic myocardium (Wythe et al., 2011). The unique subcellular localization and tissue distribution of PLEKHA7 distinguish it from both ZO-1 and E-cadherin (Pulimeno et al., 2010), suggesting that the PLEKHA7/afadin-associated protein complex bridges the ZA to tight junctions (TJ) (Citi et al., 2012).

In relationship to expression in human normal and cancer tissues, PLEKHA7 was detected at junctions of normal epithelial breast tubular structures and in low grade ductal carcinomas, but not in high grade and lobular carcinomas (Tille et al., 2015). Mislocalization or loss of PLEKHA7 was independently observed in human breast and renal cancers (Kourtidis et al., 2015).

4. Biological functions

PLEKHA7 is emerging as a multifunctional adaptor protein with important roles both in the structural organization of AJ, and in their signaling functions.

The complex between PLEKHA7, nezha and the minus-end directed motor kinesin KIFC3 allows PLEKHA7 to tether the E-cadherin complex to the minus end of noncentrosomal microtubules, thus stabilizing E-cadherin-based junctions (Meng et al., 2008) (Fig. 2B). By binding to afadin, PLEKHA7 is also indirectly linked to microfilaments (Fig. 2B). In MDCK cells, PLEKHA7 is required for the junctional localization of the zonular protein paracingulin, through their direct interaction (Pulimeno et al., 2011) (Fig. 2B). By recruiting PDZD11 to AJ, PLEKHA7 stabilizes nectins, the second major class of transmembrane adhesion receptors of AJ (Guerrera et al., 2016) (Fig. 2B). Thus, by binding to the E-cadherin complex through redundant direct and indirect interactions (p120-ctn, paracingulin, afadin), and to the nectin complex through PDZD11 and afadin, PLEKHA7 connects these two protein complexes within the ZA (Guerrera et al., 2016) (Fig. 2B). Although PLEKHA7 is not required for the formation of functional TJ (Kurita et al., 2013; Paschoud et al., 2014), overexpression experiments show that PLEKHA7 stabilizes TJ barrier function in a microtubule- and AJ-dependent manner (Paschoud et al., 2014).

In colon epithelial carcinoma cells (Caco2) the interaction with PLEKHA7 differentiates two pools of p120-catenin: an apical complex (unphosphorylated inactive p120-catenin), bound to PLEKHA7; and a basolateral complex (p120-catenin phosphorylated by activated Src), which signals to promote cell cycle progression and cancer. Indeed, Caco2 cells depleted of PLEKHA7 show increased anchorage independent growth and expression of transformation and mesenchymal markers (Kourtidis et al., 2015). Analysis of PLEKHA7 immunoprecipitates reveals the presence of components of the miRNA processing complex (DROSHA and DGCR8), allowing the processing and regulation of miR-24, miR-30a, miR30-b and let7-g, which suppress the expression of growth promoting proteins SNAIL, MYC and cyclin D1 at junctions (Kourtidis et al., 2015; Kourtidis and Anastasiadis, 2016). Consequently, in cells depleted of PLEKHA7 the junctional localization of the microprocessor complex is lost, and there is a decrease in the levels of the above mentioned miRNAs. Since reintroduction

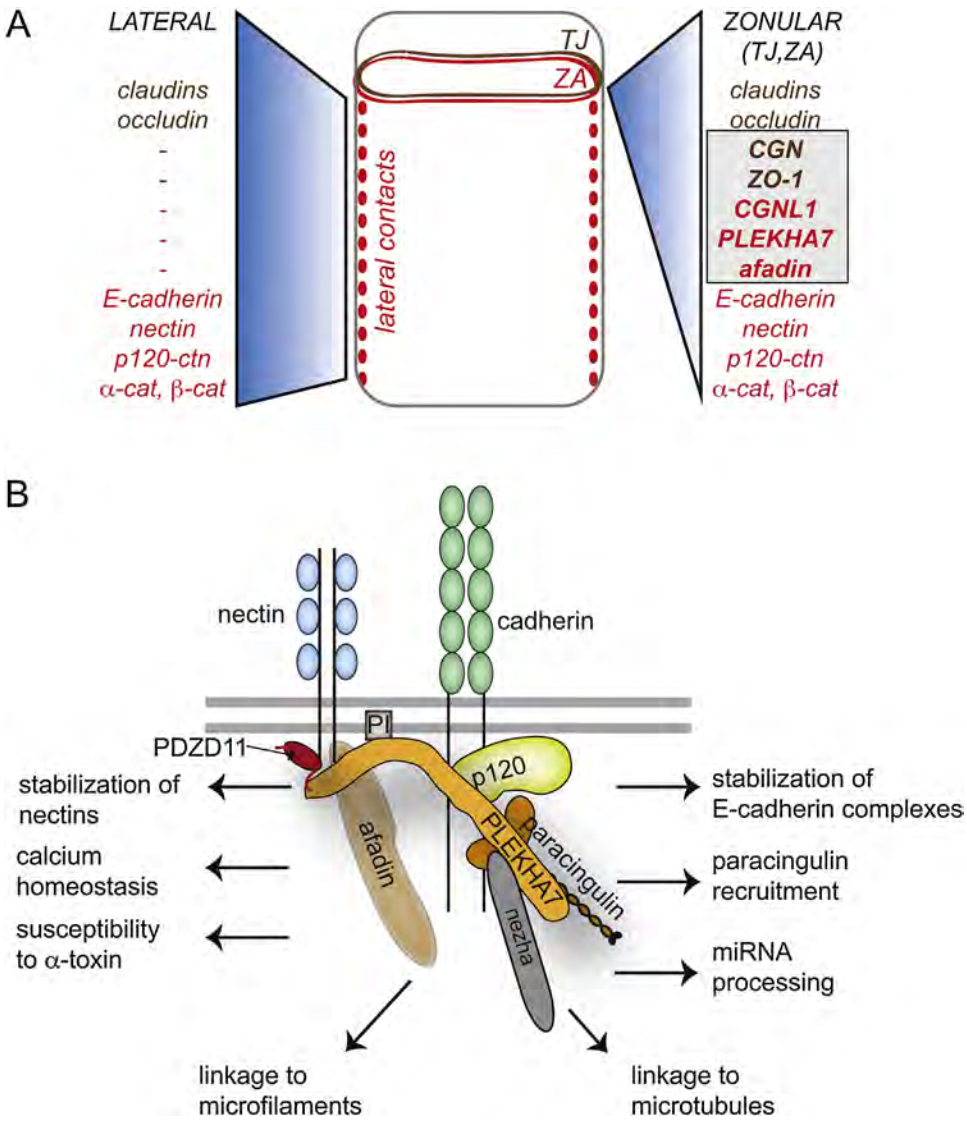

Fig. 2. The localization and functions of PLEKHA7. (A) Schematic drawing of a polarized epithelial cell, with the subcellular localizations of zonular junctions (TJ, ZA) and lateral contacts indicated by apical continuous circles and lateral dotted lines, respectively. Text on the sides indicates non-exhaustive lists of transmembrane and cytoplasmic junctional proteins localized both at zonular and lateral junctions (claudins, occludin, E-cadherin, nectin and catenins) or exclusively at the apical "*zonulae*", for example cingulin and ZO-1 for TJ, and paracingulin (CGNL1), PLEKHA7 and afadin for ZA (highlighted in the grey box), in polarized epithelial cells. (B) Schematic drawing of the *zonula adhaerens*, where PLEKHA7 is shown interacting with PDZD11, afadin, membrane phosphorylated phosphatidylinositols (PI), nezha (CAMSAP3), p120ctn and paracingulin. Ig-like and EC domains of nectin(s) and E-cadherin are shown by blue and green ovals, respectively. Functions of PLEKHA7 are indicated by arrows and text on each side of the scheme. Stabilization of the E-cadherin and nectin complexes is mediated by nezha-dependent linkage to microtubules, and by the PDZD11 and afadin interactors (the latter binding to actin filaments), respectively.

of miR-30b in PLEKHA7 knockdown cells rescues the abnormal increased levels of SNAIL, MYC and cyclin D1, the p120-catenin-PLEKHA7-microprocessor complex antagonizes the effects of the tumor-promoting basolateral p120 complex (Kourtidis et al., 2015) (Fig. 2B).

PLEKHA7 was recently shown to be important in the cytotoxic effect of α-toxin, the most potent virulence factor of *Staphylococcus aureus* (Popov et al., 2015) (Fig. 2B). PLEKHA7 was in fact identified in a genetic screen designed to determine host cellular factors required for alpha-toxin cytotoxicity. A library of mutagenized haploid human cells (HAP1) was screened to identify clones that survived upon treatment with α-toxin. Besides the α-toxin receptor (ADAM10) the most enriched gene in the screen was PLEKHA7 (Popov et al., 2015). In PLEKHA7-KO mice, which are viable and otherwise show no apparent additional phenotype, necrotic inflammatory effects of *S. aureus* on the skin were resolved with a significantly reduced tissue loss, with respect to WT (Popov et al., 2015). Live imaging analysis reveals that WT and PLEKHA7-KO HAP1 cells undergo similar levels of initial cell injury after alpha-toxin treatment (Popov et al., 2015). This cytopathic effect is absent in the ADAM10-KO HAP1 cells, suggesting that PLEKHA7 might play a role in the recovery process in a step downstream of ADAM10 interaction and pore formation by the toxin.

Depletion of the PLEKHA7 homologue Hadp1 in zebrafish demonstrates its role in cardiac morphogenesis and contractility (Wythe et al., 2011). The loss of Hadp1 alters Ca^{2+} signaling in cardiomyocytes, leading to an increase in the amplitude and duration of the calcium transient (Wythe et al., 2011). This was explained by a reduced rate of extrusion of cytoplasmic calcium during diastole, through the interaction of Hadp1 with phosphatidylinositol 4-kinase signaling (Wythe et al., 2011). It was proposed that Hadp1 inhibits the generation of phosphatidylinositol (4,5)-biphosphate and/or its hydrolysis, regulating the calcium released by the sarcomeric reticulum, the reuptake of Ca^{2+} from the cytoplasm and the

plasma membrane calcium conductance (Wythe et al., 2011). An alternative hypothesis for a mechanism through which PLEKHA7 modulates calcium homeostasis, proposed following the discovery of its new interactor PDZD11, is by acting on the calcium pump Plasma Membrane Calcium ATPase (Guerrera et al., 2016), which is known to interact with PDZD11 (Goellner et al., 2003) (Fig. 2B).

Specific single nucleotide polymorphisms of the PLEKHA7 gene have been identified in different human cohort studies as associated with hypertension (Levy et al., 2009; Hong et al., 2010; Lin et al., 2011) albeit not in African-Americans (Fox et al., 2011). The implication of PLEKHA7 in the regulation of blood pressure was confirmed experimentally in a rat PLEKHA7-KO model, whereby the loss of PLEKHA7 resulted in lower blood pressure, and hence reduced kidney and cardiac damage (Endres et al., 2014). The vasodilatory effect of PLEKHA7 KO was shown to correlate with increased intracellular Ca^{2+} and eNOS signaling in endothelial cells (Endres et al., 2014). Thus, PLEKHA7 plays a role in cardiac contractility and blood pressure regulation through its involvement in intracellular calcium dynamics (Fig. 2B). However, additional studies are required to characterize the different hypothetical mechanisms by which PLEKHA7 regulates intracellular Ca^{2+} levels in these tissues.

Genetic variants of PLEKHA7 are also associated with primary angle closure glaucoma, one of the leading causes of irreversible blindness (Vithana et al., 2012; Day et al., 2013; Shuai et al., 2015). Glaucoma is characterized by the increase in intraocular pressure, due to reduced trabecular meshwork function. The molecular mechanism through which PLEKHA7 is implicated in glaucoma is not clear, but PLEKHA7 is expressed in different structures that might be involved in the increase of intraocular pressure, such as the iris, ciliary body and vasculature (Lee et al., 2014).

5. Medical applications

As mentioned above, studies on human cohorts and animal models show that PLEKHA7 is implicated in the control of cardiac morphogenesis and contractility, in hypertension, in glaucoma and in susceptibility to *S. aureus* α-toxin. This, and recent studies on the role of PLEKHA7 in regulating microRNA processing, make PLEKHA7 an interesting candidate for the development of new therapeutic approaches for cardiovascular and infectious diseases, and cancer.

Based on observations on PLEKHA7-KO rats (Endres et al., 2014) it could be hypothesized that a reduction of PLEKHA7 expression/function in endothelial cells could help to control blood pressure. Possibly PLEKHA7 mutations in hypertensive patients may lead to increased blood pressure through an increase in PLEKHA7 levels. Drugs targeting PLEKHA7 might allow to modulate vascular tone, as well as cardiac contractility, and also primary angle closure glaucoma.

Since PLEKHA7 is mislocalized, drastically reduced or lost in different human tumors (Tille et al., 2015; Kourtidis et al., 2015), PLEKHA7 is a potential new marker of tumor progression, and a possible candidate for gene therapy. Reintroduction of PLEKHA7 in cells showing a reduced expression, or introduction of miRNAs, whose maturation is specifically regulated by PLEKHA7, could be a successful strategy to prevent tumor formation and progression. Similarly, manipulation of PLEKHA7 levels or function could be helpful to reduce the cytotoxic effects of *S. aureus* infection in epithelial cells.

As our understanding of the molecular mechanisms through which PLEKHA7 controls endothelial and epithelial cell and tissue functions improves, it will be possible to develop targeted approaches to treat diseases involving PLEKHA7.

Acknowledgements

We are grateful to the Swiss National Science Foundation, the Swiss Cancer league and the Republic and Canton of Geneva for financial support of research projects in the Citi laboratory.

References

Citi, S., Pulimeno, P., Paschoud, S., 2012. Cingulin, paracingulin, and PLEKHA7: signaling and cytoskeletal adaptors at the apical junctional complex. Ann. N. Y. Acad. Sci. 1257, 125–132.
Citi, S., Guerrera, D., Spadaro, D., Shah, J., 2014. Epithelial junctions and Rho family GTPases: the zonular signalosome. Small GTPases 5, 1–15.
Day, A.C., Luben, R., Khawaja, A.P., Low, S., Hayat, S., Dalzell, N., Wareham, N.J., Khaw, K.-T., Foster, P.J., 2013. Genotype-phenotype analysis of SNPs associated with primary angle closure glaucoma (rs1015213, rs3753841 and rs11024102) and ocular biometry in the EPICNorfolk Eye Study. Br. J. Ophthalmol. 97, 704–707.
Endres, B.T., Priestley, J.R., Palygin, O., Flister, M.J., Hoffman, M.J., Weinberg, B.D., Grzybowski, M., Lombard, J.H., Staruschenko, A., Moreno, C., Jacob, H.J., Geurts, A.M., 2014. Mutation of Plekha7 attenuates salt-sensitive hypertension in the rat. Proc. Natl. Acad. Sci. U. S. A. 111, 12817–12822.
Fox, E.R., Young, J.H., Li, Y., Dreisbach, A.W., Keating, B.J., Musani, S.K., Liu, K., Morrison, A.C., Ganesh, S., Kutlar, A., et al., 2011. Association of genetic variation with systolic and diastolic blood pressure among African Americans: the Candidate Gene Association Resource study. Hum. Mol. Genet. 20, 2273–2284.
Goellner, G.M., DeMarco, S.J., Strehler, E.E., 2003. Characterization of PISP, a novel single-PDZ protein that binds to all plasma membrane Ca2+-ATPase b-splice variants. Ann. N. Y. Acad. Sci. 986, 461–471.
Guerrera, D., Shah, J., Vasileva, E., Sluysmans, S., Mean, I., Jond, L., Poser, I., Mann, M., Hyman, A.A., Citi, S., 2016. PLEKHA7 recruits PDZD11 to adherens junctions to stabilize nectins. J. Biol. Chem, http://dx.doi.org/10.1074/jbc.M115.712935.
Hong, K.-W., Jin, H.-S., Lim, J.-E., Kim, S., Go, M.J., Oh, B., 2010. Recapitulation of two genomewide association studies on blood pressure and essential hypertension in the Korean population. J. Hum. Genet. 55, 336–341.
Kasanov, J., Pirozzi, G., Uveges, A.J., Kay, B.K., 2001. Characterizing Class I WW domains defines key specificity determinants and generates mutant domains with novel specificities. Chem. Biol. 8, 231–241.
Kourtidis, A., Anastasiadis, P.Z., 2016. PLEKHA7 defines an apical junctional complex with cytoskeletal associations and miRNA-mediated growth implications. Cell Cycle 15 (4), 498–505, http://dx.doi.org/10.1080/15384101.2016.1141840.
Kourtidis, A., Ngok, S.P., Pulimeno, P., Feathers, R.W., Carpio, L.R., Baker, T.R., Carr, J.M., Yan, I.K., Borges, S., Perez, E.A., et al., 2015. Distinct E-cadherin-based complexes regulate cell behaviour through miRNA processing or Src and p120 catenin activity. Nat. Cell Biol. 17, 1145–1157.
Kurita, S., Yamada, T., Rikitsu, E., Ikeda, W., Takai, Y., 2013. Binding between the junctional proteins afadin and PLEKHA7 and implication in the formation of adherens junction in epithelial cells. J. Biol. Chem. 288, 29356–29368.
Lee, M.C., Chan, A.S.Y., Goh, S.R., Hilmy, M.H., Nongpiur, M.E., Hong, W., Aung, T., Hunziker, W., Vithana, E.N., 2014. Expression of the primary angle closure glaucoma (PACG) susceptibility gene PLEKHA7 in endothelial and epithelial cell junctions in the eye. Invest. Ophthalmol. Vis. Sci. 55, 3833–3841.
Levy, D., Ehret, G.B., Rice, K., Verwoert, G.C., Launer, L.J., Dehghan, A., Glazer, N.L., Morrison, A.C., Johnson, A.D., Aspelund, T., et al., 2009. Genome-wide association study of blood pressure and hypertension. Nat. Genet. 41, 677–687.
Lin, Y., Lai, X., Chen, B., Xu, Y., Huang, B., Chen, Z., Zhu, S., Yao, J., Jiang, Q., Huang, H., et al., 2011. Genetic variations in CYP17A1, CACNB2 and PLEKHA7 are associated with blood pressure and/or hypertension in she ethnic minority of China. Atherosclerosis 219, 709–714.
Martinez-Rodriguez, S., Bacarizo, J., Luque, I., Camara-Artigas, A., 2015. Crystal structure of the first WW domain of human YAP2 isoform. J. Struct. Biol. 191, 381–387.
Meng, W., Mushika, Y., Ichii, T., Takeichi, M., 2008. Anchorage of microtubule minus ends to adherens junctions regulates epithelial cell–cell contacts. Cell 135, 948–959.
Paschoud, S., Jond, L., Guerrera, D., Citi, S., 2014. PLEKHA7 modulates epithelial tight junction barrier function. Tissue Barriers 2, e28755.
Popov, L.M., Marceau, C.D., Starkl, P.M., Lumb, J.H., Shah, J., Guerrera, D., Cooper, R.L., Merakou, C., Bouley, D.M., Meng, W., et al., 2015. The adherens junctions control susceptibility to Staphylococcus aureus alpha-toxin. Proc. Natl. Acad. Sci. U. S. A. 112, 14337–14342.
Pulimeno, P., Bauer, C., Stutz, J., Citi, S., 2010. PLEKHA7 is an adherens junction protein with a tissue distribution and subcellular localization distinct from ZO-1 and E-Cadherin. PLoS One 5, http://dx.doi.org/10.1371/journal.pone.0012207.
Pulimeno, P., Paschoud, S., Citi, S., 2011. A role for ZO-1 and PLEKHA7 in recruiting paracingulin to tight and adherens junctions of epithelial cells. J. Biol. Chem. 286, 16743–16750.
Shuai, P., Yu, M., Li, X., Zhou, Y., Liu, X., Liu, Y., Zhang, D.D., Gong, B., 2015. Genetic associations in PLEKHA7 and COL11A1 with primary angle closure glaucoma: a meta-analysis. Clin. Exp. Ophthalmol. 43, 523–530.

Tille, J.-C., Ho, L., Shah, J., Seyde, O., McKee, T.A., Citi, S., 2015. The expression of the zonula adhaerens protein PLEKHA7 is strongly decreased in high grade ductal and lobular breast carcinomas. PLoS One 10, e0135442.

Vithana, E.N., Khor, C.-C., Qiao, C., Nongpiur, M.E., George, R., Chen, L.-J., Do, T., Abu-Amero, K., Huang, C.K., Low, S., et al., 2012. Genome-wide association analyses identify three new susceptibility loci for primary angle closure glaucoma. Nat. Genet. 44, 1142–1146.

Wythe, J.D., Jurynec, M.J., Urness, L.D., Jones, C.A., Sabeh, M.K., Werdich, A.A., Sato, M., Yost, H.J., Grunwald, D.J., Macrae, C.A., et al., 2011. Hadp1, a newly identified pleckstrin homology domain protein, is required for cardiac contractility in zebrafish. Dis. Model Mech. 4, 607–621.

DISCUSSION AND PERSPECTIVES

The junctional complex plays fundamental roles in the physiology of epithelial tissues and organs. Therefore, dissecting the molecular composition of the junctional complex and the functions of its molecular components is of critical importance to understand their implication in tissue morphogenesis, physiology and disease.

PLEKHA7 is a junctional adaptor protein localized at AJ of epithelial and endothelial cells, and it interacts with both major adhesion complexes of AJ (based on either E-cadherin or nectin), through its binding to p120ctn and afadin, respectively [5, 7]. Although the functional relevance of the interaction of PLEKHA7 with the E-cadherin complex has been characterized by previous studies [5, 8, 81], the specific role of PLEKHA7 at nectin-based complexes was not known. The results presented in this thesis provide new information in this perspective.

The exclusive localization of PLEKHA7 and afadin at the zonular apical region could be relevant for their participation in the molecular linking of the two junctional structures of the apical junctional complex, AJ and TJ. Only when exogenous PLEKHA7 is overexpressed can it localize also to lateral contacts, suggesting a differential affinity of binding for the two complexes. In fact, afadin has been found either at AJ in complex with nectins, or at TJ where it binds JAM, ZO-1 and cingulin [47, 58, 59]. In contrast, , PLEKHA7 binds and recruits paracingulin to AJ, the latter being present also at TJ in association with ZO-1 and cingulin [81]. Thus, PLEKHA7 could further strengthen the linkage provided by the interaction of afadin-ponsin with α-

catenin-vinculin. Our recent findings that PLEKHA7 modulate TJ barrier function, and its association in epithelial cells with the TJ proteins ZO-1 and cingulin strongly support the idea that all the mentioned proteins are part of a molecular framework linking TJ to AJ, with PLEKHA7 having a key role in it. The observation that PLEKHA7, similarly to afadin but unlike p120ctn, is excluded from lateral discontinuous AJ, points to a major role of the afadin-PLEKHA7 interaction in its cellular localization, and possibly function.

Considering the emerging role of PLEKHA7 as an adaptor protein conferring stability to the apical junctional complex, its recent implication in signaling regulating miRNA processing and tumor growth [8], and its implication in human pathologies, like hypertension and glaucoma [9, 11], it is essential to learn more about its molecular interactors to gain more insight in its role in physiological and pathological conditions.

In this perspective, through different approaches, we identified PDZD11 as a novel molecular partner of PLEKHA7. Interestingly, two distinct screening technologies, yeast two-hybrid and mass spectrometry, gave both as top hit PDZD11 among PLEKHA7 interactors, drawing our attention to this relatively unknown new partner as a potentially critical mediator of PLEKHA7 function in epithelial and endothelial cells. PDZD11 is a small (17 kDa) single PDZ domain-containing protein, and litlle information has been published about it so far. PDZD11 is ubiquitously expressed, and is also known as PISP (Plasma membrane Ca-ATPase Interacting Single-PDZ protein) or AIPP1 (ATPase-Interacting PDZ Protein 1), since it was first identified as an interactor of the plasma membrane calcium ATPase b-splice variants (PMCA) and of the menkes copper ATPase (ATP7A), regulating copper homeostasis

[189, 190]. Moreover, it also interacts with the sodium multivitamin transporter (SMVT) regulating biotin uptake [191]. These studies proposed a function for PDZD11 as a scaffold for these transmembrane proteins, by binding, through its class I PDZ domain (Table 1), to the PDZ-binding motif at their C-terminal tail. In agreement with this idea, PDZD11 depletion resulted in a reduced cell surface expression of the sodium-dependent multivitamin transporter, as assessed by cell surface biotinylation assay [191].

PDZ domains are widely expressed protein interaction modules, which are often found in scaffold proteins. In humans more than 150 PDZ domain-containing proteins with more than 250 non-redundant PDZ domain sequences have been identified [192]. Due to their abundance and diversity in the cells of various organisms, together with protein domains like WW, SH3, SH2 and PH, that mediates dynamic protein-protein interactions, they are involved in many cellular and biological functions. The lack of intrinsic catalytic activities in most PDZ proteins suggest a pure scaffolding function in signal transduction complexes assembled through PDZ-mediated interactions. For example, PDZ domain proteins are involved in cell polarity establishment and maintenance, cell migration, cell proliferation and differentiation, embryonic development, through the trafficking and clustering of membrane proteins, receptors and ion channels at specific membrane regions and connecting membrane and cytoskeletal structures [192-197]. A canonical PDZ domain comprises ~90 amino acids, and is organized in six β-strands which form a partially opened barrel, and two α-helices, each capping the opening sides [198, 199]. The binding site of the PDZ domains is located between the α-helix and the β-strand, and comprises the GLGF motif or more in general

XΦGΦ motif (where X is any amino acid and Φ represents hydrophobic amino acids), QLGF in the case of PDZD11. Its conformation is fundamental for the binding specificities of PDZ domains. PDZ domains can bind either another PDZ domain or a PDZ consensus motif localized on the C-terminal tail of target proteins, mainly membrane proteins. The classical classification of PDZ domains is based on the binding preference for different consensus motifs: class I domains recognize the motif S/T-X- Φ; class II domains recognize the motif Φ -X- Φ; class III domains recognize the motif D/E-X- Φ. However, recently the importance for upstream positions within the PDZ ligand has emerged, with the position -3 and -4 from the C-terminus being also important for the binding specificity, leading to the definition of sixteen classes of PDZ domains [192, 200]. PDZD11 so far has been shown to have preference for class I motif, based on the PDZ-consensus motif recognized on the known intercators (Table 1) [189-191]. Additional single PDZ domain proteins exist, with some of them showing high similarity to the PDZ domain of PDZD11, like GOPC, β2-syntrophin and MALS family proteins. These proteins are implicated in the intracellular trafficking or targeting of their molecular partners. MALS binds the polarity complex protein PALS1, thus stabilizing it, and is involved in the regulation of TJ formation [201]. β2-syntrophin is an activator of the Rac GEF Tiam1 at AJ, and is required for correct apico-basal polarization [179]. Future studies should determine if PDZD11 also plays this role, for example by promoting the efficient transport of PDZ-binding proteins to the cell surface.

Table 1. PDZD11 interactors and PDZ consensus motif classes.

Protein	C-terminal residues	Motif class	Reference
PMCA1b	LE**TSL**	classI (S/T-X-Φ)	[189]
PMCA2b	LE**TSL**	classI (S/T-X-Φ)	[189]
PMCA3b	VE**TSL**	classI (S/T-X-Φ)	[189]
PMCA4b	LE**TSV**	classI (S/T-X-Φ)	[189]
ATP7A	DD**TAL**	classI (S/T-X-Φ)	[190]
SMVT	QE**STL**	classI (S/T-X-Φ)	[191]
Nectin-1	KE**WYV**	classII (Φ -X- Φ)	[202]

PDZD11 could mediate several functions for PLEKHA7, connecting it with a variety of membrane or signaling proteins, helping in proteins stabilization or signal transduction. However, PLEKHA7 does not contain either a PDZ domain or a PDZ binding motif that could mediate an interaction with PDZD11. In fact, by biochemical direct in vitro binding assays, not only we confirmed the direct interaction of PLEKHA7 with PDZD11 identified through the two screening technologies, but we also showed that the N-terminal regions of both proteins are implicated in their interaction. Specifically, the first WW domain of PLEKHA7 is sufficient for interaction with PDZD11, whereas the PDZ domain of PDZD11 is not required for PLEKHA7 binding, but it interacts through a short unstructured N-terminal region that does not show any homology to the N-terminal sequences of other single PDZ domain proteins. For this reason, we proposed to call it PLEKHA7 Interacting Domain (P7-ID). The P7-ID may function as an additional module of the PDZ domain, increasing the specificity of interaction of PDZD11 for its target sequences. Indeed, the affinity of binding of a PDZ domain with its target

sequence and its specificity can be modulated by several regulatory mechanisms, among them allosteric interactions and phosphorylation in specific residues of the PDZ domain. Several studies investigated the effect of allostery in PDZ-containing protein, showing that allosteric interactions modulate the binding preferences of PDZ domain [192]. For example, this is the case of NHERF1: ezrin binding to its C-terminal region leads to conformational changes that increase the binding capabilities of both PDZ domain of NHERF1 [203]. Thus, PLEKHA7 interacts with the P7-ID of PDZD11, leaving the PDZ domain free to interact with other molecular partners that could mediate different biological functions for the PLEKHA7-PDZD11 complex. Moreover, PLEKHA7 binding to this region may also modulate the affinity of binding of the PDZ domain of PDZD11 with its target sequences. Future studies should address whether PDZD11 present possible phosphorylation sites and protein kinases consensus motifs in its PDZ domain, that could regulate the binding with molecular partners and possible function of the PLEKHA7-PDZD11 complex.

On the other hand, PLEKHA7 contains in its N-terminal region two WW domains. WW domains are the smallest occurring protein modules and comprise ~40 amino acids; the name comes from the two hallmark tryptophan residues that are typically spaced 20-22 amino acids apart, and are present in most of the known WW domains. WW domains have a compact conformation with three-stranded antiparallel β-sheets, and recognize proline-rich linear sequences. WW domains are very abundant, with more than 200 identified so far in many different proteins implicated in signaling complexes [204]. The binding properties and specificity of WW domains can be modulated by the

presence of tandem WW domains and by tyrosine residue phosphorylation present in the core of WW domain [205, 206]. WW domains are classified based on the ligand predilection among the proline-rich motifs: the class I binds the minimal core consensus PPXY; the class II binds the PPLP motif; the class III prefers poly-proline motifs flanked by arginine or lysine, PP-R/K; the class IV binds short sequences comprising phosphorylated serine or threonine, p-S/T-P [204]. PLEKHA7 contains two class I WW domains each of 33 residues separated by a spacer region of 11 residues; the first is characterized by two signature tryptophan residues, the second by a tryptophan and a phenylananine residue [207] . Notably, the sequence of the P7-ID of PDZD11 comprises eight proline residues, including two proline (PP) residues, but none of them is part of a consensus ligand sequence belonging to any of the four previously described WW-binding motif groups [204]. Additional experiments are required to determine whether the proline motifs of PDZD11 constitute a new group of WW-interacting sequences, and which residues within the WW domain of PLEKHA7 are implicated in its interaction with PDZD11. Interestingly, we showed that the first WW domain of PLEKHA7 alone, but not the second, is sufficient to bind PDZD11. However, in line with previously reported studies suggesting that the presence of WW domains in tandem could influence their binding properties [205, 208], we found that the fragment comprising the two WW domains showed a stronger interaction with PDZD11. This suggests that the presence of the second WW domain in tandem could support the binding capabilities of the first WW domain. Moreover, it is interesting to note that PLEKHA7 presents two proline-rich domains in its C-terminal region, and although the structural conformation of

PLEKHA7 is not known, we cannot exclude that its WW domains and proline-rich regions interact together, promoting a "folded" conformation of PLEKHA7. The binding of PDZD11 to PLEKHA7 could be either inhibited by this self-interaction or promote the open conformation of PLEKHA7, with consequent regulation of activity. In the first case, additional regulation of both proteins would be needed to promote their binding, like phosphorylation within either the proline-rich motifs or the WW domains. Further studies are needed to address these questions, with additional in vitro binding analysis of PLEKHA7 N-terminal and C-terminal fragments, and analysis of the possible phosphorylation sites on both proteins. In summary, we assigned a specific protein-interaction function to the most N-terminal, WW region of PLEKHA7, which so far was never implicated in any protein interaction, and we dissected the structure-function relationships in PDZD11.

Although PDZD11 was reported to bind several transmembrane pumps, its subcellular localization was never clearly established, probably due to the lack of good antibodies against the endogenous protein. To overcome this problem, we developed a rabbit antiserum against PDZD11, using a GST fusion protein of full-length PDZD11, produced in bacterial cells, as an antigen. We could thus show for the first time that both exogenous and endogenous PDZD11 accumulate at junctions, in particular colocalizing with markers of AJ, thus identifying PDZD11 as a novel AJ protein. Moreover, from the analysis of epithelial cells KO for PLEKHA7, and rescued with different fragments of the protein, we showed that PDZD11 is recruited by PLEKHA7 at AJ, and, in accordance with the in vitro binding analysis, the WW domain of PLEKHA7 is required for PDZD11 junctional accumulation. These results

confirm the relevance of the PLEKHA7-PDZD11 interaction, strengthening the idea that PDZD11 could act as a mediator of PLEKHA7 function either in the stabilization of junctional complexes or in the regulation of signaling complexes. Indeed, we showed that PDZD11 can form a complex with nectins in vivo, and also binds in vitro to nectin-1, and this interaction occurs between the PDZ domain of PDZD11 and the PDZ consensus motif present at the C-terminal tail of nectin-1. However, the PDZ domain of PDZD11 has been shown to prefer class I consensus motif so far, whereas nectins contain a class II PDZ consensus motif [209] (Table 1). We could speculate, based on the previously reported allosteric modulation of PDZ domains binding specificities [192], that the binding of PLEKHA7 to the P7-ID of PDZD11 modifies its binding preferences, favoring the binding with the class II consensus motif of nectin-1. Supporting this idea, we showed that PDZD11 is recruited at AJ by PLEKHA7, and only then it can bind nectins, since its junctional accumulation is completely lost upon PLEKHA7 KO. Furthermore, we provided evidence that PDZD11 binding is important for nectins stabilization at junctions by preventing their proteasomal degradation, since PDZD11 KO in epithelial cells results in reduced protein levels and junctional accumulation of nectins. Thus, we discovered a new role for PDZD11 in promoting the efficient recruitment and stabilization of nectins at AJ of epithelial cells. The C-terminal tail of nectins was previously reported to interact with the PDZ domains of several junctional partners, primarily with afadin, which can interact with all the nectins and was shown to be important for the accumulation of nectin-1 at AJ [123, 128]. Depending on nectin isoform, additional scaffolding PDZ-containing interactors of nectins have

been reported, such as Par-3 [125], PATJ, MUPP1 [126], PICK-1 [124], and MPP3 [210]. These observations suggest that redundant interactions can stabilize nectins at junctions [1]. Consistent with this notion, from our observations on epithelial cells KO for PDZD11, we reported that the absence of PDZD11 does not result in the complete loss of junctional nectins. PDZD11 may function not only through direct scaffolding of nectins, but also indirectly; for example, the interaction of PDZD11 with the N-terminal region of PLEKHA7 could affect the conformation of PLEKHA7. Since the N-terminal region of PLEKHA7 interacts also with afadin, PDZD11 could affect PLEKHA7-afadin interaction, and the ability of afadin to form an efficient scaffold for nectins. Consistent with our reported results and this idea, PLEKHA7 KO in epithelial cells phenocopies the effects of PDZD11 KO. Thus, PDZD11 is recruited by PLEKHA7 to AJ, to promote the efficient junctional recruitment and stabilization of nectins in epithelial cells. These results confirm the relevance of the PLEKHA7-PDZD11 interaction and uncover a new function for PLEKHA7: PLEKHA7, through PDZD11, can organize the junctional clustering of PDZ-interacting proteins. Furthermore, the reported results highlight the importance of PLEKHA7 in stabilizing both the major adhesion transmembrane proteins of AJ, cadherins and nectins, through the binding of cytoplasmic components associated with the two complexes: p120catenin/paracingulin for E-cadherin, and PDZD11-afadin, for nectins.

Since we showed that the PLEKHA7-PDZD11 complex promotes the efficient recruitment of nectins to ZA, it is possible to hypothesize that one cellular function of PDZD11 may be related to the biological function of

nectins. In few studies the role of nectins in cultured epithelial cells was investigated. Nectins mutations in the extracellular domain that prevent their trans-interaction affect junction formation in MDCK cells, resulting in a delay in AJ formation [135]. Consistent with the reduction of junctional nectin levels observed in the PDZD11 KO cells, and the fundamental role played by nectins in initiating junction assembly, the KO of PDZD11 resulted in a reduction of the efficiency of assembly of zonular junctions, that was observed only in the very early time points of junction assembly, up to 30 minutes after calcium re-addiction. Junction assembly resumed to normal kinetics at later time points, probably due to the residual nectin molecules, that are not completely lost in PDZD11 KO cells, and the cooperative adhesion functions of E-cadherins, which are not affected by the absence of PDZD11. Thus, the PLEKHA7-PDZD11 complex is important in the regulation of initial steps of junction assembly and in the correct kinetics of this process.

In summary, PLEKHA7 is at center stage in the cytoplasmic complex bridging nectin and E-cadherin complexes. By binding to p120ctn and paracingulin on one side, and to PDZD11 and afadin on the other, PLEKHA7 connects and stabilizes the two major adhesion complexes at ZA, in addition to the previously reported connection provided through the afadin-ponsin complex interacting with the α-catenin-vinculin complex [132]. PLEKHA7 recruitment of PDZD11 to AJ contributes to the recruitment and stabilization of nectins to the ZA. The interaction of PLEKHA7 with both afadin and PDZD11 strengthens the cytoplasmic scaffold provided by these two PDZ proteins for nectins. Finally, thanks to the interaction with the actin cytoskeleton mediated by afadin [86], and with the microtubules through nezha [5], PLEKHA7

reinforces the cytoskeletal anchoring of nectin and cadherin adhesion molecules (Fig. 8).

The PLEKHA7-PDZD11 complex that we characterized defines a new module capable to bring PDZ-binding membrane proteins to the AJ in epithelial and endothelial cells (Fig. 8). This function is extremely important to explore new mechanistic hypotheses to understand at the molecular level the role of PLEKHA7 in tissue physiology and pathology. Recently, in the study conducted with our collaborators, through a genetic screening in haploid cells, PLEKHA7 and other AJ proteins have been implicated in the cytotoxicity of the *Staphylococcus aureus* α-toxin. Interestingly, PDZD11 was also found in this screen, where its KO reduced the cytotoxic effects of the staphylococcal α-toxin, promoting increased cell survival. PLEKHA7 KO cells were more resistant to the effect of the α-toxin, with significantly reduced cell death upon intoxication. Upon intoxication, wild-type cells show high potassium extrusion and drastically decreased intracellular ATP levels; the KO cells initially show the same phenotype but are capable to recover. However, the molecular mechanisms underlying PLEKHA7 involvement in the mechanisms of action of α-toxin are not identified yet. Our new findings that PLEKHA7 form a complex with PDZD11 at AJ are consistent with the data of the genetic screening, and suggest that the complex formation with PDZD11 could be relevant for the mechanism of action of α-toxin. In particular, PDZD11 could mediate the interactions with transmembrane ionic pumps and the regulation of their functions possibly underlies the molecular mechanisms implicated in the cytotoxic effects of α-toxin. Indeed, PDZD11 was previously shown to

interact with the Plasma Membrane Calcium ATPase (PMCA) a key regulator of intracellular calcium homeostasis [189].

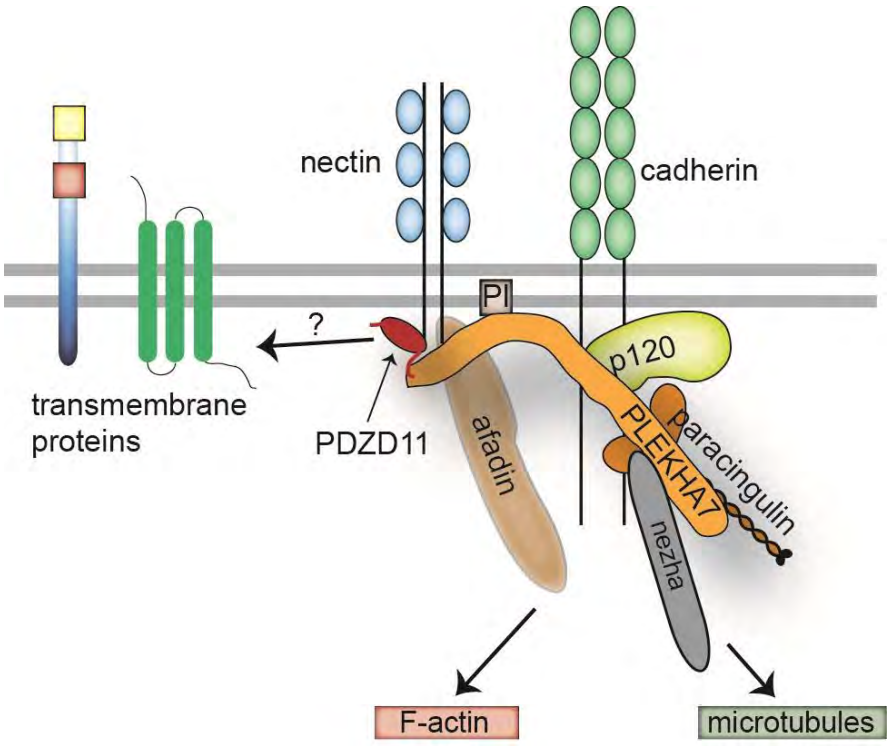

Figure 8. Schematic representation of PLEKHA7 interactions at AJ.
PLEKHA7 interaction with its partners at AJ allow the bridging of the nectin and E-cadherin complexes, stabilizing and connecting the two complexes with the actin and microtubule cytoskeleton**.** PLEKHA7 could recruit and stabilize PDZ-binding transmembrane proteins at AJ.

Genetic studies on zebrafish show that the PLEKHA7 homologue hadp1 is implicated in cardiac development and contractility, since its loss leads to a reduced rate of extrusion of cytoplasmic calcium during diastole [10]. Genome-wide analyses have identified SNPs in PLEKHA7 locus to be associated with high systolic blood pressure and primary angle closure glaucoma [9, 11]. Furthermore, genome-wide data were confirmed in vivo in a PLEKHA7 KO rat model, where the absence of PLEKHA7 reduced the blood pressure and attenuated the salt-induced hypertension. Aortic endothelial cells from PLEKHA7 KO rats showed increased intracellular

calcium levels and synthesis of nitric oxide [168], in agreement with the idea that PLEKHA7 promotes endothelial-mediated smooth muscle relaxation through endothelial nitric oxide synthase (eNOS) signaling [211]. However, the molecular mechanism through which PLEKHA7 may regulate intracellular calcium homeostasis is still completely unknown. Our recent findings lead us to hypothesize a possible mechanism for the PLEKHA7-dependent regulation of intracellular calcium through its molecular partners at AJ. Significantly, we showed that both PDZD11 and PLEKHA7 are localized at endothelial junctions. Thus, it is possible to hypothesize that PLEKHA7 and its partner PDZD11 regulate PMCA and in turn calcium and nitric oxide (NO) signaling in endothelial cells. The PLEKHA7-PDZD11 complex could be involved in the accumulation, stabilization and junctional clustering of PMCA and/or in the direct or indirect regulation of its function and in turn of NO production and signaling in endothelial cells, with systemic effects on blood pressure regulation. Future studies are needed in this direction to assess whether PLEKHA7 regulates PMCA, and hence calcium homeostasis, through PDZD11, to clarify mechanistically its role in the regulation of blood pressure, cardiac contractility, and glaucoma. Alternatively, PLEKHA7-PDZD11 complex could bind and regulate several others transmembrane proteins and receptors involved in calcium and NO signaling. For example, 20% of known human G protein coupled receptors (GPCRs) contain a PDZ-binding motif [192]. GPCRs are involved in calcium signaling; upon agonists binding they promote the activation of phospholipase C (PLC) and formation of IP_3, promoting calcium signaling [211]. Furthermore, shear stress can directly activate eNOS and NO production independently of calcium signaling, through

phosphorylation mediated by PI3K-AKT pathway [212]. PLEKHA7 can bind, through its PH domain, different types of phosphorylated phosphatidylinositols, including PIP_2 [10]. In this manner, PLEKHA7 could prevent PKC-mediated conversion of PIP_2 in PIP_3 and the subsequent activation of the AKT pathway. Finally, a similar mechanism could be involved in the regulation of calcium signaling. By binding to PIP_2, PLEKHA7 could prevent its PLC-mediated conversion in IP_3 and DAG that activate calcium signaling, leading to an increased calcium response in the absence of PLEKHA7.

In summary, we described a new protein complex, where the single PDZ domain protein PDZD11, through the binding to PLEKHA7, connects nectins to the cadherin complex and the cytoskeleton. This complex formation is relevant for the stabilization of nectins at AJ and to promote efficient early assembly of junctions. These results also point to a role for PLEKHA7 in regulating the function and membrane organization of proteins involved in calcium homeostasis, through PDZD11, providing new insight in the potential molecular mechanism that could explain PLEKHA7 implication in vascular and cardiac pathophysiology.

REFERENCES

1. Rikitake, Y., K. Mandai, and Y. Takai, *The role of nectins in different types of cell-cell adhesion.* J Cell Sci, 2012. **125**(Pt 16): p. 3713-22.
2. Takai, Y., et al., *Nectins and nectin-like molecules: roles in contact inhibition of cell movement and proliferation.* Nat Rev Mol Cell Biol, 2008. **9**(8): p. 603-15.
3. Guttman, J.A. and B.B. Finlay, *Tight junctions as targets of infectious agents.* Biochim Biophys Acta, 2009. **1788**(4): p. 832-41.
4. Guillemot, L., et al., *The cytoplasmic plaque of tight junctions: a scaffolding and signalling center.* Biochim Biophys Acta, 2008. **1778**(3): p. 601-13.
5. Meng, W., et al., *Anchorage of microtubule minus ends to adherens junctions regulates epithelial cell-cell contacts.* Cell, 2008. **135**(5): p. 948-59.
6. Pulimeno, P., et al., *PLEKHA7 is an adherens junction protein with a tissue distribution and subcellular localization distinct from ZO-1 and E-cadherin.* PLoS One, 2010. **5**(8): p. e12207.
7. Kurita, S., et al., *Binding between the junctional proteins afadin and PLEKHA7 and implication in the formation of adherens junction in epithelial cells.* J Biol Chem, 2013. **288**(41): p. 29356-68.
8. Kourtidis, A., et al., *Distinct E-cadherin-based complexes regulate cell behaviour through miRNA processing or Src and p120 catenin activity.* Nat Cell Biol, 2015. **17**(9): p. 1145-57.

9. Levy, D., et al., *Genome-wide association study of blood pressure and hypertension.* Nat Genet, 2009. **41**(6): p. 677-87.

10. Wythe, J.D., et al., *Hadp1, a newly identified pleckstrin homology domain protein, is required for cardiac contractility in zebrafish.* Dis Model Mech, 2011. **4**(5): p. 607-21.

11. Vithana, E.N., et al., *Genome-wide association analyses identify three new susceptibility loci for primary angle closure glaucoma.* Nat Genet, 2012. **44**(10): p. 1142-6.

12. Satir, P. and N.B. Gilula, *THE CELL JUNCTION IN A LAMELLIBRANCH GILL CILIATED EPITHELIUM : Localization of Pyroantimonate Precipitate.* J Cell Biol, 1970. **47**(2): p. 468-87.

13. Farquhar, M.G. and G.E. Palade, *Junctional complexes in various epithelia.* J Cell Biol, 1963. **17**: p. 375-412.

14. Hartsock, A. and W.J. Nelson, *Adherens and tight junctions: structure, function and connections to the actin cytoskeleton.* Biochim Biophys Acta, 2008. **1778**(3): p. 660-9.

15. Wang, Q. and B. Margolis, *Apical junctional complexes and cell polarity.* Kidney Int, 2007. **72**(12): p. 1448-58.

16. Diamond, J.M., *Twenty-first Bowditch lecture. The epithelial junction: bridge, gate, and fence.* Physiologist, 1977. **20**(1): p. 10-8.

17. Citi, S., et al., *Epithelial junctions and Rho family GTPases: the zonular signalosome.* Small GTPases, 2014. **5**(4): p. 1-15.

18. Meng, W. and M. Takeichi, *Adherens junction: molecular architecture and regulation.* Cold Spring Harb Perspect Biol, 2009. **1**(6): p. a002899.

19. Diamond, J.M., *Channels in epithelial cell membranes and junctions.* Fed Proc, 1978. **37**(12): p. 2639-43.

20. Powell, D.W., *Barrier function of epithelia.* Am J Physiol, 1981. **241**(4): p. G275-88.

21. Anderson, J.M. and C.M. Van Itallie, *Physiology and function of the tight junction.* Cold Spring Harb Perspect Biol, 2009. **1**(2): p. a002584.

22. Vogelmann, R., et al., *Breaking into the epithelial apical-junctional complex--news from pathogen hackers.* Curr Opin Cell Biol, 2004. **16**(1): p. 86-93.

23. Oka, T., et al., *Functional complexes between YAP2 and ZO-2 are PDZ domain-dependent, and regulate YAP2 nuclear localization and signalling.* Biochem J, 2010. **432**(3): p. 461-72.

24. Spadaro, D., et al., *ZO proteins redundantly regulate the transcription factor DbpA/ZONAB.* J Biol Chem, 2014. **289**(32): p. 22500-11.

25. Zhao, B., et al., *Angiomotin is a novel Hippo pathway component that inhibits YAP oncoprotein.* Genes Dev, 2011. **25**(1): p. 51-63.

26. Guillemot, L. and S. Citi, *Cingulin regulates claudin-2 expression and cell proliferation through the small GTPase RhoA.* Mol Biol Cell, 2006. **17**(8): p. 3569-77.

27. Guillemot, L., et al., *Paracingulin regulates the activity of Rac1 and RhoA GTPases by recruiting Tiam1 and GEF-H1 to epithelial junctions.* Mol Biol Cell, 2008. **19**(10): p. 4442-53.

28. Furuse, M., *Molecular basis of the core structure of tight junctions.* Cold Spring Harb Perspect Biol, 2010. **2**(1): p. a002907.

29. Furuse, M., et al., *Occludin: a novel integral membrane protein localizing at tight junctions.* J Cell Biol, 1993. **123**(6 Pt 2): p. 1777-88.

30. Sakakibara, A., et al., *Possible involvement of phosphorylation of occludin in tight junction formation.* J Cell Biol, 1997. **137**(6): p. 1393-401.

31. Wong, V., *Phosphorylation of occludin correlates with occludin localization and function at the tight junction.* Am J Physiol, 1997. **273**(6 Pt 1): p. C1859-67.

32. Furuse, M., et al., *Direct association of occludin with ZO-1 and its possible involvement in the localization of occludin at tight junctions.* J Cell Biol, 1994. **127**(6 Pt 1): p. 1617-26.

33. Wittchen, E.S., J. Haskins, and B.R. Stevenson, *Protein interactions at the tight junction. Actin has multiple binding partners, and ZO-1 forms independent complexes with ZO-2 and ZO-3.* J Biol Chem, 1999. **274**(49): p. 35179-85.

34. Furuse, M., et al., *A single gene product, claudin-1 or -2, reconstitutes tight junction strands and recruits occludin in fibroblasts.* J Cell Biol, 1998. **143**(2): p. 391-401.

35. Wong, V. and B.M. Gumbiner, *A synthetic peptide corresponding to the extracellular domain of occludin perturbs the tight junction permeability barrier.* J Cell Biol, 1997. **136**(2): p. 399-409.

36. Saitou, M., et al., *Occludin-deficient embryonic stem cells can differentiate into polarized epithelial cells bearing tight junctions.* J Cell Biol, 1998. **141**(2): p. 397-408.

37. Saitou, M., et al., *Complex phenotype of mice lacking occludin, a component of tight junction strands.* Mol Biol Cell, 2000. **11**(12): p. 4131-42.

38. Furuse, M., et al., *Claudin-1 and -2: novel integral membrane proteins localizing at tight junctions with no sequence similarity to occludin.* J Cell Biol, 1998. **141**(7): p. 1539-50.

39. Tsukita, S., M. Furuse, and M. Itoh, *Multifunctional strands in tight junctions.* Nat Rev Mol Cell Biol, 2001. **2**(4): p. 285-93.

40. Hamazaki, Y., et al., *Multi-PDZ domain protein 1 (MUPP1) is concentrated at tight junctions through its possible interaction with claudin-1 and junctional adhesion molecule.* J Biol Chem, 2002. **277**(1): p. 455-61.

41. Itoh, M., et al., *Direct binding of three tight junction-associated MAGUKs, ZO-1, ZO-2, and ZO-3, with the COOH termini of claudins.* J Cell Biol, 1999. **147**(6): p. 1351-63.

42. Roh, M.H., et al., *The carboxyl terminus of zona occludens-3 binds and recruits a mammalian homologue of discs lost to tight junctions.* J Biol Chem, 2002. **277**(30): p. 27501-9.

43. Furuse, M., H. Sasaki, and S. Tsukita, *Manner of interaction of heterogeneous claudin species within and between tight junction strands.* J Cell Biol, 1999. **147**(4): p. 891-903.

44. Furuse, M., et al., *Claudin-based tight junctions are crucial for the mammalian epidermal barrier: a lesson from claudin-1-deficient mice.* J Cell Biol, 2002. **156**(6): p. 1099-111.

45. Escudero-Esparza, A., W.G. Jiang, and T.A. Martin, *The Claudin family and its role in cancer and metastasis.* Front Biosci (Landmark Ed), 2011. **16**: p. 1069-83.

46. Bazzoni, G., et al., *Interaction of junctional adhesion molecule with the tight junction components ZO-1, cingulin, and occludin.* J Biol Chem, 2000. **275**(27): p. 20520-6.

47. Ebnet, K., et al., *Junctional adhesion molecule interacts with the PDZ domain-containing proteins AF-6 and ZO-1.* J Biol Chem, 2000. **275**(36): p. 27979-88.

48. Itoh, M., et al., *Junctional adhesion molecule (JAM) binds to PAR-3: a possible mechanism for the recruitment of PAR-3 to tight junctions.* J Cell Biol, 2001. **154**(3): p. 491-7.

49. Cohen, C.J., et al., *The coxsackievirus and adenovirus receptor is a transmembrane component of the tight junction.* Proc Natl Acad Sci U S A, 2001. **98**(26): p. 15191-6.

50. Liu, Y., et al., *Human junction adhesion molecule regulates tight junction resealing in epithelia.* J Cell Sci, 2000. **113 (Pt 13)**: p. 2363-74.

51. Fanning, A.S. and J.M. Anderson, *Zonula occludens-1 and -2 are cytosolic scaffolds that regulate the assembly of cellular junctions.* Ann N Y Acad Sci, 2009. **1165**: p. 113-20.

52. Stevenson, B.R., et al., *Identification of ZO-1: a high molecular weight polypeptide associated with the tight junction (zonula occludens) in a variety of epithelia.* J Cell Biol, 1986. **103**(3): p. 755-66.

53. Balda, M.S., et al., *Assembly of the tight junction: the role of diacylglycerol.* J Cell Biol, 1993. **123**(2): p. 293-302.

54. Gumbiner, B., T. Lowenkopf, and D. Apatira, *Identification of a 160-kDa polypeptide that binds to the tight junction protein ZO-1.* Proc Natl Acad Sci U S A, 1991. **88**(8): p. 3460-4.

55. Utepbergenov, D.I., A.S. Fanning, and J.M. Anderson, *Dimerization of the scaffolding protein ZO-1 through the second PDZ domain.* J Biol Chem, 2006. **281**(34): p. 24671-7.

56. Umeda, K., et al., *ZO-1 and ZO-2 independently determine where claudins are polymerized in tight-junction strand formation.* Cell, 2006. **126**(4): p. 741-54.

57. Adachi, M., et al., *Normal establishment of epithelial tight junctions in mice and cultured cells lacking expression of ZO-3, a tight-junction MAGUK protein.* Mol Cell Biol, 2006. **26**(23): p. 9003-15.

58. Cordenonsi, M., et al., *Cingulin contains globular and coiled-coil domains and interacts with ZO-1, ZO-2, ZO-3, and myosin.* J Cell Biol, 1999. **147**(7): p. 1569-82.

59. Yamamoto, T., et al., *The Ras target AF-6 interacts with ZO-1 and serves as a peripheral component of tight junctions in epithelial cells.* J Cell Biol, 1997. **139**(3): p. 785-95.

60. Yokoyama, S., et al., *alpha-catenin-independent recruitment of ZO-1 to nectin-based cell-cell adhesion sites through afadin.* Mol Biol Cell, 2001. **12**(6): p. 1595-609.

61. Fanning, A.S., et al., *The tight junction protein ZO-1 establishes a link between the transmembrane protein occludin and the actin cytoskeleton.* J Biol Chem, 1998. **273**(45): p. 29745-53.

62. Katsuno, T., et al., *Deficiency of zonula occludens-1 causes embryonic lethal phenotype associated with defected yolk sac angiogenesis and apoptosis of embryonic cells.* Mol Biol Cell, 2008. **19**(6): p. 2465-75.

63. Xu, J., et al., *Early embryonic lethality of mice lacking ZO-2, but Not ZO-3, reveals critical and nonredundant roles for individual zonula occludens proteins in mammalian development.* Mol Cell Biol, 2008. **28**(5): p. 1669-78.

64. Assemat, E., et al., *Polarity complex proteins.* Biochim Biophys Acta, 2008. **1778**(3): p. 614-30.

65. Izumi, Y., et al., *An atypical PKC directly associates and colocalizes at the epithelial tight junction with ASIP, a mammalian homologue of Caenorhabditis elegans polarity protein PAR-3.* J Cell Biol, 1998. **143**(1): p. 95-106.

66. Johansson, A., M. Driessens, and P. Aspenstrom, *The mammalian homologue of the Caenorhabditis elegans polarity protein PAR-6 is a binding partner for the Rho GTPases Cdc42 and Rac1.* J Cell Sci, 2000. **113 (Pt 18)**: p. 3267-75.

67. Chen, X. and I.G. Macara, *Par-3 controls tight junction assembly through the Rac exchange factor Tiam1.* Nat Cell Biol, 2005. **7**(3): p. 262-9.

68. Michel, D., et al., *PATJ connects and stabilizes apical and lateral components of tight junctions in human intestinal cells.* J Cell Sci, 2005. **118**(Pt 17): p. 4049-57.

69. Citi, S., et al., *Cingulin, a new peripheral component of tight junctions.* Nature, 1988. **333**(6170): p. 272-6.

70. D'Atri, F. and S. Citi, *Cingulin interacts with F-actin in vitro.* FEBS Lett, 2001. **507**(1): p. 21-4.

71. Yano, T., et al., *The association of microtubules with tight junctions is promoted by cingulin phosphorylation by AMPK.* J Cell Biol, 2013. **203**(4): p. 605-14.

72. D'Atri, F., F. Nadalutti, and S. Citi, *Evidence for a functional interaction between cingulin and ZO-1 in cultured cells.* J Biol Chem, 2002. **277**(31): p. 27757-64.

73. Umeda, K., et al., *Establishment and characterization of cultured epithelial cells lacking expression of ZO-1.* J Biol Chem, 2004. **279**(43): p. 44785-94.

74. Guillemot, L., et al., *Disruption of the cingulin gene does not prevent tight junction formation but alters gene expression.* J Cell Sci, 2004. **117**(Pt 22): p. 5245-56.

75. Aijaz, S., et al., *Binding of GEF-H1 to the tight junction-associated adaptor cingulin results in inhibition of Rho signaling and G1/S phase transition.* Dev Cell, 2005. **8**(5): p. 777-86.

76. Guillemot, L., et al., *Cingulin is dispensable for epithelial barrier function and tight junction structure, and plays a role in the control of*

claudin-2 expression and response to duodenal mucosa injury. Journal of Cell Science, 2012. **125**(21): p. 5005-5014.

77. Terry, S.J., et al., *Spatially restricted activation of RhoA signalling at epithelial junctions by p114RhoGEF drives junction formation and morphogenesis.* Nat Cell Biol, 2011. **13**(2): p. 159-66.

78. Schossleitner, K., et al., *Evidence That Cingulin Regulates Endothelial Barrier Function In Vitro and In Vivo.* Arterioscler Thromb Vasc Biol, 2016. **36**(4): p. 647-54.

79. Ohnishi, H., et al., *JACOP, a novel plaque protein localizing at the apical junctional complex with sequence similarity to cingulin.* J Biol Chem, 2004. **279**(44): p. 46014-22.

80. Paschoud, S., et al., *Cingulin and paracingulin show similar dynamic behaviour, but are recruited independently to junctions.* Mol Membr Biol, 2011. **28**(2): p. 123-35.

81. Pulimeno, P., S. Paschoud, and S. Citi, *A role for ZO-1 and PLEKHA7 in recruiting paracingulin to tight and adherens junctions of epithelial cells.* J Biol Chem, 2011. **286**(19): p. 16743-50.

82. Miyaguchi, K., *Ultrastructure of the zonula adherens revealed by rapid-freeze deep-etching.* J Struct Biol, 2000. **132**(3): p. 169-78.

83. Franke, W.W., H.P. Kapprell, and P. Cowin, *Immunolocalization of plakoglobin in endothelial junctions: identification as a special type of Zonulae adhaerentes.* Biol Cell, 1987. **59**(3): p. 205-18.

84. Yonemura, S., et al., *Cell-to-cell adherens junction formation and actin filament organization: similarities and differences between non-*

polarized fibroblasts and polarized epithelial cells. J Cell Sci, 1995. **108 (Pt 1)**: p. 127-42.

85. Rimm, D.L., et al., *Alpha 1(E)-catenin is an actin-binding and -bundling protein mediating the attachment of F-actin to the membrane adhesion complex.* Proc Natl Acad Sci U S A, 1995. **92**(19): p. 8813-7.
86. Mandai, K., et al., *Afadin: A novel actin filament-binding protein with one PDZ domain localized at cadherin-based cell-to-cell adherens junction.* J Cell Biol, 1997. **139**(2): p. 517-28.
87. Watabe-Uchida, M., et al., *alpha-Catenin-vinculin interaction functions to organize the apical junctional complex in epithelial cells.* J Cell Biol, 1998. **142**(3): p. 847-57.
88. Maul, R.S., et al., *EPLIN regulates actin dynamics by cross-linking and stabilizing filaments.* J Cell Biol, 2003. **160**(3): p. 399-407.
89. Holmes, G.R., D.E. Goll, and A. Suzuki, *Effect of -actinin on actin viscosity.* Biochim Biophys Acta, 1971. **253**(1): p. 240-53.
90. Takeichi, M., *Dynamic contacts: rearranging adherens junctions to drive epithelial remodelling.* Nat Rev Mol Cell Biol, 2014. **15**(6): p. 397-410.
91. Ligon, L.A., et al., *Dynein binds to beta-catenin and may tether microtubules at adherens junctions.* Nat Cell Biol, 2001. **3**(10): p. 913-7.
92. Klezovitch, O. and V. Vasioukhin, *Cadherin signaling: keeping cells in touch.* F1000Res, 2015. **4**(F1000 Faculty Rev): p. 550.

93. McCrea, P.D., D. Gu, and M.S. Balda, *Junctional music that the nucleus hears: cell-cell contact signaling and the modulation of gene activity.* Cold Spring Harb Perspect Biol, 2009. **1**(4): p. a002923.

94. Silvis, M.R., et al., *alpha-catenin is a tumor suppressor that controls cell accumulation by regulating the localization and activity of the transcriptional coactivator Yap1.* Sci Signal, 2011. **4**(174): p. ra33.

95. Giampietro, C., et al., *The actin-binding protein EPS8 binds VE-cadherin and modulates YAP localization and signaling.* J Cell Biol, 2015. **211**(6): p. 1177-92.

96. Takeichi, M., *The cadherins: cell-cell adhesion molecules controlling animal morphogenesis.* Development, 1988. **102**(4): p. 639-55.

97. Yoshida, C. and M. Takeichi, *Teratocarcinoma cell adhesion: identification of a cell-surface protein involved in calcium-dependent cell aggregation.* Cell, 1982. **28**(2): p. 217-24.

98. Pokutta, S., et al., *Conformational changes of the recombinant extracellular domain of E-cadherin upon calcium binding.* Eur J Biochem, 1994. **223**(3): p. 1019-26.

99. Takeda, H., et al., *E-cadherin functions as a cis-dimer at the cell-cell adhesive interface in vivo.* Nat Struct Biol, 1999. **6**(4): p. 310-2.

100. Yap, A.S., et al., *Lateral clustering of the adhesive ectodomain: a fundamental determinant of cadherin function.* Curr Biol, 1997. **7**(5): p. 308-15.

101. Buxton, R.S. and A.I. Magee, *Structure and interactions of desmosomal and other cadherins.* Semin Cell Biol, 1992. **3**(3): p. 157-67.

102. Wheeler, G.N., et al., *Desmosomal glycoproteins I, II and III: novel members of the cadherin superfamily.* Biochem Soc Trans, 1991. **19**(4): p. 1060-4.

103. Aberle, H., et al., *Assembly of the cadherin-catenin complex in vitro with recombinant proteins.* J Cell Sci, 1994. **107 (Pt 12)**: p. 3655-63.

104. McCrea, P.D., C.W. Turck, and B. Gumbiner, *A homolog of the armadillo protein in Drosophila (plakoglobin) associated with E-cadherin.* Science, 1991. **254**(5036): p. 1359-61.

105. Yap, A.S., C.M. Niessen, and B.M. Gumbiner, *The juxtamembrane region of the cadherin cytoplasmic tail supports lateral clustering, adhesive strengthening, and interaction with p120ctn.* J Cell Biol, 1998. **141**(3): p. 779-89.

106. Fujita, Y., et al., *Hakai, a c-Cbl-like protein, ubiquitinates and induces endocytosis of the E-cadherin complex.* Nat Cell Biol, 2002. **4**(3): p. 222-31.

107. Miyashita, Y. and M. Ozawa, *Increased internalization of p120-uncoupled E-cadherin and a requirement for a dileucine motif in the cytoplasmic domain for endocytosis of the protein.* J Biol Chem, 2007. **282**(15): p. 11540-8.

108. Troyanovsky, R.B., E.P. Sokolov, and S.M. Troyanovsky, *Endocytosis of cadherin from intracellular junctions is the driving force for cadherin adhesive dimer disassembly.* Mol Biol Cell, 2006. **17**(8): p. 3484-93.

109. Sako-Kubota, K., et al., *Minus end-directed motor KIFC3 suppresses E-cadherin degradation by recruiting USP47 to adherens junctions.* Mol Biol Cell, 2014. **25**(24): p. 3851-60.

110. McEwen, A.E., et al., *E-cadherin phosphorylation occurs during its biosynthesis to promote its cell surface stability and adhesion.* Mol Biol Cell, 2014. **25**(16): p. 2365-74.

111. Maiden, S.L., et al., *Specific conserved C-terminal amino acids of Caenorhabditis elegans HMP-1/alpha-catenin modulate F-actin binding independently of vinculin.* J Biol Chem, 2013. **288**(8): p. 5694-706.

112. Orsulic, S., et al., *E-cadherin binding prevents beta-catenin nuclear localization and beta-catenin/LEF-1-mediated transactivation.* J Cell Sci, 1999. **112 (Pt 8)**: p. 1237-45.

113. Capaldo, C.T. and I.G. Macara, *Depletion of E-cadherin disrupts establishment but not maintenance of cell junctions in Madin-Darby canine kidney epithelial cells.* Mol Biol Cell, 2007. **18**(1): p. 189-200.

114. Larue, L., et al., *E-cadherin null mutant embryos fail to form a trophectoderm epithelium.* Proc Natl Acad Sci U S A, 1994. **91**(17): p. 8263-7.

115. Tinkle, C.L., et al., *Conditional targeting of E-cadherin in skin: insights into hyperproliferative and degenerative responses.* Proc Natl Acad Sci U S A, 2004. **101**(2): p. 552-7.

116. Tunggal, J.A., et al., *E-cadherin is essential for in vivo epidermal barrier function by regulating tight junctions.* EMBO J, 2005. **24**(6): p. 1146-56.

117. Schneider, M.R. and F.T. Kolligs, *E-cadherin's role in development, tissue homeostasis and disease: Insights from mouse models: Tissue-specific inactivation of the adhesion protein E-cadherin in mice reveals its functions in health and disease.* Bioessays, 2015. **37**(3): p. 294-304.

118. Takai, Y., et al., *The immunoglobulin-like cell adhesion molecule nectin and its associated protein afadin.* Annu Rev Cell Dev Biol, 2008. **24**: p. 309-42.

119. Eberle, F., et al., *The human PRR2 gene, related to the human poliovirus receptor gene (PVR), is the true homolog of the murine MPH gene.* Gene, 1995. **159**(2): p. 267-72.

120. Morrison, M.E. and V.R. Racaniello, *Molecular cloning and expression of a murine homolog of the human poliovirus receptor gene.* J Virol, 1992. **66**(5): p. 2807-13.

121. Mandai, K., et al., *Nectins and nectin-like molecules in development and disease.* Curr Top Dev Biol, 2015. **112**: p. 197-231.

122. Samanta, D. and S.C. Almo, *Nectin family of cell-adhesion molecules: structural and molecular aspects of function and specificity.* Cell Mol Life Sci, 2015. **72**(4): p. 645-58.

123. Takahashi, K., et al., *Nectin/PRR: an immunoglobulin-like cell adhesion molecule recruited to cadherin-based adherens junctions through interaction with Afadin, a PDZ domain-containing protein.* J Cell Biol, 1999. **145**(3): p. 539-49.

124. Reymond, N., et al., *PICK-1: a scaffold protein that interacts with Nectins and JAMs at cell junctions.* FEBS Lett, 2005. **579**(10): p. 2243-9.

125. Takekuni, K., et al., *Direct binding of cell polarity protein PAR-3 to cell-cell adhesion molecule nectin at neuroepithelial cells of developing mouse.* J Biol Chem, 2003. **278**(8): p. 5497-500.

126. Adachi, M., et al., *Similar and distinct properties of MUPP1 and Patj, two homologous PDZ domain-containing tight-junction proteins.* Mol Cell Biol, 2009. **29**(9): p. 2372-89.

127. Call, G.S., et al., *Zyxin phosphorylation at serine 142 modulates the zyxin head-tail interaction to alter cell-cell adhesion.* Biochem Biophys Res Commun, 2011. **404**(3): p. 780-4.

128. Ishiuchi, T. and M. Takeichi, *Nectins localize Willin to cell-cell junctions.* Genes Cells, 2012. **17**(5): p. 387-97.

129. Miyahara, M., et al., *Interaction of nectin with afadin is necessary for its clustering at cell-cell contact sites but not for its cis dimerization or trans interaction.* J Biol Chem, 2000. **275**(1): p. 613-8.

130. Tachibana, K., et al., *Two cell adhesion molecules, nectin and cadherin, interact through their cytoplasmic domain-associated proteins.* J Cell Biol, 2000. **150**(5): p. 1161-76.

131. Asakura, T., et al., *Similar and differential behaviour between the nectin-afadin-ponsin and cadherin-catenin systems during the formation and disruption of the polarized junctional alignment in epithelial cells.* Genes Cells, 1999. **4**(10): p. 573-81.

132. Mandai, K., et al., *Ponsin/SH3P12: an l-afadin- and vinculin-binding protein localized at cell-cell and cell-matrix adherens junctions.* J Cell Biol, 1999. **144**(5): p. 1001-17.

133. Fukuhara, A., et al., *Involvement of nectin in the localization of junctional adhesion molecule at tight junctions.* Oncogene, 2002. **21**(50): p. 7642-55.

134. Fukuhara, A., et al., *Role of nectin in organization of tight junctions in epithelial cells.* Genes Cells, 2002. **7**(10): p. 1059-72.

135. Hoshino, T., et al., *A novel role of nectins in inhibition of the E-cadherin-induced activation of Rac and formation of cell-cell adherens junctions.* Mol Biol Cell, 2004. **15**(3): p. 1077-88.

136. Inagaki, M., et al., *Role of cell adhesion molecule nectin-3 in spermatid development.* Genes Cells, 2006. **11**(9): p. 1125-32.

137. Inagaki, M., et al., *Roles of cell-adhesion molecules nectin 1 and nectin 3 in ciliary body development.* Development, 2005. **132**(7): p. 1525-37.

138. Togashi, H., et al., *Nectins establish a checkerboard-like cellular pattern in the auditory epithelium.* Science, 2011. **333**(6046): p. 1144-7.

139. Drees, F., et al., *Alpha-catenin is a molecular switch that binds E-cadherin-beta-catenin and regulates actin-filament assembly.* Cell, 2005. **123**(5): p. 903-15.

140. Scott, J.A. and A.S. Yap, *Cinderella no longer: alpha-catenin steps out of cadherin's shadow.* J Cell Sci, 2006. **119**(Pt 22): p. 4599-605.

141. Torres, M., et al., *An alpha-E-catenin gene trap mutation defines its function in preimplantation development.* Proc Natl Acad Sci U S A, 1997. **94**(3): p. 901-6.

142. Vasioukhin, V., et al., *Hyperproliferation and defects in epithelial polarity upon conditional ablation of alpha-catenin in skin.* Cell, 2001. **104**(4): p. 605-17.

143. Behrens, J., et al., *Functional interaction of beta-catenin with the transcription factor LEF-1.* Nature, 1996. **382**(6592): p. 638-42.

144. Orford, K., et al., *Serine phosphorylation-regulated ubiquitination and degradation of beta-catenin.* J Biol Chem, 1997. **272**(40): p. 24735-8.

145. Klaus, A. and W. Birchmeier, *Wnt signalling and its impact on development and cancer.* Nat Rev Cancer, 2008. **8**(5): p. 387-98.

146. Chen, Y.T., D.B. Stewart, and W.J. Nelson, *Coupling assembly of the E-cadherin/beta-catenin complex to efficient endoplasmic reticulum exit and basal-lateral membrane targeting of E-cadherin in polarized MDCK cells.* J Cell Biol, 1999. **144**(4): p. 687-99.

147. Miyashita, Y. and M. Ozawa, *A dileucine motif in its cytoplasmic domain directs beta-catenin-uncoupled E-cadherin to the lysosome.* J Cell Sci, 2007. **120**(Pt 24): p. 4395-406.

148. Stepniak, E., G.L. Radice, and V. Vasioukhin, *Adhesive and signaling functions of cadherins and catenins in vertebrate development.* Cold Spring Harb Perspect Biol, 2009. **1**(5): p. a002949.

149. Reynolds, A.B., et al., *Identification of a new catenin: the tyrosine kinase substrate p120cas associates with E-cadherin complexes.* Mol Cell Biol, 1994. **14**(12): p. 8333-42.

150. Kinch, M.S., et al., *Tyrosine phosphorylation regulates the adhesions of ras-transformed breast epithelia.* J Cell Biol, 1995. **130**(2): p. 461-71.

151. Davis, M.A., R.C. Ireton, and A.B. Reynolds, *A core function for p120-catenin in cadherin turnover.* J Cell Biol, 2003. **163**(3): p. 525-34.

152. Ishiyama, N., et al., *Dynamic and static interactions between p120 catenin and E-cadherin regulate the stability of cell-cell adhesion.* Cell, 2010. **141**(1): p. 117-28.

153. Anastasiadis, P.Z., et al., *Inhibition of RhoA by p120 catenin.* Nat Cell Biol, 2000. **2**(9): p. 637-44.

154. Wildenberg, G.A., et al., *p120-catenin and p190RhoGAP regulate cell-cell adhesion by coordinating antagonism between Rac and Rho.* Cell, 2006. **127**(5): p. 1027-39.

155. Yu, H.H., et al., *p120-catenin controls contractility along the vertical axis of epithelial lateral membranes.* J Cell Sci, 2016. **129**(1): p. 80-94.

156. Kelly, K.F., et al., *NLS-dependent nuclear localization of p120(ctn) is necessary to relieve Kaiso-mediated transcriptional repression. (vol 117, pg 2675, 2004).* Journal of Cell Science, 2004. **117**(15): p. 3405-3405.

157. Kourtidis, A., et al., *Pro-Tumorigenic Phosphorylation of p120 Catenin in Renal and Breast Cancer.* PLoS One, 2015. **10**(6): p. e0129964.

158. Davis, M.A. and A.B. Reynolds, *Blocked acinar development, E-cadherin reduction, and intraepithelial neoplasia upon ablation of p120-catenin in the mouse salivary gland.* Dev Cell, 2006. **10**(1): p. 21-31.

159. Perez-Moreno, M., et al., *p120-catenin mediates inflammatory responses in the skin.* Cell, 2006. **124**(3): p. 631-44.

160. Smalley-Freed, W.G., et al., *p120-catenin is essential for maintenance of barrier function and intestinal homeostasis in mice.* J Clin Invest, 2010. **120**(6): p. 1824-35.

161. Radziwill, G., et al., *Regulation of c-Src by binding to the PDZ domain of AF-6.* EMBO J, 2007. **26**(11): p. 2633-44.

162. Boettner, B., et al., *The junctional multidomain protein AF-6 is a binding partner of the Rap1A GTPase and associates with the actin*

cytoskeletal regulator profilin. Proc Natl Acad Sci U S A, 2000. **97**(16): p. 9064-9.

163. Ooshio, T., et al., *Involvement of LMO7 in the association of two cell-cell adhesion molecules, nectin and E-cadherin, through afadin and alpha-actinin in epithelial cells.* J Biol Chem, 2004. **279**(30): p. 31365-73.

164. Sato, T., et al., *Regulation of the assembly and adhesion activity of E-cadherin by nectin and afadin for the formation of adherens junctions in Madin-Darby canine kidney cells.* J Biol Chem, 2006. **281**(8): p. 5288-99.

165. Ikeda, W., et al., *Afadin: A key molecule essential for structural organization of cell-cell junctions of polarized epithelia during embryogenesis.* J Cell Biol, 1999. **146**(5): p. 1117-32.

166. Komura, H., et al., *Establishment of cell polarity by afadin during the formation of embryoid bodies.* Genes Cells, 2008. **13**(1): p. 79-90.

167. Tille, J.C., et al., *The Expression of the Zonula Adhaerens Protein PLEKHA7 Is Strongly Decreased in High Grade Ductal and Lobular Breast Carcinomas.* PLoS One, 2015. **10**(8): p. e0135442.

168. Endres, B.T., et al., *Mutation of Plekha7 attenuates salt-sensitive hypertension in the rat.* Proc Natl Acad Sci U S A, 2014. **111**(35): p. 12817-22.

169. Nusrat, A., et al., *Rho protein regulates tight junctions and perijunctional actin organization in polarized epithelia.* Proc Natl Acad Sci U S A, 1995. **92**(23): p. 10629-33.

170. Braga, V.M., et al., *The small GTPases Rho and Rac are required for the establishment of cadherin-dependent cell-cell contacts.* J Cell Biol, 1997. **137**(6): p. 1421-31.

171. Jou, T.S. and W.J. Nelson, *Effects of regulated expression of mutant RhoA and Rac1 small GTPases on the development of epithelial (MDCK) cell polarity.* J Cell Biol, 1998. **142**(1): p. 85-100.

172. Kovacs, E.M., et al., *Cadherin-directed actin assembly: E-cadherin physically associates with the Arp2/3 complex to direct actin assembly in nascent adhesive contacts.* Curr Biol, 2002. **12**(5): p. 379-82.

173. Vasioukhin, V. and E. Fuchs, *Actin dynamics and cell-cell adhesion in epithelia.* Curr Opin Cell Biol, 2001. **13**(1): p. 76-84.

174. Amano, M., M. Nakayama, and K. Kaibuchi, *Rho-kinase/ROCK: A key regulator of the cytoskeleton and cell polarity.* Cytoskeleton (Hoboken), 2010. **67**(9): p. 545-54.

175. Samarin, S.N., et al., *Rho/Rho-associated kinase-II signaling mediates disassembly of epithelial apical junctions.* Mol Biol Cell, 2007. **18**(9): p. 3429-39.

176. Nakajima, H. and T. Tanoue, *Lulu2 regulates the circumferential actomyosin tensile system in epithelial cells through p114RhoGEF.* J Cell Biol, 2011. **195**(2): p. 245-61.

177. Itoh, M., et al., *Rho GTP exchange factor ARHGEF11 regulates the integrity of epithelial junctions by connecting ZO-1 and RhoA-myosin II signaling.* Proc Natl Acad Sci U S A, 2012. **109**(25): p. 9905-10.

178. Ratheesh, A., et al., *Centralspindlin and alpha-catenin regulate Rho signalling at the epithelial zonula adherens.* Nat Cell Biol, 2012. **14**(8): p. 818-28.

179. Mack, N.A., et al., *beta2-syntrophin and Par-3 promote an apicobasal Rac activity gradient at cell-cell junctions by differentially regulating Tiam1 activity.* Nat Cell Biol, 2012. **14**(11): p. 1169-80.

180. Yi, C., et al., *A tight junction-associated Merlin-angiomotin complex mediates Merlin's regulation of mitogenic signaling and tumor suppressive functions.* Cancer Cell, 2011. **19**(4): p. 527-40.

181. Otani, T., et al., *Cdc42 GEF Tuba regulates the junctional configuration of simple epithelial cells.* J Cell Biol, 2006. **175**(1): p. 135-46.

182. Elbediwy, A., et al., *Epithelial junction formation requires confinement of Cdc42 activity by a novel SH3BP1 complex.* J Cell Biol, 2012. **198**(4): p. 677-93.

183. Citi, S., et al., *Regulation of small GTPases at epithelial cell-cell junctions.* Mol Membr Biol, 2011. **28**(7-8): p. 427-44.

184. Itoh, M., et al., *The 220-kD protein colocalizing with cadherins in non-epithelial cells is identical to ZO-1, a tight junction-associated protein in epithelial cells: cDNA cloning and immunoelectron microscopy.* J Cell Biol, 1993. **121**(3): p. 491-502.

185. Itoh, M., et al., *Involvement of ZO-1 in cadherin-based cell adhesion through its direct binding to alpha catenin and actin filaments.* J Cell Biol, 1997. **138**(1): p. 181-92.

186. Maiers, J.L., et al., *ZO-1 recruitment to alpha-catenin--a novel mechanism for coupling the assembly of tight junctions to adherens junctions.* J Cell Sci, 2013. **126**(Pt 17): p. 3904-15.

187. Yap, A.S., et al., *Microtubule integrity is necessary for the epithelial barrier function of cultured thyroid cell monolayers.* Exp Cell Res, 1995. **218**(2): p. 540-50.

188. Ivanov, A.I., et al., *Microtubules regulate disassembly of epithelial apical junctions.* BMC Cell Biol, 2006. **7**: p. 12.

189. Goellner, G.M., S.J. DeMarco, and E.E. Strehler, *Characterization of PISP, a novel single-PDZ protein that binds to all plasma membrane Ca2+-ATPase b-splice variants.* Ann N Y Acad Sci, 2003. **986**: p. 461-71.

190. Stephenson, S.E., et al., *A single PDZ domain protein interacts with the Menkes copper ATPase, ATP7A. A new protein implicated in copper homeostasis.* J Biol Chem, 2005. **280**(39): p. 33270-9.

191. Nabokina, S.M., V.S. Subramanian, and H.M. Said, *Association of PDZ-containing protein PDZD11 with the human sodium-dependent multivitamin transporter.* Am J Physiol Gastrointest Liver Physiol, 2011. **300**(4): p. G561-7.

192. Lee, H.J. and J.J. Zheng, *PDZ domains and their binding partners: structure, specificity, and modification.* Cell Commun Signal, 2010. **8**: p. 8.

193. Garner, C.C., J. Nash, and R.L. Huganir, *PDZ domains in synapse assembly and signalling.* Trends Cell Biol, 2000. **10**(7): p. 274-80.

194. Harris, B.Z. and W.A. Lim, *Mechanism and role of PDZ domains in signaling complex assembly.* J Cell Sci, 2001. **114**(Pt 18): p. 3219-31.

195. Zhang, M. and W. Wang, *Organization of signaling complexes by PDZ-domain scaffold proteins.* Acc Chem Res, 2003. **36**(7): p. 530-8.

196. Brone, B. and J. Eggermont, *PDZ proteins retain and regulate membrane transporters in polarized epithelial cell membranes.* Am J Physiol Cell Physiol, 2005. **288**(1): p. C20-9.

197. Roh, M.H. and B. Margolis, *Composition and function of PDZ protein complexes during cell polarization.* Am J Physiol Renal Physiol, 2003. **285**(3): p. F377-87.

198. Doyle, D.A., et al., *Crystal structures of a complexed and peptide-free membrane protein-binding domain: molecular basis of peptide recognition by PDZ.* Cell, 1996. **85**(7): p. 1067-76.

199. Morais Cabral, J.H., et al., *Crystal structure of a PDZ domain.* Nature, 1996. **382**(6592): p. 649-52.

200. Ye, F. and M. Zhang, *Structures and target recognition modes of PDZ domains: recurring themes and emerging pictures.* Biochem J, 2013. **455**(1): p. 1-14.

201. Straight, S.W., et al., *Mammalian lin-7 stabilizes polarity protein complexes.* J Biol Chem, 2006. **281**(49): p. 37738-47.

202. Guerrera, D., et al., *PLEKHA7 Recruits PDZD11 to Adherens Junctions to Stabilize Nectins.* J Biol Chem, 2016. **291**(21): p. 11016-29.

203. Li, J., D.J. Callaway, and Z. Bu, *Ezrin induces long-range interdomain allostery in the scaffolding protein NHERF1.* J Mol Biol, 2009. **392**(1): p. 166-80.

204. Sudol, M. and T. Hunter, *NeW wrinkles for an old domain.* Cell, 2000. **103**(7): p. 1001-4.

205. Dodson, E.J., et al., *Versatile communication strategies among tandem WW domain repeats.* Exp Biol Med (Maywood), 2015. **240**(3): p. 351-60.

206. Reuven, N., M. Shanzer, and Y. Shaul, *Tyrosine phosphorylation of WW proteins.* Exp Biol Med (Maywood), 2015. **240**(3): p. 375-82.

207. Shah, J., et al., *PLEKHA7: Cytoskeletal adaptor protein at center stage in junctional organization and signaling.* Int J Biochem Cell Biol, 2016. **75**: p. 112-6.

208. Iglesias-Bexiga, M., et al., *WW domains of the yes-kinase-associated-protein (YAP) transcriptional regulator behave as independent units with different binding preferences for PPxY motif-containing ligands.* PLoS One, 2015. **10**(1): p. e0113828.

209. Fujiwara, Y., et al., *Crystal structure of afadin PDZ domain-nectin-3 complex shows the structural plasticity of the ligand-binding site.* Protein Sci, 2015. **24**(3): p. 376-85.

210. Dudak, A., et al., *Membrane palmitoylated proteins regulate trafficking and processing of nectins.* Eur J Cell Biol, 2011. **90**(5): p. 365-75.

211. Zhao, Y., P.M. Vanhoutte, and S.W. Leung, *Vascular nitric oxide: Beyond eNOS.* J Pharmacol Sci, 2015. **129**(2): p. 83-94.

212. Dimmeler, S., et al., *Activation of nitric oxide synthase in endothelial cells by Akt-dependent phosphorylation.* Nature, 1999. **399**(6736): p. 601-5.